Faculté de Pharmacie et des Sciences Biomédicales
Louvain Drug Research Institute
Groupe de recherche en Pharmacognosie

Development and validation of analytical methods for the identification and quantification of phenolic compounds from *Euterpe oleracea* fruits

Aécio L. S. DIAS

Thèse présentée en vue de l'obtention du grade de
Docteur en Sciences Pharmaceutiques et Biomédicales

Promoteurs: **Prof. Joëlle QUETIN-LECLERCQ, LDRI/UCL**

Prof. Hervé ROGEZ, FEA and CVACBA/UFPA

Année académique 2013-2014

Faculté de Pharmacie et des Sciences Biomédicales
Louvain Drug Research Institute
Groupe de recherche en Pharmacognosie

Development and validation of analytical methods for the identification and quantification of phenolic compounds from *Euterpe oleracea* fruits

Aécio Luís de Sousa Dias

Thèse présentée en vue de l'obtention du grade de
Docteur en Sciences Pharmaceutiques et Biomédicales

Promoteurs : Pr. Joëlle Quetin-Leclercq (UCL-LDRI)
Pr. Hervé Rogez (UFPA-CVACBA)

Membres du jury : Pr. Sandra Apers (UA, NatuRA)
Pr. Georges Lognay (ULg-GxABT)
Dr. Eric Rozet (ULg-CIRM)
Pr. Yvan Lorondelle (UCL-ISV)
Pr. Giulio Muccioli (UCL-LDRI)

Président du jury : Pr. Nathalie Delzenne (UCL-LDRI)

Année académique 2013-2014

To Emmanuelle and Céci who is the most beautiful fruit of my life, to my parents Maria and Arnaldo, and to my siblings Arnaldo Júnior, Mara, Alan and Alder.

Acknowledgements

A PhD thesis deals with many challenges, many questions and answers, a lot of learning, and the participation of so many people. In fact, this work relies on an immense network of dependencies to which justice can hardly be done with a brief acknowledgment page. I would like to express my gratitude to all the people who participated directly or indirectly to this project.

My deepest gratitude goes to my three promoters with whom I have had the great pleasure of working and from whom I have learned very much : Prof. Joëlle Quetin-Leclercq, Prof. Hervé Rogez and Prof. Jean-Louis Habib Jiwan (*in memoriam*). Many thanks for their scientific orientations and the precious time devoted to this work. Their knowledge, experience, and many other qualities and contributions were fundamental to the completion of this thesis. I want to specify some of these qualities and contributions. I owe a debt of gratitude to Prof. J. Quetin-Leclercq for her scientific rigor, rich and decisive orientation, efficiency in solving problems, corrections, and for her management of so many projects including this one, a quality that I admire very much, for welcoming me in her research group and for her confidence. I appreciated her willingness to discuss even with so many works to manage. I would like to express my immense gratitude to Prof. H. Rogez who sparked my interest in research along with J.N.S Souza several years ago yet during my graduation. Many thanks for his confidence, support, encouragements, and help in several periods of this thesis. His knowledge on açai and several other Amazonian plants was so important for the planification and completion of this project. I would like to thank him also for his management of students, producers and traders, etc., during acquisitions and processing of the fruit samples that was a hard work and needed so much time. Even per Skype, he was a real presence in all steps of this thesis. *Valeu!!! Muito obrigado por tudo!!!!* I am extremely grateful to Prof. J-L Habib Jiwan (*in memoriam*) for his confidence in accepting me as a PhD student. His knowledge and experience contributed very much to this thesis. I appreciated his rich orientations, calm, and politeness. Even for a relatively short period I learned much with him.

I am also obliged to the scientific committee that devoted their time all along this thesis and contributed to the development of this project with interesting discussions, advices and commentaries. I am very grateful to the jury members Prof. S. Apers and Prof. G. Lognay who accepted to honour this work with their participation in the last step of this thesis.

Particular mention must go to Dr. E. Rozet and Prof. Y. Larondelle who participated in the publication of the articles with critical revisions. Dr. E. Rozet was an essential support to the completion of this project, participating in the experimental planifications, treatment of the results and discussions with always a lot of kindness. Prof. Y. Larondelle also provided a fellowship at the final step of the work for which I am really gratefull and financial support to this research from a PIC project coordinated by him via CUD-Belgium and UCL-ADRI, and he also contributed to several other steps of this project. I also remain indebted to Prof. G. Muccioli who helped me especially with the efficient troubleshooting related to the LC-MS system. His precious help was very frequent and, sometimes, even at the weekend!!! I am deeply grateful for his devoted availability. Moreover, I want to express my gratitude to Prof. Nathalie Delzenne who agreed to devote her time to preside the jury.

I am also very grateful to Prof. Philippe Hubert (ULg-CIRM) who participated with his knowledge and experience in the articles publicated from this thesis and in fruitful discussions on analytical problems. I extend my appreciation to Dr. Vincent Baeten (CRA-W) who kindly donated some standard compounds and along with Aline Gato participated in the transport of samples from Brazil to Belgium.

UCL-ADRI is acknowledged by the financial support from a fellowship during the major part of this thesis. Thanks again to CUD-Belgium and the PIC project (2009-2013) coordinated by Y. Larondelle by their financial support via UCL-ADRI for this research and by another fellowship provided at the last step of this work.

Special thanks to Dr. Gabrielle Chataigné who, at the beginning of this thesis, devoted part of her time to contribute with my formation on the LC-PDA-HRMS and in several discussions on my preliminary results. Her presence was always very pleasant. Furthermore, in the same sphere, I also had the assistance of Dr. Marie-France Hérent, Julien Masquelier and Dr. Aubert Maquille to whom I would like to express my appreciation.

Many thanks to my Brazilian colleagues of the laboratories “Usina de alimentos” and CVACBA who contributed in important steps of the project involving the samples: Jesus, Darly, Karissa, Taiana, Bianca and Tatiana. Specially, Ana Caroline, Cézar, Larissa, Luciana and Risaldo are gratefully acknowledged for their participation in the acquisition and preparation of the samples that were laborious works and took a lot of time. *Muito obrigado!!!*

I am again very grateful to Hervé and Jesus who helped me in this project in its origins.

Thank you very much to all the colleagues of Belgian laboratories that shared time, discussions, kindness and help me in many different ways: Emmanuelle, Joseph (Jupp), Salim, Habib, Achille, Joanne, Françoise, Mamy, Marie-Christine, Ramazan, Jean-Paul, Alphonse, Marie-Yvonne, Emilie, Claire Beaufay, Claire Mourgues, Lucy, Maude, Vincent, Julien, Aubert, Thomas, Valentin, Owen, Mireille, Adam, Salomé, Aurélie, Andrea, Pascale, Ouma, Cynthia.

Special thanks to Sophie and Ian for their friendship, and hospitality at the beginning of my stay in Belgium. Their kind family gave me very happy moments. I extend my appreciation to the friends Kleber, Wânia, Marta, Tien, Benoît and Alex. Especially at the beginning of this thesis, they were a great support that helped me in the adaptation in the loved Belgium.

I am deeply grateful to my wife, Emmanuelle, and my daughter, Céci, to whom I want to speak in Portuguese, the language of my heart : *Muito obrigado Emmanuelle pelo apoio, encorajamento, paciência e compreensão durante esses anos, especialmente nos longos dias e dias longos de trabalho. Obrigado pelos conselhos científicos, pelas discussões, ajuda analítica que me ajudaram a responder tantas questões, entre tantas outras ajudas. Ceci, tu és tão pequena e de aparência tão frágil, mas tu me deste tanta força que foi muito importante durante esse trabalho, e claro tu és uma fonte de muita alegria para mim. Obrigado, minha querida.*

I am also very grateful to my French family, Jocelyne, Jacky and Marianne for their great kindness and support from different forms.

I would also like to thank to the numerous members of my Brazilian family, parents, brothers, sister, sisters-in-law, nephews, nieces, uncles, cousins, grandfathers/grandmothers (*in memoriam*), etc, who have participated in my life. I am specially grateful to my mother, father, and brothers to whom I would also like to express my appreciation in Portuguese : *mãe, pai, irmãos, vocês foram uma presença constante em meus pensamentos durante esses cinco anos e um solido suporte em muitos momentos desse trabalho. Agredeço muito à vocês pela força e coragem que vocês me deram e pelas participações nas diferentes etapas e esferas da minha vida. Muito obrigado!!!*

Legend of açai

Many years ago, there was an Indian tribe in the region of the Pará state in Brazil that became very numerous. There was a period of food scarcity. Therefore, the Indian chief, Itaki, had to make the very hard decision to have all newborn babies sacrificed.

This chief had a daughter called Iaçá, who soon gave birth to a baby girl, who had to be sacrificed. Iaçá was devastated and cried day and night, going for long days without food or drink and not leaving her house at all. She remained in her hut praying to Tupã the jungle god that she might show her father another way to help her people and save the tribe without sacrificing any more babies.

Then one night, she heard the crying of a baby coming from the forest. She followed the sound and found her baby at the base of a palm. She darted out and hugged her baby. However, mysteriously, her baby disappeared.

Iaçá, heartbroken, cried until death. Days after, Itaki found her lifeless body, her arms wrapped around the trunk of a palm tree, her face was peaceful with a smile and her eyes were open and strangely fixed to the top of the palm that was laden with dark purple fruit.

Itaki then ordered that the fruits be harvested, tasted and noted that they were tasty and sustaining. In homage to his daughter he named the berry Açai (Iaçá spelled backwards). The chief lifted his order, saving the babies, and the tribe prospered thereafter.

Story of the Amazonian folklore

Abbreviations

AAPH : 2,2'-azobis(2-amidinopropane) dihydrochloride

AA : arachidonic acid

ACN : acetonitrile

AGEs : advanced glycation end products

Akt : also known as "Protein Kinase B" (PKB) (a serine/threonine-specific-protein kinase)

amu : atomic mass unit

AP-1 : activator protein-1

APCI : atmospheric pressure chemical ionization

API : atmospheric pressure ionization

ASK-1 : apoptosis signal-regulating kinase 1

ABC : adenosine triphosphate-binding cassette

C8, C18 : reversed-phase column-packing designations, indicating length of alkyl ligand bonded to the particle

CBG : cytosolic β-glucosidase

CEM : channel electron multiplier

COMTs : catechol-*O*-methyltransferases

COX : cyclooxygenase

CID : collision-induced dissociation

CREB : cAMP response element-binding protein

CRM : consecutive reaction monitoring

cy3glu : cyanidin 3-glucoside

cy3rut, cyanidin 3-rutinoside

Da : Dalton

DAD : diode-array detector, also PDA detector

EIC : extracted-ion chromatogram

eNOS : endothelial nitric oxide synthase

EOF : *Euterpe oleracea* fruits

EOJ : *Euterpe oleracea* juice

ERK : extracellular-signal-regulated kinase

ESI : electrospray ionization

EtOAc : ethyl acetate

FT : Fourier transform

FT−ICR : Fourier transform−ion cyclotron resonance

FTMS : Fourier transform mass spectrometry

FWHM : full width at half maximum

HPLC : high-performance liquid chromatography

GLUT1-2 : glucose transporter 1 or 2

HPLC−MS : high-performance liquid chromatography−mass spectrometry

HRMS : high resolution mass spectrometry

ICAM-1 : intercellular adhesion molecule 1

ICR : ion cyclotron resonance

i.d. : internal diameter

IL : interleukin

iNOS : inducible nitric oxide synthase

IS : internal standard

IT : ion trap

JNK : c-Jun N-terminal kinase

LC : liquid chromatography

LC−MS : liquid chromatography−mass spectrometry

LDL : low-density lipoprotein

LIT : linear ion trap, also called LTQ

LLE : liquid–liquid extraction

LOD : limit of detection

LOX : lipoxygenase

LOQ : limit of quantitation

LPH : lactase phlorizin hydrolase

LPS : Lipopolysaccharide

LTQ : linear trap quadrupole or quadrupole linear ion trap, also LIT

m/*z* : mass-to-charge ratio

MA : mass accuracy

MAPK : mitogen-activated protein kinase

mAU : milli-absorbance units

ME : matrix effect

MeOH : methanol

MEW : mass extraction window

MRP1,-2-3 : multidrug resistance protein 1, 2 or 3

MS : mass spectrometry

MS/MS : tandem mass spectrometry

MS^n : multiple-stage mass spectrometry, where "n" is the number of product ion stages (n^{th}-generation product ions)

NADPH oxydase : nicotinamide adenine dinucleotide phosphate-oxidase

NAF : non-anhocyanin flavonoids

NF-κB ; nuclear factor-kappa B

NO : nitric oxide

NOS : nitric oxide synthase

OAT2 : organic anion transporter 2

ORAC : oxygen radical absorbance capacity

p38 MAPK : p38 mitogen-activated protein kinase

PDA : photodiode-array (detector); also DAD

PE : process efficiency

PIC : projet interuniversitaire ciblé

PI3 kinase : phosphatidylinositol 3-kinase

PKC : protein kinase C

PLA2 : phospholipase 2

ppm : parts per million

Q : quadrupole

RAGE : receptor for advanced glycation end products (AGEs)

RDA : retro-Diels–Alder

RE : recovery

RP : resolving power

RSD : relative standard deviation

S/N : signal-to-noise ratio

SEM : secondary-electron multiplier

SGLT1 : sodium-dependent glucose transporter 1

SIM : selected-ion monitoring

SMCT1-2 : sodium-coupled monocarboxylate transporter 1 or 2

SPE : solid-phase extraction

SRM : selected reaction monitoring

STAT-1 : signal transducer and activator of transcription-1

SULTs : sulfotransferases

TIC or TICC : total ion chromatogram or total ion current chromatogram (synonymous).

TNF-α : tumor necrosis factor-α

TEAC : trolox equivalent antioxidant capacity

TOF : time of flight

TOSC : total oxidant scavenging capacity

TRAP : total radical trapping antioxidant parameter

UFPA : universidade federal do Pará

UGTs : uridine-5'-diphosphate glucuronosyltransferases

UHPLC : ultra-high pressure liquid chromatography, also ultra-high performance liquid chromatography

UV : ultraviolet

VCAM-1 : vascular cell adhesion molecule 1

Table of contents

General introduction

Euterpe oleracea is a palm tree very abundant in the Brazilian Amazon forest. The juice produced from its fruits, called "açaí" is the most commonly consumed beverage in the Amazon region, where the individual consumption can reach one litre per day. The fruits have been acclaimed as "superfruit" and have received much attention of the food industry and health sector, because of their abundance in bioactive compounds, mainly phenolic derivatives. The interest for phenolic compounds has remarkably increased in the last fifteen years because of their elevated antioxidant activity, and scavenging potential of free radicals associated to various diseases. The increasing commercialization of these fruits have directly improved the benefits of small cooperatives, organized for the harvest, transport and process of the fruits to juice and other derived products [1].

The general context of this thesis is a collaboration between Peruvian (UNALM, Lima), Brazilian (UFPA, Belém) and Belgian (UCL and ULB, Louvain-la-Neuve and Bruxelles) universities from a Projet Interuniversitaire Ciblé (PIC) entitled « Etudes approfondies sur la valorisation de composés bioactifs de plantes andines et amazoniennes pour un développement régional durable ». This project has the financial support of the Commission Universitaire pour le Développment (CUD). The main objective of the PIC is to give added value to different plant products from the Andean and Amazonian biodiversity, through a better knowledge on their bioactive compounds, for a sustainable regional development. In this project, chemical, biochemical, toxicological and engineering studies have been performed to achieve this objective. In this context, this thesis selected the fruits of *E. oleracea* palm in order to perform their phenolic characterization and quantification. *E. oleracea* fruits were chosen because of their economic importance for the Amazon region. Additionally, their characterization and quantification are crucial steps for their valorization because they can help producers and research institutions to improve the quality of the fruits and derived products.

In the first part of this work, a general review of the scientific literature will be presented about (a) validation of analytical methods, (b) phenolic compounds, including their chemical structures and analytical methods used for their characterization, and finally, (c) generalities about *E. oleracea* fruits, including the current knowledge about their phenolic composition. After that, the objectives of the thesis will be detailed. Chapter 2, a validated analytical method that allowed the identification and quantification of anthocyanins in fruit extracts of *E. oleracea* palm will be described. The anthocyanins correspond to the first group of phenolic compounds studied in this work. Due to the specificities of the different classes of

phenolic compounds, another analytical method was developed and validated for the identification and quantification of non-anthocyanin flavonoids in juices of *E. oleracea*. It will be presented in Chapter 3. Then, a general discussion will be performed regarding the results obtained in those experimental chapters. Finally, the conclusions and perspectives will be presented.

1. Bibliographic review

1.1. Validation of analytical methods

Analytical method validation is a mandatory step before routine analysis in analytical laboratories of the chemical, pharmaceutical, biopharmaceutical and agro-food industries [2–5]. The validation of quantitative procedures gives guarantees that each measure that will be performed in routine analysis will be close enough to the unknown true value of the sample to be analysed [6,7].

Today, several international organisations offer guidelines on method validation and related topics, e.g. AOAC [8], FDA [9–11], ICH [12], ISO [2,5], EURACHEM [4]. These organisations proposed several validation criteria that should be tested in order to ensure the reliability of the developed method. The criteria that will be discussed here are:

- Selectivity
- Response function
- Trueness
- Precision (repeatability and intermediate precision)
- Accuracy
- Linearity
- Limit of detection (LOD)
- Limit of quantitation (LOQ)
- Dosing range

Although the consensus on which criteria should be evaluated during the validation analytical methods, some confusion about terminologies of these validation criteria were observed between the references. Some papers have discussed the incoherencies and confusions established about these terminologies [6,13–16]. Some of the main ambiguities will be noted in the next section.

In this context, a commission of the « Société Française des Sciences et Techniques Pharmaceutiques » (SFSTP) [6,13,14,17,18] looked for a consensus on the norms usually recognized for the validation, and principally proposed a harmonized approach for quantitative method validation that uses the accuracy profile as decision tool, based on the β-

expectation tolerance interval and the concept of total error. This approach gives predictions about the quality of the future results that will be produced.

This approach of method validation, as well as this consensus about the terminologies of validation criteria discussed in these references were used in this work.

1.1.1. Objectives of method validation

Before addressing the purpose of the method validation, we can define the objective of a quantitative analytical procedure as the quantification, as accurate as possible, of each of the unknown quantities of analytes that the laboratory will have to determine, which means that the difference between the obtained result and the unknown true value of the analyte will be inferior to acceptance limits (Eq. 1):

$$-\lambda < x - \mu_T < \lambda \Leftrightarrow \left| x - \mu_T \right| < \lambda \quad \text{Eq. 1}$$

where x is the result obtained by the analytical method, μ_T is the true value of the sample, and λ is the acceptance limit. The acceptance limits are fixed a priori by the analyst according to the objective of the analytical procedure. The objective is linked to the requirements usually admitted by the practice. In biological matrices as in our case (vegetal extracts) the acceptance limits between ± 20% and ± 30% can be used [17].

The objective of method validation is then to provide by examination evidences that an analytical procedure meets its objective. In other words, the objective of validation is to give guarantees that each of the future results that the laboratory will obtain with the validated method during routine analysis will be accurate enough, so sufficiently closed to the true value.

1.1.2. Validation criteria

1.1.2.1. Selectivity and Specificity

Selectivity refers to the extent to which the method can be used to determine particular analytes in mixtures or matrices without interferences from other components of similar

behavior [19]. A method, which is perfectly selective for an analyte is said to be specific [20]. Therefore, specificity can be considered as the ultimate selectivity, meaning that no interferences are supposed to occur [19]. Selectivity can be graded while specificity is an absolute characteristic [19,21].

A clear distinction should be made as discussed in a recent review [22] "A specific reaction or test is one that occurs only with the substance of interest, while a selective reaction or test is one that can occur with other substances but exhibits a degree of preference for the substance of interest. Few reactions are specific, but many exhibit selectivity". This is consistent with the above definitions of selectivity and specificity.

As recommended by the IUPAC [19], the term selectivity should be promoted in analytical chemistry and particularly in chromatographic techniques and the term specificity should be discouraged. Therefore, in the present work, selectivity will be used instead of specificity. The selectivity level of chromatographic methods depends on the quality of the chromatographic separation and on the intrinsic selectivity of the detection method [17].

In plant extract analysis, it is impossible to obtain a blank sample (containing all compounds, except the analyte(s)) to evaluate the selectivity. Nevertheless, this parameter can be evaluated by checking the deviation of the retention time which should fall within the range of ±0.5% [23] and mainly by checking the peak purity of the chromatographic peak, by comparing the spectra (i.e. UV, MS or MS/MS) at different levels of the peak, with standard compound data [24–27]. This may be done by softwares in several analytical instruments.

1.1.2.2. Response function

The response function of an analytical procedure is the relationship between the response (signal, e.g. area under the curve, peak height) and the concentration (quantity) of the analyte in the sample, within a specified range. The calibration curve is the most appropriate response function. The response function can be linear (straight line) or non linear, depending on the detection method or the concentration range. Non linear models have often been observed in bioanalytical methods using LC–MS/MS [28,29].

As the purpose of an analytical procedure is to give accurate measurements, the standard curve must be evaluated on its ability to provide accurate results. This may be evaluated by the accuracy profile by analysing which response function gives the best accurate results

[16,29–31]. Explanations on the use of accuracy profile, as a decision tool to evaluate the accuracy of the results, will be given in *1.1.2.6. Accuracy* section.

1.1.2.3. Linearity

The linearity of an analytical procedure is the proportional relationship within a definite range between the results and the concentrations of the analyte in the sample that were back-calculated from the calibration curve. As discussed in a recent review [16] linearity is confused with response function, e.g. the ICH Q2 (R1) document [12] is ambiguous : in one section of the document, linearity is defined as aforementioned, but in another section it is mentioned that it should be evaluated from a visual inspection of a plot of signals as function of the concentrations. The notion of signals *vs* concentration is presented in other references [32,33].

Figure 1 [14] illustrates the linearity graphic with the intercept, the slope (close to 1) and r^2 estimations.

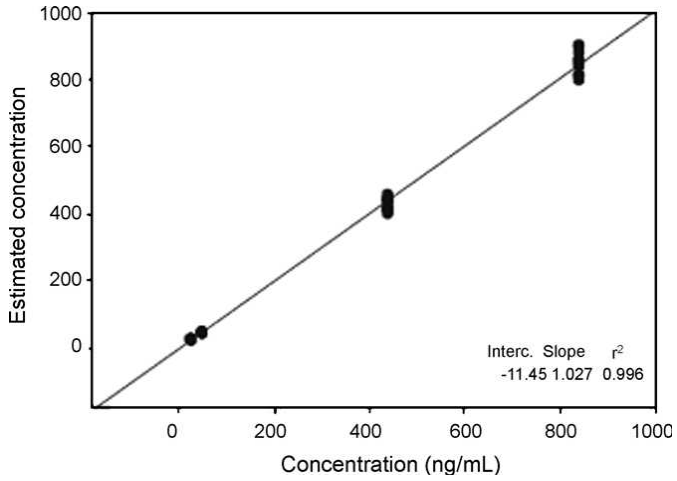

Figure 1 Representation of the linearity of an analytical procedure, with the estimations of the intercept, the slope and r^2 [14]. The dots represent the back-calculated concentrations obtained from a linear regression as response function. The line represents the linear regression model that was fitted on the back-calculated concentrations (experimental results) as a function of the target concentrations (introduced concentrations in the validation standards).

1.1.2.4. Precision

Precision of an analytical procedure expresses the closeness of agreement between a series of measurements obtained from multiple sampling of the same homogeneous sample (independent assays) under the prescribed conditions. It gives some information on random errors. Considering "within laboratory evaluation", precision can be estimated at two levels, repeatability and intermediate precision, both are expressed in terms of standard deviation (SD) and relative standard deviation (RSD) values:

1) Repeatability expresses the precision under conditions where the results of independent assays are obtained by the same analytical procedure on identical samples in the same laboratory, by the same operator, using the same equipment and during a short interval of time (intra-day);

2) Intermediate precision expresses the precision under conditions where the results of independent assays are obtained by the same analytical procedure on identical samples in the same laboratory, with different operators, using different equipment, on different days, etc.

The following notations will be employed in the equations:

- i series index (ranging from 1 to I)
- j concentration level index (ranging from 1 to J)
- k repetition index (ranging from 1 to K)

Repeatability and intermediate precision are evaluated by analysis of variance (ANOVA) of the back-calculated results coming from the validation standards for each concentration level j. Here, we will consider that the design is balanced, i.e. the same numbers of replicates per series for each concentration level.

For each concentration level *j*:

- $\bar{x}_i$ is the mean of the back-calculated concentrations of *K* repetitions and one *i* series (intra-series mean) (Eq. 2):

$$\bar{x}_i = \frac{\sum_{k=1}^{K} x_{ik}}{K} \quad \text{Eq. 2}$$

- $\bar{x}_{ik}$ is the overall mean of the back-calculated concentrations of the *I* series and *K* repetitions of a concentration level (Eq. 3):

$$\bar{x}_{ik} = \frac{\sum_{i=1}^{I} \sum_{k=1}^{K} x_{ik}}{I \times K} \quad \text{Eq. 3}$$

- S^2_{intra} is the estimator of the intra-series variance (Eq. 4):

$$S^2_{intra} = \frac{\sum_{i=1}^{I} \sum_{k=1}^{K} (x_{ik} - \bar{x}_i)^2}{I(K-1)} \quad \text{Eq. 4}$$

where x_{ik} is the back-calculated concentration of th i^{th} series and k^{th} repetition.

- S^2_{inter} is the estimator of the inter-series variance (Eq. 5):

$$S^2_{inter} = \frac{\frac{\sum_{k=1}^{K}\sum_{i=1}^{I}(\bar{x}_i - \bar{x}_{ik})^2}{K-1} - S^2_{intra}}{I} \quad \text{Eq. 5}$$

If $S^2_{\text{inter}} \leq 0$, then this estimator must be 0.

Finally, the repeatability is expressed by the standard deviation of the S^2_{intra} and will be represented by S_{intra} (Eq. 6):

$$S_{intra} = \sqrt{S^2_{intra}} \quad \text{Eq. 6}$$

In addition, the sum of the intra and inter-series variance estimators gives the intermediate precision estimation represented by S^2_{IP} (Eq. 7):

$$S^2_{IP} = S^2_{intra} + S^2_{inter} \quad \text{Eq. 7}$$

Intermediate precision is expressed as a standard deviation (S_{IP}) (Eq. 8):

$$S_{IP} = \sqrt{S^2_{intra} + S^2_{inter}} \quad \text{Eq. 8}$$

or as a relative standard deviation (RSD_{IP}) (Eq. 9):

$$RSD_{IP} = \frac{S_{IP}}{\bar{x}_{ik}} \times 100 \quad \text{Eq. 9}$$

1.1.2.5. Trueness

Trueness of an analytical procedure refers to the closeness of agreement between a conventionally accepted value and a mean experimental one obtained from a series of measurements. The first one can be obtained by the use of validation standards, which corresponds to samples prepared with a known amount of the analyte. The trueness is estimated for each concentration level of the dosing range and gives information on systematic error.

This criterion is generally expressed in terms of absolute bias (Eq. 10), relative bias (%) (Eq. 11) or recovery (%) (Eq. 12) and calculated as follows:

$$Absolute\ bias = \overline{x}_{ik} - \overline{\mu}_T \quad \text{Eq. 10}$$

$$Relative\ bias\ (\%) = 100 \times \frac{\overline{x}_{ik} - \overline{\mu}_T}{\overline{\mu}_T} \quad \text{Eq. 11}$$

$$Recovery\ (\%) = 100 \times \frac{\overline{x}_i}{\overline{\mu}_T} \quad \text{Eq. 12}$$

where $\overline{x}_{ik}$ is the mean of the back-calculated concentrations obtained in the I series and K repetitions; and $\overline{\mu}_T$ is the mean of the introduced concentrations that are conventionally considered as the true values.

Trueness is confused with accuracy in some documents, but this terminology is not recommended [13,16].

1.1.2.6. Accuracy

The accuracy of an analytical procedure expresses the closeness of agreement between the value obtained by this procedure and the value that is accepted either as a conventional true value or as an accepted reference value. The closeness of agreement observed is the resultant of the sum of the systematic and random errors, i.e. the total error linked to the result. Consequently, the accuracy is the expression of the sum of the trueness (or bias) and precision, as shown below for a X measurement and a μ_T conventional true value:

$$X = \mu_T + bias + precision$$

$$X - \mu_T = bias + precision$$

$$X - \mu_T = \text{total error}$$

$$X - \mu_T = \text{accuracy}$$

Therefore, the total error of an analytical procedure evaluates its ability to produce accurate results. Thus, the total error estimation of a procedure is fundamental to assess the validity of a method. Additionally, another aspect of method validation is to give guarantees about the quality of future results. This is the role of the β-expectation tolerance interval, which is a prediction interval where β is the proportion of the future results expected to fall into the acceptance limits $\pm\lambda$. Values of β are usually chosen between 80% and 95% [29,34–36].

β-expectation tolerance interval (*TI*) can be calculated from the relative bias (%) (Eq. 11) and the relative standard deviation of the intermediate precision RSD_{IP} (Eq. 9), following the equation proposed by Mee R. Mee (Eq. 13) [14,37].

For each concentration level j :

$$TI = bias(\%) \pm kRSD_{IP}(\%) \quad \text{Eq. 13}$$

where k is a cover factor of the *TI* calculated as follows (Eq. 14):

$$k = Q_t\left(v; \frac{1+\beta}{2}\right)\sqrt{1+\frac{IS^2_{inter} + S^2_{intra}}{I \times K(S^2_{inter} + S^2_{intra})}} \quad \text{Eq. 14}$$

with S^2_{intra} and S^2_{inter} being the intra-series and inter-series variances, respectively;

and $Q_t\left(v;\frac{1+\beta}{2}\right)$ the β quantile of the Student's distribution with v degrees of freedom.

The v (number of degrees of freedom) is calculated as follows (Eq. 15):

$$v = \frac{(R+1)^2}{\frac{\left(R+\frac{1}{I}\right)^2}{K-1}\frac{1-\frac{1}{I}}{KI}} \quad \text{Eq. 15}$$

where R is the ratio of the inter-series over the intra-series variance (Eq. 16):

$$R = \frac{S^2_{Inter}}{S^2_{Intra}} \quad \text{Eq. 16}$$

In order to simplify the equation 14, the term B can be used (Eq. 17):

$$B = \sqrt{\frac{R+1}{K\times R+1}} \quad \text{Eq. 17}$$

The lower and upper limits of the *TI* are calculated as follows (Eq. 18 and Eq. 19):

$$TI_{lower} = bias(\%) - Q_t\left(v; \frac{1+\beta}{2}\right)\sqrt{1+\frac{1}{IKB^2}}RSD_{IP} \quad \text{Eq. 18}$$

$$TI_{upper} = bias(\%) + Q_t\left(v; \frac{1+\beta}{2}\right)\sqrt{1+\frac{1}{IKB^2}}RSD_{IP} \quad \text{Eq. 19}$$

As shown in Eq. 18 and 19, the tolerance interval limits are constituted by the bias (trueness) and the RSD_{IP} (intermediate precision) multiplied by a factor that is proportional to Q_t. Additionally, the intermediate precision includes the intra and inter-series variances (Eq. 8). As discussed above, the accuracy is the expression of the sum of the trueness (bias) and precision. Consequently, as the tolerance interval limits contain these two terms, they can be considered as expressing the results accuracy. Furthermore the *TI* integrates another dimension, the chance (β chance level) for future results to fall within the acceptance limits. The β probability is expressed in the β quantile of the Student's distribution (Eq. 14).

The limits of the *TI* are calculated for each concentration level and finally the accuracy profile is obtained by connecting the lower limits between themselves and, in the same way, the upper limits.

The accuracy profile is a decision criterion from which we can decide about the validity of the analytical method. Figure 2 illustrates the accuracy profile.

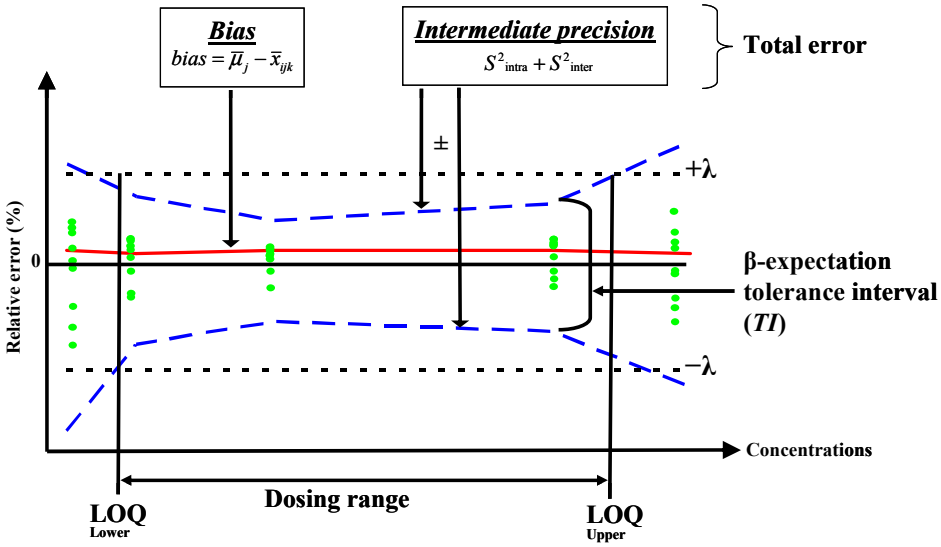

Figure 2 Schematic representation of the accuracy profile in relative values.
The green dots represent the relative error of the back-calculated concentrations of the validation standards and were back-calculated from the calibration standards, the dots are plotted with respect to their targeted concentration; the continuous line represents the relative bias; the blue dashed lines the *β*-expectation tolerance limits and the black dashed lines represent the acceptance limits.

The tolerance interval is the region in which it is expected to find the future results with a probability *β* %. The method is considered as valid within the range for which the *β*-expectation tolerance interval is comprised inside the acceptance limits (± λ). LOQ (lower and upper) is the lower and upper limits of quantification (Figure 2).

1.1.2.7. Limits of detection

The limit of detection (LOD) is the smallest quantity of the targeted substance that can be detected, but not accurately quantified in the sample in the experimental conditions of the analytical procedure.

Several approaches for determining the detection limits are described and they may give somewhat different results. We will discuss here the two most used. The LOD can be estimated based on the signal-to-noise ratio (S/N). The signal is measured from the middle of the baseline noise to the top of the peak (Figure 3). Both the S and N are illustrated in Figure 3. A signal-to-noise ratio of 3 is generally considered acceptable for estimating the detection

limit.

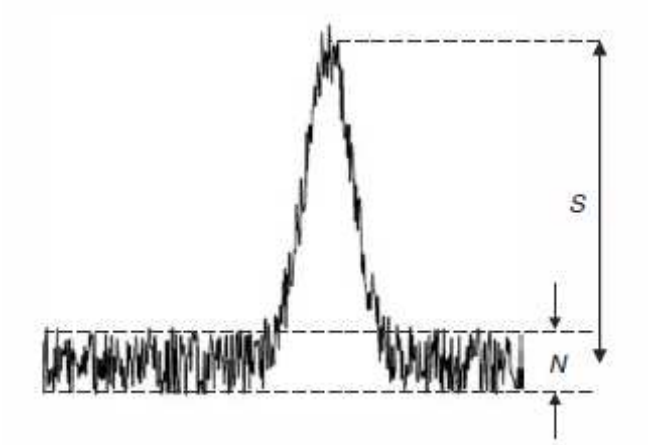

Figure 3 Measurement of chromatographic signal (S) and noise (N) [23].

LOD can also be estimated by Eq. 20, depending on the residual standard-deviation of the standard curve and its slope (Eq. 20).

$$\mathrm{LOD} = \frac{3.3\sigma}{\mathrm{Y}} \quad \text{Eq. 20}$$

where Y is the slope of the calibration curve of the analyte and σ is the residual standard deviation of the ANOVA of the regression line.

1.1.2.8. Limits of quantification

The lower limit of quantitation is the smallest quantity of the targeted substance in the sample that can be assayed under experimental conditions with well-defined accuracy (Figure 2). The definition can also be applicable to the upper limit of quantitation, which is the highest quantity of the targeted substance in the sample that can be assayed under experimental conditions with well-defined accuracy.

1.1.2.9. Dosing range

The dosing range is the interval between the lower and upper limits (including these limits) where the analytical procedure achieves adequate accuracy (trueness + precision) and linearity.

1.2. Phenolic compounds

Phenolic compounds are a large category of plant secondary metabolites. These compounds have a common structural feature, a phenol, which is an aromatic ring bearing at least one hydroxyl substituent, which can be in its free form or involved in another function: ether and ester. A general classification divides this broad category in simple phenols (only one phenol in the structure) and polyphenols (containing at least two phenol groups) [38,39]. Phenolic compounds have a wide variety of roles in plant life as structural, growth, reproduction, protection against pathogens or UV light, etc [40,41].

In foods, phenolic compounds are associated with colour, sensory qualities, and antioxidant properties [42]. Fruits, vegetables and cereals are important dietary sources of phenolic compounds and their phenolic levels depend on cultivation techniques, cultivars, growing conditions, ripening stage and process, as well as processing and storage conditions, among others [43–45]. They are mainly used in the food industry as colorant, dietary supplement, or natural preservative ingredient, and are also often found in the cosmetic sector. The level of phenolic compounds in foods and extracts is of high importance because of the health benefits of these compounds. In fact, the literature provides a lot of information that correlates the consumption of fruits and vegetables with the disease prevention. This effect is partly attributed to the phenolic compounds. Several works associated the high antioxidant activity of the phenolic compounds with the inhibition of oxidative damage diseases such as coronary heart disease, stroke, and cancers [46–48].

Because of their health implications, plant polyphenols have received much attention of the complementary medicine and food industry [49]. We can quote for example the tropical “exotic” fruits, whose production, trade and consumption have increased significantly on the domestic and international markets, not only due to their attractive sensory properties but also to a growing recognition of their nutritional and therapeutic values, that are partly associated with the presence of phenolic compounds [50,51]. In addition we can mention the potentialities of “exotic” plants from which polyphenol-rich extracts are produced and have

contributed to regional development in Latin American countries [52–57]. The large and yet growing interest of medicine and food industry in phenolic compounds is one of the reasons of the great effort that has been made in the development of analytical methods and in the chemical characterization of several plant matrices [58–60].

1.2.1. Biosynthesis and chemical structure of phenolic compounds

Plant secondary metabolites known as phenolic compounds are a wide group of substances, from simple phenols to polymeric molecules. The most important phenolic compounds are derived from two major routes: the shikimate and/or acetate pathways [61,62].

In general terms, the shikimate pathway is closely interlinked with the aromatic amino acid and phenylpropanoid pathways (Figure 4). L-phenylalanine and L-tyrosine amino acids are produced from the shikimate route, and deamination of L-phenylalanine produces cinnamic acid (Figure 4), that is followed by the production of its many derivatives such as phenolic acids, lignans, coumarines, etc. [63–65].

The acetate pathway begins with combinations of two-carbon units derived from the acetate, which lead to the formation of poly-*β*-keto chains of variable length. Cyclization of a poly-*β*-keto chain by Claisen or aldol reactions frequently promotes the formation of polycyclic compounds such as anthraquinones, chromones, etc. [61,62,66,67].

The diversity of the phenolic compounds is improved by the possibility of a simultaneous participation of the shikimate and the acetate pathways to the biosynthesis of compounds of mixed origin, such as flavonoids, pyrones, xanthones, etc. [61,68,69].

A brief explanation about the biosynthesis of some classes of phenolic compounds will be done, as well as a discussion about their chemical structures.

1.2.2. Phenolic acids

Phenolic acids have only one phenol subunit and one carboxylic acid functionality. They contain two constitutive carbon frameworks: benzoic acid derivatives (C_6-C_1, e.g. gallic acid in Figure 4) and cinnamic acid derivatives (C_6-C_3, e.g. 4-coumaric acid) [61,70]. The shikimate pathway comprises the early steps for the biosynthesis of these compounds as well as for several plant secondary metabolites. The different steps of this metabolic route are

discussed in some reviews [71–73] from which a detailed background can be found. In Figure 4, the main steps of the phenolic acid biosynthesis are shown. The shikimate pathway begins from phosphoenolpyruvate and erythrose 4-phosphate and comprises seven reactions catalyzed by six enzymes to produce chorismate. Phosphoenolpyruvate and erythrose 4-phosphate are respectively derived from the glycolysis and the non-oxidative branch of the pentose phosphate pathway. Chorismate is a central metabolite in plant cells, serving as a common precursor for the synthesis of three aromatic amino acids, L-tryptophan, L-phenylalanine and L-tyrosine. The two latter are the precursors of the cinnamic acid derivatives [63].

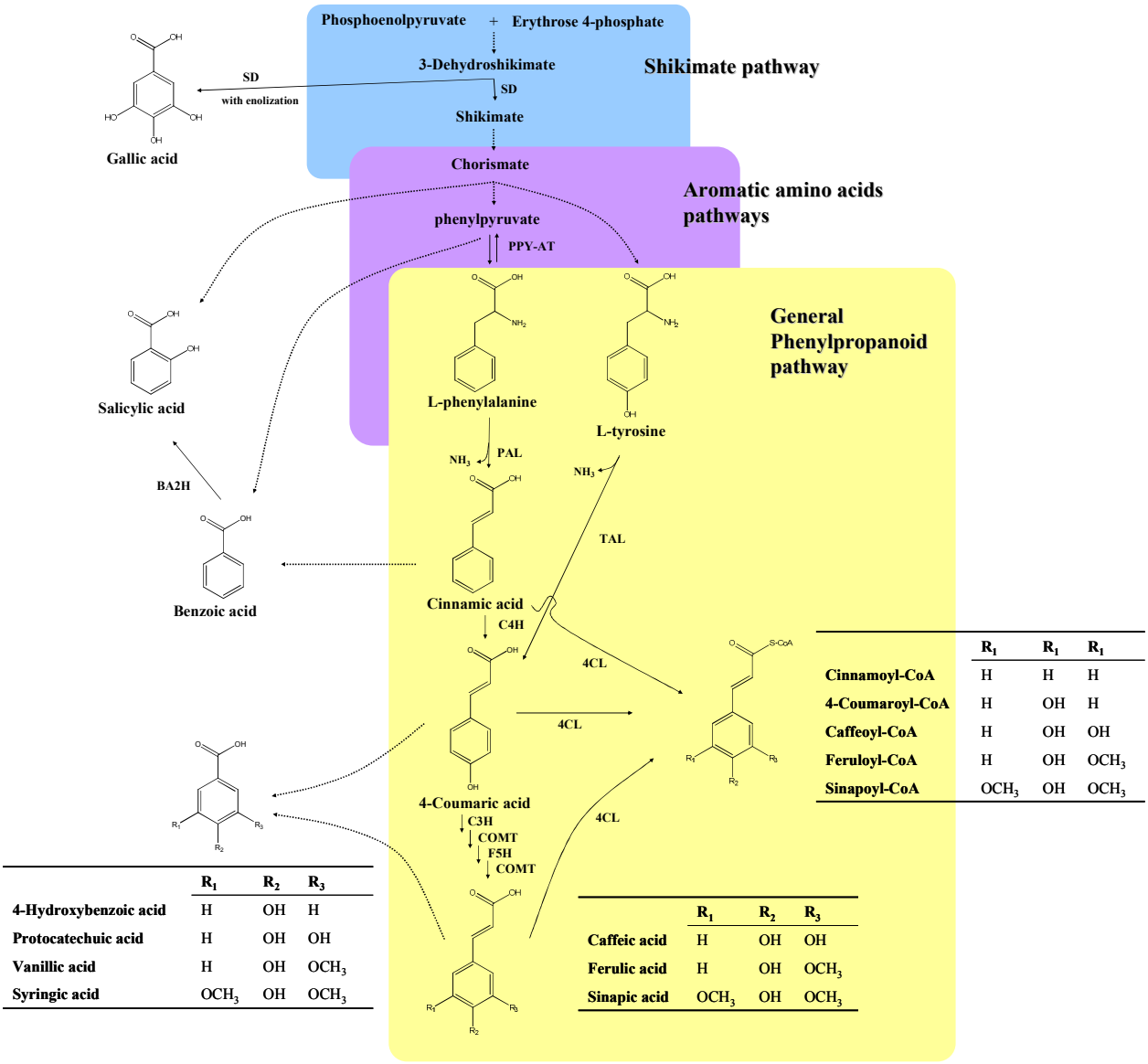

	R_1	R_2	R_3
4-Hydroxybenzoic acid	H	OH	H
Protocatechuic acid	H	OH	OH
Vanillic acid	H	OH	OCH_3
Syringic acid	OCH_3	OH	OCH_3

	R_1	R_2	R_3
Caffeic acid	H	OH	OH
Ferulic acid	H	OH	OCH_3
Sinapic acid	OCH_3	OH	OCH_3

	R_1	R_1	R_1
Cinnamoyl-CoA	H	H	H
4-Coumaroyl-CoA	H	OH	H
Caffeoyl-CoA	H	OH	OH
Feruloyl-CoA	H	OH	OCH_3
Sinapoyl-CoA	OCH_3	OH	OCH_3

Figure 4 General biosynthetic pathways of benzoic and cinnamic acid derivatives. Dotted lines represent multi-step reactions. Enzymes are described in Table 1. Figure adapted from [61,63,70,72,74].

L-phenylalanine is the principal precursor of the cinnamic acid derivatives. Phenylalanine ammonia-lyase (PAL), one of the most studied enzymes in plant metabolism, catalyzes the non-oxidative deamination of L-phenylalanine to *trans*-cinnamic acid. Cinnamic acid 4-hydroxylase (C4H) is a cytochrome P450 monooxygenase which catalyzes the hydroxylation of *trans*-cinnamic acid at C-4 position to yield 4-coumaric acid [75,76]. In some plant species, 4-coumaric acid may not only be synthesized from L-phenylalanine, but may also be synthesized directly from L-tyrosine by Tyrosine ammonia-lyase (TAL) [63,77]. 4-Coumaric acid can be hydroxylated by the action of the enzyme C3H to form caffeic acid, which can be methylated (enzyme COMT) to form ferulic acid, and this last acid can be hydroxylated and methylated (enzyme F5H and COMT, respectively) to produce sinapic acid [78]. The cinnamic acid as well as the cinnamic acid derivatives can be activated to form the corresponding Coenzyme A (CoA) thioester through a reaction catalyzed by 4-coumarate: CoA ligase (4CL). This enzyme accept several substrates, however 4-coumaric and caffeic acids are generally the preferred ones. This activation will facilitate further conversion to other secondary metabolites, as the flavonoids [40,78].

Concerning benzoic acid derivatives, generally they are formed by removal of a two-carbon fragment from the three-carbon side-chain of the correspondent cinnamic acid derivatives. For example, 4-hydroxybenzoic acid, protocatechuic acid, vanillic acid and syringic acid can be produced from the 4-coumaric acid, caffeic acid, ferulic acid and sinapic acid, respectively [79,62,70,38]. They can also be formed from 3-dehydroshikimate (intermediate product of the shikimate pathway), as the direct synthesis of gallic acid [80]; from chorismate that produces salicylic acid via isochorismate [81]; or from hydroxylations of benzoic acid [82]. Formation of benzoic acid, itself, can be performed from cinnamic acid, which also requires shortening of the C3 side chain by two carbons [83]. An alternative pathway could involve oxidative decarboxylation of phenylpyruvic acid to phenylacetic acid, followed by benzylic hydroxylation to produce a benzylic alcohol. Further oxidation and decarboxylation of this benzylic alcohol gives benzoic acid [38].

Table 1 Some enzymes directly or indirectly associated with biosynthesis of benzoic and cinnamic acid derivatives. Substrates and products of the reactions are presented in **Figure 4**.

Enzyme	Abbreviation	EC number
Shikimatedehydrogenase	SD	1.1.1.25
Phenylpyruvate aminotransferase	PPY-AT	2.6.1.5
Phenylalanine ammonia-lyase	PAL	4.3.1.5
Tyrosine ammonia-lyase	TAL	4.3.1
Cinnamate 4-hydroxylase	C4H	1.14.13.11
4-coumarate 3-hydroxylase	C3H	1.14.14.9
Caffeate *O*-methyltransferase	COMT	2.1.1.68
Ferulate 5-hydroxylase	F5H	1.14.-.-
4-Coumarate:CoA ligase	4CL	6.2.1.12
Benzoate 2-hydroxylase	BA2H	–

Both benzoic acid and cinnamic acid derivatives can be found in plants in different forms: free form, dimers, glycosylated, esterified to one or more hydroxyl groups of the sugar of flavonoid glycosides or esterified directly to a flavonoid hydroxyl, etc. In addition gallic acid and its dimer, the hexahydroxydiphenic acid, are constituents of hydrolyzable tannins [61,84–86].

1.2.3. Flavonoids

Flavonoids are formed out of the products of shikimate and acetate pathways. Main routes for biosynthesis of the principal flavonoid classes and proanthocyanidins in plants are shown in Figure 5. Flavonoids are synthetized from the condensation of a cinnamoyl-CoA thioester with 3 molecules of malonyl-CoA. The first element is the final product of the phenylpropanoid pathway (Figure 4). In most cases, the suitable CoA thioester is the 4-coumaroyl-CoA, but in a few species caffeoyl-CoA and feruloyl-CoA may also be used as substrates. On the other hand, one molecule of malonyl-CoA is produced from the acetyl-CoA by action of acetyl-CoA carboxylase (ACC) (Figure 5) [61,87]. Initially, the three sequential reactions of 4-coumaroyl-CoA with malonyl-CoA give a poly-β-keto chain intermediate, which according to the nature of the enzyme responsible, can be folded in two different ways, by aldol or Claisen reaction, e.g. the flavonoid naringenin chalcone is produced by Claisen reaction catalized by chalcone synthase (CHS) [62,88]. Chalcones are the precursor metabolites for the biosynthesis of compounds belonging to different classes of flavonoids. Stilbenes correspond to another class of phenolic compounds, biosynthetically close to the

flavonoids. The several enzymes associated with the flavonoid and proanthocyanidin biosynthesis (Figure 5) are presented in Table 2. Detailed information about the different enzymes and reactions shown in Figure 5 are discussed in several sources in the scientific literature, including books, reviews and papers [40,87,89–91].

Table 2 Principal enzymes associated with flavonoid biosynthesis. Substrates and products of the reactions are presented in **Figure 5**.

Enzyme	Abbreviation	EC number
Acetyl-CoA carboxylase	ACC	6.4.1.2
Chalcone synthase	CHS	2.3.1.74
Chalcone isomerase	CHI	5.5.1.6
Flavonoid 3'-hydroxylase	F3'H	1.14.13.21
Flavonoid 3',5'-hydroxylase	F3',5'H	1.14.13.88
Flavone synthase I	FNSI	1.14.11.22
Flavone synthase II	FNSII	1.14.13.-
Flavanone 3-hydroxylase	F3H	1.14.13.21
Flavonol synthase	FLS	1.14.11.23
Dihydroflavonol 4-reductase	DFR	1.1.1.219
Anthocyanidin synthase	ANS	1.14.11.19
Leucoanthocyanidin reductase	LAR	1.17.1.3
Anthocyanidin reductase	ANR	1.3.1.77

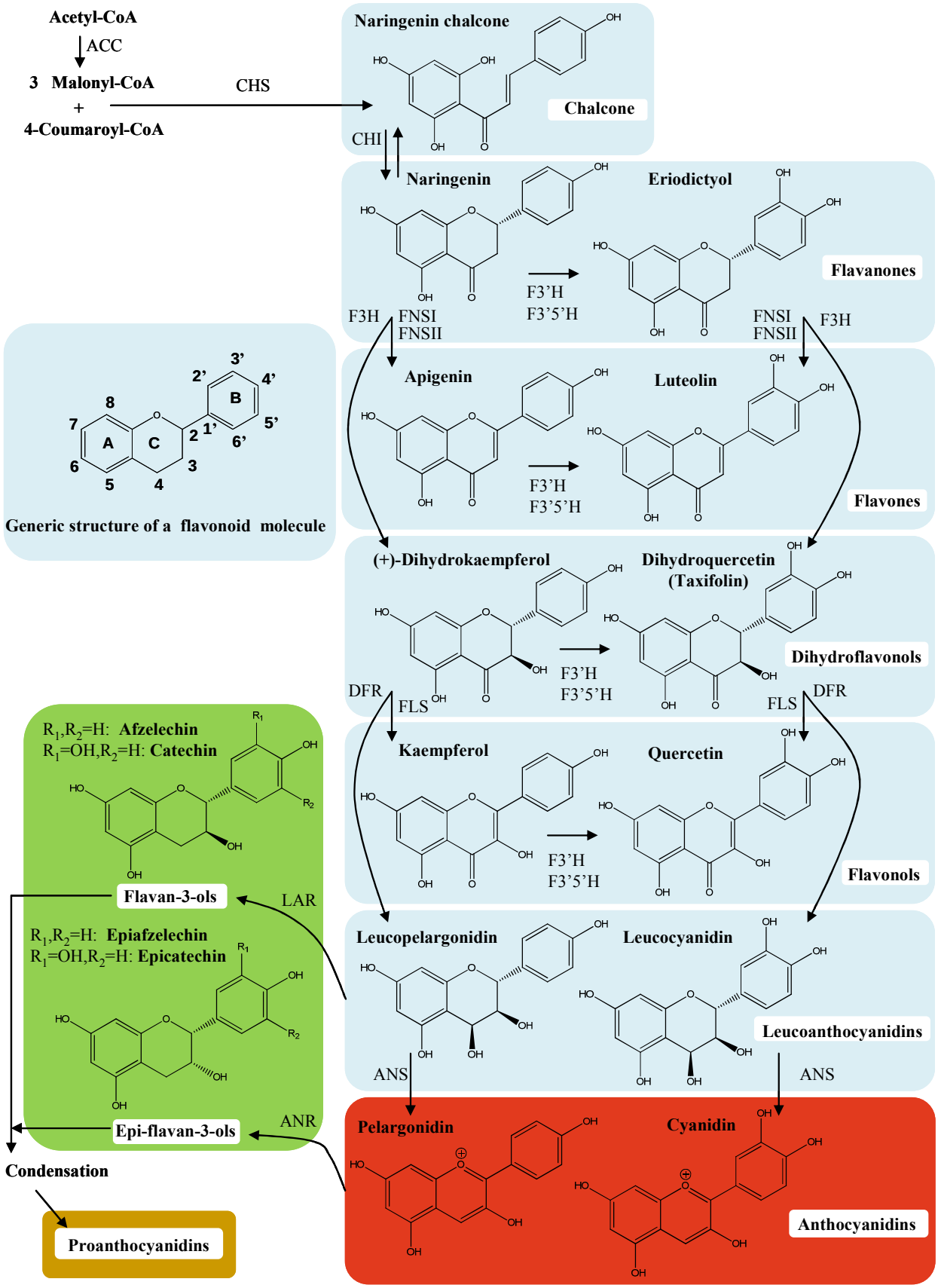

Figure 5 Principal routes for biosynthesis of flavonoids and proanthocyanidins, and generic molecular structure of flavonoids. For enzyme abbreviation definitions see Table 2. Figure adapted from [87,90–92].

The most common transformations that the aglycones can undergo are methylations, glycosylations and acylations. For glycosylation, the heteroside is more commonly glucose, arabinose and xylose. Sugars can be *O*-linked at the phenolic hydroxyl group, which is the case of *O*-glycosylation. In the case of diglycosylation in a same position, firstly a glycose unit is attached, followed by another one. Tri, tetra and pentaglycosylation are also observed [40,93]. When anthocyanidins are glycosylated they are called anthocyanins. Glycosylation can also be performed directly on the flavonoid skeleton by a C-C bond. It has been demonstrated for flavones that the *C*-glycosylation takes place as an early reaction during flavonoid biosynthesis [94,95]. Figure 6 shows a proposed biosynthesis pathway for *C*-glucosylflavones in plants. Finally, several aliphatic acids (e.g. acetic, malonic, lactic, etc.) and aromatic acids (e.g. 4-hydroxybenzoic, gallic, 4-coumaric, etc.) can be esterified to one or more hydroxyl groups of flavonoid glycosides or directly to a flavonoid hydroxyl [84].

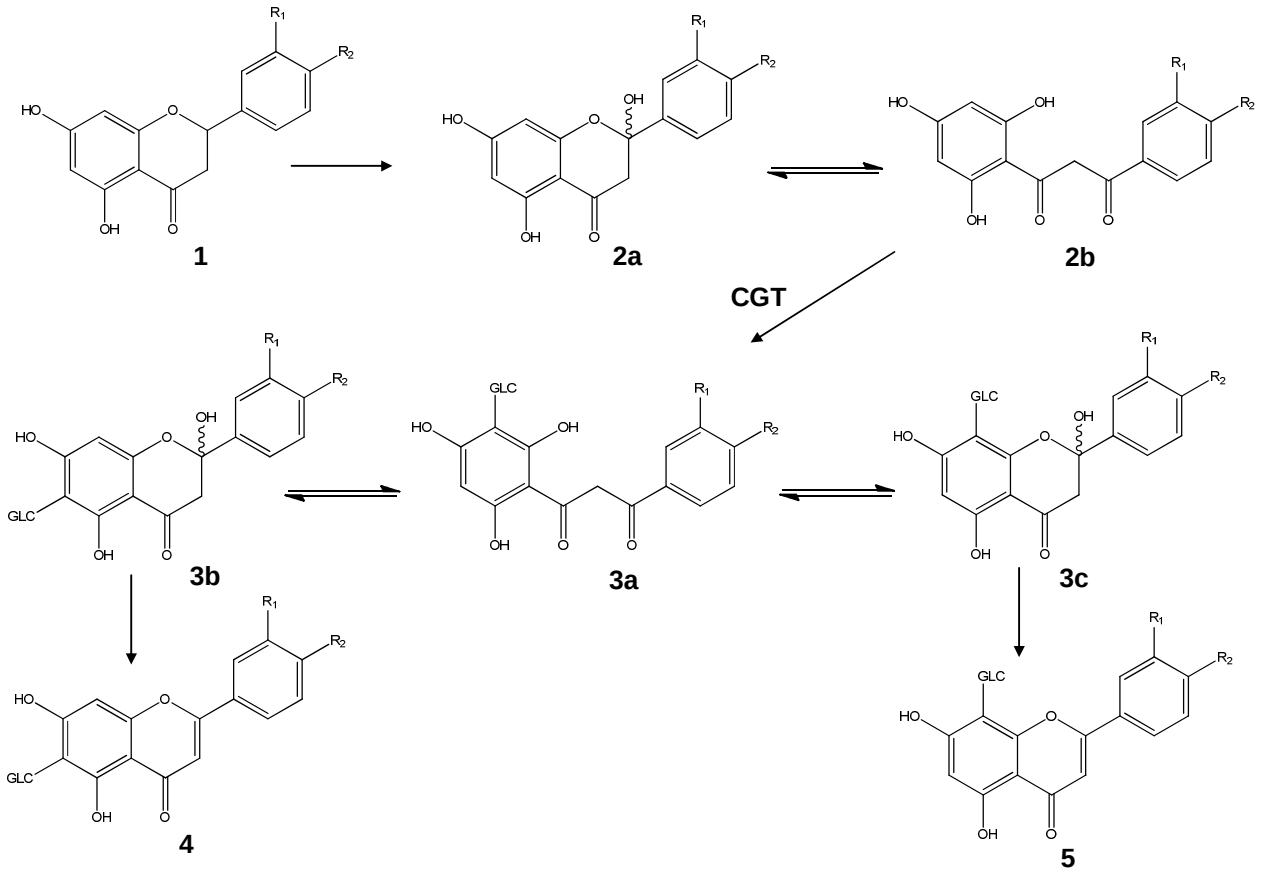

Figure 6 Biosynthesis pathway for *C*-glucosylflavones in plants. Flavanone (compound **1**) undergoes conversion to the 2-hydroxyflavanone (compound **2a**), which exists in equilibrium with its open-chain form (compound **2b**), the latter is transformed to 2-hydroxyflavanone *C*-glucosides (compounds **3**, **a–c**) by the action of the *C*-glucosyltransferase (CGT). These are then dehydrated to yield the flavone-6*C*-glucoside (compound **4**) and flavone-8*C*-glucoside (compound **5**). Figure adapted from [94,95].

Flavonoids are low molecular weight compounds, consisting of fifteen carbon atoms, arranged in a C6–C3–C6 configuration. Essentially, the structure consists of two aromatic rings A and B, joined by a 3-carbon bridge, usually in the form of a heterocyclic ring C (Figure 5). Variations in substitution patterns to ring C result in the major flavonoid classes. Among the many classes of flavonoids, those of particular interest to this work are flavanones, flavones, flavonols, dihydroflavonols, flavan-3-ols and anthocyanidins. Substitutions to rings A and B give rise to the different compounds within each class of flavonoids. These substitutions may include oxygenation, alkylation, glycosylation, acylation, and sulfatation [96]. Important characteristics of some flavonoid classes are given below.

Flavanones are characterized by having a saturated C−ring and the C4 carbonyl group. Flavones differ from flavanones in having a double bond between carbons C2 and C3. Additionally in both classes there is no substituent at C3. Flavonols differ from flavones by their hydroxyl group at C3. Dihydroflavonols constitute a related class that differs in lacking the double bond between C2 and C3. Flavan-3-ols have also a hydroxyl group at the C3 position and lack the C4 carbonyl. Finally, anthocyanidins differ from the other flavonoids mainly by possessing a charged oxygen atom in the C ring [97]. These compounds and their glycosylated forms, the anthocyanins, can be found in different chemical forms in equilibrium which depend on the pH of the solution [98–100], as shown in Figure 7. At pH < 2, the flavylium cation is the predominant and stable form and contributes to purple and red colours (Figure 7A). At pH values between 2 and 4, the quinoidal blue species are predominant (Figure 7B–D). At pH values between 5 and 6 two colourless species can be observed, which are a carbinol pseudobase (Figure 7E) and a chalcone (Figure 7F), respectively. At pH values higher than 7, the anthocyanins are degraded depending on their substituent groups.

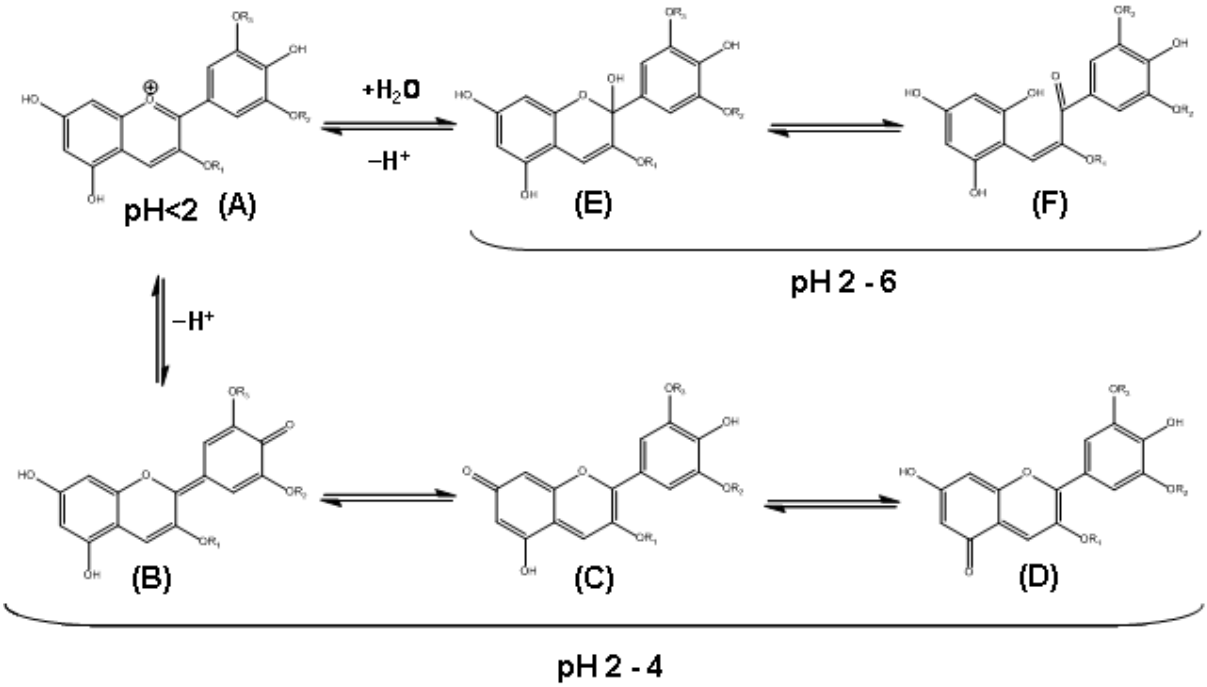

Figure 7 Predominant chemical forms of anthocyanin depending on pH. Where R1 = H or saccharide, R2 and R3 = H or Methyl. A: flavylium, B-D: quinoidal, E: pseudobase, and F: chalcone forms [100].

1.2.4. Bioavailability of phenolic compounds

Phenolic compounds are naturally occurring compounds widespread in plant-derived foodstuffs and therefore abundant in our diet. There are evidences regarding the positive association of their intake with healthy biological effects displayed *in vivo*. This section will review the recent advances on the absorption, bioavailability, biotransformation and elimination of these compounds and their metabolites.

Some studies demonstrated a polyphenol absorption in the oral cavity. In a recent work, black raspberry anthocyanins could be detected in their hydrolysed aglycone form (anthocyanidins) in the oral cavity, resulting from the activity of *β*-glycosidase derived from both bacteria and oral epithelial cells [101]. In this same study, parent anthocyanins and protocatechuic acid, a metabolite of cyanidin-3-glucoside, were detected in the saliva. Furthermore, saliva samples revealed the presence of glucuronidated anthocyanin conjugates, consistent with intracellular uptake and phase II metabolism of anthocyanins. Another study also demonstrated that flavonoid glucosides, such as quercetin 4'-glucoside and genistein 7-glucoside can be hydrolyzed in the oral cavity by both bacteria and epithelial cells to deliver the aglycones at the surface of the epithelial cells [102]. The importance of these oral

transformation reactions for local biological effects in the oral epithelium is difficult to assess considering the relatively short residence time of most foods in the oral cavity [103].

At the gastric level, Talavéra et al. [104] demonstrated that a high proportion (approximately 25%) of anthocyanin monoglycosides, including cyanidin 3-glucoside, and in their flavylium cation form, were absorbed from the stomach in rats, whereas absorption of cyanidin 3-rutinoside was lower (approximately 8%). They also showed that cyanidin 3-glucoside was rapidly excreted into the bile as intact and metabolized forms. Analysis of bile samples revealed that cyanidin 3-glucoside appeared in bile after as little as 20 min after in situ gastric administration. Peonidin 3-glucoside (the methylated form of cyanidin 3-glycoside) as well as other unknown anthocyanin metabolites were also observed in bile. Felgines et al. [105] examined the gastric absorption of pelargonidin-3-glucoside using rat models. Once more, a high proportion of this anthocyanin monoglycoside was found to be rapidly absorbed from the stomach (23%). From these studies, it appears that anthocyanins (mainly monoglycosides) are absorbed in high proportions in the stomach and reach the systemic circulation in their native or metabolized forms, being available to exert their biological activities approximately 30 min after ingestion. There are also a few references concerning the gastric absorption of flavonoid aglycones. Quercetin, but not quercetin 3-*O*-glucoside nor quercetin 3-*O*-rutinoside, was found to be absorbed in rat stomach [106]. Additionally, some phenolic acids were also found to be absorbed at the gastric epithelium [107].

The mechanism of phenolic compound gastric absorption remains unknown. Some transporter candidates may include GLUT1, OAT2, SMCT1 and SMCT2, since the expression of these transporters has already been detected in stomach tissue [108–110]

Regarding intestinal absorption, flavonoids (aglycones and glycosides) are typically absorbed in the small and large intestine. The absorption of flavonoid glycosides, as illustrated in Figure 11, is associated with sugar cleavage and release of the aglycone as a result of the action of lactase phlorizin hydrolase (LPH) in the brush border of the small intestine epithelial cells. The released aglycone may then enter the epithelial cells by passive diffusion as a result of its increased lipophilicity and its proximity to the cellular membrane [111]. An alternative hydrolytic step is mediated by a cytosolic *β*-glucosidase (CBG) within the epithelial cells. For CBG-catalyzed hydrolysis to occur, the polar glucosides must be transported into the epithelial cells, possibly with the involvement of the active sodium-dependent glucose transporter 1 (SGLT1) [112] and the glucose transporter 2 (GLUT2) [113].

Thus, there are two possible routes by which the glycoside conjugates are hydrolyzed, and the resultant aglycones appear in the epithelial cells, namely LPH/ diffusion and transport/CBG (Figure 11). The flavonoid glycosides into the enterocyte can also be transported to the blood stream by action of GLUT2, or back into the lumen of the small intestine by action of the multidrug resistance protein (MRP) 1 or 2 (Figure 11).

Before going into the blood stream, the aglycones can undergo some degree of phase II metabolism forming sulfate, glucuronide, and/or methylated metabolites through the respective action of sulfotransferases (SULTs), uridine-5'-diphosphate glucuronosyltransferases (UGT), and catechol-*O*-methyltransferases (COMTs). There is also efflux of some of the metabolites back into the lumen of the small intestine, and this is thought to involve MRP1 or MRP2 (Figure 11). The MRP3 and the GLUT2 have also been implicated in the efflux of metabolites from the basolateral membrane of the enterocytes [114,115]. Once in the portal bloodstream, metabolites rapidly reach the liver, where they can be subjected to further phase II metabolism, and enterohepatic recirculation may result in some recycling back to the small intestine through bile excretion [116].

The anthocyanins, mainly in their carbinol pseudobase form (predominant form in the basic condition of the small intestine) are also absorbed in the small intestine [117]. Their potential mechanisms of absorption may involve the GLUT2 and SGLT1 transporters. They can also be hydrolyzed by brush border enzymes, such as LPH, prior to passive diffusion of the aglycone [103].

(Poly)phenol conjugates with sugar moieties that did not undergo the action of LPH/CBG are not absorbed in the small intestine and pass to the colon. Analysis of ileal fluid after the ingestion of various foodstuffs has shown that even when dietary (poly)phenols are absorbed in the proximal gastrointestinal tract, substantial quantities nonetheless pass from the small to the large intestine [118], where the colonic microbiota cleave conjugating moieties, and the resultant aglycones undergo ring fission leading to the production of smaller molecules, including phenolic acids and hydroxycinnamates. These can be absorbed and may be subjected to metabolism in the liver before being excreted in urine [119].

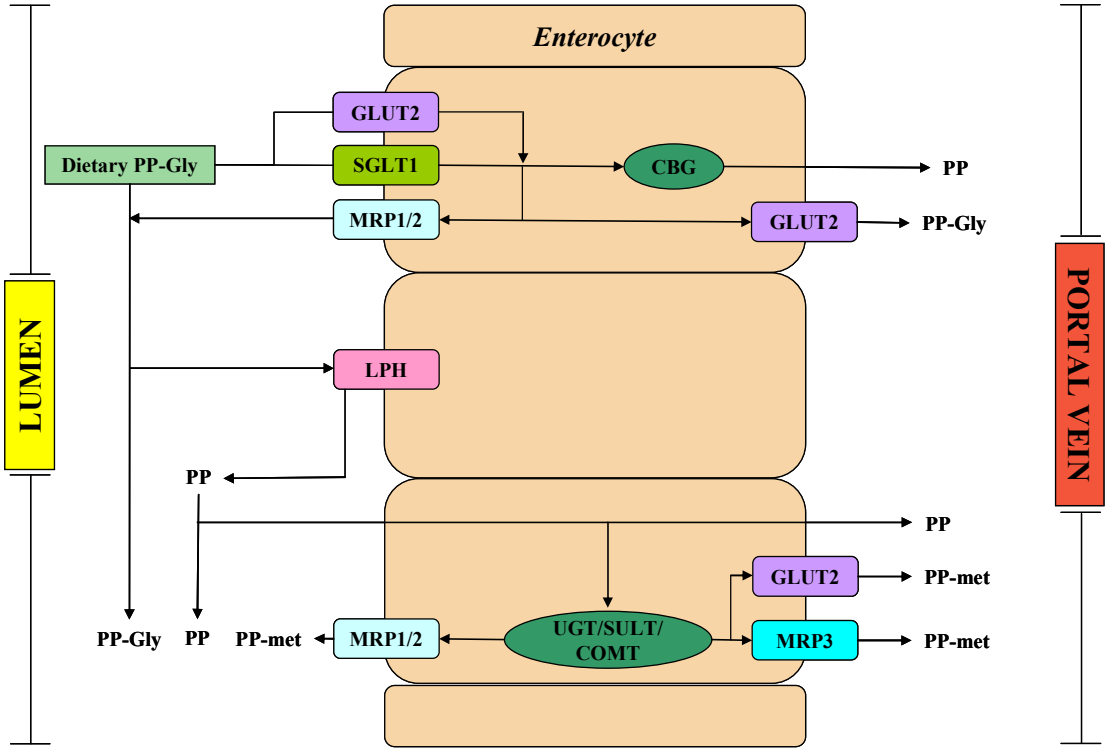

Figure 11 Proposed mechanisms for the absorption and metabolism of (poly)phenolic compounds in the small intestine. CBG, cytosolic *β*-glucosidase; COMT, catechol-*O*-methyl transferase; GLUT2, glucose transporter; LPH, lactase phlorizin hydrolase; MRP1-2–3, multidrug-resistant proteins; PP, (poly)phenol aglycone; PP-gly, (poly)phenol glycoside, PP-met, polyphenol sulfate/glucuronide/methyl metabolites; SGLT1, sodium dependent glucose transporter; SULT, sulfotransferase; UGT, uridine-5'-diphosphate glucuronosyltransferase [120].

Concerning tissue distribution of phenolic compounds, intact anthocyanins were detected in liver, eye, cortex, and cerebellum in pigs after ingestion of blueberries for 4 weeks. The results suggest that anthocyanins can accumulate in tissues, including tissues beyond the blood–brain barrier [121]. In a more recent work, proportions of anthocyanin derivatives (methylated anthocyanins and glucurono-conjugated derivatives) were identified in various organs (bladder, prostate, testes, heart, and adipose tissue) in rats fed with a blackberry anthocyanin-enriched diet for 12 days [122]

Non-anthocyanin flavonoids, such as quercetin, can also accumulate in brain tissue [123]. Others, like (−)-epigallocatechin gallate and its metabolites were detected in lungs, heart, liver, spleen, pancreas, kidney, brain, bone, bladder and skin in mice [124]. Finally, catechins cross the placenta and reach the foetal organs in rats (~ nM concentration) 0.5−1 hour after the mother received the dose [125].

In a pharmacokinetic perspective, in human studies, a recent review [126] discusses pharmacokinetic data of several classes of phenolic compounds, including anthocyanins, flavonols, flavones, flavanones, flavan-3-ols and isoflavones. In this review, some phenolic compounds exhibit rapid absorption and appearance in plasma, e.g., t_{max} (time for maximum plasma concentration to appear) were the fastest for anthocyanins, for which they ranged from 0.5 hours [127] to 2.2 hours [128]. On the other hand, other compounds show slow absorption, e.g., t_{max} of isoflavones were the slowest. They ranged between 2.5 and 11 hours [129]. The values of C_{max} (maximal plasma concentration (peak) after single dose oral ingestion) ranged from 0.56 nM for anthocyanins (after ingestion of a juice containing 94 mg of anthocyaninis) [130] to 25.4 μM for isoflavones (after ingestion of purified isoflavones in a dose of 25 mg/kg)[129]. However, nM concentrations were predominant considering all the classes of phenolic compounds reviewed. The $t_{1/2}$ (elimination half-life) values ranged from 0.42 hours (for flavan-3-ols) [131] to 28.1 hours (for flavonols) [132].

Flavonoid bioavailability is very low, due to extensive metabolism at the intestinal level and low overall permeability. However, the low bioavailability of phenolic compounds must not be confused with low bioactivity. Recent studies suggest that some of the flavonoid metabolites also have the potential to possess similar pharmacodynamics as the parent compound [133]. Moreover, a given flavonoid could have opposite, additive, or synergistic effects with its metabolites; therefore, the bioactivity observed in *in vivo* settings depends on the particular phenolic profile. The synergistic bioactivity of multiple flavonoids, as found in food matrices, is also important. For instance, the antiproliferative activity in vascular smooth muscle cells of four red wine polyphenols, i.e., resveratrol, quercetin, ethyl gallate and (+)-catechin, was stronger than the predicted additive activity of each individual substance [134].

Moreover, low concentrations of flavonoids (in the physiological range: nM and μM concentrations) can affect the expression of genes involved in vascular aging. For instance, treatment of cultured human umbilical vein endothelial cells with ferulic acid, quercetin or resveratrol (in 0.1 μM concentration) resulted in down-regulation (> 2-fold) of 363 genes and up-regulation (> 2-fold) of 233 genes. [135]. Furthermore, cellular antioxidant activity assay showed that both monomeric cyanidin 3-glucoside and a mixture of 15 bilberry anthocyanins [136,137] have strong intracellular antioxidant activity in the low concentration range (nM), which correlates with the typical human plasma concentrations. The effects of polyphenols at physiological concentrations along with the possibility of synergistic activities suggests an explanation for several epidemiological observations whereby dietary flavonoids, even if

present in low concentrations (nM range) in plasma, display health-protective properties [138–140] .

1.2.5. Antioxidant properties of phenolic compounds

In the last decades, phenolic compounds have attracted much interest because of their association with the prevention of cardiovascular and neurodegenerative diseases, by acting as antioxidants [141,142]. This interest was improved by the discovery of the so-called ‘‘French Paradox”, i.e. the observation that although the French people have smoking tendency and a fat rich diet, they show much reduced rates of coronary heart diseases when compared with northern European nations such as UK and Germany [143]. This has been partially explained by the French high consumption of red wines, which are rich in phenolic compounds [144].

The best described property of phenolics is the antioxidant activity towards free radicals and reactive oxygen species (ROS), which are chemically reactive molecules containing oxygen and comprising free radical and non-free radical species. They are normally produced by cell metabolism or in response to external factors, such as pollutants, tobacco, smoke, drugs, etc [145]. These species can damage biomolecules such as lipids, nucleic acids, proteins, cause cellular membrane peroxidation, and attract various inflammatory mediators [146,147]. Polyphenols scavenge free radicals that are in turn made inactive [148].

Phenolic compounds have been reported to have several other activities, such as antinflammatory, antiallergic, antiviral, etc. Flavonoids also demonstrated chemopreventive or antitumor effects, whose mechanisms seem to depend on their structure, each compound displaying various biological potency and mechanism(s) of action [149]. However, the essential feature of flavonoids is their free radical scavenging activity, partially responsible for these antitumor effects [150].

The molecular basis for the antioxidant properties of polyphenols is recognised into three main mechanisms, arising from the direct reaction with free radicals and from the chelation of free metals, which are involved in reactions that generate free radicals [145], but they can also inhibit prooxidant enzymes, associated with the production of ROS, such as xanthine oxidase. Flavonoids, in particular quercetin and luteolin, are potent inhibitors of xanthine oxidase, which is implicated in oxidative injury, as it reacts with molecular oxygen and releases superoxide [151].

Polyphenols inactivate free radicals by a hydrogen atom transfer (Figure 8A) or a single electron transfer mechanism (Figure 8B). In the first transfer mechanism, the antioxidant polyphenol, ArOH, reacts with the free radical, $R^{\bullet}$, by transferring a hydrogen atom, through homolytic rupture of the O–H bond. The products of the reaction are the harmless RH species and the oxidised $ArO^{\bullet}$ radical, which is less reactive with respect to $R^{\bullet}$. In the single electron transfer mechanism, an electron is donated to $R^{\bullet}$. The anion R^{-} is an energetically stable species with an even number of electrons, while the cation radical $ArOH^{+\bullet}$ is also in this case a less reactive radical species. The $ArO^{\bullet}$ and $ArOH^{+\bullet}$ are aromatic structures in which the odd electron, originated by the reactions with the free radical, has the possibility to be spread over the molecule, resulting into a radical stabilization.

Chelation of transition metals is another antioxidant mechanism that arises from the possibility that transition metal ions (M^{n+}) may be chelated by polyphenols, leading to stable complexed compounds [145]. Flavonoids with their multiple hydroxyl groups and the carbonyl group at the 4 position on ring C (Figure 8C) may offer several available sites for metal complexation.

Some metals in their low oxidation state (mainly Fe^{2+}) may be involved in Fenton reactions with hydrogen peroxide [152], from which $OH^{\bullet}$ is formed:

$$H_2O_2 + M^{n+} \rightarrow HO^{-} + HO^{\bullet} + M^{(n+1)+}$$

The $OH^{\bullet}$ is generally accepted to be one of the most reactive radicals. It has a very short half-life (around 10^{-9} s) and a very high reactivity. This hydroxyl radical cannot be eliminated by enzymatic reactions, in contrast to hydroperoxides that are metabolized by catalase and glutathione peroxidase. Transition metals like copper, manganese, and cobalt are able to catalyse the above mentioned reaction, when these metal ions are not bound to proteins or chelators. Fenton-like reaction may take place and cause site specific accumulation of free radicals and initiate biomolecule damage processes [145]. Fenton reactions can occur in dopaminergic neurons of the nervous tissue, where normally dopamine catabolism produces some levels of hydrogen peroxide. The accumulation of free radicals in these neurons may be recognised as the main aetiological agent of Parkinson disease [152].

A. Hydrogen Atom Transfer

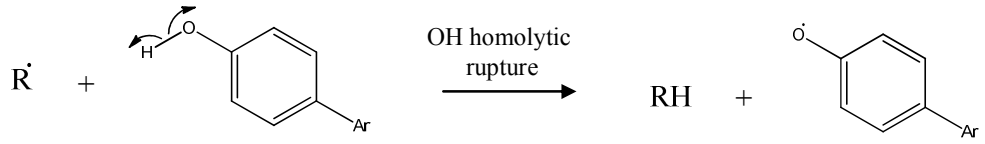

B. Single Electron Transfer

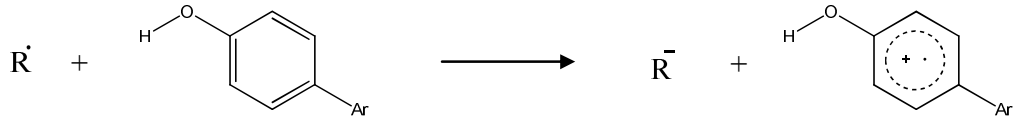

C. Transition Metals Chelation

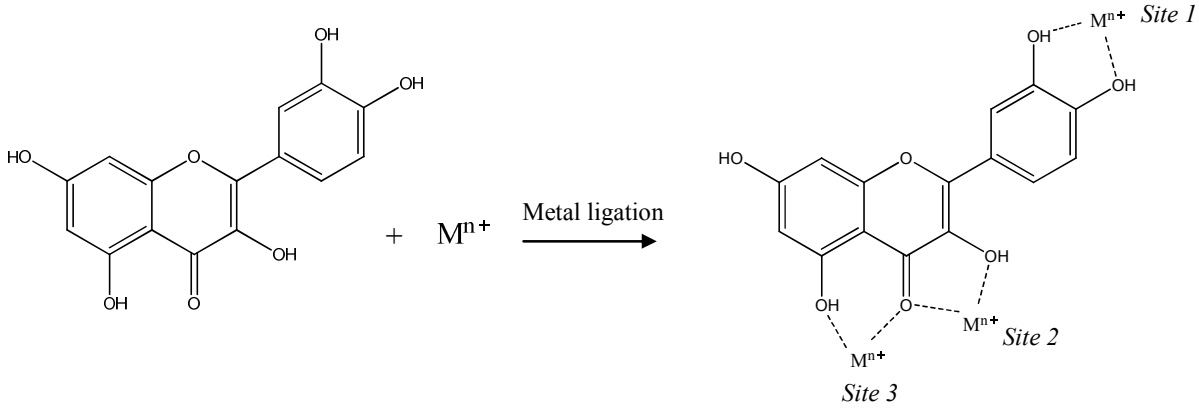

Figure 8 Main mechanisms for the antioxidant activity of phenolic compounds.

In the literature, the *in vitro* antioxidant activity of juice and extracts derived from açai were mainly measured by the ORAC method (oxygen radical absorbance capacity). The mechanism of the test is based on the degradation of fluorescein (a fluorescent substrate) by peroxyl radicals produced by the thermal decomposition of the 2,2'-azobis(2-amidinopropane) dihydrochloride (AAPH) in aqueous phase [153]. The presence of an antioxidant compound inactives peroxyl radicals, pretecting the fluorescein. Thus, the more effective the antioxidant, the lower the observed decrease of the fluorescence. These reactions occur in particular conditions: temperature of 37°C and serum pH of 7.4 [154].

In the ORAC assay, the difference between the area under the fluorescence decay curves obtained in the presence and absence of an antioxidant is measured for the quantification (Figure 9) and accounts for all the phases of the kinetic curve in a single value. This is an advantage in relation to other similar methods (e.g., the total radical trapping antioxidant

parameter (TRAP*)), because this helps to avoid an underestimation of antioxidant activity and to account for potential effects of secondary antioxidant products. Additionally, the ORAC method is considered as a reference method, used by food industries [155]

The ORAC values are reported in equivalent of trolox (6-hydroxy-2,5,7,8-tetramethylchroman-2-carboxylic acid) which is the water-soluble analog of vitamin E.

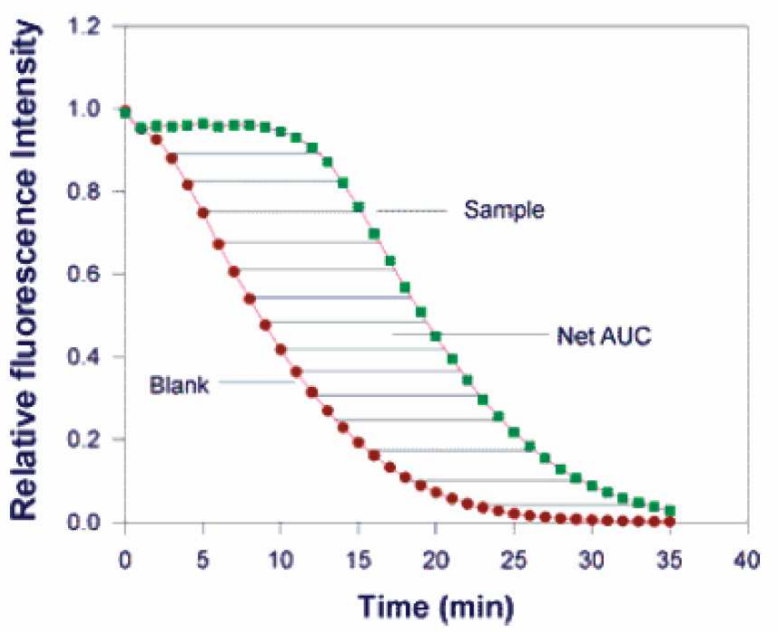

Figure 9 Antioxidant activity of a sample measured by the ORAC method from the net area under the curve (Net AUC) [155].

1.2.6. Anti-inflammatory properties of phenolic compounds

Inflammation is an orchestrated biological process, induced by microbial infection or tissue injury. A major trigger of inflammation is the recognition of microbes by specific receptors of the innate immune system, which play a crucial role in the induction of early signals initiating and establishing the inflammatory setting [156]. A main function of inflammation is to resolve infection and to repair the damage in order to achieve homeostasis equilibrium. Thus, the ideal inflammatory response is rapid and destructive, yet specific and self-limiting [157]. Inflammation and the immune system are intimately tied. Indeed, an over

* TRAP assay. This method is based on the oxygen uptake associated to the peroxidation process of human plasma. The method evaluates the induction period (lag time), generated in the kinetic profiles of oxygen uptake during the incubation of human plasma with AAPH (a peroxyl radical generator).

activation of innate immune response can cause chronic infection or chronic inflammation due to an inefficient regulation or resolution of the inflammatory response [158]. In addition, inflammation is increasingly found to be involved in the development of several chronic diseases such as arteriosclerosis, obesity, diabetes, neurodegenerative diseases and even cancer [159].

Many investigations have shown that a variety of flavonoid molecules exhibit anti-inflammatory activity both, *in vitro* and in various animal models of inflammation [160,161]. The most important are described here.

Several mechanisms explaining the anti-inflammatory activity of flavonoids have been described, including (a) regulation of cellular activities of inflammation-related cells, (b) modulation of the activities of arachidonic acid metabolism enzymes (phospholipase A2, cyclooxygenase, lipoxygenase) and nitric oxide synthase, (c) modulation of the production of other proinflammatory molecules, (d) modulation of proinflammatory gene expression.

a) Modulation of inflammatory related cell functions

The immune system is integrated by a highly complex regulated group of cells that may interact in a cell–cell manner and may also respond to intercellular messages including hormones, cytokines and autacoids. The immune response can be modified by diet, pharmacological agents, environmental pollutants, and naturally occurring food chemicals such as vitamins and flavonoids [162–164]. Some flavonoids display a remarkable array of biochemical and pharmacological actions that affect the function of immune and inflammatory cells such as T cells, B cells, macrophages, neutrophils, mast cells, or basophils [165].

Several flavonoids specifically affect enzyme systems critically involved in the generation of inflammatory processes, especially tyrosine and serine-threonine protein kinases. These enzymes are involved in signaling transduction and cell activation processes such as T cell proliferation [166], B lymphocyte activation [167] or cytokine production by stimulated monocytes [168].

They also exhibit an effect on secretory processes of inflammatory cells. Thus, Bennett et al. [169] have shown that several flavonoids were capable of inhibiting stimulated rabbit neutrophil lysosomal enzyme release. In other studies, quercetin impaired secretion of lysosomal enzyme from human polymorphonuclear leukocytes induced by concanavalin A

[170]. Quercetin also inhibited human neutrophil degranulation as well as catalytic activity of the released elastase [171].

b) Modulation of proinflammatory enzyme activities

Many investigations have shown that different flavonoid molecules modulate the activity of arachidonic acid (AA) metabolizing enzymes such as phospholipase A2 (PLA2) [172,173], cyclooxygenase (COX) and lipoxygenase (LOX) [174] and the nitric oxide (NO) producing enzyme, nitric oxide synthase (NOS) [175,176]. The inhibition of these enzymes reduces the production of AA, prostaglandins, leucotrienes, and NO, which are crucial mediators of inflammation. Thus, the inhibition of these enzymes by flavonoids may be one of the most important mechanisms for their anti-inflammatory activity.

c) Modulation of the production of other proinflammatory molecules

Several cytokines are deeply associated with inflammatory diseases. In particular, tumor necrosis factor-α (TNF-α), interleukin-6 (IL-6) and IL-1b are prominent contributors to chronic inflammatory responses. Genistein was reported to inhibit IL-1b, IL-6 and TNF-α production at a concentration of 37 μM in LPS-induced human blood monocytes [168]. The inhibitory effect of genistein on IL-6 production has been shown in different settings: cultured human intestinal cells Caco-2 [177], osteoblast cells [178], and human gastric epithelial cells [179]. In these studies the the inhibitory effects were observed in the range between 10 and 50 μM. In another work, pretreatment of RAW 264.7 with luteolin, luteolin-7-glucoside, quercetin, and genistein inhibited both the LPS-stimulated TNF-α and IL-6 release, whereas eriodictyol and hesperetin only inhibited TNF-α release. From the compounds tested luteolin and quercetin were the most potent in inhibiting cytokine production with an IC_{50} of less than 1 and 5 μM for TNF-α release, respectively [180].

The comparison of molecular structures from different flavonoids shows that the presence of a double bond at position C2–C3 of the C ring with oxo function at position 4, along with the presence of OH groups at positions 3’ and 4’ of the B ring, are required for optimal inhibition of LPS stimulated TNF-α release [180].

d) Modulation of proinflammatory gene expression

Several lines of evidence have supported the idea that certain flavonoids are modulators of proinflammatory gene expression, thus leading to the attenuation of the inflammatory response. The mechanisms by which flavonoids block proinflammatory gene expression involve an effect on transcriptional activity suppression in response to inflammatory stimuli [181].

Flavonoids inhibiting COX-2 activity are rarely reported, but some studies have demonstrated an effect on suppression of COX-2 expression. Thus, apigenin, genistein, and kaempferol inhibited COX-2 induction in LPS-stimulated macrophages (IC_{50} < 15 μM) [182]. Other experiments using the gene-reporter assay to express COX-2 showed that some flavones and flavonols were effective suppressors (IC_{50} range = 10.5 − 52.5) in human colon cancer DLD-1 cells [183]. Luteolin decreases protein and mRNA levels of the proinflammatory iNOS and COX-2 at a concentration of 25 μM in LPS-stimulated macrophages [184].

Several studies have shown that some flavonoids inhibit NO production in response to inflammatory stimuli [185,186]. Hämäläinen et al. [187] compared the effects of a series of compounds on NO production in activated macrophages. The flavonoid classes containing the most effective compounds were isoflavones and flavonols. They identified eight compounds as being able to inhibit LPS-induced iNOS expression at a concentration range between 30 and 100 μM: flavone, daidzein, genistein, isorhamnetin, kaempferol, quercetin, naringenin and pelargonidin.

Cellular mechanisms of flavonoids modulating gene expression have been actively studied. The most prominent keys of cellular regulation affected by flavonoids are the various protein kinases involved in signal transduction including protein kinase C (PKC) and mitogen-activated protein kinase (MAPK). Through the inhibition of these enzymes, DNA-binding capacity of transcription factors such as nuclear factor-kappa B (NF-κB) or activator protein-1 (AP-1) is regulated, and the expression rate of the gene target is controlled [188].

Mitogen-activated protein kinases (MAPKs) are a family of serine/threonine kinases, which connect inflammatory and other extracellular signals to intracellular responses, such as gene expression. The three better characterized MAPKs are extracellular signal-regulated kinase 1 and 2 (Erk1/2), p38, and c-Jun N-terminal kinase (JNK) [189].

Inhibition of MAPKs is likely to result in a suppression of inflammatory mediators and these kinases may be targets for anti-inflammatory approaches. Xagorari et al. [190] have shown that the exposure of RAW 264.7 macrophages to LPS caused phosphorylation of ERK1/2, p38 and JNK pathways, and pretreatment of cells with luteolin at a concentration of 10μM abolished the LPS-induced stimulation of ERK1/2 and p38, but not JNK phosphorylation. Simultaneous inhibition of the two pathways results in drastic reduction of TNF-α release in macrophages [190]. Similar results have been obtained with quercetin, which inhibited ERK and p38 activation in concentration range between 50 and 200 μM on LPS-stimulated RAW 264.7 cells, but not JNK activation [191].

Another control point of gene expression is the NF-κB transcriptional system, which is a major effector pathway involved in inflammation and innate immune responses. Many genes that are implicated in the initiation of inflammatory responses are regulated at the level of transcription by NF-κB. Activation of this nuclear factor is regulated by its endogenous inhibitor IκB, which complexes and sequesters NF-κB in the cytoplasm. Following stimulation, the successive activation of various kinases leads to the phosphorylation and degradation of IκB and subsequent release of NF-κB, which then translocates to the nucleus and activates the transcription of multiple genes, including TNF-α, IL-6, IL-8, and other chemokines, ICAM-1, iNOS, COX-2, etc. [192]. Several flavonoids have been shown to downregulate the production of inflammatory mediators through the blockade of NF-κB pathway at different levels.

In this context, luteolin has shown potent anti-inflammatory properties by inhibiting LPS-induced proinflammatory molecule expression both *in vitro* [193] and *in vivo* [194]. The molecular mechanisms of luteolin mediated immunomodulation have been studied in different cellular lines. In murine macrophages RAW 264.7, luteolin inhibits gene expression and proinflammatory cytokine production at a concentration of 1μM by blocking protein tyrosine phosphorylation and NF-κB activation [180]. It has been reported in mouse alveolar macrophages that luteolin inhibits LPS-induced inflammatory reactions, at a concentration of 25 μM, by blocking the NF-κB and AP-1 activation pathways [184]. Another study demonstrated that genistein, kaempferol, quercetin, daidzein inhibited both NF-κB and STAT-1 activation at a concentration range between 30 and 100 μM, in activated macrophages [187].

1.2.7. Health benefits of phenolic compounds

Phenolic compounds have been positively associated with several diseases, mainly due to their antioxidant and anti-inflammatory properties discussed in the previous sections. Among these diseases, cardiovascular diseases (CVD) and cancer are the main causes of mortality in many countries [195,196], and neurodegenerative diseases represent an increasing problem in our aging societies, as there is an increase prevalence of these diseases with age [197]. In this section, the health benefits of these compounds related to cancer, cardiovascular (CVD) and neurodegenerative diseases will be discussed. This section is not an exhaustive review, but a series of recent publications related to each disease are mentioned.

1.2.7.1. Polyphenols and cancer

Cancer is a hyperproliferative disorder that involves morphological cellular transformation, dysregulation of apoptosis, uncontrolled cellular proliferation, invasion, angiogenesis, and metastasis [198]. Indeed, the unbalanced control of cellular proliferation is a primary characteristic of cancer cells and, as such, any molecule capable of inhibiting transformation of normal cell to cancer cell, may be useful as a potential chemopreventive agent [199]. Plant foods contain a wide variety of phytochemicals with potential bioactivities that may contribute to the prevention of cancer. Among then, flavonoids are especially promising candidates [200]. Recently, several cohort investigations have shown an inverse association between fruits and vegetables consumption and the risk of development of various types of cancer [138,201]. An 8-year study by cancer researchers found that the consumption of a diet rich in three flavonols, kaempferol, myricetin, and quercetin, as well as catechin, a flavan-3-ol, resulted in a 23% reduced risk of developing pancreatic cancer [202].

In addition to their chemopreventive activities, polyphenols were also shown to have a direct toxicity or antiproliferative effects on cancer cells. Several *in vitro* studies demonstrated that polyphenols can interfere in the modulation of cancer cell signaling [203] and cell cycle progression [204], and promotion of apoptosis [205]. Their metabolites have also showed anticancer effects. Forester and Waterhouse [206] tested *in vitro* the anthocyanin microbial catabolites produced from the gut microbiota for their ability to inhibit cell proliferation in a colon cancer model using Caco-2 cells. Gallic acid, 3-*O*-methyl-gallic acid, and 2,4,6-trihydroxybenzaldehyde all reduced cell proliferation (IC_{50} = 68, 24, and 76 μM, respectively) without being cytotoxic and were more effective than the parent anthocyanins. However, in

these cases, phenolic compounds should be used not in their natural (from foods), but perhaps in their pure form for the therapy, where large doses may be needed.

In terms of mechanism of action, the enhancement of glutathione peroxidase, catalase, NADPH-quinone oxidoreductase, glutathione S-transferase and/or cytochrome P450 enzyme activity by polyphenols may help in the detoxification of carcinogenic agents [207]. This modulation of enzymatic activities can respond to the chemopreventive effects of these compounds.

They may also modulate the activity of signaling pathways [208] (i.e., MAPK kinase and PI3 kinase), which are involved in cancer cell proliferation [209]. This can respond to some of the chemotherapeutic effects of polypheonols. The three better characterized MAPKs are extracellular signal-regulated kinase 1 and 2 (ERK1/2), p38, and c-Jun N-terminal kinase (JNK) [210]. The MAPK signaling pathway has long been viewed as an attractive pathway for anticancer therapies, based on its central role in regulating the growth and survival of cells from a broad spectrum of human cancers [211], and its role in the transcriptional and post-transcriptional activation of COX-2 [212] (Figure 10). Modulation of cell signalling pathways may also respond to the chemopreventive effects of polyphenols, since it can interfere in inflammatory processes that lead to cell transformation, hyperproliferation, and initiation of carcinogenesis.

Phenolic compounds of olive oil extract, including hydroxytyrosol, tyrosol and oleuropein have been shown to exert a strong inhibitory effect on the *in vitro* growth of colon adenocarcinoma cells through the inhibition of p38/CREB signaling and a decrease in COX-2 expression [213]. In addition, (−)-epicatechin and procyanidin B2 [214] have been shown to inhibit ERK1/2 phosphorylation and downstream cyclin D1 expression leading to a block in the *in vitro* cell cycle progression of Caco-2 cells (Figure 10). Alternatively, polyphenols such as hydroxytyrosol and tea flavanols such as epigallocatechin gallate have been shown to reduce COX-2 over-expression, which is associated with colorectal neoplasia in colorectal cancer [215–217]. Additionally, several anthocyanins have also shown the ability to down-regulate COX-2 expression and enzyme activity, a mechanism which could explain its antiproliferative actions on many different human cancer cell lines *in vitro* [218,219].

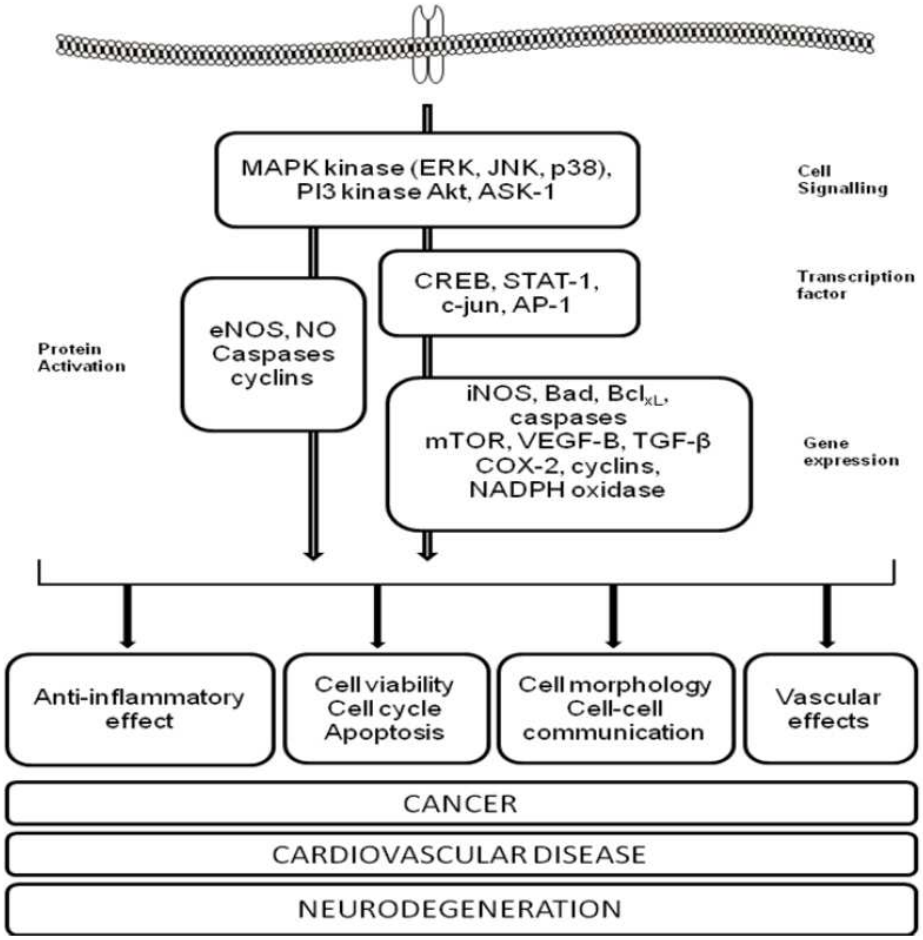

Figure 10 The interaction of polyphenols with cellular signaling pathways involved in chronic disease. Flavonoid-induced activation and/or inhibition of MAP kinase and PI3 kinase signaling leads to the activation of transcription factors which drive gene expression. For example, activation of ERK/Akt and the downstream transcription factor CREB by flavonoids may promote changes in neuronal viability and synaptic plasticity, which ultimately influence neurodegenerative processes. Polyphenol-induced inhibition of the JNK, ASK1 and p38 pathways leads to inhibition of both apoptosis in neurons and a reduction of neuroinflammatory reactions in microglia (reduced iNOS expression and $NO^{\bullet}$ release). Alternatively, their interaction with signaling may lead to direct activation of proteins such as eNOS, which controls nitric oxide release in the vasculature and thus influences cardiovascular diseases risk. Additionally, polyphenols may exert a inhibitory effect on the growth of cancer cells through the inhibition of p38/CREB signaling and a decrease in COX-2 expression, they may also inhibit ERK1/2 phosphorylation and downstream cyclins expression leading to a block of the cell cycle progression [220].

Tumors are also characterized by an increase in glucose uptake and a high rate of glycolysis, which can led to the non-enzymatic glycation of proteins and the generation of so called advanced glycation end products (AGEs). Indeed, the detection of two AGEs, Nϵ-carboxymethyllysine (CML) and argpyrimidine in several human tumors has been linked to

cancer progression [221]. Certain polyphenols, such as rutin, theaflavin 3-3'-digallate and (−)-epigallocatechin, have been proposed to counteract AGE formation both *in vivo* and *in vitro* and thus may limit their impact on the carcinogenesis process [222,223]. Furthermore, as receptors for AGEs (RAGE), are activated by ligand, they promotes an oxidative stress and an increase of the inflammatory response, which is associated with cancer cell invasion and metastasis. Therefore, they also are a target for for cancer therapy [224]. Flavanols such as epigallocatechin gallate may inhibit the cancer cell proliferation by blocking RAGE related signaling [225].

1.2.7.2. Polyphenols and cardiovascular diseases

Coronary heart disease, a type of cardiovascular disease (CVD), is a leading cause of death and disability worldwide. It occurs predominantly in older age groups with a lower prevalence in women than men [195]. CVD is a chronic, multi-factorial disease in which a range of genetic and environmental factors plays a role in its initiation, progression and development. For example, smoking, high saturated fat diets and physical inactivity are well known environmental factors that are considered to increase the risk of CVD [226,227]. There is considerable epidemiological evidence indicating that the regular consumption of diets rich in fruit and vegetables is associated with a reduction in the risk of CVD [139,228,229]. The health benefits provided by fruits and vegetable consumption are partly associated with their polyphenol contents. Recently, a prospective study of postmenopausal women showed that dietary intakes of flavanones, anthocyanidins, and certain foods rich in flavonoids were associated with a reduced risk of death due to coronary heart and cardiovascular diseases [230]. Additionally, a decrease in blood pressure has been reported after chronic intakes of anthocyanins rich tea, flavonoids rich extract from chokeberry fruits, blueberries, and Concord grape juice by hypertensive individuals, myocardial infarction survivors, and those with markers of the metabolic syndrome [231–234]. Improvements in vascular function have been reported with pure anthocyanins (12 weeks, improved endothelium-dependent vasodilation) [235], and after consumption of cranberry juice (4 weeks; decrease in carotid femoral pulse wave velocity) [236]. It was also showed that berries, including Concord grape juice, inhibited platelet aggregation [237,238].

One suggested mechanism for the action of polyphenols on vascular function involves their ability to modulate the levels and activity of nitric oxide synthase (eNOS) and therefore nitric oxide (NO) bioavailability to the endothelium [239,240] (Figure 10). This regulation of

vascular nitric oxide is thought to involve the ability of polyphenols to interact with kinase signaling pathways such as the PI3 kinase/Akt pathway and intracellular Ca^{+2} , inducing eNOS phosphorylation and subsequent NO production [241,242] (Figure 10). As well as activating eNOS, trans-resveratrol has also been shown to increase eNOS expression [243].

Furthermore, flavanoids may act to prevent AGE-related vascular injury via their regulation of MAPK signaling through RAGE (see section 1.2.7.1.) [244] and the down-regulation of transcription factors such as NF-*k*B leading to the suppression of NADPH oxidase [245] (Figure 10).

In addition, flavonoids contributes to the prevention of atherosclerosis [246]. One of the earliest events in the arterial wall to initiatie atherosclerosis is the adherence of mononuclear cells to endothelium, which is triggered by a number of adhesion molecules such as P-selectin, E-selectin [161], vascular cell adhesion molecule-1 (VCAM-1) and intercellular adhesion molecule-1 (ICAM-1) [162]. These molecules are expressed by endothelial and/or vascular smooth muscle cells upon proatherogenic stimuli such as oxidized LDL or oxidative free radicals [163, 164]. After that, a series of inflammatory responses will induce the accumulation of lipids and fibrous elements in the large arteries. As demonstrated by many studies, phenolic compounds and their phase II metabolites have shown antioxidant activity, which can be a mechanism for their effects on atherosclerosis by preventing LDL oxidation [247].

1.2.7.3. Polyphenols and neurodegeneration

Alzheimer's disease is the first most common neurodegenerative disorder followed by Parkinson's disease. Both diseases are expected to impose an increasing social and economic burden on societies as populations age [197]. These and other neurodegenerative disorders appear to be triggered by multi-factorial events including neuroinflammation, glutamatergic excitotoxicity, increases in oxidative stress, iron and/or depletion of endogenous antioxidants [248]. Epidemiological studies have suggested that moderate wine consumption may reduce the incidence of certain age-related neurological disorders including Alzheimer’s disease [249,250]. Furthermore, in a study of the dietary intake of 1367 subjects, aged of 65 years or older, it was found that the intake of flavonoids from fruits and vegetables was inversely associated with dementia. In this study, the regular dietary intake of flavonoids was associated with 50% reduction in the risk of dementia [251] Another population-based study on the

association between flavonoids intake and disability due to Alzheimer's disease and related dementias found that the higher the consumption of dietary flavonoids, particularly flavonols, the lower the rate of dementia [140]. Other studies demonstrated that the consumption of flavonoid-rich plant foods may also be capable of inducing improvements in cognitive performance [252].

Many studies have reported the bioavailability of polyphenols in the systemic circulation. Whilst less is known regarding their degree of brain bioavailability, flavanones such as naringenin and their *in vivo* metabolites, as well as quercetin (a flavonol) have been shown to cross the blood-brain barrier in relevant *in vitro* and *in situ* models [253]. Moreover, several anthocyanins have also been identified in the cortex and cerebellum of rat [254] and pig [121] following feeding with blueberries. Together, these results suggest that polyphenols are able to transverse the blood-brain barrier, albeit to varying degrees depending on their structure. Thus, such compounds are likely to be candidates for direct neuroprotective and neuromodulatory actions.

Flavonoids may act to protect the brain in a number of ways, including the protection of vulnerable neurons, the enhancement of existing neuronal function or by stimulating neuronal regeneration [255]. For example, (+)-cathechin has been shown to protect neurons against oxidative stress [256], which is generally caused by the excessive accumulation of ROS in cells and has been implicated in the development of many neurodegenerative diseases, including Parkinson's disease, Huntington's disease, amyotrophic lateral sclerosis, and Alzheimer's disease [257]. Polyphenol-rich *Ginkgo biloba* extracts have also been shown to be neuroprotective by protecting hippocampal neurons from nitric oxide-induced toxicity [258]. In addition, tyrosol, caffeic acid, and gallic acid have also been shown to protect the neurons against peroxynitrite neurotoxicity *in vitro* [259].

There is a growing interest in the potential of polyphenols to improve memory, learning and general cognitive ability [260]. The effects of polyphenols on cognition and against neurodegenerative processes appear to be mediated via their interactions with neuronal and glial signaling pathways that affect gene expression and interfere with the cell death mechanisms [261]. For example, flavonoids may exert direct modulation of protein and lipid kinase signaling pathways via the inhibition of MAPK signaling cascades, such as p38 or ERK1/2 (Figure 10) [262]. The effects of flavonoids on these kinases may influence downstream transcription factors, including NF-κB [263], which responds to p38 signaling and is involved in iNOS induction [264]. This suggests that there may be interference between

signaling pathways, transcription factors and cytokine production in determining the neuroinflammatory response in the CNS (Figure 10). In addition, the actions of flavonoids on neuronal signaling may mediate their ability to protect against neurotoxicity induced by AGEs [265]. Verzelloni et al. [266] observed that 3'-hydroxyphenylacetic acid, 3',4'-dihydroxyphenylacetic acid, and 3'-methoxy-4'-hydroxyphenylacetic acid, known anthocyanin microbial catabolites (gut microbiota), at physiological concentrations, inhibited the formation of AGEs. The same set of catabolites was effective in preserving cultivated neuron cells from death due to oxidative stress.

1.3. Analytical methods for separation, identification and quantification of phenolic compounds

Phenolic compounds can be separated, identified and quantified in one operation by high-performance liquid chromatography (HPLC) coupled to detectors such as diode array detectors (DAD, also called photodiode-array (PDA)), and mass spectrometers [267]. More details will be given on mass spectrometry (MS) in the present section. On the other hand, spectrophotometric methods can also be used for the determination of the total (or a specific class) of phenolic content in plant and food extracts, using several reagents. Folin-Ciocalteu reagent is the classic reagent used for the determination of total phenols. These methods are less expensive than (U)HPLC methods. However, the spectrophotometric measurements can show poor selectivity and can give an over-estimation of the phenolic content [268,269].

1.3.1. High-Performance Liquid Chromatography

In HPLC methods, not only for phenolic compound analysis, the stationary phase, solvent, and gradient need to be optimized for separation of the different compounds. Vegetable matrices, as crude extracts, are very complex, containing several classes of polyphenols and other compounds that may interfere in the polyphenol analysis. This complexity hampers the optimization of the separation of compounds in a single chromatographic run. Mobile phases such as acetonitrile-water or methanol-water mixtures are very common in reversed-phase systems. Additionally, small amounts of acid are very often used in the mobile phases, mainly formic acid and acetic acid. In the case of anthocyanin analysis, for the best resolution of the peaks, structure equilibria have to be displaced toward their flavylium forms by increasing the acid concentration in the solvent,

generally between 3 and 10%, v/v. In these conditions, peak tailing is minimized and peak sharpness is improved. Polyphenol separations are performed mainly on octadecylsilyl bonded (C18) phases and less frequently on octasilyl bonded (C8) phases. Among these stationary phases, C18 columns are the most used. Generally, the column lengths have between 100 and 300 mm and with internal diameters between 2 and 5 mm. Granulometry vary from 3 to 10 μm, and more frequently it is 5 μm. Separation runs are in general up to 60 minutes [40,270].

Over recent decades, different advances in the development of silica-based particles have been made with the aim of improving the separation efficiency of the HPLC analysis. As a result of these improvements in the packing material used for the chromatographic separations, an advanced form of liquid chromatography has been reported. This novel technique is known as ultra-high performance liquid chromatography (UHPLC), also known as ultra-high pressure liquid chromatography. This technique uses narrow-bore columns packed with very small particles, sub-2μm (from 1.7 to 1.9 μm), and mobile phase delivery systems operating at high back-pressures (up to 1300 bar or 15,000 psi). The major advantages of UHPLC over conventional HPLC are higher separation efficiency and resolution, the increased speed of analysis, higher sensitivity and much lower solvent consumption. On the other hand, the main drawback of UHPLC is that columns packed with small particles generate higher backpressures, which are inversely proportional to the particle size. This makes the use of dedicated instrumentation mandatory [271–273]. UHPLC is a very interesting technology for the analysis of complex matrices. It allows the separation of several compounds in a short run time. Several works used this technology for the analysis of phenolic compounds of plant and food samples [273–275].

Separated compounds are currently detected by UV detectors and/or analyzed and detected by mass spectrometers. The coupling of liquid chromatography to MS (LC-MS) will be discussed in section *1.3.5*.

1.3.2. HPLC−UV detection

Since all phenolics contain at least one aromatic ring, they can consequently absorb UV light. So, UV detectors are used to detect this absorbance. However, UV detectors can be operated in only one wavelength per chromatographic run. On the other hand, the DAD enables simultaneous recording of chromatograms at different wavelengths, as well as to

obtain UV–Visible (UV–Vis) spectral data, allowing compound characterization and rapid diagnosis of certain structural features of each eluted compound. In fact, each class of phenolics, in general, has a distinctive UV or UV–Vis spectra [276]. However, the UV-Vis spectra of the different phenolic classes can be variable in function of the solvent and the concentration of the analytes. As many of the absorption spectra can be very similar within a class of phenolic compounds, peak assignments are made from the retention times, as well as by comparing the UV-Vis spectra of analytes to purchased standards. An important advantage of DAD is that it improves the possibilities of quantification because detection can be performed at the wavelength of maximum absorption (λ_{max}) of each compound. Table 3 shows the maximum absorbance wavelengths of several classes of phenolic compounds. In the case of anthocyanins, the flavylium cations are coloured and can be selectively detected in the visible region, avoiding the interference of other phenolics and flavonoids that may be present in a same extract [40,277,278].

Table 3 Absorption spectra of the various classes of phenolic compound. Adapted from [279].

Class of compounds	UV Band II[a]	UV Band I[a]	Visible[a]
Benzoic acids	270–280		
Cinnamic acids	(290–300)	305–330	
Anthocyanic pigments	240–280	(315–325)[b]	450–560
Flavonols	250–270	(300) 350–380	
Flavanols	270–280		
Coumarins	220–230	310–350	
Flavones	250–270	330–350	
Flavanones, Flavanonols	270–295	(300–330)	
Chalcones	220–270	(300–320) 340–390	
Aurones	240–270		340–370
Isoflavones	245–270	300–340	

[a] Usual solvent is methanol except methanol-HCl for anthocyanins.
[b] In the case of acylation by cinnamic acids.

1.3.3. Mass spectrometry: instrumentation and techniques

Regardless of the type of instrument, a mass spectrometer is composed of three main components as illustrated in Figure 12, and consists of 1) an **ion source** to produce ions from the sample, in the case of ESI source the ions are also partially preformed in the solution; 2) one or several **mass analyzer(s)** to separate the various ions according to their mass-to-charge

ratio; 3) a **detector** to detect the ions emerging from the last analyser and measure their abundance. The signals from the detector are processed in a data processing system that produces the mass spectra [280,281].

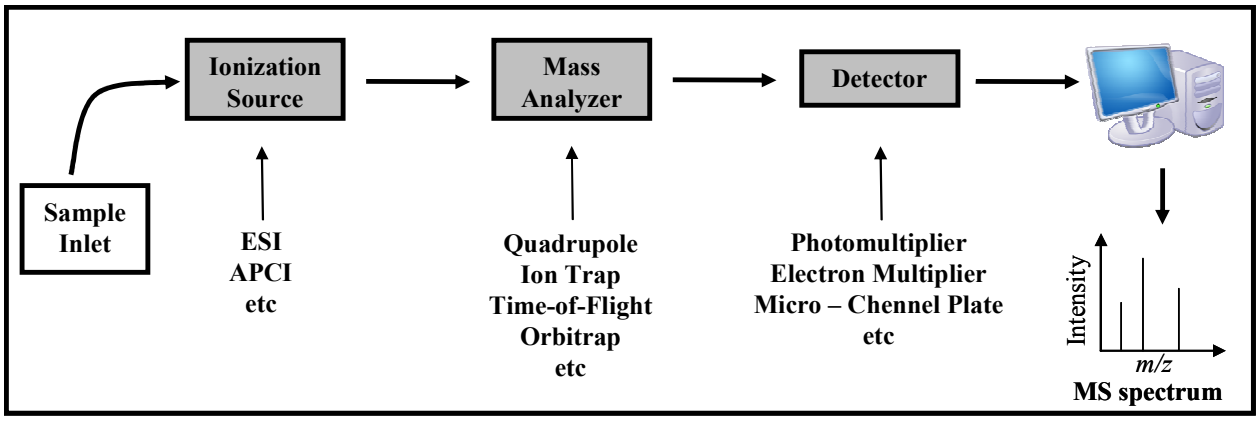

Figure 12 The basic components of a mass spectrometer. ESI, Electrospray Ionization; APCI, Atmospheric Pressure Chemical Ionization. Adapted from [282,283].

1.3.3.1. Ionization sources in LC–MS

The popularity of LC–MS today is largely due to Atmospheric Pressure Ionization (API) interfaces, where solvent elimination and ionization steps are combined in the source and take place at atmospheric pressure. API, known as a soft ionization technique which means the formation of gas-phase ions without extensive fragmentation, mainly includes electrospray ionization (ESI) and atmospheric pressure chemical ionization (APCI).

APCI is suitable for low and moderate polarity compounds, while ESI is most widely used for the analysis of polar molecules. Moreover, ESI technique allows the analysis of compounds of high molecular weights (Figure 13), as proteins, etc. Both techniques are applied for polyphenol analysis [284], but the most employed ion source is ESI because both the polarity and molecular weight of most of these analytes match well the requirements of this interface [285].

ESI in the negative ion mode is more selective in the analysis of phenolic compounds, but may also be more sensitive, because they are often better ionized negatively. Their hydroxyl group can easily lose a proton. However, in acidic conditions, the flavylium cation is the predominant species of the anthocyanins, i.e. naturally these compounds are positively charged and, consequently, higher sensitivity is obtained from ESI in the positive ion mode [270,271]. When ESI source is operated in the positive ion mode, the ions detected by the

mass spectrometer are mainly protonated molecules $[M+H]^+$, but also occasional adducts can be detected, such as $[M+Na]^+$, $[M+K]^+$. In the case of anthocyanins, they are detected in their flavylium cation forms $[M]^+$. In ESI negative ion mode the ions are mainly detected in their deprotonated forms $[M–H]^-$, but some other species can be observed, such as adducted ions $[M+Cl]^-$, $[M–H–HCOOH]^-$ [286–288].

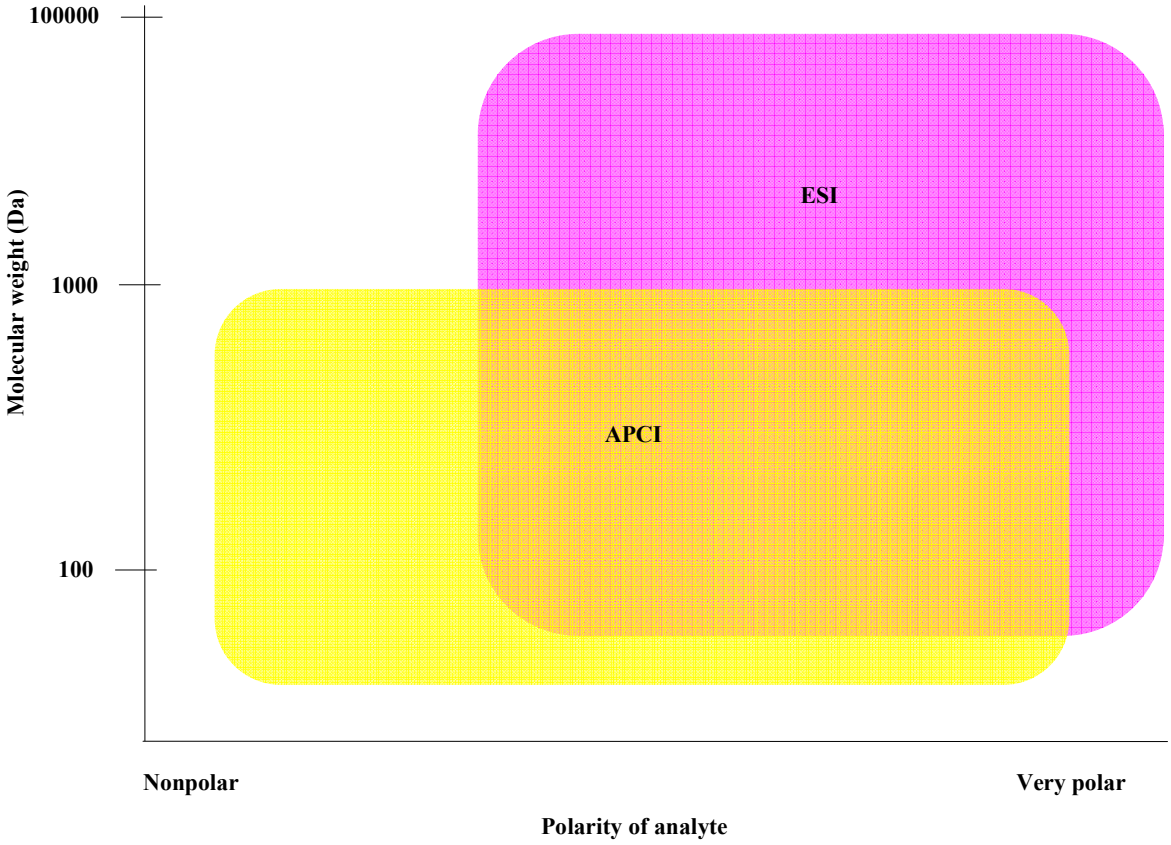

Figure 13 Diagram showing the mass range and polarity range covered by different ESI and APCI sources [289].

Particularly, a representation of the ESI source is shown in Figure 14A. The analyte solution is injected through a metal capillary (Figure 14A). A very high voltage is applied to the tip of the metal capillary relative to the surrounding ion sweep cone or heated capillary. This strong electric field causes the dispersion of the sample solution into an aerosol of highly charged electrospray droplets. An inner coaxial sheath gas (most often N_2) flow around the capillary results in better nebulization. This gas flow also helps to direct the spray emerging from the capillary tip into the mass spectrometer. Another gas participates during operation of

the ESI, the auxiliary gas is the outer coaxial gas that assists the sheath gas in the nebulization and evaporation of sample solutions. The charged droplets diminish in size by solvent evaporation. Finally, the charged analytes are released from the droplets, most of which pass through a sampling cone and the orifice of a heated capillary (kept in the interface of atmospheric pressure and the high vacuum) toward the analyzer of the mass spectrometer, which is held under high vacuum. The heated capillary causes the complete desolvation of the ions passing through it and removes the last solvent molecules [280,282].

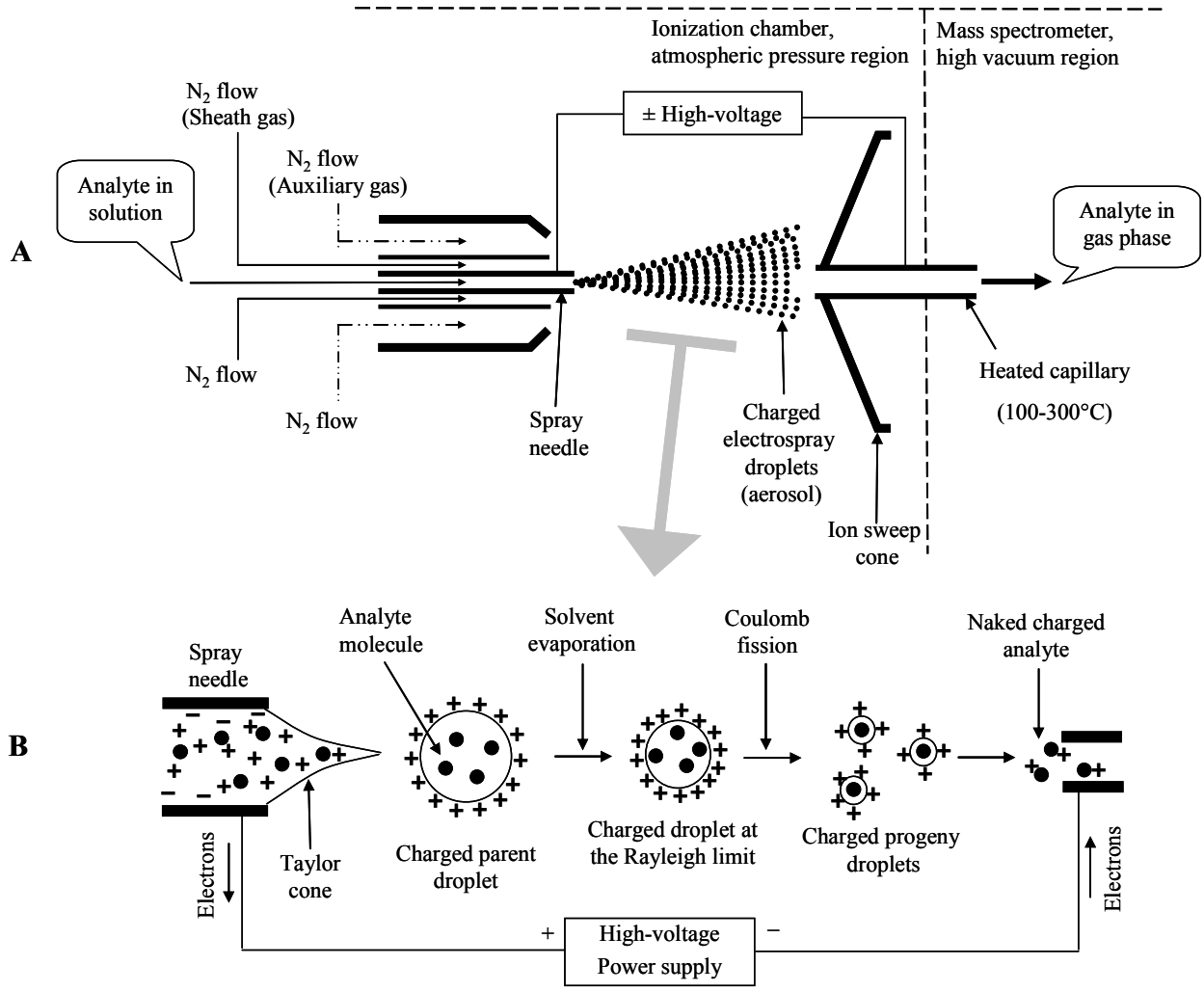

Figure 14 A schematic representation of (A) the ESI-ion source and (B) the electrospray ionization process in positive ion mode (Adapted from [282]).

ESI transforms ions in solution to ions in the gas phase prior to their mass analysis in a mass spectrometer. The source can be operated in positive or negative ion modes to extract positive or negative ions for analysis, respectively. The mechanism of ESI is represented in Figure 14B for the positive ion mode (in this paragraph, information about the negative ion mode will be given in parentheses). Since the introduction of ESI source for mass-spectrometric analysis by the Fenn group in the mid 1980s, its ionization mechanism is the object of extensive research and was not yet fully understood. ESI can be viewed as a special type of electrolytic cell. The analyte is pumped through the high-voltage spray needle, and an electrochemical oxidation (or reduction) reaction of species in the solution at the spray needle tip occurs, when the polarity of this capillary is positive (or negative). These reactions cause an electron flow from the spray needle (or to the spray needle), as illustrated in Figure 14B. In addition, they also supply extra positive (or negative) ions to the solution that prevents the build-up of a charge imbalance [280,282,290]. The origins and nature of these additional ions are very complex and depend on the experimental conditions. Solvents like water, methanol, acetonitrile, etc. can easily undergo electrochemical reactions in the spray needle. The positive charges mainly come from protons, whereas the negative charges mainly come from some negative ions such as OH^-. Redox reactions of water and methanol are shown in Table 4 [282]. Additionally, metal ions of the spray needle could be entering the solution causing a release of electrons to the circuit [290]. These different ions generated by the redox reactions from different species may contribute for the ionization of analytes. The analytes themselves can undergo these redox reactions and be ionized. However, analyte ions can also be preformed in solution, before the arrival of the analyte solution in the ionization source [270,290,291].

The solution delivered to the tip of the spray needle experiences the electric field associated with the positive (or negative) high-voltage applied to the needle. Assuming a positive potential, positive ions in solution will accumulate at the solution-air interface, which is thus drawn out in a down field direction to establish a “Taylor cone”. At a high enough imposed field, the cone is drawn to a filament which produces positively charged droplets via a “budding” process when the surface tension is exceeded by the applied electrostatic force [292]. Solvent evaporation occurs when the droplets traverse the space between the spray needle and the heated capillary, which leads to a reduction in diameter until a point called “Rayleigh limit”, where the surface tension can no longer sustain the Coulomb force of repulsion between the charges on the droplets surface. At this point, “Coulomb fission”

occurs. The process of solvent evaporation and Coulomb fission occurs repeatedly to generate smaller and smaller progeny droplets and finally the charged nanodroplets from which the gas-phase charged analyte molecules are formed [282].

Table 4 Typical redox reactions of the solvents expected to occur in the electrospray emitter (spray needle).

Solvent systems	**Positive-ion mode** *Oxidation reactions*	**Negative ion-mode** *Reduction reactions*
Water	$2H_2O = O_2 + 4H^+ + 2e^-$ $2H_2O = H_2O_2 + 2H^+ + 2e^-$	$2H_2O + O_2 + 4e^- = 4OH^-$ $H_2O + O_2^- + e^- = HO_2^- + OH^-$ $2H_2O + 2e^- = H_2^- + 2OH^-$ $2H_2O + O_2 + 2e^- = H_2O_2 + 2OH^-$ $H_2O + O_2 + 2e^- = HO_2^- + OH^-$
Methanol	$CH_3OH = HCHO + 2H^+ + 2e^-$ $CH_3OH + H_2O = HCOOH + 4H^+ + 4e^-$ $HCOOH = CO_2 + 2H^+ + 2e^-$	$CH_3OH + H_2O + 2e^- = CH_4 + 2OH^-$ $CH_3OH + 2H^+ + 2e^- = CH_4 + H_2O$

Two main mechanisms have been proposed to account for the formation of gas-phase analyte ions from very small highly charged droplets, the *charge residue model* (CRM) and the *ion evaporation model* (IEM). For the first one, as a result of a series of solvent evaporation and Coulomb fission, an extremely small charged droplet is formed (radius $R \approx 1$ nm) which contains only one analyte molecule as well as the ionic charges on the surface of the droplet. Solvent evaporation of this droplet causes its charges to land on the analyte molecules. For IEM, after repeated solvent evaporation and Coulomb fission, the radii of the charged droplets decrease to a given size, when the electric field due to the charges at the surface of the droplet is strong enough to cause direct emission of the solvated ions. Typically, when the droplet reaches the radius $R \leq 10$ nm, the ion emission dominates over Coulomb fission. Thus, unlike CRM, this mechanism does not require the production of very small droplets ($R \approx 1$ nm) that contain only one analyte molecule. [282,290].

1.3.3.2. Mass analyzer

Several mass instruments including the single quadruple (Q), ion trap (IT), time-of-flight (TOF), Fourier transform ion cyclotron resonance (FT-ICR) and Orbitrap can be used as on-line analyzers. The physical property of ions that is measured by a mass analyzer is their mass-to-charge ratio (*m/z*). The main characteristics for measuring the performance of a mass analyzer are the resolving power, the mass accuracy, the *m/z* range, and the acquisition speed.

Resolving power (*RP*) is the mass spectrometer's ability to resolve two adjacent mass peaks and is defined, in the current LC–MS practice, as the *m/z* value (*m*) of a particular peak divided by the peak width *Δm* at *x* % of the peak height (Eq. 21). *x* is often taken to be 50% and *Δm* is designated as full width at half maximum (FWHM)[280,293,294]:

$$RP = \frac{m}{\Delta m} \quad \text{Eq. 21}$$

Definition of FWHM is represented in Figure 15.

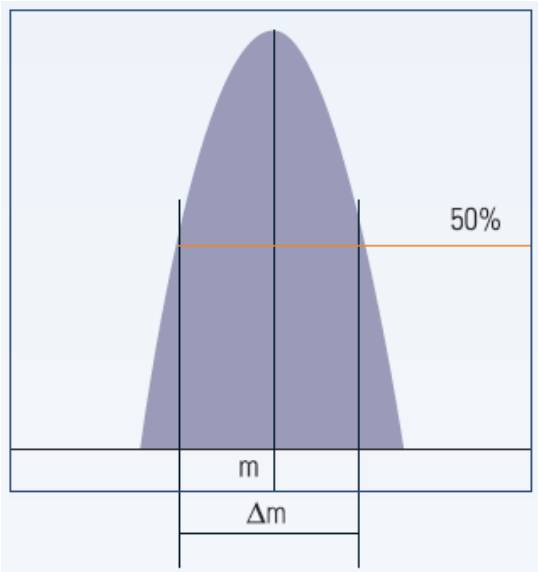

Figure 15 Representation of the "full width at half maximum" (FWHM) definition.

"Resolving power" and "resolution" are used synonymously in most of the scientific publications and commercial manuscripts [280,294–297]. Additionally, most of the manufacturers of mass spectrometers use the value of *RP* defined in terms of FWHM to compare the performances of their instruments. Nevertheless, "resolution" can be calculated as follows, according to some references [295,298]: resolution = *m*/*RP*. To avoid confusions, here the two terms will be used as synonyms, and calculated according to Eq. 21, using FWHM.

Low resolution or high resolution is usually used to describe analyzers with resolving power that is less or greater than 10 000, respectively [280].

Mass accuracy (*MA*) is defined as the relative difference between the experimental *m/z* value (m_{exp}) and theoretical (calculated) *m/z* value (m_{theor}), including the sign (plus or minus) and expressed in ppm (Eq. 22) [280,294,295]:

$$MA = \frac{(m_{\exp} - m_{theor})}{m_{theor}} \times 10^6 \quad \text{Eq. 22}$$

The ***m/z* range** (also called "mass range") determines the limits (lower and upper limits) of *m/z* over which the mass analyzer can measure ions [280].

Acquisition speed (also called "analysis speed" and "scan speed") is the rate at which the analyzer measures over a particular mass range. It is typically expressed in technical specifications in Da/s for low-resolution mass analyzers and in Hz for high-resolution ones. In Table 5 all values are in Hz over the mass range of 1000 *m/z* to allow the comparison among all instruments [280,295].

A general view of the recent performances of different mass analyzers is shown in Table 5. Details of performance values for a specific instrument can be found in the following references [295,297].

Table 5 General values for common performance parameters of mass analyzers used in LC−MS.

Mass analyzer type[a]	Maximum Resolving power [x 10^3]	Mass accuracy (ppm)	*m/z* range (upper limit) [x 10^3] [b]	Acquisition speed (Hz)
Q	**3−5**	**Low**	**2−3**	**2−10**
IT	**4−20**	**Low**	**4−6**	**2−10**
TOF	**10−60**	**1−5**	**10−20**	**10−50**
Orbitrap	**100−240**	**1−3**	**4**	**1−5**
FT−ICR	**750−2500**	**0.3−1**	**4−10**	**0.5−2**

[a] Include different mass spectrometers on the market containing these analyzers [295,297].
[b] Values for the typical measurement range of 1000 *m/z*.

Better values of RP and MA are achieved by FT-ICR analyzer, followed by Orbitrap and TOF analyzers, respectively. Higher resolving power values result in a higher capacity to

separate adjacent ions of slightly different *m/z* values, which is the case of isobaric compounds that have the same nominal mass but different molecular formula. High MA (<5ppm) obtained by these analyzers allows determination of analyte elemental composition, unlike the low resolution analyzers, which have typical MA of about 100 ppm [280]. Obviously, a better MA results in more reliable determination of the elemental composition of analytes. TOF instruments in LC−MS configuration can analyze a mass range having upper limits of ≥ 10 000 *m/z*. Therefore it is an interesting option for the analysis in LC−MS of macromolecules. As the molecular weight of most of the polyphenols classes is inferior to 1000 amu, they can be analyzed by all instruments of Table 5. Acquisition speed is especially important for LC−MS methods for quantitative purposes because higher analysis speed results in more data points on the chromatographic peaks. Additional discussion in this respect will be given in the item "a" of the *1.3.5.2.* section that deals with LC-MS.

Prices of mass spectrometers strongly depend on the particular configuration of the instruments and individual offers from the manufacturer. In general, Q analyzers are simplest and cheapest devices followed by IT. TOF analyzer is the cheapest high-resolution mass analyzer with relatively good RP and MA and some interesting characteristics in terms of acquisition speed and *m/z* range. FT mass analyzers, Orbitrap and ICR, are high-end MS technologies with the best operational parameters, but they have an additional investment cost. FT−ICR instrument provides better RP and MA, but it has the highest price. Orbitrap has a lower cost and a much simpler and compact design than FT−ICR instruments. Therefore, in general terms, it can be considered, among these three HR mass spectrometers, as a good compromise in terms of RP, MA and cost.

Additionally, it has been reported that Orbitrap provides high accuracy in a much more stable fashion than TOF analyzers, which can have mass shifts between 5 and 20 ppm within 24 h, and this stability over time becomes worse with slight temperature fluctuations [294]. This capacity to provide reproducible MA over time is important in LC−MS analysis because sometimes a series of experiments can take more than 24 h, even with UHPLC runs.

Another important consideration is that both TOF and Orbitrap analyzers can have a hybrid configuration with a Q or IT. These combinations allow at least MS/MS experiments, which improve the characterization of compounds. HRMS is now widespread for polyphenols analysis, specially using TOF analyzers, but the recent Orbitrap technology has gained much attention. On the other hand, only a few papers using FT−ICR instruments for polyphenols analysis has been reported [271].

Brief information about instrumentation and principle of operation will be given for the Orbitrap mass analyzer.

The Orbitrap analyzer itself is an electrostatic ion trap that, as the FT-ICR, uses the Fourier transform to obtain mass spectra. The first commercial mass spectrometer containing an Orbitrap was introduced on the market by the Thermo Electron Corporation in June 2005. Figure 16 illustrates the analyzer.

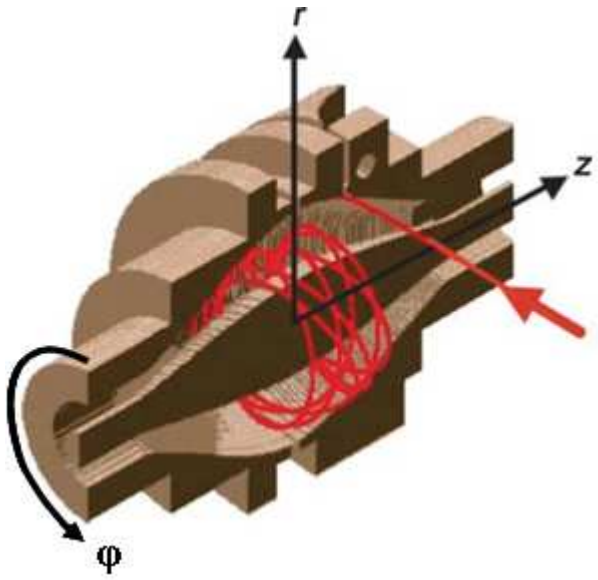

Figure 16 Cutaway view of the Orbitrap mass analyzer. Ions are injected into the Orbitrap at a point (arrow) offset from its equator plane ($z = 0$) and perpendicular to the z-axis; where they begin coherent axial oscillations without the need for any further excitation. The ion trajectories also involve angular (φ) and radial (r) motions (Adapted from [299,300]).

The Orbitrap analyzer consists of two axially symmetrical electrodes: an outer barrel-like electrode and a central spindle-like electrode. The first one is split in two parts in the equator plane ($z = 0$) of the Orbitrap, and one of these parts has a small entrance aperture, through which the ions enter into the analyzer (Figure 16) [299,300].

Ions are injected into the Orbitrap at a position where $z \neq 0$, and perpendicularly to the z-axis, after application of an increasing voltage to the central electrode, while the outer electrode is maintained at ground potential [300]. The voltage of the central electrode is increasing only in this first step when the ions are injected and trapped into the analyzer. Under these conditions, and thanks to the astute geometry of the Orbitrap, the electrodes

create an electric field that can be divided in fields that have axial (z) and radial (r) direction. Axial field strength is at zero in the equator plane of the Orbitrap, but increases uniformly in opposing directions along the z-axis as the two coaxial electrodes become progressively closer. As it reaches substantial values at the point of entry of the ions, it starts to pull all ions towards the equator plane as soon as they enter the field. This initiates axial oscillations without any additional excitation, in a manner analogous to pulling back a pendulum bob and then releasing it to oscillate. Ions of a given m/z enter into the Orbitrap practically simultaneously, in the form of a packet. The axial size of the ion packet remains almost unchanged (i.e. the ion packet remains with small thickness, considering the axial amplitude of the central electrode). The radial field increases very fast with time and being stronger near the central electrode, attracts the ions towards this electrode. This field bends the trajectories of the ions into circular arcs. The radii of the arcs become progressively smaller, so that ions cannot return to the entrance radius to hit the outer electrode as they begin their axial oscillations, and thus be lost for detection [300,301].

After stabilizing the central electrode voltage (outer electrode remains at ground potential), the electric field between the two electrodes is also stabilized, being thus termed electrostatic field. This field has a quadro-logarithmic potential distribution thanks to the shape of the electrodes. In these conditions, stable ion trajectories within the Orbitrap are obtained, and involve oscillations along the z-axis and rotation (composed of radial and angular (φ) motion) around the central electrode [280,300,302]. Frequency ω of axial ion oscillations depends only on ion mass/charge ratio (m/z) and field curvature k (that is held constant) (Eq. 23). The parameter k is determined by the exact shape of the electrodes and the stabilized applied potential between the outer and central electrodes [302]:

$$\omega = \sqrt{(z/m)\,k} \quad \text{Eq. 23}$$

On the other hand, frequencies of the φ and r motions of the ions (Figure 16) are strongly dependent on other initial parameters of the ions, as kinetic energy, position, and angle of ions. Because of this, each ion packet (that have ions of a same m/z, but with slightly different initial ion parameters) quickly spreads (i.e. dephase) over the angular coordinate and forms a thin rotating ring [301]. Unlike angular and radial frequencies, axial frequencies are completely independent of initial ion parameters. Therefore, the thin ring continues to

oscillate along the *z*-axis, remaining in-phase (i.e. with axial thickness of the ion ring remaining small compared with the axial amplitude of the central electrode) [299–301].

Moving from one half outer electrode to the other, this ring will induce opposite currents on these halves (detection electrodes), thus creating a signal called of "image current" that is detected by differential amplification [299]. The image current is acquired as a time-domain signal (signal intensity as a function of time). This time domain signal, containing all the characteristic frequencies of the measured ions at intensities corresponding to the amount of the molecular species in the sample, is converted by a fast Fourier transform into a frequency spectrum (intensity as a function of frequency). Each frequency can be assigned to a specific *m/z* ratio by Eq. 23, and finally a MS spectrum (intensity as a function of *m/z* ratio) is obtained [280,300–302].

It is important to note that a nonzero image current can be detected only if ions are moving in-phase with each other. This means that ions of each *m/z* inside the Orbitrap analyzer should be concentrated in packets that have an axial length shorter than the amplitude of oscillations, *i.e.* ions should oscillate *coherently*. Radial and angular frequencies do not appear in the frequency spectrum precisely because of the fast loss of coherence caused by dependence of these frequencies on the initial parameters of the ions [301].

This method of detection brings Orbitrap analyzer into the family of Fourier transform (FT) mass spectrometers which was, until recently, represented by FT−ICR alone. Very high fidelity of frequency determination is inherent to FT mass spectrometry, consequently very high resolving power and mass accuracy are achieved by this family of instruments [303].

1.3.3.3. Detector

The ions pass through the mass analyzer and are then detected and transformed into a usable signal by a detector. Detectors are able to generate from the incident ions an electric current that is proportional to their abundance [280]. Among several ion detectors in mass spectrometry, the most widely used is the electron multiplier, also called secondary-electron multiplier (SEM). Several Qs, ITs, and TOF instruments are connected to this detector type [304]. It works on the phenomenon of secondary electron emission. A variety of designs are in common use. The most used are: discrete-dynode SEM, and continuous-dynode SEM, also known as channel electron multiplier (CEM). The first one consists of a series of dynodes, generally 16 or 20 dynodes, usually made of copper–beryllium (Figure 17). The first dynode,

called a conversion dynode, is held at a high voltage generally from ±1 to ±30 kV, opposite to the charge on the detected ions. The other sequential dynodes are held at decreasing potentials, from the conversion dynode, e.g. ±0.7 kV, ±0.5 kV, etc. A positive or negative ion striking the conversion dynode causes the emission of several secondary particules. These secondary particles can include positive ions, negative ions, electrons and neutrals. When positive ions strike the negative high-voltage conversion dynode, the secondary particles of interest are negative ions and electrons. When negative ions strike the positive high-voltage conversion dynode, the secondary particles of interest are positive ions. As shown in Figure 17, for positive ions, the secondary particles emitted by the conversion dynode are accelerated to the next dynode because it is held at a lower (negative or positive) potential. They strike the second dynode, where the secondary particles are converted to secondary electrons. This process continues as the secondary electrons travel towards the last dynode (the anode). For each dynode, more secondary electrons are emitted for each electron that has struck the dynodes. Thus a cascade of electrons is created and the final flow of electrons provides an electric current at the last dynode. This dynode is called anode, because it collects the negative charges (electrons). The electric current is then increased by conventional electronic amplification to provide a gain in excess of 10^7 electrons for each incident ion [280,305].

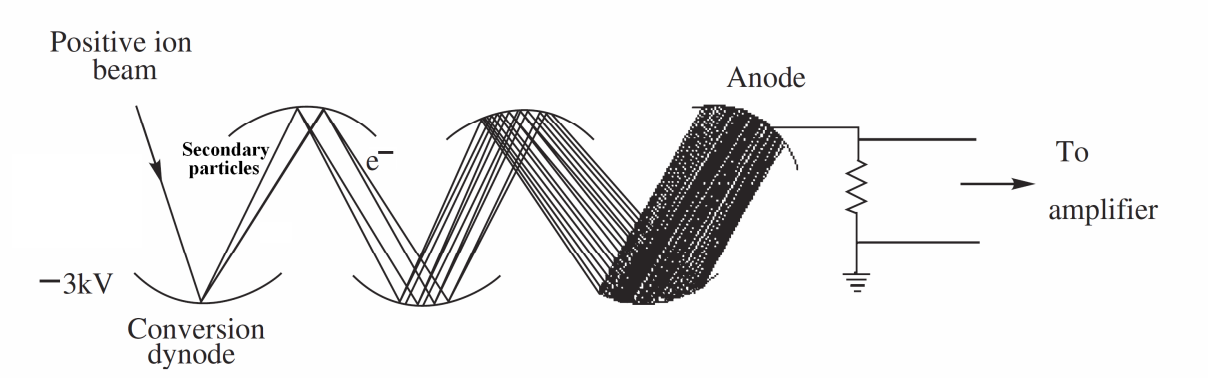

Figure 17 Principle of ion detection by the discrete-dynode electron multiplier. Adapted from [305].

The CEM is a horn-shaped or funnel-shaped assembly, in which a conducting surface acts as an array of continuous electrodes (Figure 18). Generraly, it is constructed from a special type of glass that has either been heavily doped with lead or whose inner surface is coated with beryllium. A high voltage is impressed across the two ends of the tube to create a

uniform field throughout the length of the tube. The beam of ions coming from the analyzer strikes the surface of a conversion dynode, generating secondary particles, in the same way that for the discrete-dynode SEM, previously described. These secondary particles collide with the curved inner wall at the detector entrance, and produce secondary electrons. The electrons ejected are reflected toward the opposite surface until they reach a metal anode located at the other end of the detector. With each impact on the inner surface of the tube, the current is amplified, due to the emission of more electrons for each striking electron. Finally, a metal anode collects the stream of secondary electrons and the current is amplified. A CEM is more compact and less expensive than a discrete dynode SEM and provides gains as high as 10^8 [280,305].

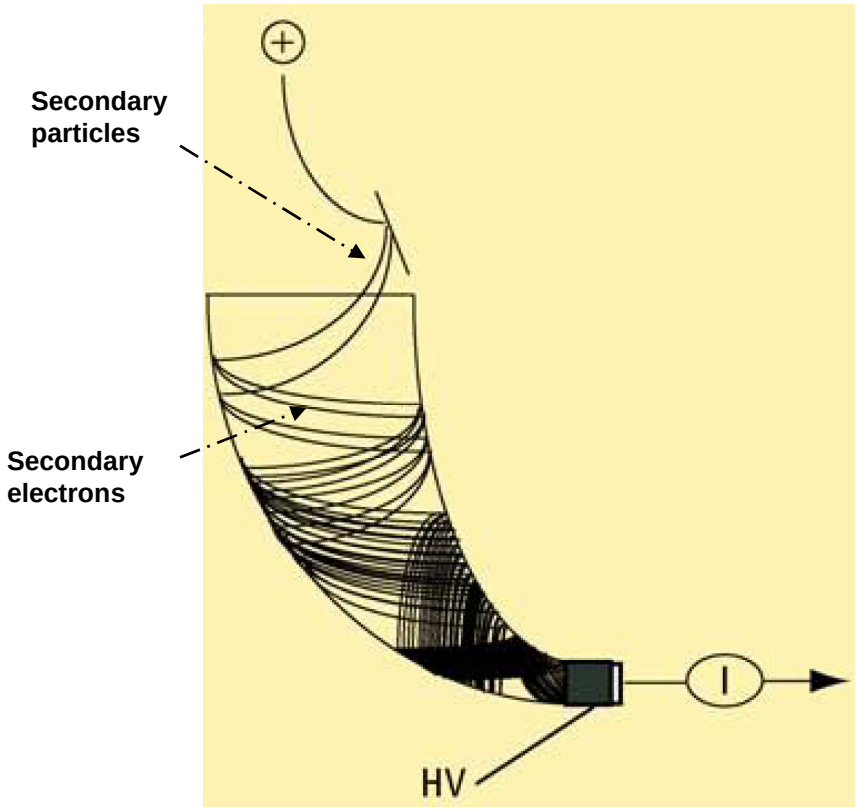

Figure 18 Principle of ion detection by the continous-dynode electron multiplier. HV: high voltage (negative for positive ions). I: electric current [304].

LTQ−Orbitrap instrument (model XL) consists of a hybrid system that has two mass analyzers, which are a linear trap quadrupole (LTQ) and an Orbitrap. The particularity of the LTQ XL analyzer is that it is connected to two CEM detectors, each one is combined to a conversion dynode. Two detectors improve the signal by a factor of two, as compared with

the signal obtained by only one detector. Figure 19 illustrates the general operation steps of the ion detection system connected to the LTQ XL analyzer.

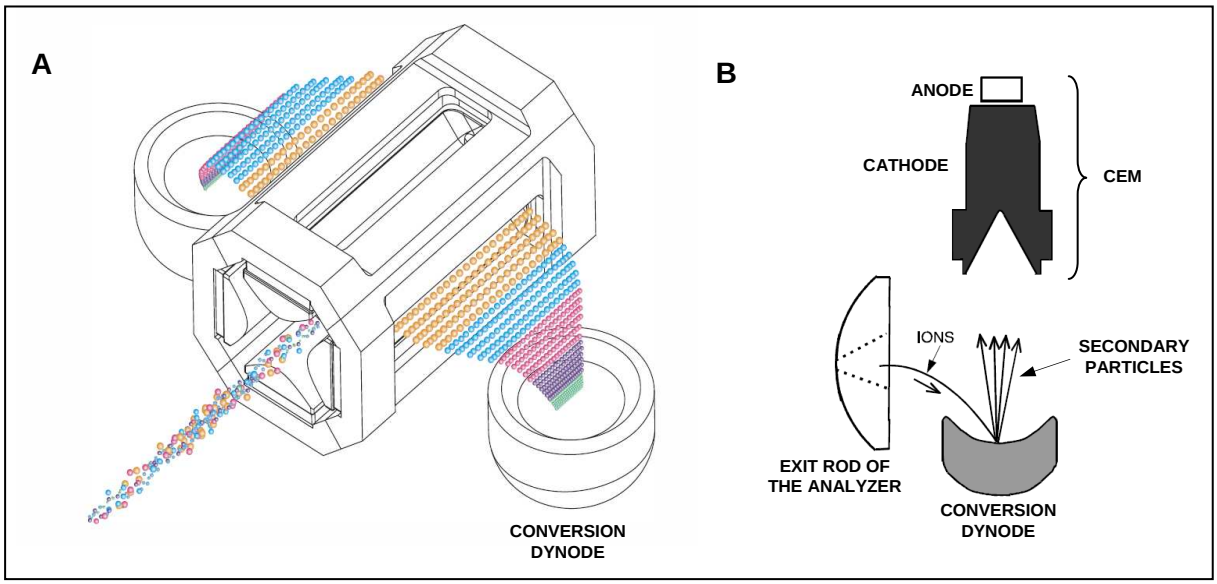

Figure 19 Summary of ion detection system operation associated with the linear trap quadrupole XL. **(A)** Different ions (represented by the colored or gray shaded spheres) are ejected from the trap in order of increasing mass-to-charge ratio. The ions exit the trap through slots in the exit rods. The ions then strike the conversion dynodes on each side of the trap. **(B)** Collision of the ions on a conversion dynode produces secondary particles that are ejected towards the cathode of the channel electron multiplier (CEM). The secondary particles strike the inner walls of the cathode to eject electrons. They strike again the inner walls of the cathode in a sequential process so that a cascade of electrons is created. Finally the electrons are collected by the anode of the CEM. The final electric current obtained is proportional to the number of secondary particles striking the cathode. The current is converted to a voltage by the electrometer circuit and recorded by the system. Adapted from [283,306].

Detection of ions in FT analyzers, FT−ICR and Orbitrap, is characteristically different of the detection by electron multipliers. In this case, the detector consists of a pair of electrodes within the mass analyser region close to the ion trajectories. Ions are detected by the image current that they produce in a circuit connecting the electrodes [280,289,307]. Ion detection in the Orbitrap analyzer was described in *1.3.3.2* section.

1.3.4. Tandem mass spectrometry

Tandem mass spectrometry is a multistage mass spectrometry technique that can precisely ascertain the progeny of ions. It involves mass selection of a precursor ion, activation and fragmentation of the mass-selected precursor, and mass analysis of the charged products. This is labelled as a MS/MS experiment. It is possible to increase the number of steps by selecting ions from the obtained fragments to perform further fragmentation and mass analysis of the product ions, and so on. This is labelled as a MS^n experiment (where n refers to the number of generations of ions being analyzed) [280,305].

1.3.4.1. Tandem mass spectrometry in space or in time

Tandem mass spectrometry instruments are classified into two broad categories: tandem in-space and tandem in-time. In tandem in-space instruments, two or more physically distinct instruments are coupled to perform MS/MS or MS^n experiments. Common space instruments have two mass analysers, allowing MS/MS experiments to be performed. A frequently used instrument of this type is the triple quadrupole (QqQ). The QqQ configuration indicates an instrument with two quadrupoles analyzers (Q) and one quadrupole collision cell (q). To improve the ion-transport efficiency, some contemporary instruments are outfitted with an octopole or hexapole collision cell in place of a conventional quadrupole cell. In the triple quadrupole the first analyser is used to isolate a precursor ion, which then undergoes activation and fragmentation in the collision cell to yield product ions that are analyzed by the second quadrupole analyzer [288,297]. To obtain higher order MS^n spectra requires *n* analysers (Q) to be combined. Successive analysers can be arranged in any number, but because the fraction of ions transmitted at each step is low, the practical maximum is three [280,305]. TOF/TOF instruments, and hybrid instruments are also examples of tandem in-space instruments. Hybrid tandem mass spectrometers are constructed by coupling two different types of mass analyzers with the objective of accruing the benefits of the best performance features of each analyzer type. This arrangement enhances the capabilities of a single type of mass analyzer. Some examples of hybrid systems are IT−TOF, Q−TOF, LTQ−Orbitrap, etc. In LTQ−Orbitrap instruments, the LTQ is an ion trap analyzer type also known as Linear Ion Trap (LIT), or two-dimensional ion trap (2D ion trap) [305].

Tandem in-time instruments perform MS/MS or MS^n experiments in the same region but by using a temporal sequence. Ion traps and FT–ICR instruments fall into the latter

category. The basic steps performed by these instruments are: accumulation into the analyzer of the ions coming from the ionization source, isolation of the precursor ions by ejection of all other ions, then activation and fragmentation of the selected ions, finally, analysis of fragment ions. The main advantage of IT instruments is the possibility to perform MS^n experiments. The maximum practical number of steps for these instruments is seven to eight [280,305].

1.3.4.2. Scan modes in mass spectrometry

In single MS analysis two scan modes can be performed, full scan and selected-ion monitoring (SIM). Other scan modes can be performed only with multiple MS analysis, thus they are performed in tandem mass spectrometers (tandem in-space or in-time). Some classical scan modes are described below [280,297,308,309]:

Full scan: in this scan mode all ions of a wide mass range are detected.

SIM: consists in recording ions signals of one or more specific *m/z* values. As several ions with different *m/z* ratios have to be detected, the analyser goes rapidly from one mass to another.

The four main scan modes available using tandem mass spectrometry are described below[280,305]:

1. *Product ion scan* consists of selecting a precursor ion of a chosen mass-to-charge ratio and determining all of the product ions resulting from the activation and fragmentation process of this precursor ion.

2. *Precursor ion scan* consists of choosing a product ion and determining the precursor ions. This method is called 'precursor scan' because the 'precursor ions' are identified. This scan mode cannot be performed with time-based mass spectrometers. This scan requires the focusing of the second spectrometer on a selected ion while scanning the masses using the first spectrometer. All of the precursor ions that produce ions with the selected mass through fragmentations thus are detected.

3. *Neutral loss scan* consists of selecting a neutral fragment and detecting all the fragmentations leading to the loss of that neutral. As in the case of the precursor ion scan, this scan mode is not available with time-based mass spectrometers. This scan requires that both mass spectrometers are scanned together, but with a constant mass offset between the two. Thus, for a mass difference *a*, when an ion of mass *m* goes through the first mass

spectrometer, detection occurs only if this ion has produced a fragment ion of mass ($m-a$) when it leaves the collision cell.

4. Selected reaction monitoring (SRM) consists of selecting a fragmentation reaction. For this scan, both the first and second analysers are focused on selected masses. The method is analogous to selected ion monitoring. But here the ions selected by the first mass analyser are only detected if they produce a given fragment, by a selected reaction. A triple-quadrupole instrument is ideally suited for SRM experiments, although IT instruments have also been used.

1.3.4.3. Collision-Induced Dissociation

To gather information about structure-specific fragment ions in tandem mass spectrometry, ion activation and dissociation of the mass-selected precursor is essential. There are several reasons for this activation step: (1) the abundance of the ion source–activated ions that fragment spontaneously in the field-free regions is usually low; (2) only a few selected reaction pathways are detectable from those spontaneously fragmenting ions; and (3) ions that are generated by currently popular softer modes of ionization (API ion sources) are either stable or exhibit a weaker fragmentation pattern to yield any meaningful structural information. Ion activation not only increases the population of precursor ions with energies beyond the threshold of dissociation, but the number of dissociation channels increase as well, to provide useful structural information. A variety of ion-activation techniques are available as *collision-induced dissociation* (CID), *surface-induced dissociation* (SID), *ultraviolet photodissociation* (PD), *infrared multiphoton dissociation* (IRMPD), *electron-capture dissociation* (ECD), etc.

By far the most common means of ion activation and dissociation for ions of phenolic compounds is CID [271]. In this technique, collisions between a fast precursor ion and a neutral target gas molecule lead to an increase in internal energy of the ion through the conversion of part of its translational energy into internal energy. If the internal energy imparted is beyond the threshold for dissociation, precursor ion fragmentation may occur [310].

To achieve collisional activation in MS/MS instruments with spatially separate analysers, a collision cell is placed between the two mass analysers. This cell often corresponds simply to a small chamber with entrance and exit apertures and contains an inert

target gas at a pressure sufficient for collisions with ions to occur. In MS/MS instruments based on time-separated mass analysis steps, an inert gas is simply introduced into the mass analyzer. In more sophisticated devices, this gas is only introduced into a certain region or at a particular time in the operating sequence using a pulsed valve [280].

1.3.5. Liquid chromatography coupled to mass spectrometry

Liquid chromatography coupled to mass spectrometry (LC–MS) is a technique that combines the chromatographic separation of a mixture of compounds of a complex matrix with the selectivity and sensitivity of the MS detector to allow the identification and quantification of individual compounds. The technique is diversified by the use of UHPLC systems, tandem mass spectrometers and high resolution mass spectrometers. When LC is coupled to tandem mass spectrometry, the technique is abbreviated as LC−MS/MS. In the text, when it is not important whether the system is LC-MS or LC-MS/MS, the term LC-MS will be used.

LC−MS is very popular to analyze non volatile compounds of complex mixtures, such as natural products. API sources (described in *1.3.3.1.* section), allowing ionization of analytes from solutions, are ideal for coupling liquid chromatography with mass spectrometry. Generally, these ion sources can tolerate flow rates up to 1 ml/min (APCI) or 0.5 mL/min (ESI), allowing an easy coupling to an (U)HPLC system. Nevertheless, buffers and pH modifiers should be volatile [280,287]. For the analysis of phenolic compounds, formic acid and acetic acid are the most employed pH modifers, and the most used solvents are methanol and acetonitrile [271]. Acidification provides a better retention and separation on the C8 and C18 columns which are almost exclusively employed. In the negative ion mode, a concentration of 0.1% formic acid or 5 mM ammonium acetate buffer seems to be preferable, whilst the addition of basic eluents has a negative influence on both the LC separation and the ESI process [311,312].

LC–MS techniques are nowadays the best analytical approach to study polyphenols from different biological sources. LC−MS instruments are also very effective tools in the study of the structure of phenolic compounds [267]. It was also reported that the sensitivity of UHPLC–MS was 3 orders of magnitude higher than that reported using HPLC–UV detection for the determination of phenolic compounds in food samples [273,275,313].

1.3.5.1. Mass Spectral Data Acquisition

As described in *1.3.4.2.* section, mass spectra can be obtained from different scan modes. In LC-MS, different types of ion chromatograms can be retrieved from the mass spectrometry data, some examples are described below [305,314].

A *total ion chromatogram* (TIC), also called total ion current chromatogram (TICC) is the sum of the intensities (proportional to the number of ions) of all the *m/z* values in each mass spectrum plotted against the time (or less frequently versus the scan number). Figure 20A illustrates a mass spectrum obtained by the full scan mode, where the ions were detected in the 100−1000 *m/z* range. Figure 20B shows the intensities of all the *m/z* values of this mass spectrum. The sum of the intensities obtained for all *m/z* values at a retention time is called of "total ion current" (Figure 20B). This term is also abbreviated as TIC, which can cause some confusion with total ion current chromatogram. Here, total ion current will not be abbreviated. Figure 20C shows a segment of a TICC, between 17.5 and 21 min of a chromatographic run, where three peaks can be observed. The total ion currents obtained for each scan are shown. For example, the total ion current presented in Figure 20B corresponds to the scan of number 429 in Figure 20C. Therefore, the TICC is obtained by plotting the total ion currents of all scans performed as a function of time. By connecting all total ion currents, the TIC chromatogram is obtained, showing the peaks of the detected compounds.

The retention times of peaks of a TICC can be used for identification purposes. Additionally, a mass spectrum can be retrieved for any chosen retention time of a TICC to provide qualitative informations of on a compound.

A

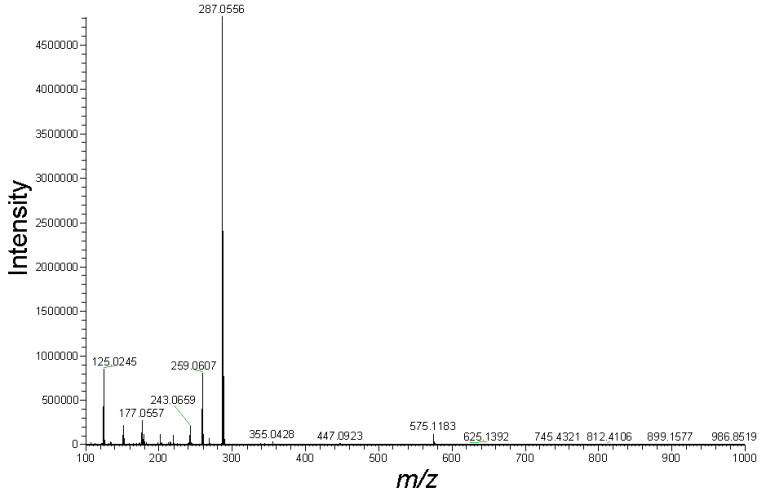

B

m/z	Intensity	Relative intensity (%) [a]
(…)	(…)	(…)
125.0245	868185.8	17.96
(…)	(…)	(…)
151.0037	218665.3	4.52
(…)	(…)	(…)
177.0557	276626.2	5.72
(…)	(…)	(…)
243.0659	203906.6	4.22
(…)	(…)	(…)
259.0607	807910.6	16.71
(…)	(…)	(…)
287.0556	4834376	100
(…)	(…)	(…)
288.0587	785176.8	16.24
(…)	(…)	(…)
355.0428	36286.2	0.75
(…)	(…)	(…)
575.1183	122181	2.53
(…)	(…)	(…)
	10550986.1	
	Total ion current	

C

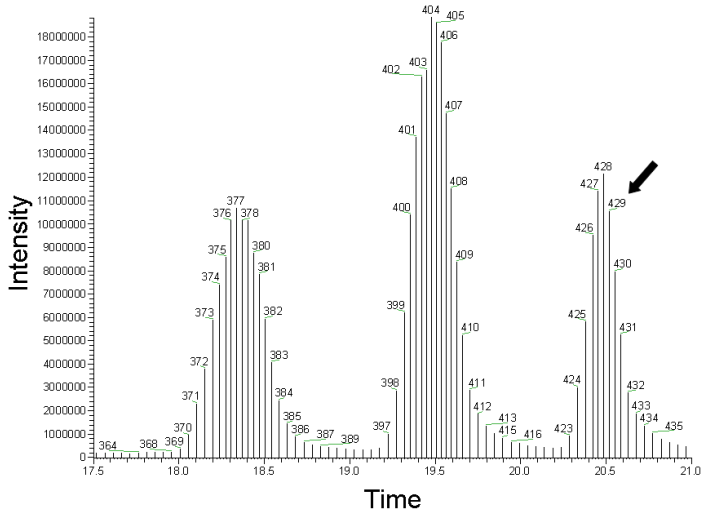

D

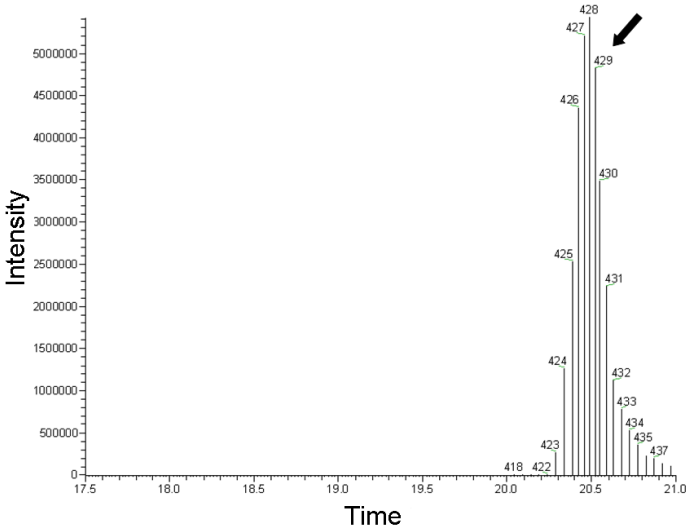

Figure 20 Generation of ion chromatograms. (A) mass spectrum obtained by the full scan mode and (B) its total ion current. (C) segment of a total ion current chromatogram, showing the number of scan. (D) extracted-ion chromatogram for the ion at *m/z* 287.0556, assuming a MEW of 5 ppm.
(…): data not shown. [a] Intensity relative to the highest intensity, obtained for the *m/z* 287.1.

An *extracted-ion chromatogram (EIC)*, also known by various other names, such as *ion-extraction chromatogram*, *reconstructed ion chromatogram* and *mass chromatogram*, is a plot of the intensity of a defined *m/z* value versus time (or less frequently versus the scan number). It is obtained by selecting a *m/z* value, among all values of the mass range of the scan, and a limit of error around this *m/z* value. This limit is known as the "mass extraction window" (MEW). Figure 20D shows an EIC for the ion at *m/z* 287.0556, assuming a MEW of 5 ppm. The intensity plotted in Figure 20D corresponds to the intensity of the ion at *m/z* 287.0556 in Figure 20A. The EIC is a useful means to distinguish coeluting components and to identify a homologous series of compounds.

A *selected-ion monitoring* (SIM) *chromatogram* is similar to the EIC. It is acquired by recording the ion signal due to only one or more compound-specific ions as a function of time. However, in this case the mass spectrometry data are only monitored for one or some *m/z* values. Consequently, the SIM chromatogram can only be retrieved for these *m/z* values, but not for other *m/z*.

A *selected reaction monitoring (SRM) chromatogram* is obtained from the intensities of a specific product ion from a specific precursor ion, so using the SRM scan mode.

The last three types of ion chromatograms are the most used for quantitative purposes, as discussed in the next section.

1.3.5.2. Considerations in quantitative analysis using LC−MS systems

Quantitative analysis by mass spectrometry involves establishing the accurate correlation of the ion signal of a compound with the quantity of the compound in the sample [280,305]. Several quantitative analysis methods using mass spectrometry have been developed for phenolic compounds in plant and food samples and recently the most used mass analyzers were TOF, Orbitrap and triple quadrupole [271].

a. Data acquisition

LC−MS systems equipped with low resolution mass spectrometers, such as IT, Q, and triple Q are operated in the SIM or SRM scan mode for quantification purposes. In the later case tandem mass spectrometer instrument is necessary.

For quantification, the area (or less frequently the height) of the analyte peak is recorded. Although an extracted-ion chromatogram and an SIM chromatogram are identical in terms of selectivity, the latter provides much higher sensitivity, owing to the increased time spent monitoring each ion selected. The selecitivity of both ion chromatograms can be compromised because of the low resolution of the instruments (unit-mass resolution), that does not distinguish very close *m/z* values. Additionally, in SIM chromatograms, some analytical information is lost due to the monitoring of only one or a few ions.

A triple quadrupole instrument is ideally suited for SRM experiments and widely used for quantification of phenolic compounds [309,313]. Using SRM scan mode for quantification, the precursor–product reaction must be unique to the analyte and should provide a strong ion current signal. Additionally the collision energy, collision gas pressure and cone voltage should be optimized in order to improve the sensitivity of the method [272,288]. An obvious advantage of SRM over SIM is the increased level of selectivity because of the exclusive structural link that is maintained during the analysis between the mass-selected precursor ion and its product ion. On the other hand, as for SIM scan mode, in SRM scan mode only the precursor and product ion are monitored and thus there is a lack of information in relation to other compounds for post-acquisition analysis.

Several LC−MS systems equipped with high resolution mass spectrometers can be operated in the SIM and SRM scan modes. However, they are more frequently operated in the full scan MS mode. In these instruments, all ions of the mass spectra obtained from full scan MS mode are acquired with high resolution and high mass accuracy. From these spectra, EIC can be obtained using the exact mass of any ion, and a narrow MEW, which is generally of some ppms. Consequently, high selectivity of the chromatographic peaks is achieved by elimination of interferent signals of isobaric compounds. The selectivity obtained by high resolution mass spectrometry (HRMS) is comparable with the selectivity obtained in LC−SRM experiments using triple quadrupole instruments [295]. A disadvantage of these last instruments is that they need optimization of MS/MS parameters which is avoided in LC−HRMS analysis when full scan mode is used. On the other hand in a LC−HRMS method the MEW must be optimized for the acquisition of EICs. When a large mass extraction window is used, the selectivity is poor and accurate quantitation is impossible. If the extraction window is narrowed, the selectivity is improved, allowing accurate quantitation [272,288], but this step is much easier to optimize as compared with the MS/MS optimization for LC−SRM methods. Additionally, in contrast to LC−SRM, LC−HRMS instruments have

the ability to detect adducted ions (sodium or ammonium adducts, etc.) generated from the target analyte, and also ions generated from other compounds in the injected sample. Adducted compounds give additional information for the characterization of analytes [309]. Accordingly, post-acquisition data queries can be conducted if the need arises to obtain information about components other than the target analyte. Thus, qualitative information about compounds can be obtained from the same sample injection used for the quantitation of the target analyte. Therefore, HRMS coupled to fast-LC separation is now becoming one of the most important techniques in the field of quantitative bioanalysis [272].

HPLC separations provide peaks of relatively narrow width, even narrower when using UHPLC separations. For quantification purposes the higher acquisition speed of the mass analyzer, the higher is the number of data points across the chromatographic peak, consequently a better integration of the peaks is obtained. FT analyzers have the RP inversely proportional to the acquisition speed (i.e. the higher resolving power, the slower acquisition speed) [294,295,315]. Consequently in most of the qualitative and quantitative studies on polyphenols, using (U)HPLC coupled to a LTQ−Orbitrap XL instrument, the Orbitrap analyzer was set to operate with a RP ≤30000, which is as a compromise between RP and acquisition speed [316–319]. It is worth noting that with this RP value, the Orbitrap provide sufficiently high MA (<5 ppm). However, the last generation of Orbitrap instruments (Exactive Plus Orbitrap mass spectrometer) can easily be set to RP of 70000 as coupled to UHPLC. Using TOF-MS, RP is not affected by acquisition rates. A last generation quadrupole-TOF mass spectrometer (Synapt G2 Q-TOF mass spectrometer) is claimed to provide high RP (max. 40000) at acquisition frequencies compatible with UHPLC [320].

b. Matrix effect

Matrix effect appears when coeluting compounds induce a change in ionization efficiency of the analyte. It is considered to be the main obstacle of quantitative LC–MS methods. The exact mechanism of matrix effect is unknown, but it probably originates from the competition between an analyte and the coeluting matrix components. It is probably based on competition, during evaporation in the ionization source, between non-volatile matrix components and analyte ions for the access to the droplet surface and for the transfer to the gas phase. The coeluting compounds can alter the signal response causing either ion suppression or enhancement, which can compromise not only the accuracy, but also the

trueness of the method, since the results can be biased [272]. More detailed informations about matrix effect can be obtained in [321]. To evaluate the matrix effect, the post-extraction addition was the main strategy for the determination of phenolic compounds in food samples by UHPLC–MS. In this approach, the signal of the analyte in a standard solution was compared to that of a post-extraction spiked sample at the same concentration (matrix-matched standard) [322]. In LC–MS method, there is a need to remove or minimize the presence of matrix effect.

A strategy to avoid or minimize the matrix effect is the use of internal standards. The best internal standard is the isotopically labelled analog whose physico-chemical properties including the retention behavior, fragmentation behavior and extraction efficiency are almost identical, as compared with those of the analyte. Isotopically labelled standard [323] as well as deuterium-labelled standard [324] have been used for polyphenols quantification to reduce signal variability and improve precision. However, these compounds are not always available and most of them are very expensive.

An alternative to isotopically labelled and deuterium-labelled standards is to use as internal standards compounds closely related to the compounds of interest. Nevertheless in the case of the analysis of plant and food extracts, that contain several compounds and classes of compounds, the use of several internal standards is not practical. So generally one or up to three internal standards are selected as a compromise among all compounds that will be quantified. To improve the compensation of the matrix effect by the internal standard method, a combination of internal standard with matrix-matched calibration was suggested [325]. In this case the standards used for the calibration were prepared in the matrix.

The use of an extensive clean-up procedure prior to UHPLC–MS analysis, such as off-line LLE and off-line SPE is another reported strategy to reduce the presence of interfering components for the quantification of phenolic compounds in food samples. By using an extensive sample pre-treatment in combination with UHPLC, that provides efficient chromatographic separation, the matrix effect was reported to be low (lower than 20%) for the determination of phenolic compounds in two food samples [326,327].

1.3.5.3. Structural characterization of phenolic compounds by LC−MS/MS analysis

LC-MS techniques are very well suited for the analysis of phenolic compounds in plants and foodstuffs and play a key role on the characterization, since they can provide significant

structural information on small quantities of complex samples. LC-MS is rarely used for full structure characterization, but it provides the nominal molecular mass of the different constituents, and in the case of HRMS, the molecular formula can be assigned. With these knowledges, LC-MS/MS can be pursued for further structure characterization. The last approach has mainly been made in combination with collision-induced dissociation (CID) that provides several structural informations from the fragment ions yielded.

Useful information about the classes of the analytes can be obtained from the chromatographic retention times. For the C18- or C8-reversed-phase columns, the most frequently used, the retention time, in general, follows the expected reversed-phase pattern of benzoic acids < cinnamic acids < flavonoid glycosides < flavonoid aglycones [328].

In this section some aspects about CID-MS/MS characteristic fragmentation for the characterization of different groups or subgroup of polyphenols will be discussed.

a. Fragment nomenclature

Fragment ions yielded by mass spectrometric analysis of flavonoids are usually designated according to a widely accepted nomenclature system elaborated for aglycones [329] and glycosylated compounds [330]. The applied labels are depicted in Figure 21.

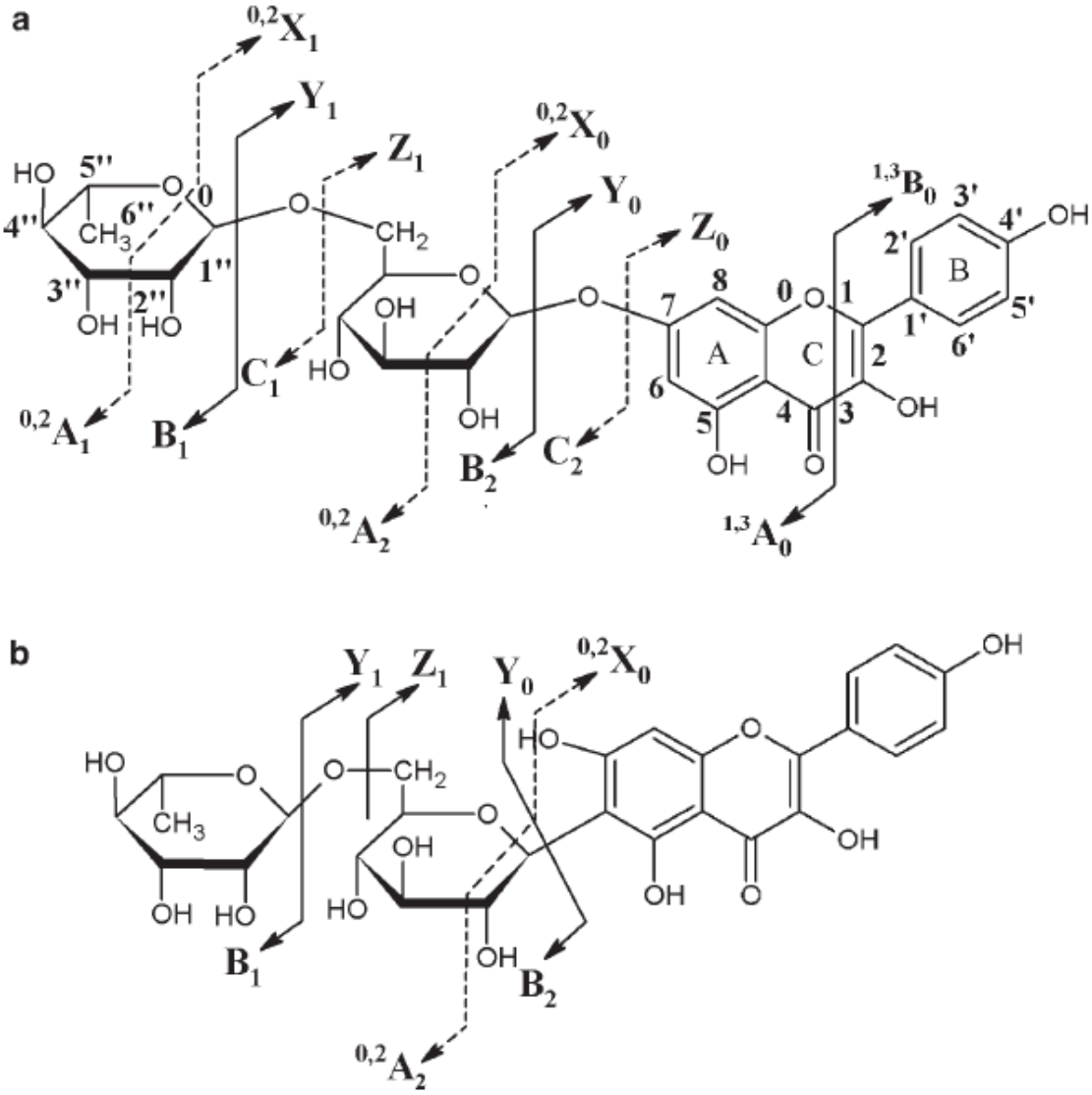

Figure 21 Fragment nomenclature commonly applied for (a) *O*-glycosides and (b) *C*,*O*- and *C*-glycosides [331].

For free aglycones, labels ${}^{i,j}A_0$ and ${}^{i,j}B_0$ are used to refer to fragments containing intact A- and B-rings, respectively, where superscripts *i* and *j* indicate the broken C-ring bonds. Glycoside fragments, with retained charges on the carbohydrate portion, are designated as ${}^{k,l}A_i$, B_i, and C_i, where *i* represents the number of glycosidic bond(s) cleaved, counted from the terminal sugar unit, and the superscripts *k* and *l* indicate the cleavages within the carbohydrate rings. A is used when cleavages are inside the sugar ring, B when the cleavage occurs in the first bond of the interglycosidic link, and C when it is observed in the second bond of the interglycosidic link (see Figure 21). On the other hand, ions containing the aglycone are labeled as ${}^{k,l}X_j$, Y_j, and Z_j, where *j* is the number of the cleaved related

interglycosidic bond, counted from the aglycone. The glycosidic bond linking to the aglycone is numbered 0. In the case of *C*,*O*-glycosides *O*-glycosylated on the *C*-glycosyl moiety (Figure 21b), as the *C*-glycosidic moiety is linked directly on the A-ring of the aglycone, the Z_0 fragment observed for *O*-glycosides is absent, as well as the last C_i fragment, corresponding to C_2 fragment in Figure 21a. For anthocyanins the discussion will be made considering MS/MS fragmentation in the positive ion mode. Therefore, the fragments aforementioned will be presented with a superscript (+), representing the charge of the fragment ion, e.g. Y_0^+, ${}^{0,2}X_0^+$, etc. For all other phenolic classes, the discussion will be based in the negative ion mode and the negative ions will be presented as Y_0^-, ${}^{0,2}X_0^-$, etc.

b. Flavonoid aglycones

Flavonoid aglycones generally undergo both losses of small molecules, such as CO, CO_2 and C_2H_2O, and retro Diels-Alder (RDA) fragmentation [328,332]. Figure 22 shows important RDA fragments observed for flavonoid aglycones. Cleavage of the C-ring by a RDA mechanism leads to ions that provide information on the number and type of substituents in the A and B-rings [333].

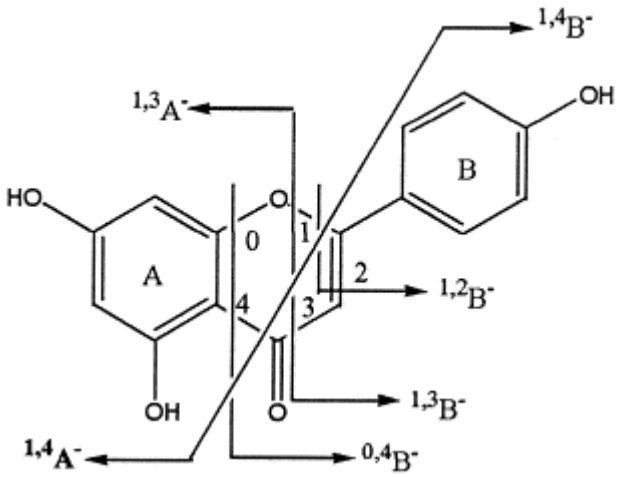

Figure 22 Nomenclature for different retro Diels-Alder (RDA) cleavages for flavonoid aglycones [332].

Figure 23 illustrates the proposed MS/MS fragmentation for luteolin (**1a**), as example of flavone aglycone fragmentation [332]. **1b** and **1f** represent neutral losses (CO and CO_2). In

further fragmentation, **1b** and **1f** lose CO or CO_2 group from the A ring, leading to fragments **1c**, **g** and **h**. Another small neutral loss, sometimes prominent, concerns C_2H_2O. This fragmentation may occur on the C ring followed by a new cyclization implying the B ring and the carbons 3 and 4 of the C ring, leading to the two plausible fragments **1d** or **1d'**. The consecutive losses of CO_2 from **1d** or **1d'** give rise to **1e** or **1e'** fragments. This latter cleavage also concerns the contraction of the A ring. In addition, the C_3O_2 loss from **1a** also implies the A ring. The resulting **1i** fragment proposed includes a methyl group and undergoes further C_2H_2O loss leading to two plausible fragments (**1j** and **1j'**). In a similar way as proposed for **1d** and **1d'**, the C_2H_2O loss involves the C ring and a cyclization implying the B ring. This allows the formation of two bicyclic fragments (**1j** or **1j'**) depending on the free rotation of the bond between carbons 2 and 1'. Concerning the RDA fragmentations, the $^{1,3}A^-$ ion can undergo further CO_2 loss leading to an ion noted as $^{1,3}A^- - CO_2$.

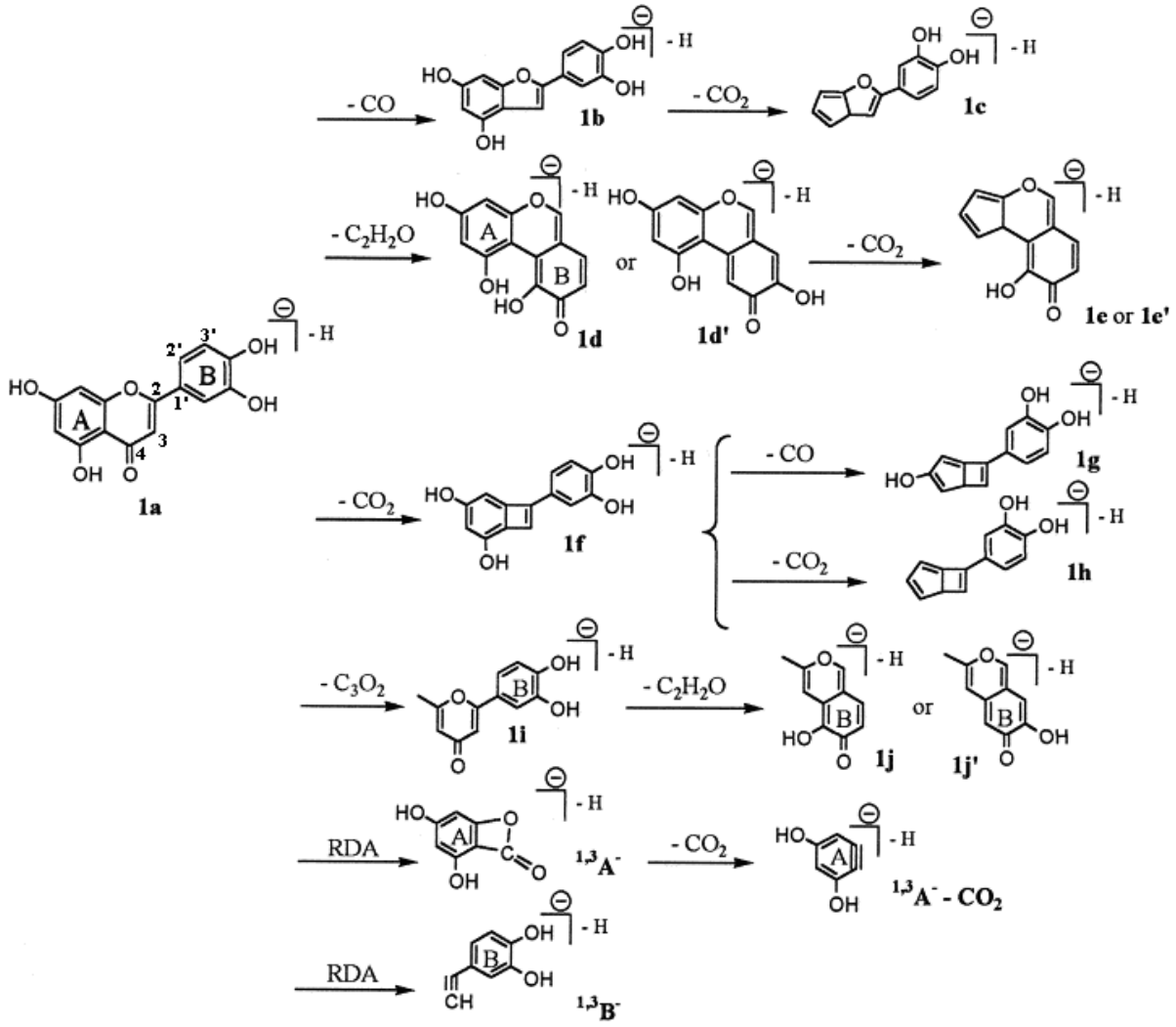

Figure 23 Proposed MS/MS fragmentation of luteolin, supported by MS^n experiments and comparison with several other flavonoid aglycones. **1c** and $^{1,3}A^- - CO_2$ ions were observed only in MS^3 experiment. Adapted from the reference [334].

The fragmentation pattern of **la** is similar to the fragmentation of other flavone compounds, as well as several flavanone and flavonol aglycones, notably by the occurrence of the initial small neutral losses of CO, CO_2, C_3O_2 and C_2H_2O groups and the $^{1,3}A^-$ fragment ion [332,335]. For flavanones, this last fragment ion is frequently reported as the major fragment ion [328,332]. Additionally, methylated aglycones are characterized by the loss of 15 u resulting in a $[M-H-CH_3]^{-\bullet}$ radical ion which generally constitutes the base peak [336].

c. Flavonoid O-glycoside, di-O-glycosides, and O-diglycoside

For *O*-glycosides, the fragmentation results in heterolytic cleavage of their hemi-acetal O–C bonds, yielding distinctive Y_i^- fragments (Figure 21). These fragments may be used for an easy characterization of the type of sugar unit, from the difference of the mass of the parent ion and the mass of the corresponding Y_i^- fragment ions. For example, differences (neutral losses) of 132 u, 146 u, and 162 u correspond to pentose, deoxyhexose and hexose losses, respectively. Di-*O*-glycosylated flavonoids present combinations of these neutral losses, e.g. 308 (146+162), 324 (162+162), etc, corresponding to deoxyhexose + hexose, or dihexoses, respectively. Additionally the Y_0^- fragment ion characterizes the aglycone moiety, which is also characterized by RDA fragment ions (see Figure 21) [337].

Differences were observed in the relative abundances of some ions for two *O*-glycosyl isomer forms, *O*-diglycosides and di-*O*-glycosides. For *O*-diglycosides, the Y_0^- ion was reported to be the base peak (100% relative abundance), and the Y_1^- of medium (approximately 22%) or low (approximately 3%) intensity. On the other hand for di-*O*-glycosides, the ions that corresponded to the loss of one sugar unit (Y_1^-ions), exhibited the highest abundance, while the ion corresponding to the loss of two sugar units (Y_0^- ions) showed approximately 30% relative abundance [338]. This approach can be useful to differentiate *O*-diglycosides and di-*O*-glycosides particularly if the two forms are present in the samples.

d. Flavonoid C-glycoside

In *C*-glycosylated flavonoids, the sugar is directly linked to the flavonoid nucleus via an acid-resistant C−C bond. The major MS/MS fragmentation pathways for these compounds are obtained by cross-ring cleavages of the saccharidic residue (Figure 24), and the loss of molecules of water [333]. In several works that analyzed different *C*-glycosylated flavonoids, the neutral losses of 60 u, 90 u or 120 u were the most reported ones [339,340], the losses of 120 u and 60 u characterizing the presence of an hexose or a pentose, respectively. Isomer compounds differing by the glycosylation at position C6 or C8, such as vitexin (apigenin-8-*C*-glucoside), isovitexin (apigenin-6-*C*-glucoside), orientin (luteolin-8-*C*-glucoside) and homoorientin (luteolin-6-*C*-glucoside) were distinguished on the basis of the intensity of the $[M-H-90]^-$ MS/MS fragment ion which was more pronounced for 8*C*-glycosylated flavonoids [339].

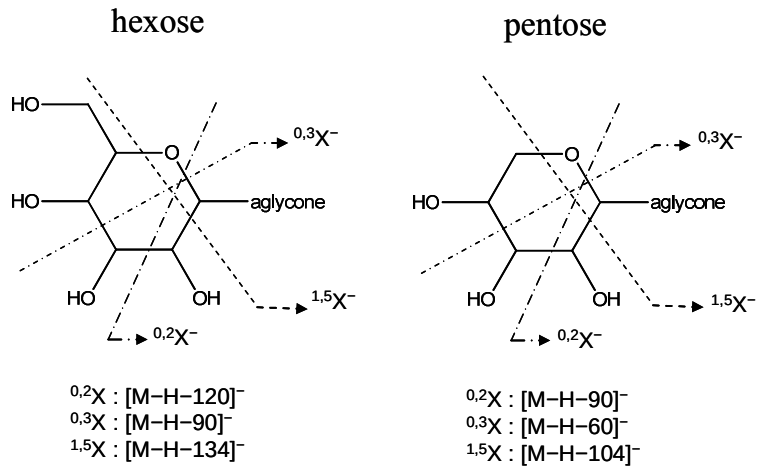

Figure 24 Characteristic product ions formed by cross-ring cleavages in a hexose and pentose residue [312].

e. Flavonoid di-C-glycosides and C-diglycosides

Di-*C*-glycosylated flavonoids have similar characteristics than the mono-*C*-glycosylated flavonoids, concerning MS/MS fragmentation, but for di-*C*-glycosides additional neutral losses are observed, corresponding to the intraglycosidic cleavages (Figure 24) occurring simultaneously in both sugar units. For example, for a di-*C*-glycoside flavonoid the following neutral losses are frequently observed: 90 u, 120 u, corresponding to the intraglycosidic cleavages of one of the two hexoses, and 210 u (90+120) and 240 u (120+120), corresponding to the intraglycosidic cleavages of the two hexoses simultaneouly [339,340]. When the oses were different (6*C*-pentose and 8*C*-hexose or vice versa), their positions were distinguished for isomer compounds, considering the relative abundances of some ions [339].

Flavonoids *C*-diglycosides correspond to compounds that are *O*-glycosylated on the sugar linked to the aglycone by a C−C bond, forming a disaccharidic unit. The intense ion corresponding to the Z_1^- ion (Figure 21) is characteristic for this type of heteroside. Neutral loss obtained from this ion (parent ion – Z_1^-) also characterizes the terminal sugar: neutral losses of 150 u, 164 u and 180 u correspond to pentose, rhamnose, and hexose, respectively [340,341].

f. Flavonoid di-C,O-glycosides

In this group of compounds, the two glycose units are attached in different positions, forming monosaccharides, corresponding to an *O*-glycosilation and a *C*-glycosilation. MS/MS fragmentation of this group presents characteristic neutral losses of both *C*-glycosylated and *O*-glycosylated flavonoids. However the main characteristic is the abundant Y_0^- ion resulting from a loss of a sugar moiety from *O*-glycosylation on a phenolic hydroxyl group [341,342].

g. Anthocyanidins and anthocyanins

MS/MS anthocyanidin fragmentation, analogously to the fragmentation observed for other flavonoid aglycone classes, can generally be classified into cross-ring cleavage of the C-ring; and ring-opening followed by subsequent loss of small neutral molecules, such as CO, C_2H_2O or H_2O (Figure 25). Crossring cleavage involves the breaking of two bonds of the C-ring. The A-type fragments are the same for most common anthocyanidin species, but the B-type fragments will differ based on the anthocyanidin type, due to changes of the substituents on the B ring [343,344]. Additionally, the loss of a 15 u, corresponding to the radical anion $CH_3^{\bullet}$ was reported to be distinctive for methoxy group containing anthocyanidins [344].

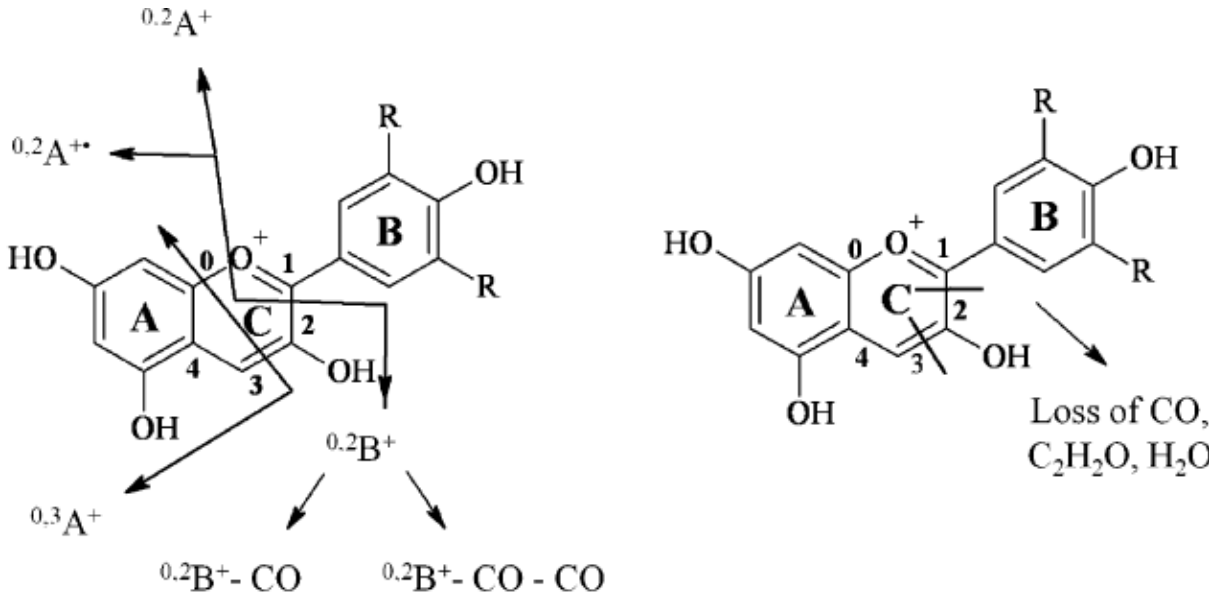

Figure 25 Fragmentation of the anthocyanidin by (left) cross-ring cleavage or by (right) neutral small molecule loss from ring opening [343].

Analysis of the *O*-diglycosylated and di-*O*-glycosylated anthocyanins showed that they also produced the above discussed $^{i,j}X_j^+$ and Y_j^+ fragments (Figure 21) [345–347].

h. Phenolic acids

Hydroxybenzoic and hydroxycinnamic acids show in their MS/MS spectra fragment ions corresponding to the loss of a CO_2 group $[M-H-44]^-$. This loss is generated from the carboxylic acid function. Aside from this loss, methoxylated compounds show the loss of a $CH_3^{\bullet}$ radical anion. For dimer compounds, a monomer is lost, as for chlorogenic acid (quinic acid + caffeic acid) that shows quinic acid as product ion. For *O*-glycosylated phenolic acids, the glycosyl type may be determined in a same way as for *O*-glycosylated flavonoids [328,348].

1.4. Generalities about *E. oleracea* fruits

1.4.1. Botanical description and geographic distribution

Euterpe oleracea Martius belongs to the Arecaceae family and is a multi-stemmed, monoecious palm with a tall, slender stem that grows up to 25 m height. The fruits form green clusters during the immature stages and become deep purple when fully ripe. Each berry has one large seed of 7–20 mm. The hard, purple epicarp is a very thin layer and the mesocarp (pulp + epicarp as shown in Figure 26) is only 1 to 2 mm thick. The seed represents the main volume of the fruit (80–95%) [1,349].

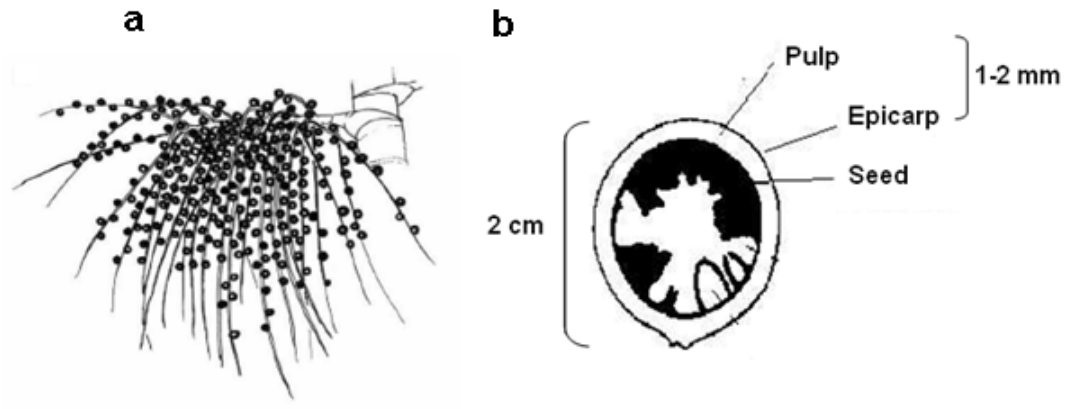

Figure 26 A bunch of *Euterpe oleracea* fruits (a) and a cross section of a fruit (b). Adapted from the references [350,351].

The *E. oleracea* palm is widely distributed in the northern part of South America, with its greatest abundance in the Amazon estuary floodplains. In these areas the islands and lands along the rivers and channels are flooded twice a day, for the regions close to the Atlantic Ocean, or in one period (≈ 5 months: January – May) of the year, for the regions where the influence of the Atlantic Ocean is lower or absent. The Pará state, in the Brazilian Amazon, is the area that has the highest abundance of this palm (Figure 27).

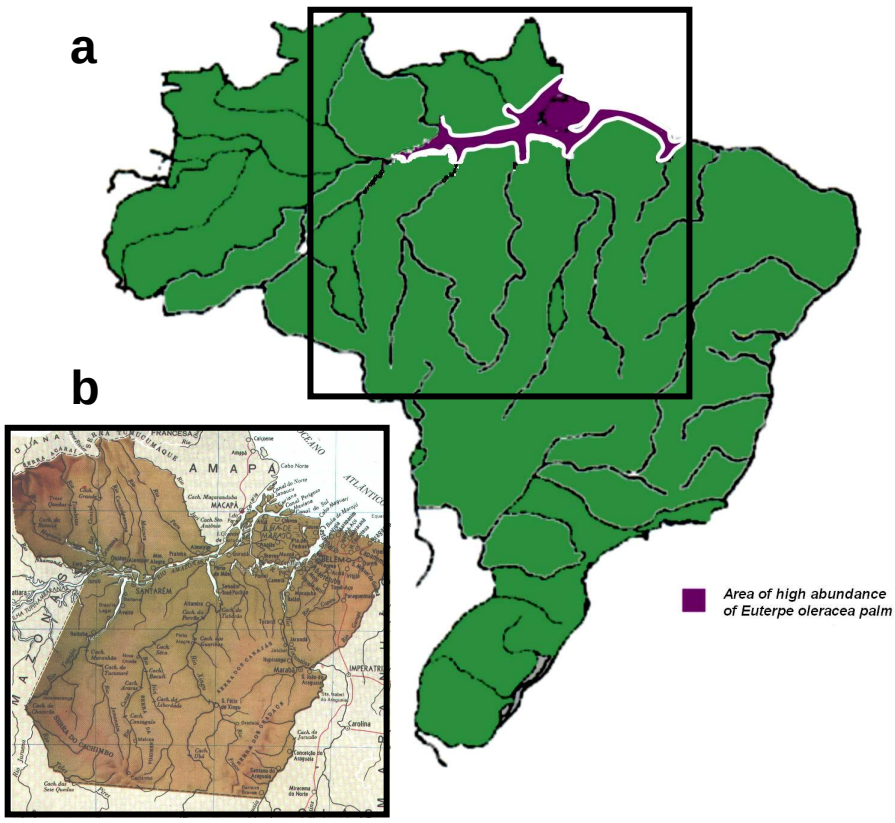

Figure 27 Area of high abundance of *Euterpe oleracea* palm in Brazil (1cm = 500 km) (a), this area is located in the Pará state (1cm = 350 km) (b). Adapted from [351].

E. oleracea fruits can be harvested throughout the year with higher yields and better organoleptic qualities during the 'dry months', August−December representing the high harvest season [286] in the delta of the Amazon schematized in Figure 27. Overall, the management of açai (systematic and organized harvest in some areas) is preferred over a systematic cultivation due to its abundance in the Amazon estuary, its adaptability to flooding and its productivity in both the forest environment as well as intensive management [352].

1.4.2. Traditional uses

The juice of *E. oleracea* fruits, called "açai juice" or simply "açai", is the most commonly consumed beverage in the eastern Amazon region, where individual consumption can reach one litre per day. Basic steps for the preparation of the juice include weighting the fruits, washing them, pulp softening and pulp crushing, and finally, filtration of the pulp to obtain the açai juice. The pulp softening consists of a maceration of the fruits in lukewarm water. The step of pulp crushing is made in an adapted juice extractor that has a cylindrical form and is placed in a vertical position. The pulp is obtained by the rotation motion of a metal shaft inside of the machine while water is added. At the bottom of the extractor there is a metallic filter for the final step of filtration [350,353]. The juice has a significant proportion of lipids, ranging from 40.7 to 60.4 percents of its dry matter, and contains 6.7 to 10.5 percent protein.

Locally, the fruits have also been used in traditional medicinal practices. The grated fruit rind is used topically for skin ulcers and infusion of toasted crushed seeds is used for fever. The seeds of *E. oleracea* were also shown to contain phenolic compounds: five different procyanidins (from di- to pentameric derivatives), furthermore, protocatechuic acid and (−)-epicatechin were identified as minor compounds [354]. It is likely that the procyanidins are partly responsible for the activities of the seeds.

Indigenous healers used the berries to treat skin complications, digestive disorders and parasitic infections such as eczema, diarrhoea, and helminth infections [352].

1.4.3. Production and global trade

Until the end of the 90's, *E. oleracea* juice was almost exclusively consumed in the Amazon region, mainly in the Pará state. From the years 2000, the Pará state started the exportation of açai juice. In 2000, the consumption in the state was of 120000 tons, 2000 tons in the rest of Brazil, and only 100 tons abroad. Since, the consumption increased significantly. In 2012, the local consumption was of approximately 240000 tons, 100000 in the rest of the country, and 25000 in other countries [355]. Exportations concern not only açai juice but also other derived products as açai juice blended with other fruits such as acerola (*Malpighia emarginata* DC.) and guarana (*Paullinia cupana* Mart.). Acerola and guarana are found to contain high levels of vitamin C and caffeine, respectively [349,356]. According to W&G Global Trade, recent açai sales from Brazil were estimated to US$45 million per year. The

Pará state is responsible for approximately 95% of the Brazilian production of açai, which is equivalent to US$63 million per year in domestic revenue. This intense economic activity is a significant source of jobs, and income, mainly for the Pará state, but also in other Brazilian regions [352].

Exports from Brazil are mainly destined to United States, Japan, Italy and the Netherlands. The US has the largest functional food and beverage market in the world and it was estimated to have an annual growth rate of 6.1 percent between 2007 and 2012. Concerns about health is driving a number of sub-trends in the US market and fuelling interest in certain ingredients, such as low-calorie sweeteners, fiber, probiotics, omega fatty acids, and antioxidants. Antioxidants are turning up in all sorts of food products, from beverages to baby food. These products are using 'superfruits' as ingredients, which are fruits that have high ORAC values. Common superfruits include blueberries, pomegranate, açai and cranberry. Overall, between 2003 and 2008, pomegranate and açai appeared in the greatest number of new products. These trends demonstrate that consumers are increasingly looking for antioxidants, which they associate with health promotion, mainly in terms of the prevention of cancer, cardiovascular diseases, and neutralization of free radicals [1].

1.4.4. Phenolic compounds of E. oleracea *fruits*

The major phenolics of ripe *E. oleracea* fruits are the anthocyanins, mainly cyanidin 3-glucoside and cyanidin 3-rutinoside. The individual concentrations of these compounds are very variable [286,353,357]. The highest value already reported for the sum of these two compounds was 2890 mg/Kg fruits. Other anthocyanins were reported, such as peonidin 3-rutinoside, peonidin 3-glucoside, pelargonidin 3-glucoside, but at very low concentrations [358]. In contrast, much more different non-anthocyanin polyphenols have been identified e.g. rutin, homoorientin, orientin, taxifolin deoxyhexose, isovitexin, scoparin, (+)-catechin, (−)-epicathechin, procyanidin dimers and trimers [359], phenolic acids, such as protocatechuic, vanillic and caffeic acids, etc [353], but in quantitative terms, they have a lower total concentration than the anthocyanins [359]. Among them, there are also two major compounds, orientin and homoorientin. The sum of their concentrations is over 50% of the total of non-anthocyanin polyphenols [359].

1.4.5. Health benefits

Juice and pulp of *Euterpe oleracea* fruits have substantially higher antioxidant capacities compared to other dark-colored berries, fruits or vegetables, as measured either by the oxygen radical absorbance capacity (ORAC, see section 1.2.5.) [360] or the total oxidant scavenging capacity (TOSC[*]) [1,286] assays. Non-anthocyanin flavonoids isolated from *E. oleracea* pulp also presented a high antioxidant activity measured by ORAC [361].

E. oleracea juice has become a product of international interest, not only because of its exotic flavor, but also because of its potential benefits for human health. In fact, many studies demonstrated that polyphenol-rich diets are directly associated with reductions in cardiovascular diseases [141,362–366]. The presence of a high quantity and variety of antioxidant compounds in the fruits is very promising regarding health benefits. An increase in the antioxidant capacity of plasma after *E. oleracea* juice consumption by healthy volunteers was observed, using the total reactive antioxidant potential (TRAP[**]), the trolox equivalent antioxidant capacity (TEAC[***]) [367], and the ORAC methods [368], indicating that the polyphenols absorbed had antioxidant activity *in vivo*. Moreover, it has been observed *in vitro* that polyphenolic extracts of açai protected human vascular endothelial cells upon oxidative stress and inflammation [369]. Therefore, these compounds could play a role in the prevention of cardiovascular diseases.

1.4.6. Liquid chromatography based analytical methods for phenolic compounds from E. oleracea *fruits*

In general, the açai samples analyzed in the phytochemical literature are juices but they can also be derived products such as powders. In many cases the samples were acquired at the market and no detailed information is provided on the process of production of these samples [358,370]. One of the main steps during the sample preparation for analysis is the clean-up procedure by either liquid-liquid extraction (LLE) for the juices or solid-liquid extraction for

[*] The TOSC assay is based on the ethylene-yielding reaction of α-keto-γ-methiolbutyric acid with either peroxyl radicals, hydroxyl radicals, or peroxynitrite. The capacity of the analysed compound(s) or extract to inhibit this ethylene production from the three oxygen reactive species are analysed by gas chromatographic ethylene quantification.

[**] TRAP assay is based on the oxygen uptake associated to the peroxidation process of human plasma. The method evaluates the induction period (lag time), generated in the kinetic profiles of oxygen uptake during the incubation of human plasma with AAPH (a peroxyl radical generator).

[***] TEAC assay is based on the scavenging ability of antioxidants to the radical cation $ABTS^{\bullet+}$. In this assay, ABTS is oxidized by peroxyl radicals or other oxidants to its radical cation, which is intensely colored, and the antioxidant capacity is measured as the ability of test compounds to decrease the color reacting directly with the $ABTS^{\bullet+}$ radical. Results of test compounds are expressed relative to Trolox (the water-soluble analog of vitamin E).

the powders in order to eliminate lipophilic compounds. The solvents used for these procedures are mainly petroleum ether and hexane [353,371]. Solid-phase extraction (SPE), using C18 cartridges is also frequently used. This process allows not only to eliminate lipophilic compounds, but also to isolate different classes of phenolic compounds. Elution steps of the SPE procedures consisted, in a simplified form, in the elution of non-anthocyanin polyphenols with ethyl acetate, followed by an elution of the anthocyanins with methanol while the lipophilic compounds remain on the cartridge [372]. LLE has also been used to obtain different fractions of phenolic compounds. For example, when LLE is performed with ethyl acetate on an aqueous solution containing phenolic compounds, most of the non-anthocyanin polyphenols are extracted by the organic phase and the anthocyanins remain in the aqueous solution [359].

Liquid chromatographic as well as mass spectrometric conditions used for the analysis of phenolic compounds of *E. oleracea* fruits were similar to those already discussed in the previous sections related to the analysis of polyphenols. Basically, these conditions consisted in the use of (U)HPLC C18 columns, acidified aqueous solutions and methanol, acetonitrile, or mixtures of both organic solvents, as eluents. Non-anthocyanin polyphenols and anthocyanins are analyzed in the negative and positive ion mode, respectively. In general, good HPLC separation is observed for the phenolic compounds of *E. oleracea* fruits, but long run times are required, generally in the range between 60 and 90 min [286], but some important exceptions have been reported, as for the separation of major non-anthocyanins polyphenols, namely, orientin and homoorientin, for which a supplementary gradient elution was used to improve separation for quantitative purposes [353]. Recently UHPLC C18 columns have been introduced as stationary phase for the separation of phenolic compounds of *E. oleracea* fruits, in a qualitative and semi-quantitative study. Reduction of the retention times and consequently of the solvent consumption were observed, as compared to the HPLC methods. Nevertheless, full separation of major non-anthocyanin polyphenols was not reached [373]. Up till now, only few studies used this technique for polyphenols of *E. oleracea* fruits [373,374].

System detection in the analysis of phenolic compounds of *E. oleracea* is usually based on DAD and mass spectrometry. The first one is very advantageous because polyphenols exhibit a high response in terms of absorbance, as discussed in the previous section. Particularly, this system of detection is very suitable for anthocyanins, because they can be selectively distinguished from the other classes of phenolic compounds, since the other

flavonoids and phenolic acids are not detected by wavelengths >500 nm [371]. In addition, UV-Vis spectra obtained by DAD have been useful for the characterization of the classes of phenolics. The maximum wavelength of absorption gives information, at least, on the type of class to which the compound belongs [358]. On the other hand, DAD can be not sensitive enough for compounds at low concentrations, with very low signal-to-noise ratios [358,371]. In contrast, MS detection showed to be very useful to detect and quantify phenolics at low concentrations in samples of açai juice. Several compounds were quantified by Gordon et al. by a LC-MS/MS method [353]. In addition it shows better selectivity in the signal detection, because it can discriminate co-eluted or very closely eluting compounds on the basis of their molecular ions (extracted ion chromatograms (EICs) and SIM chromatograms) or on the basis of precursor–product reactions (SRM chromatograms), as also observed in some works [353,373]. On the other hand, in MS detection, it is not possible to distinguish co-eluting isomer compounds, so that, if they are not fully separated, the signal of an isomer will interfere with the signal of the other, as observed for major non-anthocyanin polyphenols in a recent work [373]. In this case, no accurate quantification can be obtained.

For quantitative analysis, both DAD [286] and MS detections [353] were used. As anthocyanins are generally present in high concentrations in the samples, DAD detection is sensitive enough to quantify them [286]. When we started our research, no validated method was published to quantify anthocyanins. We developed an UHPLC-DAD method [374] (see Chapter 2) whereas another team developed a LC-HRMS method [375]. On the other hand, other less concentrated non-anthocyanin polyphenols generally were quantified with MS detection [353]. However, an important disadvantage of the MS detection is that the analytical response of the analyte is very often compound and matrix-dependent. In MS, it is very important to quantify each analyte with its respective calibration curve, because the ionization can vary depending on the molecular structure. However, when commercial phenolic standards were not available, the phenolic compounds were tentatively quantified with respect to other similar phenolic compounds [271]. Gordon et al. used the corresponding standard for each of the several compounds quantified of *E. oleracea* juice [353]. Additionally, the matrix of the samples can interfere with the response of the analyte, so that a calibration curve in the matrix is useful to improve the accuracy of the quantification [272]. Up till now, no LC-MS method addressed the matrix effect in the analytical response of the analytes.

Thesis aims

General purposes

The general purposes of this thesis are to characterize and quantify phenolic compounds in fruits and juices of *Euterpe oleracea* in order to improve the added value of these foods and consequently to contribute to the development of the Amazon region.

Phenolic compounds have potential health benefits, mainly as antioxidant substances. Characterization of phenolic compounds in foods improves the knowledge on their phenolic profile and helps producers to determine quality parameters for their products. Therefore, the phenolic profile represents an added value to the products. Additionally, the phenolic composition of the products is a requirement of purchasers and regulatory bodies. Thus, methods used for phenolic characterization can contribute to the quality control of the products, and for research purposes, they can help to the optimization of fruit and juice processings in order to improve their quality.

General objectives

- To identify major (anthocyanins) and minor (non-anthocyanin) phenolic compounds in fruit extracts and juices of *E. oleracea*;
- To quantify both major and minor compounds.

Specific objectives:

- To develop an extraction procedure for anthocyanins directly from the fruits.
- To develop an extraction procedure for non-anthocyanin polyphenols from lyophilized juice.
- To develop two UHPLC-PDA-HRMS-MS^n methods to separate, identify and quantify
    - the anthocyanins
    - the non-anthocyanin polyphenols
- To validate the methods for the quantification of the major compounds of each group studied:
    - the anthocyanins, using PDA detection
    - the non-anthocyanin polyphenols, using HRMS detection

To apply the quantification methods on different batches of products: fruits and juices.

2. A rapid validated UHPLC-PDA method for major anthocyanin quantification from *Euterpe oleracea* fruit extracts

This chapter was adapted from the following article:

Journal of Chromatography B, 907 (2012) 108– 116

2. UHPLC-PDA method for major anthocyanins from *E. oleracea* fruit extracts

Euterpe oleracea fruits contain high quantities of anthocyanins, mainly cyanidin 3-glucoside and cyanidin 3-rutinoside. Among other reasons, the fruit juices interested the food industry because those compounds give potential health benefits, mainly associated with their antioxidant activities. Moreover, products derived from the fruits, such as purified extracts, have demonstrated several applications, as natural pigments, and dietary supplements. At the beginning of this work, no validated analytical method, based on liquid chromatography, was available in the literature for the quantification of anthocyanins of the fruits and derived products, such as fruit extracts. The validation of a method is a crucial step for the different institutions interested in the reliability of the results. Moreover, the methods of the published works were very time-consuming and some of the works showed anthocyanin profiles qualitatively and quantitatively very different. They mainly analysed commercial juices and powders, for which no detailed information was given with respect to the processing of the initial samples, which can partially explain the different profiles observed. On the other hand, for the producers and research institutions of the Amazon region, such as the partner university (UFPA), the accessibility of fruits is favored by the proximity of the production zones, so that a rapid extraction procedure directly on the fruits can be helpful, avoiding further steps for the preparation of the juices. Additionally, the partner university has the possibility to study fruits harvested in a specific location of production.

Therefore, this chapter presents the development and validation of a rapid analytical method for the identification and quantification of anthocyanins of *E. oleracea* fruit extracts. This work was performed with the collaboration of research groups of ULg, UFPA and UCL. The developed method will help producers and researchers in Brazil and in Belgium to know the anthocyanin composition of the fruits of a specific region and will be a support for other studies in order to improve the quality of the fruits.

2. UHPLC-PDA method for major anthocyanins from *E. oleracea* fruit extracts

ABSTRACT

The aim of this work is to develop the first validated UHPLC–PDA method for major anthocyanin quantification in *Euterpe oleracea* fruit extracts after fast extraction procedure and samples preparation. The separation was performed on HSS C18 column (1.8 μm) using a gradient elution with acetonitrile and 5% formic acid in a total run time of only 17 min. Total error and accuracy profiles were used as criteria for the validation process. Calibration in the matrix was found to be more accurate than calibration without matrix. Trueness (<6.76% relative bias), repeatability (<4.6% RSD), intermediate precision (<5.3% RSD), selectivity, response function and linearity for major anthocyanins, cyanidin-3-glucoside and cyanidin-3-rutinoside, were evaluated. The concentration range validated was 1–48 μg/mL for both compounds. In addition, two cyanidin-di-*O*-glycosides were detected for the fist time in this fruit. We also showed that a first extraction of the fruits with ethyl acetate removes the lipophilic compounds and allows an easier extraction by methanol and quantification of anthocyanins in this extract.

2.1. Introduction

It is generally accepted that anthocyanins are the most important pigments in vascular plants. These pigments are responsible for the blue, purple, red colors and intermediate hues present in many plant tissues. They belong to the very large class of molecules called flavonoids synthesized via the phenylpropanoid pathway. There are hundreds of anthocyanins (glycosides) in nature that are derived from several anthocyanidins (aglycones). The main differences between them are the number of hydroxylated groups, the nature and the number of bonded sugars, the aliphatic or aromatic carboxylates bonded to the sugar and the position of these bonds [376,377]. Anthocyanin extracts from fruits are of great interest for the food industry and health sector. In fact, many biological activities of the anthocyanins related to their potent antioxidant properties are described in the literature [378,379].

The palm *Euterpe oleracea* is widely distributed in northern South America. It is particularly abundant in the floodplains of the Amazonian delta where it has high economic importance. The fruits are mainly harvested between July and December. They are round-shaped drupes (diameter of about 12 mm) and associated in racemes [1]. The seed represents around 85% of the volume of the fruit. The epicarp is a thin layer and the mesocarp is 1–2 mm thick [350]. The fruit color goes from green to black during the ripening process. In addition, fully ripen fruits are covered with a wax cuticle [1]. The ripen fruits have a very high content in phenolic compounds and, notably, anthocyanins. Cyanidin-3-rutinoside (cy3rut) and cyanidin-3-glucoside (cy3glu) are the major anthocyanins in *E. oleracea* fruits (EOF) [1,371,380] and, as a consequence, the content of anthocyanins attributed to fruit or fruit juices are basically based on these two compounds [286,357]. Some other minor anthocyanins have been identified in trace levels, like pelargonidin- 3-glucoside, peonidin-3-glucoside, cyanidin-3-sambubioside, and peonidin-3-rutinoside [358,381]. The fruits have also presented substantially higher antioxidant activity than most other fruits [286,382]. This contributed to the huge increase of the exports from Brazil and internal consumption of this fruit observed recently [352].

EOF are harvested at different maturity stages. Recently, special attention has been given to the analysis of phenolic compounds of EOF during ripening [353,357] and to fingerprinting analysis of dietary supplement raw materials derived from this fruit [373]. In fact, accurate characterizations of these compounds from reliable analytical methods are very important for the post-harvest and food industry. In addition, the validation of analytical methods gives to laboratories as well as to regulatory bodies “guarantees” of the reliability of

the measures [383], which improve the confidence of producers and consumers on the products. To our knowledge, no article describing a (U)HPLC–UV method for the quantification of the major anthocyanins from EOF has been validated [286,350,353,357–359,372,381,384], probably, for some of them, because they are not so recent. One poster was found about method validation and analysis of the major anthocyanins from EOF using UPLC and HPLC methods, but no validation data were available [385]. The run times of these HPLC methods are very long. Nowadays, the use of UHPLC methods has become a trend because of improved resolution, higher sensitivity and reduction of the run time and solvent volumes [386]. A few validated UHPLC methods have been reported for the quantification of cy3glu and/or cy3rut [387–390]. But these methods analyzed milk-based products or biological fluids and tissues for bioavailability and pharmacokinetic studies. They use MS detectors for the quantification in trace levels. Therefore, the sample matrix of these methods is very different of a plant matrix. In addition, these compounds are present in EOF in high and variable concentrations [286,357]. In this case, the validation of a wide dosing range, with concentration levels covering also high concentrations, is more suitable. The use of highly sensitive MS detectors is adapted for trace analysis. However, the PDA detectors are sensitive enough for the concentration of cy3glu and cy3rut generally found in EOF [286,350,358,359,371,381]. The aim of this work is to develop and validate an UHPLC–PDA method for the cy3glu and cy3rut quantification in EOF after fast extraction procedure and sample preparation.

2.2. Experimental

2.2.1. Chemicals and plant material

Cy3glu (98.0%), cy3rut (97.2%), pelargonidin-3-glucoside (100%), peonidin-3-glucoside (95.0%), peonidin-3-rutinoside (95.5%) and cyanidin-3,5-diglucoside were purchased from Extrasynthèse (Genay, France). HPLC grade acetonitrile from Fisher Scientific (Tournai, Belgium) and formic acid from Prolabo, VWR (Leuven, Belgium) were used for the UHPLC runs. The Chromabond® C18 cartridges (1 g/6 mL) were acquired from Macherey-Nagel (Düren, Germany).

The EOF were harvested in the municipal district of Abaetetuba, between July and December 2010, at four different maturity stages, identified as A, B, C, and D, corresponding to the maturity stages 2, 6, 8, and 11, respectively, according to Rogez et al. [357]. The

following fruit characteristics were used to classify the maturity stages: 20% of black fruits and 80% of green fruits (A), 100% of black and bright fruits (B), 60% of black fruits and 40% of opaque fruits (C), and finally, 100% of black fruits with intense gray coverage due to the presence of the intense wax cuticle (D). The samples were quickly transported to the laboratory in Belém (Pará State, Brazil) and immediately processed.

2.2.2. Extraction and clean-up procedure

The fruit samples were weighed (49.1–50.3 g) and introduced in 150 mL brown glass bottles. The fruits were extracted sequentially by EtOAc (0.1% HCl), MeOH (0.1% HCl) and MeOH/H_2O (50/50, v/v) (0.1% HCl) (Figure 28). Each extraction was carried out twice with a ratio fruits/solution of 1:3 (g / mL), for 30 min, at ambient temperature and without shaking. The extracts were called EtOAc, MeOH, and MeOH 50% extracts, respectively. The extracts were centrifuged for 10 min at 4300 × g. The residue of the EtOAc extract was re-extracted in MeOH/HCOOH (99/1, v/v) (10.0 mL) by ultrasound extraction (5 min), the other residues were re-extracted in their respective extraction solution. After centrifugation, the supernatants of each extraction were mixed before drying. The supernatants of the EtOAc and MeOH extracts were evaporated to dryness with an acid-resistant CentriVap® vacuum concentrator (Labconco, Kansas City, MO) at 40 °C. The MeOH 50% extract supernatant was concentrated in the same conditions and, then, freeze dried. They were stored at −21 °C and sent to Belgium to be analyzed.

As the EtOAc extract was a little viscous, probably due to the presence of nonpolar compounds, like lipids and chlorophylls, it was purified by solid phase extraction (SPE) (Figure 28). First, the extract was reconstituted in MeOH/H_2O/HCOOH (90/9/1) to the concentration of 14 mg/mL (for all EtOAc extracts) and 0.80 mL was applied on a C18 SPE cartridge (1 g/6 mL) (Chromabond, Düren, Germany). This cartridge was previously conditioned in MeOH/H_2O/HCOOH (90/9/1). Then, the anthocyanins were eluted with 9.0 mL of MeOH/H_2O/HCOOH (90/9/1) and recovered in a test tube. Afterwards, the anthocyanin fraction was evaporated to dryness with a RapidVap multi-tube evaporator (Labconco), which was adjusted at 40 °C. The dried fraction was called “anthocyanin fraction” and was stored at −21°C until analysis.

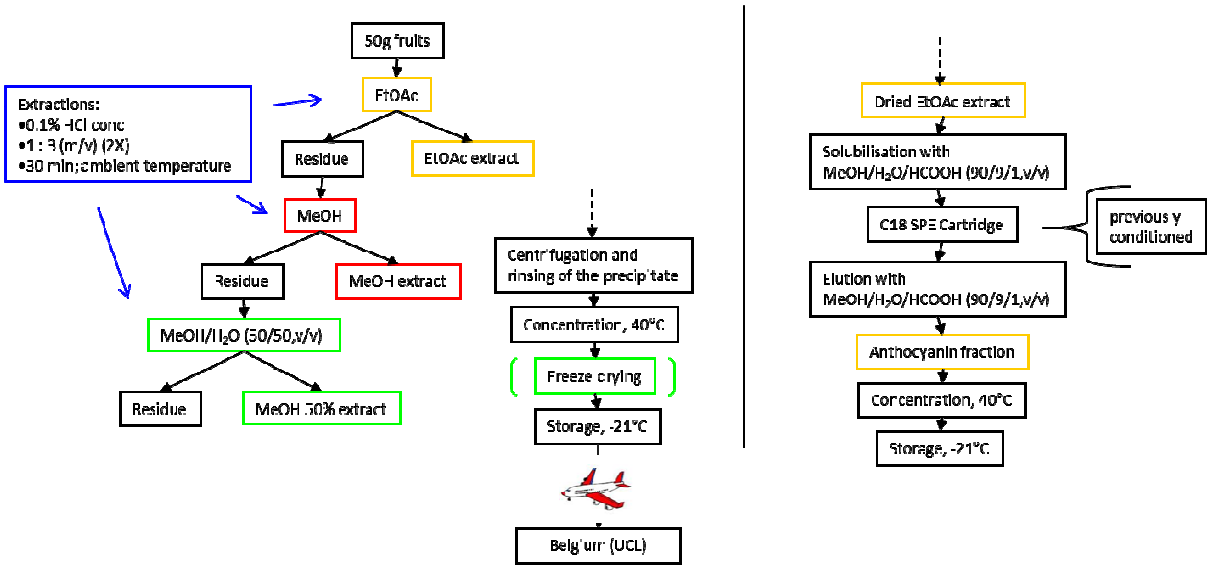

Figure 28 Extraction of *E. oleracea* fruit and clean-up procedure of the EtOAc extract.

The day of the analysis, the totality of the anthocyanin fraction, obtained from each SPE, was solubilized with 1.0 mL of MeOH/ACN/H_2O/HCOOH (15/5/75.25/4.75) (Solution S). The solubilized fraction was then filtered on a 0.2 µm filter (Interchrom, Montluçon, France) and immediately injected into UHPLC.

The solutions from dried MeOH and MeOH 50% extracts were prepared at 0.25 mg of dried extract/mL. The final solvent composition of this solution was the same as the solvent composition of the Solution S. The solutions were also filtered and directly injected into UHPLC.

2.2.3. Apparatus and UHPLC–PDA–ESI-MS/MS analysis

The analyses were performed on an Accela UHPLC system acquired from Fisher Scientific (Thermo Fisher Scientific, Bremen, Germany) that consisted of a PDA detector, an autosampler equipped with a column oven and a tray compartment cooler, and a quaternary pump with a built-in solvent degasser, all piloted by ChemoQuest software. The chromatographic separation was performed on an Acquity UPLC HSS C18 column 1.8 µm, 100 mm × 2.1 mm ID (Waters, Belfast, Ireland), which was equipped with a VanGuard UPLC HSS C18 pre-column 1.8 µm, 5 mm × 2.1 mm ID, obtained from the same supplier. 5 µL of samples was injected in a full loop injection mode. The separations were performed with a constant flow rate of 400 µL/min with the eluents being (A) H_2O/HCOOH (95/5) and (B)

CAN, and with the following gradient program: 0–10 min: 5–15% B; 10–10.1 min: 15–95% B; 10.1–12 min: 95% B; 12–12.1 min: 95–5% B; 12.1–17 min: 5% B. The column oven and tray cooler temperatures were set to 30 and 4 °C, respectively. For the quantitative analysis the PDA detector was used at 515 nm. The quantification was performed using the external calibration method.

The Accela UHPLC system was hyphenated with a LTQ−Orbitrap XL mass spectrometry system (Thermo Fisher Scientific, Bremen, Germany), from UCL MASSMET platform. This system was employed to perform the identifications and evaluation of the selectivity of the method for all extracts and all maturity stages, using the same separation conditions aforementioned. The system was equipped with an ESI interface that was used in positive ionization mode with the following conditions: capillary temperature and voltage at 270 °C and 9 V, respectively, ion spray voltage at 5 kV and tube lens voltage at 95 V. Nitrogen was used as the sheath gas and helium as auxiliary gas with a flow rate of 20 and 10 arbitrary units. The compounds were identified by comparison with reference compounds from retention times, MS and MS/MS analysis. For the MS experiments, two scan events were applied. The first was a full MS scan, for which the spectra were recorded in the range of *m/z* 100–1000 with a resolution of 30,000. The second was a data dependent scan that selected the most intense ion (or specified ions in another setting) from the first scan event, for the acquisition of MS/MS spectra. The collision-induced dissociation (CID) activation was set to a normalized collision energy of 20% or 15%. An external calibration of the equipment for mass accuracy was carried out the day before the analysis, according to the manufacturer's guidelines.

2.2.4. Standard solutions

The Stock solution containing cy3glu and cy3rut at 0.98 and 0.972 mg/mL, respectively, was prepared in MeOH/HCOOH (99/1) and stored at −21 ◦C. Good stability of anthocyanins is known in similar storage conditions [391]. An aliquot of this solution was diluted to 98.0 and 97.2 µg/mL (cy3glu and cy3rut, respectively) to have the same final solvent composition as Solution S. This solution, called "Standards Intermediate Solution 1", was diluted to obtain the calibration standards at 5 concentration levels (m = 5) ranging from 1.0 to 49.0 for cy3glu and from 1.0 to 48.6 µg/mL for cy3rut. Each concentration was analyzed three times (n = 3), for 3 series of experiments (k = 3). Another set of calibration standards was prepared in the

MeOH extract itself in order to compare the calibration with and without matrix. A solution of MeOH extract (maturity stage B) of 0.5 mg/mL was prepared (final solvent composition = Solution S composition) and was used to prepare the calibration standards in the matrix. They were prepared by diluting in the extract the same volumes of Standards Intermediate Solution 1 that were employed for the preparation of the calibration standards without matrix. The signals from the cy3glu and cy3rut, initially present in the extract, were subtracted from the peaks obtained with these solutions. The final concentration of the extract in each solution was the same (0.25 mg of extract/mL). The number of concentration levels, series and repetitions per series were the same as without matrix calibrations (m = 5, k = 3 and n = 3).

The validation standards were prepared in the same way as the matrix based calibration standards. Five concentrations were analyzed (m = 5) and the dilutions from the stock solutions of standards and extract were independent for each sample (n = 3). Three series (k = 3) of experiments were performed.

2.2.5. Evaluation of the SPE clean-up procedure and the matrix effect

For the clean-up procedure of the EtOAc extract, the recovery (RE) of the SPE process was determined, along with the overall "process efficiency" (PE) and the matrix effect (ME). It was calculated for both cy3glu and cy3rut, according to an adaptation of the procedures of Matuszewski et al. [392]. From the standard stock solution, an intermediate solution called "Standards Intermediate Solution 2" was prepared at 196.0 and 194.4 µg/mL (cy3glu and cy3rut, respectively) for a final solvent composition of MeOH/H_2O/HCOOH (90/9/1). Three different SPE called SPE 1, SPE 2 and SPE 3 were performed, each one in triplicate, as described below from a solution of EtOAc extract of the maturity stage B.

Along with the extract solution volume, an additional volume of 0.125 mL was applied on the SPE cartridges. This volume consisted of a blank solution of MeOH/H_2O/HCOOH (90/9/1) that was applied for SPE 1 and SPE 2 cartridges, while it consisted of the Standards Intermediate Solution 2 that was applied for SPE 3 cartridges (spiked with standards before SPE extraction). After SPE elution and drying of the fraction, the same volume of 0.125 mL of the blank solution was applied in the tubes containing the anthocyanin fraction obtained from SPE 1 and SPE 3, while 0.125 mL of Standards Intermediate Solution 2 was applied in the tubes containing the anthocyanin fraction obtained from SPE 2 (spiked with standards after SPE extraction). The solutions in all tubes were adjusted to 1.0 mL and the final solvent

composition was the same as the solvent composition of the Solution S, cited in section 2.2.2. Finally, in order to have a reference of the standard responses without SPE, 0.125 mL of the Standards Intermediate Solution 2 was diluted in triplicate, in new tubes, to 1.0 mL. The final concentrations of this solution were 24.5 and 24.3 µg/mL for cy3glu and cy3rut, respectively, and the final solvent composition was also the same as the Solution S. All solutions of anthocyanin fractions obtained from SPE 1, SPE 2 and SPE 3, as well as the diluted Standards Intermediate Solution 2 (reference without SPE) were filtered and injected into the UHPLC for peak area recording.

The ME, RE and PE values for the cy3glu and cy3rut were calculated as follows:

$$\text{ME}\,(\%) = \frac{\text{MPA2} - \text{MPA1}}{\text{MPAs}} \times 100 \quad \text{Eq. 24}$$

$$\text{RE}\,(\%) = \frac{\text{MPA3} - \text{MPA1}}{\text{MPA2} - \text{MPA1}} \times 100 \quad \text{Eq. 25}$$

$$\text{PE}\,(\%) = \frac{\text{MPA3} - \text{MPA1}}{\text{MPAs}} \times 100 \quad \text{Eq. 26}$$

where MPA1, MPA2 and MPA3 are the mean peak areas of the compounds of the anthocyanin fraction obtained from SPE 1, SPE 2 and SPE 3, respectively, and MPAs are the mean peak areas of reference without SPE.

The response of the cy3glu and cy3rut spiked after SPE extraction (MPA2 − MPA1) were back-calculated from a calibration curve prepared in the matrix (MeOH extract), whose preparation was explained in Section 2.2.4. Eq. 24 and the back-calculated concentrations were used to evaluate the influence of the matrix on the detection and on the quantification from a calibration curve prepared in the matrix. For the MeOH 50% extract of maturity stage B, only the matrix effect was evaluated, as it did not undergo a SPE process. The procedure for this evaluation is the same as previously described. The extract solution was prepared at 0.5 mg/mL and had the same final solvent composition of the Solution S. In order to measure MPA 2 (spiked solution referred to in Eq. 24), the extract solution was spiked with the intermediate solution 1, cited in section 2.2.4, with a final concentration of 24.5 and 24.3 µg/mL for cy3glu and cy3rut, respectively. To measure MPA 1 (not spiked), the extract

solution was diluted twice with blank solution S. Finally, the Standards Intermediate Solution 1 was diluted to the same concentration but in blank solution S in order to have the reference without matrix (MPAs in Eq. 24). All solutions were prepared in triplicate and injected into UHPLC to record the peak areas, to calculate ME and to evaluate the back-calculated concentrations, as for the EtOAc extract.

2.2.6. Validation of the method

The validation of the method was realized from three series of experiments. For each series, the eluents of the mobile phase were renewed and 78 injections were performed. From these series, the following criteria were tested: response function, linearity, selectivity, precision (repeatability and intermediate precision), trueness, accuracy, limits of detection (LOD) and quantification (LOQ) and matrix effect. Total error was used as decision criterion for the validation process [383,393–395]. The acceptance limits were set at $\lambda = \pm 20\%$ and the minimum probability to obtain future results within these limits was set at $\beta = 95\%$ (β-expectation limits). Statistical analyses were performed using the e-noval V3.0 (Arlenda, Liège, Belgium) software.

2.3. Results and discussion

2.3.1. Extraction, SPE clean-up procedure and matrix effect

A sequential extraction method with different solvents was developed for the extraction of anthocyanins. On the surface of the fruits, a thin layer of lipids could interfere with the transfer of anthocyanins, from the cells to any polar extraction solution, in the conditions of extraction used in this study. Thus, before applying quite polar extraction solutions, as MeOH, a less polar solution, the EtOAc (0.1%HCl), was applied to remove the lipids and other apolar compounds like chlorophylls and to begin the extraction of the anthocyanins.

We developed a clean-up procedure for the EtOAc extract by SPE from C18 cartridges and observed that a complete elution of the anthocyanins was obtained with 7.0 mL of MeOH/H_2O/HCOOH (90/9/1), for the different maturity stages. No further anthocyanin elution was observed after an additional elution with 6.0 mL of acidified MeOH (data not shown).

The matrix effect (ME ± SD) was calculated by Eq. 24 and gave 94.5% (±2.0) and 96.7% (±1.9) for cy3glu and cy3rut, respectively, indicating no significant influence of the matrix on the response. The back-calculated concentrations of the spiked solution from a calibration curve in the MeOH extract matrix, as described in section 2.2.5, were 23.7 (SD ± 0.5) and 24.2 µg/mL (SD ± 0.5) for cy3glu and cy3rut, respectively, which were not significantly different from the spiked concentrations of cy3glu and cy3rut (24.5 and 24.3 µg/mL, respectively). These results confirm that the responses of the "anthocyanin fraction" can be analyzed from the calibration curve in the MeOH extract matrix.

The recovery (RE ± SD) was calculated by Eq. 25, as described in section 2.2.5. The RE values were 58.7% ± 4.9 and 74.6% ± 3.6 for cy3glu and cy3rut, respectively. These values were taken into account for the calculation of their concentrations in the EtOAc extract. Recoveries of these orders can be used to correct the final results [396]. In addition, the recoveries obtained have a good repeatability. Similar values of "process efficiency" (PE ± SD) were obtained, according to Eq. 26, which corresponded to 55.4% ± 4.0 and 72.0% ± 2.4 for cy3glu and cy3rut, respectively, which is logical as no matrix effect was observed. The recovery obtained was inferior to the one obtained by Pacheco-Palencia et al. [397], who used a C18 cartridge, and an acidified MeOH as eluent, for anthocyanin extraction from the clarified *E. oleracea* juice. Considering that the SPE conditions were relatively similar, the inferior recovery we obtained could be explained by the different lipid content of the samples, or by the degradation of compounds during drying procedures, which probably was more time consuming because of the presence of water. Indeed, cy3rut is more thermostable than the cy3glu [359], which can explain its higher RE value. We also have to note that the amount of cy3glu and cy3rut in the EtOAc extract is very low, compared to the total concentrations in the fruits.

For the MeOH 50% extract (ME = 98.8% ± 3.2), also no significant matrix effect was observed, and back calculated concentrations were 24.6 µg/mL ± 0.8 for both compounds. This confirms that the quantification of cy3glu and cy3rut from this MeOH 50% extract can be performed from the calibration curve in the matrix constructed with MeOH extract.

2.3.2. Development of the UHPLC method

The UHPLC method that we developed allowed separating the major and minor anthocyanins detected in the extracts (Figure 29a) in only 10 min, on a total run time of 17

min. Some of these compounds (peaks 3–7) are the dominant anthocyanins of many other berry fruits [379], for which this separation method can be applied. Good resolution of the peaks is very important when a UV detector is used. Another work, using an UHPLC C18 column, [373] did not provide the complete chromatographic separation of the major anthocyanins of EOF, because it used an MS detector, for which no separation of peaks that have different molecular ions is necessary. In addition, the total run time of our method was 2.1× faster than this one. Regular HPLC methods for *E. oleracea* anthocyanins have a total run time between 30 and 80 min [286,350,353,357–359,371,372,381,384,398]. Our UHPLC method is 1.8–4.7× faster than these ones, which shows the advantage of UHPLC analysis for these compounds. In terms of organic mobile phase, ACN, MeOH and a mixture of ACN/MeOH (1/1) were tested. A better resolution and a faster elution of the chromatographic peaks were obtained with ACN. Moreover, this solvent has a lower viscosity than MeOH, consequently, lower back pressure is obtained, which promotes a better system stability. The acidified mobile phase allowed a predominance of the flavylium cation species and a better separation, as reported previously [391]. We used 5% formic acid in the aqueous solution of the mobile phase which corresponds to a quite low pH (1.8), because we observed that smaller acid percentages provided an increase of the retention times and decreases peaks resolution. In addition, the predominance of the flavylium cation forms provided better MS detection in positive ionization mode, which we applied for the identification studies. It was necessary to apply a linear gradient with low slope (5–15% ACN in 10 min) to separate all the peaks. From this gradient interval, convex and concave gradients were tested, but the conditions aforementioned remained the better compromise between the run time and resolution of the peaks. The samples were very well solubilized in ACN/H_2O/MeOH/HCOOH (5/75/15/5). In fact, the dissolution solvent is an important parameter for UHPLC, where it has more influence on the chromatographic separation than with conventional HPLC analysis [399].

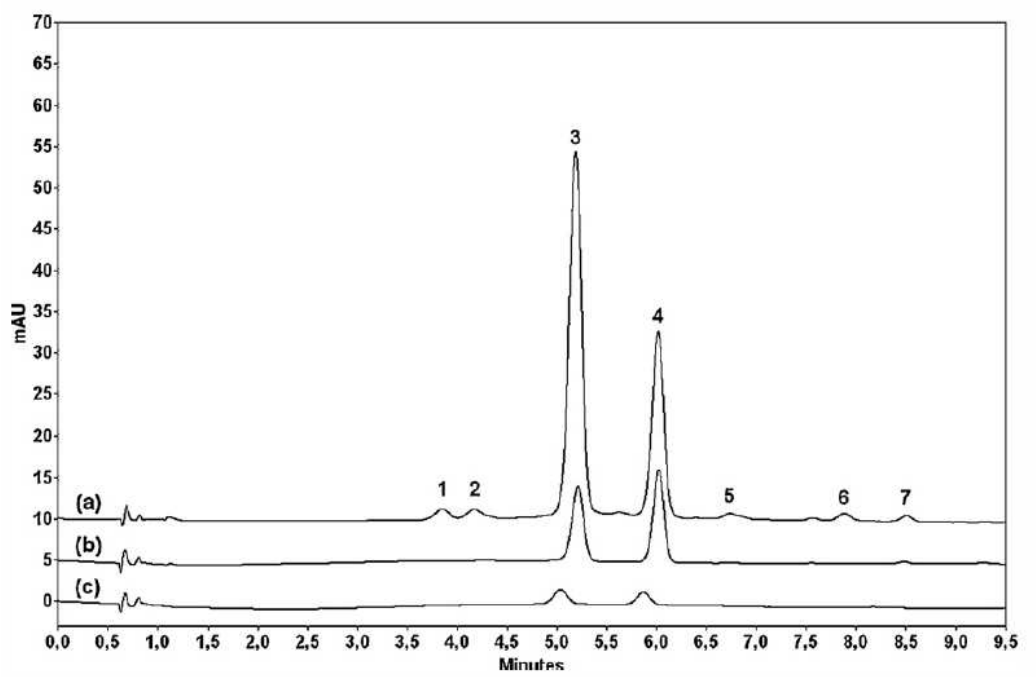

Figure 29 UHPLC–PDA chromatograms recorded at 520 nm from (a) MeOH, (b) MeOH50% extracts and (c) anthocyanin fraction of the EtOAc extract. 1: cyanidin-di-*O*-glycoside, 2: cyanidin-di-*O*-glycoside (isomer of the first), 3: cyanidin-3-glucoside, 4: cyanidin-3-rutinoside, 5: pelargonidin-3-glucoside, 6: peonidin-3-glucoside, 7: peonidin-3- rutinoside.

The final UHPLC conditions were: acetonitrile and 5% formic acid in water, as mobile phase, which was eluted at a constant flow rate of 400 μL/min, with a gradient of 5–15% ACN in the first 10 min, after that, a washing of the column with 95% ACN, followed by an equilibration of 4.9 min to the initial condition was performed.

2.3.3. Validation of the method

2.3.3.1. Identification and selectivity

From the full high resolution MS scan analysis in positive ion mode, the anthocyanin molecular ions were detected in their oxonium form and their molecular weight were directly obtained. Peak 1 showed a molecular ion at *m/z* 611.15839 $[M]^+$ (calculated mass: 611.16066) from which the formula $[C27H31O16]^+$ was deduced. From the data-dependent MS/MS acquisition (CID = 15%), the molecular ion showed two fragment ions at *m/z* 449,10614 $[M-162]^+$ and at *m/z* 287.05411 $[M-162-162]^+$ due to a sequential the loss of two hexoses (Figure 30a). The fragment ion at *m/z* 287 indicates the presence of cyanidin or an isomer in the structure of the molecule. According to the literature [400], the only disaccharide linked to

anthocyanins losing a sugar after MS/MS is rutinoside. The presence of rutinose in the structure is excluded because its fragmentation did not correspond to a sequential loss of two *m/z* 162 fragments. As we observed the fragment ion at *m/z* 449 $[M]^+$, the two hexoses must likely be attached at different positions, probably to an oxygen atom because a carbon-carbon bond of a *C*-glycosilation is more difficult to be broken, but the exact position of the sugars cannot be ensured by MS. Peak 2 showed similar MS data than peak 1 (Figure 30b and Table 6), indicating that these compounds are isomers. Nevertheless, the retention time of these two compounds was different from the standard of cyanidin 3,5-diglucoside. Peaks 1 and 2 were partially identified for the first time in EOF. The retention times and the MS data (CID = 20%) of peaks 3–7 were compared with those of standards, allowing their identification (Table 6) and confirming other studies [1,286,350,357,358,371,380,381]. All peaks were present in the MeOH extract of all evaluated maturity stages, but, in the EtOAc and MeOH 50% extract, only cy3glu and cy3rut were always observed at detectable levels.

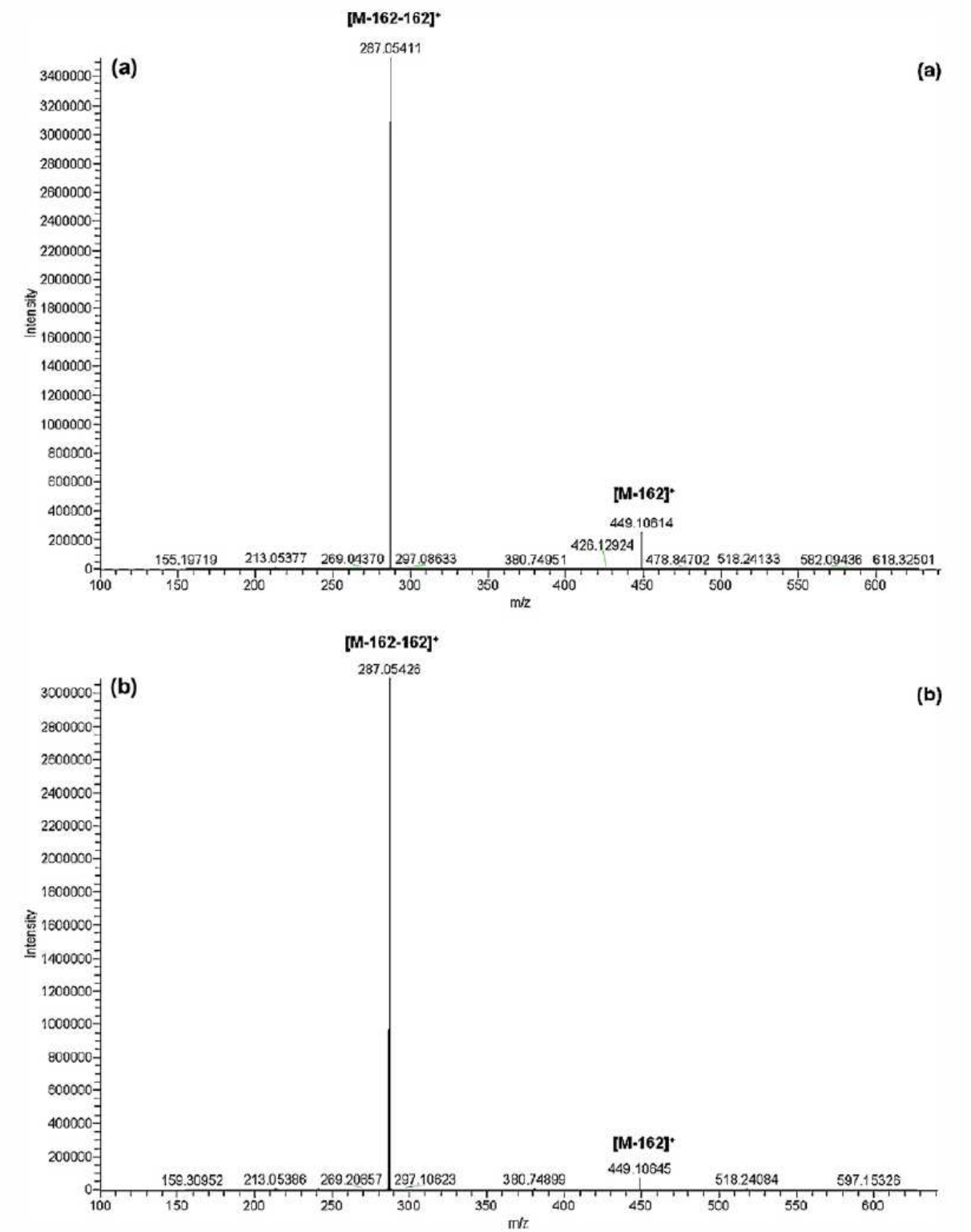

Figure 30. (a) MS/MS spectra of the molecular ion at *m/z* 611.15839 $[M]^+$ corresponding to peak 1 (Figure 29). (b) MS/MS spectra of *m/z* 611.15845 $[M]^+$ corresponding to peak 2 (Figure 29) (MeOH extract obtained from *Euterpe oleracea* fruits at maturity stage C).

Table 6 Identification of anthocyanins of *Euterpe oleracea* fruits by UHPLC–PDA–MS/MS method.

Peak[a]	RT UHPLC–PDA (min)	Experimental mass *m/z* $[M]^+$ (error: ppm)	Formula $[M]^+$	MS/MS (*m/z*)	Identification
1	3.85	611.15839 (−3.72)	$C_{27}H_{31}O_{16}$ [b]	287.05411, 449.10614	Cyanidin-di-O-glycoside[c]
2	4.18	611.15845 (−2.21)	$C_{27}H_{31}O_{16}$ [b]	287.05426, 449.10645	Cyanidin-di-O-glycoside[c]
3	5.19	449.10654 (−2.89)	$C_{21}H_{21}O_{11}$	287.05423	Cyanidin-3-glucoside[d]
4	6.01	595.16418 (−2.63)	$C_{27}H_{31}O_{15}$	287.05411, 449.10620	Cyanidin-3-rutinoside[d]
5	6.75	433.11191 (−2.34)	$C_{21}H_{21}O_{10}$	271.05939	Pelargonidin-3-glucoside[d]
6	7.90	463.12198 (−3.26)	$C_{22}H_{23}O_{11}$	301.07053	Peonidin-3-glucoside[d]
7	8.51	609.17908 (−3.803)	$C_{28}H_{33}O_{15}$	301.07056, 463.12305	Peonidin-3-rutinoside[d]

[a] The numbers correspond to Figure 29.
[b] Best fitted molecular formula obtained by HRMS.
[c] Not fully identified on the basis of the MS data.
[d] Identification were confirmed by analysis of standards.

Special attention was dedicated in the anthocyanin identifications because some studies reported different profiles, with respect to the major anthocyanins in EOF. Cyanidin-3-arabinoside and cyanidin-3-arabinosylarabinoside were reported as major anthocyanins in [401]. In another study, peonidin-3-(6”-malonylglucoside) and delphinidin 3-(6”-acetoyl)glucoside, in addition to cy3glu and cy3rut, were reported as major anthocyanins [398]. These other major anthocyanins were not detected in our study.

The selectivity of the analytical method was assessed by peak purity verification of the cy3glu and cy3rut from the UHPLC–MS analysis. Mass spectra were recorded at three retention times, corresponding to the beginning, the middle and the end of the peaks and were found to be similar for the different extracts (anthocyanin fraction of the EtOAc extract, MeOH and MeOH 50% extracts) and for all maturity stages studied. Figure 31 gives one example of MS spectra for cy3glu (Figures 31a–c) and cy3rut (Figures 31d–f), from the MeOH extract of the maturity stage C, which is the most commercialized [1].

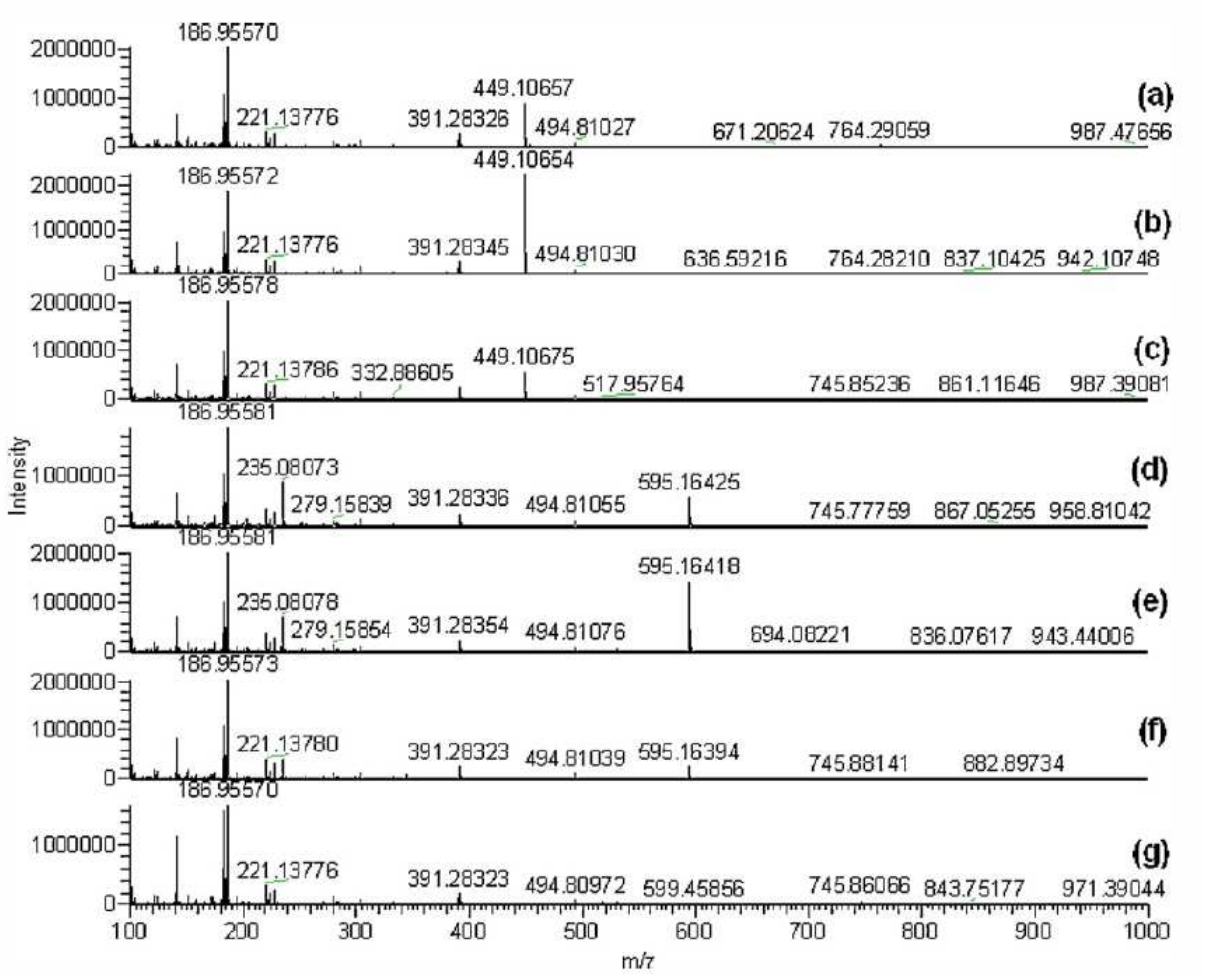

Figure 31. Positive ion mode MS spectra of cyanidin-3-glucoside (*m/z* 449 [M]+) recorded at (a) the beginning (b) the middle and (c) the end of the peak, and MS spectra of cyanidin-3-rutinoside (*m/z* 595 $[M]^+$) corresponding to (d) the beginning (e) the middle and (f) the end of the peak, and (g) MS spectrum of a blank analysis obtained from the retention time of cy3glu (A similar MS spectrum was observed in the retention time of the cy3rut).

2.3.3.2. Response function and accuracy

For both compounds, cy3glu and cy3rut, different regression models were tested such as linear, quadratic (weighted or unweighted), with or without transformations. Total error (systematic + random error) was the main decision criterion for our validation process. The suitability of the different models was assessed by plotting the accuracy profiles, using 95% *β*-expectation tolerance intervals and ±20% acceptance limits. For cy3glu, calibration in the matrix, using a linear regression, was chosen for the quantification. With this calibration model, all concentrations, except the lowest one, gave results within the acceptance limits (Figure 32a). The same linear regression, but in a calibration without matrix, showed higher values of total error for the two lowest concentration levels (Figure 32b). Improved accuracy

profiles for low concentration levels were also obtained in a calibration in the matrix for other phenolic compounds in a HPLC–UV method [402].

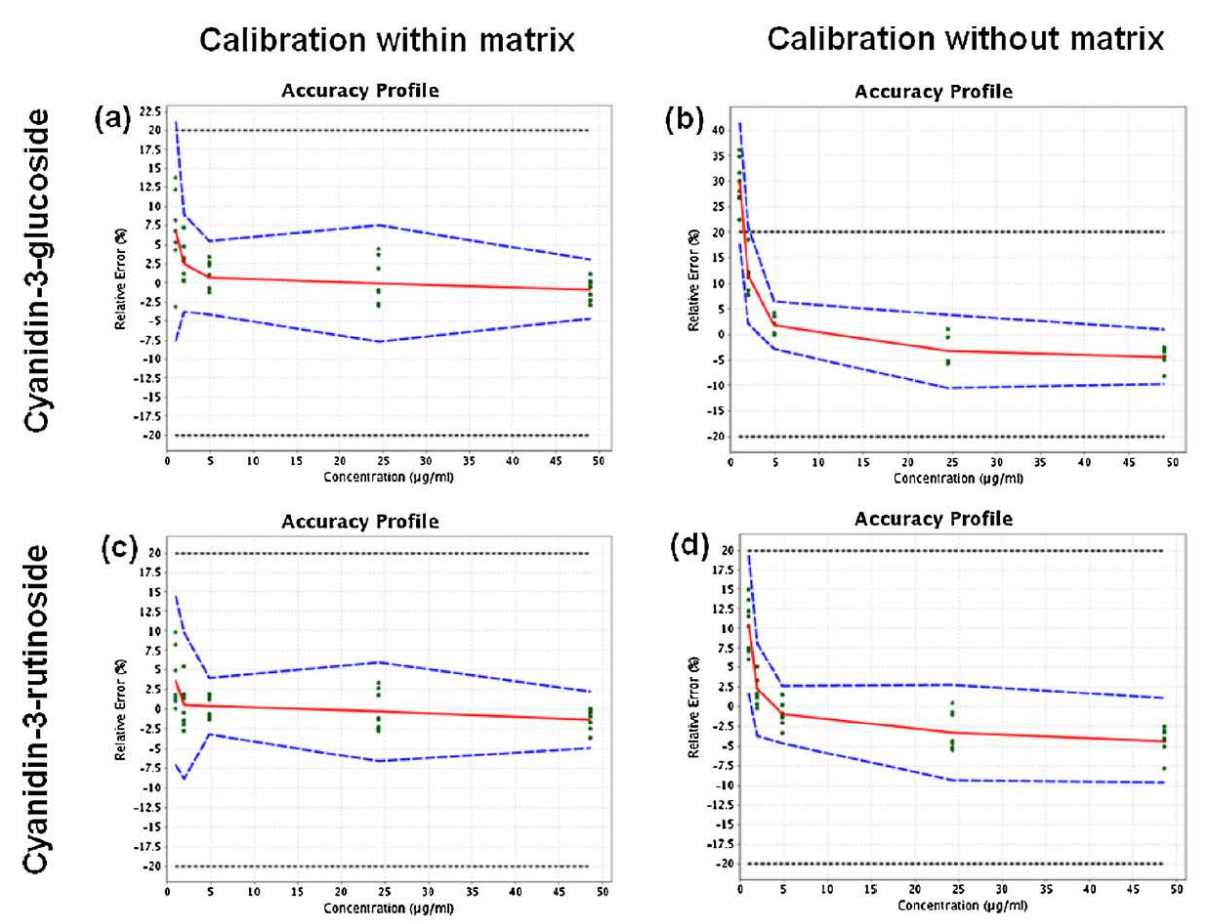

Figure 32. Accuracy profiles in relative values for different regression models using 5 points calibrations. (a) Linear regression in the matrix (MeOH extract) and (b) without matrix for cyanidin-3-glucoside, (c) weighted (1/X) linear regression in the matrix and (d) without matrix for cyanidin-3-rutinoside. The continuous line represents the relative bias, the dashed lines the 95% β-expectation tolerance limits and the dotted lines the ±20% acceptance limits.

Several calibration models for cy3rut showed relatively good accuracy profiles, with the tolerance intervals within the ±20% acceptance limits. The weighted (1/X) linear regression in the matrix was chosen for the quantification because it gave the best accuracy profile. We also observed, as for cy3glu, lower total error when calibration was made in the matrix (Figures 32c and d). Accuracy values obtained for cy3glu and cy3rut are summarized in Table 7. This work was the first that evaluated an external calibration in the matrix extract. In other quantification studies from EOF, external calibrations without matrix were applied from non-validated methods [286,350,353,357,359,372,381,384].

Table 7 Validation results for the quantification method of cyanidin-3-glucoside and cyanidin-3-rutinoside obtained in MeOH extract of *Euterpe oleracea* fruits.

Validation criteria	Cyanindin-3-glucoside		Cyanidin-3-rutinoside	
Response function	Linear regression Calibration in the matrix (5 points) Range: 1.0–49.0 μg/mL		Weighted (1/*X*) linear regression Calibration in the matrix (5 points) Range: 1.0–48.6 μg/mL	
Trueness	Concentration (μg/mL)	Relative bias (%)	Concentration (μg/mL)	Relative bias (%)
	1.0	6.76	1.0	3.60
	2.0	2.54	1.9	0.51
	4.9	0.67	4.9	0.38
	24.5	−0.07	24.3	−0.24
	49.0	−0.83	48.6	−1.29
Precision	Repeatability (RSD%)	Intermediate precision (RSD%)	Repeatability (RSD%)	Intermediate precision (RSD%)
	4.63	5.30	3.10	3.80
	2.49	2.49	1.86	2.85
	1.90	1.90	1.41	1.41
	2.99	2.99	2.47	2.47
	1.46	1.46	1.35	1.35
Accuracy	Relative β-expectation lower and upper tolerance limits (%)		Relative β-expectation lower and upper tolerance limits (%)	
	−7.6, 21.1		−7.2, 14.4	
	−3.8, 8.9		−8.8, 9.8	
	−4.1, 5.5		−3.2, 4.0	
	−7.6, 7.5		−6.5, 6.0	
	−4.7, 3.0		−4.9, 2.3	
Linearity				
Slope	0.9910		Slope	0.9873
Intercept	0.0910		Intercept	0.0829
r^2	0.9994		r^2	0.9995

2.3.3.3. Trueness, precision and linearity

The values obtained are also summarized in Table 7. Trueness expressed in terms of relative bias was generally inferior to 6.76% for cy3glu to 3.6% for cy3rut, which shows the good trueness of the method. The precision is evaluated at two levels, repeatability and intermediate precision, and were expressed in terms of relative standard deviation (RSD) values. The repeatability and intermediate precision for both compounds were very good and inferior to 5.3% (cy3glu) and 3.8% (cy3rut). In addition, they showed similar variance along the dosing range, indicating that the effect of the series did not provide significant additional variability for each compound. The linearity is the ability within a definite range to obtain results directly proportional to the concentration of the analyte. The concentrations of the validation standards were back-calculated from the calibration curve. A linear regression model was fitted on the back-calculated concentrations, as a function of the introduced concentrations. The intercept, the slope and the coefficient of determination of the equations obtained for cy3glu and cy3rut are presented in Table 7. The slopes values close to 1

demonstrate the linearity of the method. The linearity was also demonstrated because the absolute β-expectation tolerance limits were within the absolute acceptance limits [395,402,403].

2.3.3.4. Limits of detection and of quantification

The limits of detection were calculated from the residual standard-deviation and the slope of the calibration curve. The results obtained were 0.32 and 0.12 µg/mL for cy3glu and cy3rut respectively. The lower (LLOQ) and upper (ULOQ) limits of quantification were obtained by calculating the lowest and highest concentration of the targeted substance, that can be assayed under experimental conditions, for which the β-expectation limits remain inside the acceptance limits. For cy3glu, the LLOQ and the ULOQ were 1.07 and 48.99 µg/mL, respectively, and for cy3rut, they were 0.97 and 48.59 µg/mL, respectively.

2.3.4. Application of the quantification method to samples of E. oleracea *fruits*

Three EOF samples corresponding to the most commercialized maturity stage (C) were harvested in a same location of the municipal district of Abaetetuba (harvest season: 2010) and analyzed. This is the maturity stage recommended to the harvest of these fruits [357]. The calibration curves in the matrix were applied for the quantification of the major anthocyanins.

The concentrations obtained for cy3glu and cy3rut as well as the sum of these concentrations for each extract are presented in Table 8. The lowest concentration of the sum of the major anthocyanins was obtained in the EtOAc extract (0.02%) due to the low solubility of anthocyanins in this solvent. This can suggest that an EtOAc extraction can be applied to remove the wax cuticle present on the fruits, before the anthocyanin extraction by methanolic solutions, without considerable loss of the anthocyanins. This procedure can optimize the mass transfer of the anthocyanins, allow obtaining a methanolic extract without lipids and other apolar compounds such as chlorophylls that can damage (U)HPLC C18 columns and avoid SPE clean-up procedures. Almost 95% of the major anthocyanins are present in the MeOH extract. This percentage can be considered as the extraction yield because of the low content of anthocyanins in the MeOH 50% extract obtained on the residue, showing the great extraction efficiency of the MeOH solution. Thus, the last extraction can be eliminated of the protocol, reducing the time for extraction and samples preparation.

Table 8 Anthocyanin quantification results from EtOAc, MeOH and MeOH50% extracts obtained from *Euterpe oleracea* fruits at maturity stage C.

Sample	Extract	Cyanidin-3-glucoside (mg/kg fruits) ± SD	Cyanidin-3-rutinoside (mg/kg fruits) ± SD	∑Major anthocyanins (mg/kg fruits)
Sample 1	EtOAc	0.06 ± 0.00	0.05 ± 0.00	0.11 ± 0.00
	MeOH	277.45 ± 1.33	192.64 ± 0.95	470.09 ± 2.26
	MeOH50%	8.14 ± 0.88	10.16 ± 0.90	18.31 ± 1.51
	Total	285.65 ± 0.47	202.85 ± 1.09	488.50 ± 1.24
Sample 2	EtOAc	0.05 ± 0.00	0.04 ± 0.00	0.09 ± 0.00
	MeOH	328.56 ± 7.77	231.41 ± 5.38	559.97 ± 13.14
	MeOH50%	9.94 ± 0.92	13.67 ± 1.10	23.61 ± 2.01
	Total	338.55 ± 8.62	245.12 ± 6.45	583.67 ± 15.04
Sample 3	EtOAc	0.05 ± 0.00	0.05 ± 0.00	0.11 ± 0.00
	MeOH	283.37 ± 21.58	240.66 ± 17.47	524.03 ± 39.05
	MeOH50%	9.83 ± 0.19	12.68 ± 0.64	22.51 ± 0.82
	Total	293.25 ± 21.59	253.39 ± 17.39	546.65 ± 38.98

SD : standard deviation from triplicate samples

The sum of the concentrations of cy3glu and cy3rut for the three samples varied between 488 and 583 mg/kg fruits and were inferior to the concentrations obtained in a previous study on the same maturity stage C, from two different locations of the same region of Abaetetuba (800 and 1200 mg/kg fruits) [357], demonstrating the great variability of the anthocyanins content in the *E. oleracea* fruits. This variability was also reported from different juice samples [286].

Therefore considering the economic importance of the EOF, as a rich anthocyanin source, and the great concentration and ration variabilities observed, it is of crucial importance to have a validated analytical method for their quantification for producers and consumers.

2.4. Conclusions

We developed a fast protocol of anthocyanin extraction and sample preparation from EOF. Elimination of lipophilic compounds can be done by an EtOAc extraction, while anthocyanins are extracted from the residue by MeOH. Calibrations in the matrix were used for cy3glu and cy3rut quantifications and showed better accuracy profiles in comparison to calibrations without matrix. To our knowledge, this is the first article that describes a validated UHPLC–PDA method for the quantification of the major anthocyanins from *E. oleracea* fruit extracts. It was found to be faster (17 min) than other HPLC–UV methods and

allowed the separation of 3 other anthocyanins that are dominant in other common berry fruits. Furthermore, this method was selective and gave good estimators of linearity, accuracy, trueness and precision from 1 to 48 µg/mL of cy3glu and cy3rut. In addition, minor diglycosylated anthocyanins were found in EOF for the first time.

Acknowledgements

We would like to thank very much Prof. J.-L. Habib-Jiwan for his rich scientific orientation (*in memoriam*), Emmanuelle Lautié for her kind scientific and technical advices, Marie-Christine Fayt, Jean Paul Vanhelleputte and Ramazan Colak for their technical support in the LC–MS system. ADRI-UCL is acknowledged for financial support to the first author, Belgian National Fund for Scientific Research (FNRS) (FRFC 2.4555.08), the Special Fund for Research (FSR) and the faculty of medicine of UCL for their financial support for the acquisition of the LTQ−Orbitrap XL, the program PIC of the Coopération universitaire au développement (CUD), and CNPq (Brazil) for financial support on this research. A research grant from the Belgium National Fund for Scientific Research (FRS-FNRS) to E. Rozet is gratefully acknowledged.

3. Development and validation of an UHPLC−LTQ−Orbitrap MS method for non-anthocyanin flavonoids quantification in *Euterpe oleracea* juice

This chapter was adapted from the is mainly based on the article

Analytical & Bioanalytical Chemistry 405 (2013) 9235 − 9249

The previous chapter dealt with the identification and quantification of the major phenolic compounds in *Euterpe oleracea* fruit extracts, the anthocyanins. The majority of the phenolic characterization studies on the fruits and derived products were focused on these compounds. Nevertheless, the number of reports about non-anthocyanin phenolic compounds has increased. Recently, some studies isolated some of these compounds and demonstrated their biological activities, such as antioxidant and anti-inflammatory [361,404,405]. In Brazil, non published and preliminary studies, previous to this thesis, demonstrated the potential presence of flavonoids not reported in the literature. The local analytical conditions did not allow their identification, but the present scientific collaboration between UFPA and UCL allowed the utilization of a very sensitive and suitable analytical tool for the analysis of complex matrices and with a great potentiality to provide structural informations about unknown compounds.

The concentration of the non-anthocyanin polyphenols were low in the extracts described in the previous chapter and the quantities of the extracts were not sufficient to validate a method. In fact, in validation studies, generally high amounts of samples are needed for the experiments. In the present chapter, other extracts were produced, this time, from lyophilized juices. From this approach, sufficient amounts of extracts were obtained, so that the samples could be prepared in higher concentrations. Moreover, the use of lyophilized juice allowed the development of another extraction procedure.

The present chapter will present a study about the identification of non-anthocyanin phenolic compounds, as well as the validation of a method for the quantification of the major ones, and the application of this method to different juices.

ABSTRACT

Euterpe oleracea fruits have gained much attention because of their phenolic constituents that have shown potential health benefits. The aim of this work was to quantify the major non-anthocyanin flavonoids (NAF) in the fruit juice by an accurate method coupling ultra-high pressure liquid chromatography with a linear ion trap-high resolution Orbitrap mass spectrometry system (UHPLC-LTQ-Orbitrap MS). Fruits were processed to juice, and then the juice was lyophilized and defatted. The residue was then extracted in the presence of methanol by sonication. The extraction time was optimized and recovery rates of the extraction were >90 %. The extracts were dried and solubilized again in 40 %MeOH, which showed the best compromise for MS detection. For the UHPLC quantification, a HSS C18 column (1.8 μm) was used with a gradient elution of methanol and water both with 0.1 % formic acid. Total error and accuracy profiles were used as validation criteria. Seven compounds and their isomers were successfully separated, including the major NAF. Calibration in the matrix was found to be more accurate than calibration without matrix. Trueness (<15 % relative bias), repeatability, and intermediate precision (<13 % RSD), selectivity, response function, linearity, LOD (ranged from 0.04 to 0.81 μg/mL) and LOQ (0.15–5.78 μg/mL) for 12 compounds were evaluated and the quantification method was validated. Its applicability was demonstrated on real samples from different suppliers. Their qualitative and quantitative profiles were similar and some compounds were for the first time quantified. In addition, eriodictyol was identified for the first time in this fruit along with five other flavonoids for which possible structures were proposed.

3.1. Introduction

Euterpe oleracea is a widespread palm of the Amazonian floodplains. Its fruits, recently acclaimed as "super fruits," are especially rich in antioxidants like phenolic compounds and tocopherols [1,352]. Anthocyanins are their major phenolic compounds, cyanidin 3-glucoside and cyanidin 3-rutinoside being in larger concentrations [356,357,374], followed by flavonoids as orientin and homoorientin [359]. Other flavonoids belonging to the flavone, flavonol, flavanol, and dihydroflavanol families are also present, as well as phenolic acids [353,359,371,373,381]. Recently, some studies were dedicated to the isolation of NAF from *E. oleracea* pulp. The compounds isolated in these studies showed interesting anti-inflammatory and antioxidant activities [361,404,405]. Other works studied *E. oleracea* pulp and extracts derived from these fruits and showed that these compounds largely contributed to their biological activities, as discussed in a recent review [406].

Many products derived from *E. oleracea* fruits are traded: fruit juices mostly blended to produce energetic beverages, ice cream, sweets and jelly [407], cosmetics, and food supplements that are principally consumed in Brazil, USA, Japan, and some European countries [352,373]. Their phenolic compounds should be quantified by appropriate methods. For this purpose, method validation is a necessary step providing "guarantees" for regulatory bodies, producers, and consumers. Recently, UHPLC-PDA and liquid chromatography-mass spectrometry (LC-MS) methods were validated for the quantification of anthocyanins from *E. oleracea* fruits and derived dietary supplement raw materials [374,375]. Regarding NAF, some high performance liquid chromatography (HPLC) methods coupled to DAD and MS detectors [353,359,371,381,407] have been used, but no validated method is available for quantification purposes. In addition, the majority of these methods have quite long run times ranging between 50 min and 90 min. Using column packed with sub-2 μm particles, Mulabagal and Calderón [373] have obtained a shorter run time (35 min) in their fingerprinting and mass profiling of *E. oleracea* dietary supplement raw materials. However, the complete separation of the two major isomers, orientin and homoorientin, was not reached, which is critical for quantitative LC-MS methods. Gordon et al. [353] in their HPLC method had to use a supplementary gradient to reach full separation of orientin and homoorientin.

LC-MS methods are generally used to analyze NAF because of their higher sensitivity and selectivity compared to HPLC-DAD methods. The use of high resolution mass spectrometry (HRMS) further improves sensitivity and selectivity. The use of columns packed

with sub-2 µm particles also contributes to ameliorate the sensitivity. In addition, it reduces run times as compared with conventional HPLC columns [373,408]. This powerful association was not yet employed for the quantification of NAF from *E. oleracea* juice (EOJ).

In order to analyze the NAF and the anthocyanins of EOJ, generally two different extraction procedures [353,407] and HPLC-MS conditions were used, one for each group of compounds. In terms of mobile phase, NAF were eluted with a lower acid concentration than the anthocyanins. In addition, the ionization source of the MS system was operated in negative ion mode for NAF and in positive ion mode for anthocyanins [286,371,407]. Furthermore, for NAF, no attention is usually paid to the matrix effect. This phenomenon is frequently present in LC-MS methods and not yet completely understood [322,409]. It is characterized by ion suppression or enhancement caused by co-elution of the compounds of interest with undetected matrix components, which can affect the reproducibility and accuracy of the assay. It is thus interesting to evaluate the matrix effect in the quantification of these compounds to assure the accuracy of the method.

The aim of this work is to develop and validate an UHPLC−LTQ−Orbitrap MS method for the quantification of *E. oleracea* NAF after optimization of the extraction procedures and the sample preparation.

3.2. Experimental

3.2.1. Chemicals and reagents

Standards of orientin, homoorientin, vitexin, isovitexin, quercetin, luteolin, eriodictyol, kaempferol 3-rutinoside, chrysoeriol, (−)-epicatechin, taxifolin, cyanidin 3-glucoside, and cyanidin 3-rutinoside were purchased from Extrasynthèse (Genay, France). Quercetin 3-glucoside, (+)-catechin hydrate, (+)-dihydrokaempferol, rutin hydrate, 7-hydroxyflavone (internal standard-IS), protocatechuic acid, vanillic acid, and caffeic acid were purchased from Sigma-Aldrich (Steinheim, Germany). LC-MS grade methanol from Biosolve (Valkenswaard, The Netherlands) and formic acid (98 %–100 %) from Prolabo, VWR (Leuven, Belgium) were used for the UHPLC-MS runs.

3.2.2. Samples and pretreatement

Ripe fruits of *E. oleracea* were kindly provided from three suppliers from Pará state (Brazil). Fruits were harvested in February 2012 and were processed to juice within 6 h of

harvesting in our laboratory in Belém—PA (Brazil). Juices (sample P0) were obtained following classic procedures used by food industries as described by Rogez et al. [410], and then, aliquots of the juices were pasteurized at 80°C/12min and 90°C/2min to produce the samples P1 and P2, respectively. Juice samples were frozen and shipped to Belgium. Finally, fruit juices were lyophilized and stored at −21 °C, under N_2 (g) atmosphere until extraction procedures.

3.2.3. Sample preparation

Sample preparation (Figure 33) was based on a procedure described by Mulabagal et al. [373] with some modifications that are discussed in the Result section (Evaluation of the extraction). About 0.5 g of lyophilized juice (in triplicate) was quantitatively weighed in an assay tube of 15 mL. The sample was then defatted with 5.0 mL of petroleum ether 40–60° in an ultrasonic bath at room temperature for 30 min. After centrifugation at 2400×g for 10 min, the extraction was repeated three more times on the residue. Petroleum ether phases of this clean-up were eliminated. The residue was extracted with methanol by sonication under similar experimental conditions. In this case, five extractions with 5.0 mL each were performed. After centrifugation, the supernatants of each methanolic extraction were assembled before evaporating to dryness with a RapidVap multi-tube vacuum evaporator (Labconco, Kansas City, MO, USA) at 35 °C. The dried extract was stored at −21 °C under N_2 (g) atmosphere. The day of the analysis, the extracts were solubilized in 40 % methanol solution at a concentration of 4 mg of dried extract per mL. The solutions were filtered with a 0.2 µm filter (Interchrom, Montluçon, France) and directly injected into the UHPLC.

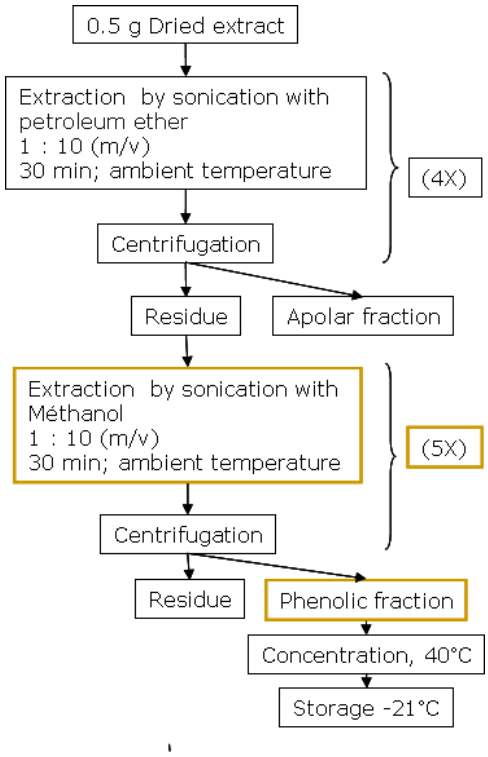

Figure 33 Extraction procedures of the dried extract (lyophilized juice) obtained from *E. oleracea* juice.

3.2.4. UHPLC-HRMS analysis

The UHPLC analysis was performed on an Accela UHPLC system acquired from Fisher Scientific (Thermo Fisher Scientific, Bremen, Germany) that consisted of an autosampler equipped with a column oven, a tray compartment cooler, and a quaternary pump with a built-in solvent degasser, all piloted by Xcalibur software. The chromatographic separation was performed on an Acquity UPLC HSS C18 column, 1.8 µm, 100 mm×2.1 mm i.d. (Waters, Belfast, Ireland), equipped with a VanGuard UPLC HSS C18 pre-column, 1.8 µm, 5 mm×2.1 mm i.d., from the same supplier. Five µL of samples were injected in a full loop injection mode. The separations were performed with a constant flow rate of 400 µL/min. The eluents were (A) 0.1 % formic acid in water and (B) 0.1 % formic acid in methanol. They were eluted with the following gradient: 0–2 min: 15 % B; 2–18 min: 15–27 % B; 18–28 min: 27–95 % B; 28–30 min: 95 % B; 30–30.1 min: 95–15 % B; 30.1–35 min: 15 % B. The column oven and tray cooler temperatures were set to 30 and 4 °C, respectively.

The Accela UHPLC system was hyphenated with a LTQ−Orbitrap XL mass spectrometer (Thermo Fisher Scientific) from the UCL MASSMET platform. The system was equipped with an ESI source that was operated in negative ion mode with the following conditions: capillary temperature and voltage at 275 °C and −21 V, respectively, source

voltage at 5 kV, and tube lens voltage at −162 V. Nitrogen was used as the sheath gas and helium as auxiliary gas with a flow rate of 80 and 30 arbitrary units, respectively. Spectra were recorded in the range of *m/z* 100–1000 with a resolution of 30,000. For identification purposes, two scan events were applied for the MS experiments. The first was in a full scan MS mode and the second was a data dependent scan that selected the most intense ion or specified ions in another setting from the first scan event for the acquisition of MS/MS spectra. The collision-induced dissociation activation was set to normalized collision energy of 25 %, except for quercetin and luteolin (35 %), vanillic, caffeic, and protocatechuic acids (20 %). The compounds were identified by comparison with reference compounds when available and with literature data, from retention times, MS, MS/MS, and MS^n analysis. An external calibration of the equipment for mass accuracy was carried out the day before the analysis according to the manufacturer's guidelines. In order to evaluate the selectivity of the method, MS/MS spectra were obtained by SRM scan type across the peaks. Product ions and their relative proportions were evaluated and compared with standards when available. For quantification, full scan MS mode was applied, and then extracted ion chromatograms of the ions of interest were generated from their theoretical exact masses using a mass tolerance of 5 ppm. After integration of the peaks, their respective areas were used for the quantifications. Finally the quantification was performed using the internal calibration method with 7-hydroxyflavone as IS.

3.2.5. Standard solutions

For the validation analysis, standard solutions of phenolic compounds were prepared as follows. Homoorientin was prepared at 0.6 mg/mL in methanol and quercetin 3- glucoside, quercetin, luteolin, eriodictyol, and kaempferol 3-rutinoside at 1 mg/mL of methanol as well. 5.0 mL of homoorientin solution was then mixed with 1.0 mL of the other solutions, giving respectively 0.3 mg/mL and 0.1 mg/mL solutions. Solutions of isovitexin, (+)-dihydrokaempferol, rutin hydrate, and (+)-catechin hydrate were prepared at 1 mg/mL in methanol and mixed to give a final concentration of 0.2 mg/mL. Chrysoeriol, orientin, and 7-hydroxyflavone (internal standard) were solubilized in methanol, to give 0.1, 0.05 and 0.1 mg/mL solutions, respectively. Vitexin, (−)-epicatechin, taxifolin, protocatechuic acid, vanillic acid, and caffeic acid were prepared at 1 mg/mL in methanol, and the solutions were

used only for identification purposes and for optimization of the chromatographic separation. All solutions were kept in the dark at 4 °C.

Standard solutions for the validation study were diluted to obtain the calibration standards at five concentration levels (m =5), except for the internal standard (7-hydroxyflavone), for which the final concentration was fixed at 0.005 mg/mL. The final solvent composition of the solutions was 40 % methanol in water. Each concentration level was analyzed three times (n=3) for three series of experiments (k =3). Another set of calibration standards was prepared in the methanolic extract itself in order to compare the calibration with and without matrix. A solution of methanolic extract of 16 mg of extract per mL was prepared in 40 % methanol in water. The calibration standards in the matrix were prepared by diluting in the methanolic extract the standards employed for the preparation of the calibration standards without matrix. The signals from the compounds initially present in the extract were subtracted from the peaks obtained with these solutions. The final concentration of the extract was always 4 mg of extract/mL. The number of concentration levels, series, and repetitions per series were the same as those implemented for the without matrix calibrations (m =5, k =3, and n =3).

The validation standards were prepared in the same way as the matrix based calibration standards. Five concentrations were analyzed (m =5) and each sample (n =3) was prepared from extracts obtained from independent extractions. Three series (k =3) were performed.

3.2.6. Evaluation of the extraction

The most appropriate methanolic extraction time was established by evaluating the peak area (LC-MS analysis) of selected compounds after 30, 90, 120, 150, and 180 min (n=3). The obtained extracts were solubilized at 4 mg of dried extract/mL in 40 % methanol in water before analysis and extraction yields were calculated according to the total extract mass obtained in each treatment.

Recovery (RE) and the overall “process efficiency” (PE) of the extraction, considering petroleum ether and methanol extractions, along with the matrix effect (ME) were determined according to an adaptation of the procedures described by Matuszewski et al. [322]. They were calculated as follows from lyophilized juices (n= 3) spiked with a known amount of standards corresponding to an intermediate concentration level of the dosing range:

$$RE(\%) = \frac{ARsps - ARnsps}{ARspe - ARnsps} \times 100 \quad \text{Eq. 27}$$

$$ME(\%) = \frac{ARspe - ARnsps}{ARstd} \times 100 \quad \text{Eq. 28}$$

$$PE(\%) = \frac{ARsps - ARnsps}{ARstd} \times 100 \quad \text{Eq. 29}$$

where *ARsps* is the area ratio (analyte/IS ratio) obtained from the spiked lyophilized juice sample (spiked *before* petroleum ether extraction), ARnsps is the area ratio of the nonspiked lyophilized juice sample before extractions, *ARspe* is the area ratio of the spiked methanolic extract (standards were spiked into the dried extract obtained after petroleum ether purification, methanolic extraction, and evaporation process), and *ARstd* is the area ratio of a solution of standards in 40 % methanol in water at the corresponding concentration.

3.2.7. Validation of the method

The validation of the method was performed during three series of experiments. The eluents of the mobile phase were renewed for each series. The following criteria were tested: selectivity, response function, linearity, precision (repeatability and intermediate precision), trueness, accuracy, limits of detection (LOD) and quantification (LOQ), and matrix effect. Total error was used as decision criterion for the validation process [411–414]. The acceptance limits were set at $\lambda = \pm 30$ %, and the minimum probability to obtain future results within these limits was set at $\beta = 90$ % (β-expectation limits). Statistical analyses were performed using the e-noval V3.0 (Arlenda, Liège, Belgium) software.

3.3. Results and discussion

3.3.1. Evaluation of the extraction

Different extraction procedures have already been described: defatted lyophilized pulp of *E. oleracea* fruits was extracted by sonication with an acetone/water/formic acid (70/29/1; v/v/v) solution, followed by a liquid–liquid extraction with ethyl acetate to obtain NAF and

phenolic acids [353]. In another work, phenolic compounds were extracted only by sonication with methanol [373], but with an extraction time longer than the previous reference. In the present work, the methanol extraction procedure by sonication was chosen because the extraction time was easier to optimize (only one extraction solution).

The lyophilized pulp was first defatted by sonication with petroleum ether 40–60°. This solvent was chosen because it is more hydrophobic than the dichloromethane used in Mulabagal et al. [373]. Chlorophylls were also extracted by petroleum ether 40–60°. The supernatants appeared clear after four 30-min extractions (4×5 mL). Phenolic compounds were then extracted by sonication in the presence of methanol. Methanolic extraction time was evaluated in the range between 30 and 180 min. Evolution of the peak areas of the selected compounds for the validation study were reported to the total extract mass. As illustrated in Figure 34, no significant difference was observed after 150-min of extraction for orientin and homoorientin (p >0.41). As they are the major compounds and contribute more to the total concentration in NAF, the methanolic extraction time was fixed to 150 min (5 × 30 min). The same was observed for chrysoeriol, quercetin, quercetin 3-glucoside, and rutin, whereas the extraction reached a maximum after 120 min for (+)-catechin, isovitexin, and kaempferol 3-rutinoside, and after 90 min for luteolin, eriodictyol, and dihydrokaempferol (data not shown). In the work of Mulabagal et al. [373], the methanolic extraction was fixed at 120 min (3 × 40 min × 100 mL), but no data about extraction time optimization were shown in that qualitative and semi-quantitative study. In addition, no data were mentioned about RE of extraction.

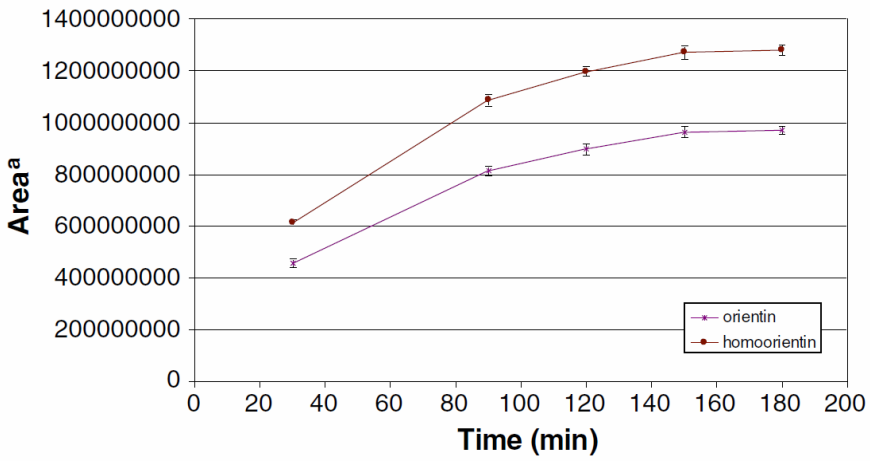

Figure 34 Changes in the extraction yields of the two major non-anthocyanin flavonoids (NAF) in function of the time of the methanolic extraction (n =3). [a] The extraction yields were calculated according to the total extract mass obtained in each treatment.

RE of the extraction was calculated by Equation 27 as described in the Experimental section. Good recoveries were obtained and were comprised between 91 % and 102 % as shown in Table 9. In addition, the recoveries obtained had good repeatabilities with SD <7 % for all evaluated compounds. ME was calculated by Equation 28. A value of >100 % indicates ionization enhancement, and a value of <100 % indicates ionization suppression. Eriodictyol, chrysoeriol, and luteolin showed no matrix effect, with ME values comprised between 92 % and 105 % as presented in Table 9. Quercetin showed an ionization enhancement effect with a value of 121 %. On the other hand, the other compounds presented values <82 % indicating ionization suppression for most of the studied compounds. In fact, ME has been often observed in LC-MS methods as discussed in a recent review [409]. Because of the ME observed, the later compounds gave PE values of <83 %. Analogously, ME could explain the high PE value of 114 % for quercetin.

Table 9 Validation results for the quantification method of non-anthocyanin flavonoids (NAF) of *E. oleracea* juice (EOJ).

Compounds / Validation criteria [a]	concentration level (μg/mL)						
(+)-Catechin	**0.5**	**1**	**2[d]**	**7**	**14**	**Linearity (Slope / Intercept / R^2)**	**RE (%)[d]**
Trueness (Relative bias %)	0.4564	1.635	−0.1081	−6.636	−1.005	0.9822 / -0.03031 / 0.9964	101±4.4
Repeatability (RSD%) [b]	11.46	12.83	6.665	2.861	3.637	**LOD / LLOQ[e] (μg/mL)**	**ME (%)[d]**
Intermediate precision (RSD%) [b]	11.46	12.83	10.15	3.723	3.637	0.15 / 0.5	56±5.6
Relative β-expectation tolerance limits (%) [c]	[−22.12, 23.03]	[−23.64, 26.91]	[−24.68, 24.47]	[−14.95, 1.67]	[−8.16, 6.15]	**validated range (μg/mL)**	**PE (%)[d]**
						0.5–14	57±5.2
(+)-Dihydrokaempferol						**Linearity (Slope / Intercept / R^2)**	**RE (%)[d]**
Trueness (Relative bias %)	−2.825	−5.506	1.447	−3.073	−0.373	0.9944 / -0.03389 / 0.9960	102±3.0
Repeatability (RSD%) [b]	6.444	5.192	5.482	1.611	3.839	**LOD / LLOQ[e] (μg/mL)**	**ME (%)[d]**
Intermediate precision (RSD%) [b]	6.444	7.537	7.319	1.611	5.454	0.12 / 0.5	82±1.7
Relative β-expectation tolerance limits (%) [c]	[−15.52, 9.86]	[−23.32, 12.31]	[−15.12, 18.01]	[−6.24, 0.09]	[−13.12, 12.38]	**validated range (μg/mL)**	**PE (%)[d]**
						0.5–14	83±4.2
Isovitexin						**Linearity (Slope / Intercept / R^2)**	**RE (%)[d]**
Trueness (Relative bias %)	−4.016	−7.029	0.3577	−5.911	−0.9025	0.9861 / -0.05954 / 0.9934	93±4.2
Repeatability (RSD%) [b]	11.18	9.68	2.352	3.766	5.867	**LOD / LLOQ[e] (μg/mL)**	**ME (%)[d]**
Intermediate precision (RSD%) [b]	14.79	10.04	6.473	6.098	5.928	0.26 / 0.85	67±3.2
Relative β-expectation tolerance limits (%) [c]	[−37.34, 29.31]	[−27.09, 13.03]	[−18.97, 19.69]	[−21.11, 9.28]	[−12.93, 11.12]	**validated range (μg/mL)**	**PE (%)[d]**
						1–14	62±3.4
Rutin						**Linearity (Slope / Intercept / R^2)**	**RE (%)[d]**
Trueness (Relative bias %)	2.364	−0.6261	−0.9349	−8.521	1.497	0.9974 / -0.08971 / 0.9878	96±4.8
Repeatability (RSD%) [b]	7.061	7.799	2.574	2.338	8.773	**LOD / LLOQ[e] (μg/mL)**	**ME (%)[d]**
Intermediate precision (RSD%) [b]	14.58	7.799	7.12	3.269	8.773	0.21 / 0.72	67±4.6
Relative β-expectation tolerance limits (%) [c]	[−37.77, 42.50]	[−15.99, 14.74]	[−22.22, 20.35]	[−16.10, -0.94]	[−17.77, 20.77]	**validated range (μg/mL)**	**PE (%)[d]**
						1–14	65±5.0
Kaempferol 3-rutinoside	**0.1**	**0.5**	**2[d]**	**4**	**10**	**Linearity (Slope / Intercept / R^2)**	**RE (%)[d]**
Trueness (Relative bias %)	1.72	−4.721	1.861	−2.711	−1.496	0.9837 / 0.005535 / 0.9955	97±6.5
Repeatability (RSD%) [b]	6.83	5.879	1.675	2.682	4.182	**LOD / LLOQ[e] (μg/mL)**	**ME (%)[d]**
Intermediate precision (RSD%) [b]	37.87	7.422	6.734	5.071	5.379	0.14 / 0.46	79±4.0
Relative β-expectation tolerance limits (%) [c]	[−122.0, 125.4]	[−21.03, 11.59]	[−19.54, 23.26]	[−16.22, 10.80]	[−13.43, 10.44]	**validated range (μg/mL)**	**PE (%)[d]**
						0.5–10	77±2.6
Quercetin 3-glucoside						**Linearity (Slope / Intercept / R^2)**	**RE (%)[d]**
Trueness (Relative bias %)	−21.37	1.695	1.915	−7.482	1.435	1.012 / -0.06427 / 0.9772	95±2.0
Repeatability (RSD%) [b]	90.77	5.787	1.963	2.866	12.46	**LOD / LLOQ[e] (μg/mL)**	**ME (%)[d]**
Intermediate precision (RSD%) [b]	90.77	6.841	5.414	4.051	12.67	0.14 / 0.47	73±4.8
Relative β-expectation tolerance limits (%) [c]	[−200.1, 157.4]	[−12.83, 16.22]	[−14.26, 18.09]	[−16.93, 1.96]	[−23.68, 26.55]	**validated range (μg/mL)**	**PE (%)[d]**
						0.5–10	70±4.1

Table 9 (continued).

Quercetin						**Linearity (Slope / Intercept / R^2)**	**RE (%)[d]**
Trueness (Relative bias %)	25.32	6.294	−8.371	−2.485	−0.7702	0.9909 / -0.02897 / 0.9957	95±4.7
Repeatability (RSD%) [b]	22.06	4.382	2.97	1.51	3.011	**LOD / LLOQ[e] (µg/mL)**	**ME (%)[d]**
Intermediate precision (RSD%) [b]	22.06	7.483	4.586	7.166	5.234	0.13 / 0.45	121±3.5
Relative β-expectation tolerance limits (%) [c]	[−18.13, 68.78]	[−12.81, 25.40]	[−19.55, 2.805]	[−25.63, 20.66]	[−14.73, 13.19]	**validated range (µg/mL)**	**PE (%)[d]**
						0.5–10	114±5.9
Eriodictyol						**Linearity (Slope / Intercept / R^2)**	**RE (%)[d]**
Trueness (Relative bias %)	−5.059	6.345	−2.747	3.733	0.952	1.011 / 0.005701 / 0.9960	102±4.5
Repeatability (RSD%) [b]	5.209	4.006	2.438	3.803	3.084	**LOD / LLOQ[e] (µg/mL)**	**ME (%)[d]**
Intermediate precision (RSD%) [b]	10.56	5.537	5.26	6.21	5.12	0.04 / 0.15	93±6.9
Relative β-expectation tolerance limits (%) [c]	[−33.95, 23.83]	[−6.414, 19.10]	[−17.44, 11.95]	[−11.80, 19.27]	[−11.96, 13.86]	**validated range (µg/mL)**	**PE (%)[d]**
						0.5–10	95±5.3
Luteolin	**0.1**	**0.5**	**2[d]**	**4**	**10**	**Linearity (Slope / Intercept / R^2)**	**RE (%)[d]**
Trueness (Relative bias %)	−29.36	14.84	1.698	−1.537	−3.348	0.9642 / 0.05855 / 0.9975	97±2.1
Repeatability (RSD%) [b]	12.8	5.392	1.688	2.069	3.251	**LOD / LLOQ[e] (µg/mL)**	**ME (%)[d]**
Intermediate precision (RSD%) [b]	39.95	5.392	5.278	2.069	4.627	0.14 / 0.47	105±3.0
Relative β-expectation tolerance limits (%) [c]	[−151.7, 93.03]	[4.224, 25.46]	[−14.47, 17.87]	[−5.61, 2.5]	[−15.73, 9.03]	**validated range (µg/mL)**	**PE (%)[d]**
						0.5–10	102±1.1
Orientin	**0.5**	**1**	**3**	**6[d]**	**18**	**Linearity (Slope / Intercept / R^2)**	**RE (%)[d]**
Trueness (Relative bias %)	5.103	14.73	1.273	−5.926	−12.39	0.8630 / 0.3059 / 0.9920	92±6.3
Repeatability (RSD%) [b]	66.82	47.31	7.495	11.34	3.616	**LOD / LLOQ[e] (µg/mL)**	**ME (%)[d]**
Intermediate precision (RSD%) [b]	66.82	47.31	7.495	11.34	3.753	0.81 / 2.69	70±5.1
Relative β-expectation tolerance limits (%) [c]	[−126.5, 136.7]	[−78.45, 107.9]	[−13.49, 16.03]	[−28.27, 16.42]	[−19.89, -4.89]	**validated range (µg/mL)**	**PE (%)[d]**
						3–18	64±4.8
Homoorientin	**0.3**	**1.5**	**6**	**12[d]**	**30**	**Linearity (Slope / Intercept / R^2)**	**RE (%)[d]**
Trueness (Relative bias %)	−11.16	−8.328	2.268	−9.187	1.015	1.003 / -0.2233 / 0.9874	92±3.9
Repeatability (RSD%) [b]	110.7	54.07	6.901	6.405	7.852	**LOD / LLOQ[e] (µg/mL)**	**ME (%)[d]**
Intermediate precision (RSD%) [b]	110.7	54.07	10.18	6.405	7.852	0.57 / 5.78	58±4.1
Relative β-expectation tolerance limits (%) [c]	[−229.2, 206.9]	[−114.8, 98.17]	[−21.99, 26.53]	[−21.80, 3.42]	[−16.23, 18.26]	**validated range (µg/mL)**	**PE (%)[d]**
						6–30	53±5.8
Chrysoeriol	**0.2**	**1**	**2[d]**	**4**	**10**	**Linearity (Slope / Intercept / R^2)**	**RE (%)[d]**
Trueness (Relative bias %)	2.361	4.547	−2.001	−3.117	0.3023	1.001 / -0.02018 / 0.9957	101±4.9
Repeatability (RSD%) [b]	10.85	3.664	1.397	2.021	4.935	**LOD / LLOQ[e] (µg/mL)**	**ME (%)[d]**
Intermediate precision (RSD%) [b]	10.85	3.887	5.547	4.492	4.958	0.06 / 0.20	92±2.0
Relative β-expectation tolerance limits (%) [c]	[−19.01, 23.73]	[−3.291, 12.39]	[−19.60, 15.60]	[−15.79, 9.555]	[−9.481, 10.09]	**validated range (µg/mL)**	**PE (%)[d]**
						0.2–10	93±3.4

[a] See text for response function and selectivity; [b] Precision was evaluated in two levels: repeatability and intermediate precision; [c] Accuracy was evaluated by the relative 90 % β-expectation tolerance limits; [d] Concentration level from which the extraction evaluation (RE, ME, PE) was performed; [e] The Upper limit of quantification (ULOQ) corresponded to the highest concentration level.

3.3.2. Development of the UHPLC−LTQ−Orbitrap MS method

Several isomers were separated (Figures 35b, c, d) under the chromatographic conditions described in the Experimental section. Orientin and homoorientin, the two major compounds, were more difficult to separate but the proposed conditions allowed this separation. A LC-HRMS method already described in a qualitative and semi-quantitative study [373] also used column packed with sub-2 μm particles to separate phenolic compounds from samples derived of *E. oleracea* fruits. Orientin and homoorientin were, however, not completely separated. The proposed method of the present work is thus an improvement. Moreover, it does not increase the total run time (35 min), compared with the published work [373]. Note that this run time is significantly smaller than those of classical HPLC runs described for the analysis of flavonoids of *E. oleracea* fruit (between 50 and 90 min) [353,359,371,381,407].

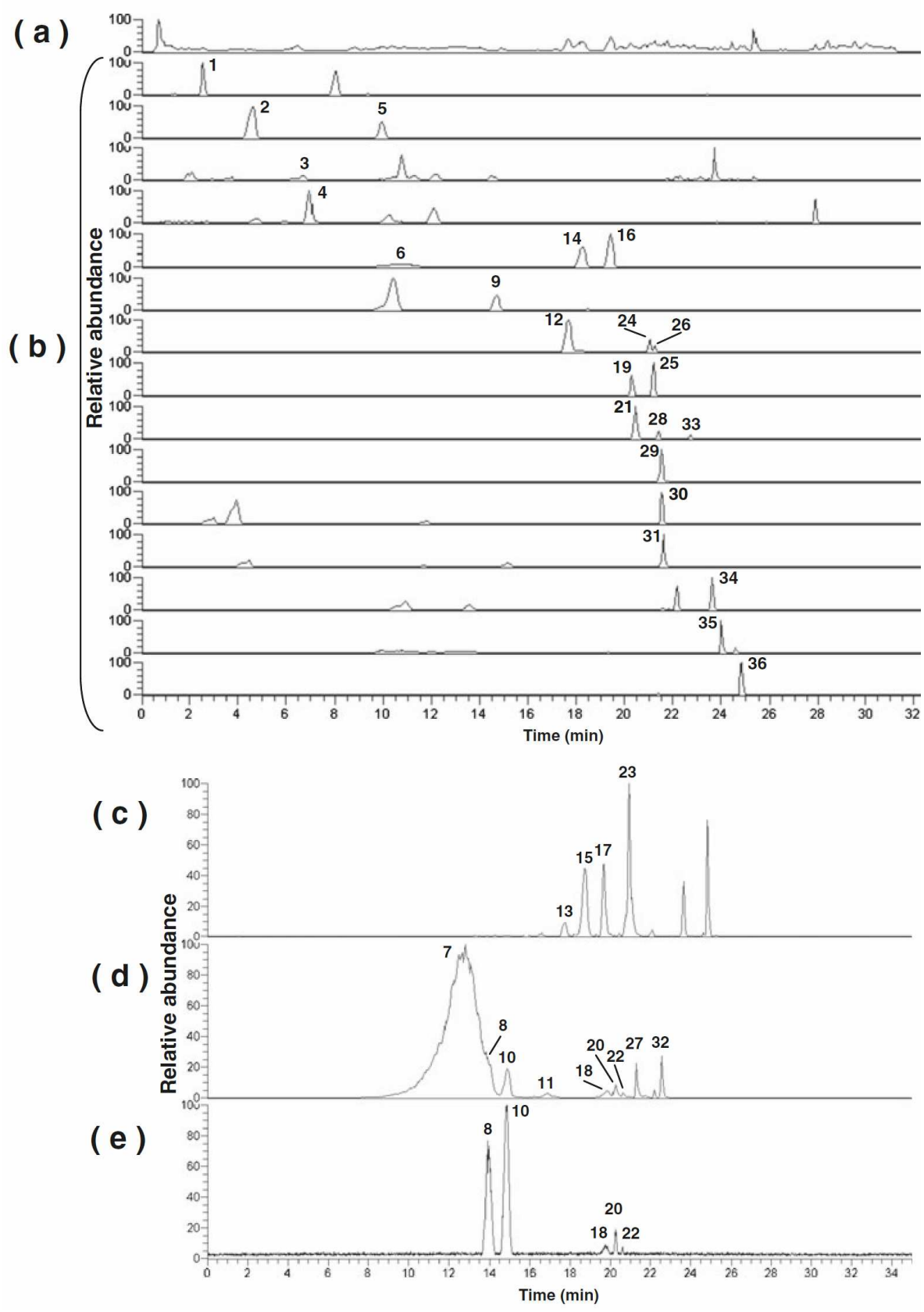

Figure 35 Phenolic compounds detected in *E. oleracea* juice (EOJ). (a) Total ion chromatogram (TIC). (b), (c), and (d) Extracted ion chromatograms of the exact masses of $[M - H]^-$ ions, using a mass extraction window of 5 ppm. (e) CRM chromatogram obtained from MS^3 experiment for the fragment ions $[M - H - 120]^-$ produced from the molecular ions $[M - H]^-$. Full details on peak numbers are available in Table 10.

7-Hydroxyflavone was chosen as IS. It was verified that extracted ion chromatograms obtained from the molecular ion of the IS did not show any interference with matrix compounds and analytes. In addition, this IS is available with a high purity level (99 %).

In the UHPLC conditions that were optimized for NAF, the width of the anthocyanin peaks was important. The analysis of these compounds in general needs the use of more acidified mobile phases [286,374,381] and ESI source operating in positive mode.

In terms of sensitivity, significant variations in the area ratio (analyte/IS ratio) of analyte peaks were observed during the development of the method depending on the methanol/water mixtures used for the sample solubilization. So peak area ratios of standards were evaluated as described by Nováková et al. [415]. A mixture of nine standards at 100 µg/mL in methanol was prepared. This mixture was then diluted to 15 µg/mL in different methanol/water ratios ranging from 15 % to 100 % methanol in water. As illustrated in Figure 36, the influence of the solvent composition on the area ratios of the studied analytes was confirmed. Between 15 % methanol (initial conditions of the chromatographic separation) and 30 % methanol, the mixtures of standards were not well solubilized. As a result, compounds, particularly aglycones, were retained during filtration before analysis, lowering observed area ratios. On the other hand, the mixture of standards was soluble in mixtures containing >30 % methanol, but important variations of the sensitivity were yet observed for high methanol contents. In addition, an increasing deterioration of the peak shapes was observed for methanol concentrations ≥50 % for catechin, ≥60 % for homoorientin, ≥70 % for rutin and isovitexin, ≥80 % for eriodictyol, and at 100 % for the other aglycones, decreasing resolution of the peaks. Therefore, a solubilization solution at 40 % methanol was chosen as a compromise for the standards and extracts.

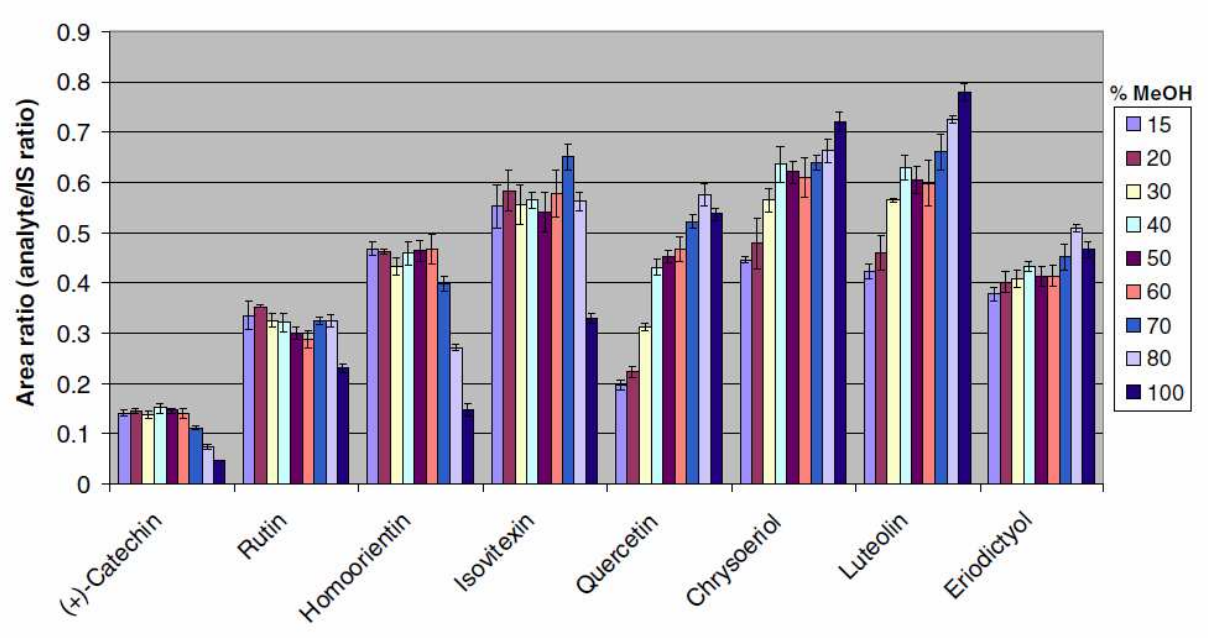

Figure 36 Area ratio (analyte/IS ratio) of several standard compounds when solubilised in different methanol/water mixtures.

ESI operated in positive ion mode was also tested but better sensitivity was obtained in negative ion mode as standards were evaluated, as already mentioned [416,417]. The negative ion mode was thus selected for the quantitative analysis.

3.3.3. Validation of the method

3.3.3.1. Identification and selectivity

This described method, which gives better chromatographic separation compared with previously published methods, allowed identifying and/or detecting known but also new NAF in the methanol extract of EOJ by HRMS and MS^n analysis. Identification data were confirmed using standards, when available in the laboratory, and by comparison with literature. Table 10 shows the proposed identifications. Compounds that were tentatively identified, on the basis of MS data, without the use of reference compounds, still need to be confirmed.

The following compounds were identified in other works: vanillic acid, (−)-epicatechin, orientin, homoorientin, isovitexin, scoparin, cyanidin 3-glucoside, cyanidin 3-rutinoside [359], quercetin, chrysoeriol, taxifolin, quercetin 3-glucoside, rutin, vitexin, kaempferol 3-

rutinoside [373], (+)-catechin [286], luteolin, protocatechuic acid, caffeic acid [353], and (+)-dihydrokaempferol [361,418].

Three peaks (21, 28, and 33) showed molecular ions at about *m/z* 287.056 $[M-H]^-$. The last one showed a MS/MS spectrum obtained from the molecular ion with a fragment ion at *m/z* 151.0037 as base peak and few other fragments at *m/z* 135.0454, 125.0245, and 107.0136. These fragment ions were consistent with the retro Diels-Alder fragmentation obtained for eriodictyol [419]. Comparison of the retention time and fragmentation pattern with a reference standard confirmed the identification. To the best of our knowledge, this is the first time that this compound is reported in EOJ. The two other isomers yielded identical MS/MS spectra with product ions generated from small neutral losses at about *m/z* 269.045 $[M-H-H2O]^-$, *m/z* 259.061 $[M-H-CO]^-$, and *m/z* 243.066 $[M–H−CO2]^-$. The fragment ion at *m/z* 125.0246 corresponded to one of the retro Diels-Alder fragments obtained for eriodictyol. Several other fragments were obtained from MS^3 experiment from $[M-H-28]^-$ produced from $[M - H]^-$, as shown in Table 10. In both cases, the fragmentation pattern corresponded to the one obtained with the (+)-dihydrokaempferol standard. As the peak 21 showed the same retention time than the standard, it was identified as (+)-dihydrokaempferol [361,418]. Peak 28 corresponded to a dihydrokaempferol isomer that has never been reported in the literature on EOJ.

Table 10 Identification of phenolic compounds of *E. oleracea* juice (EOJ) by UHPLC−LTQ−Orbitrap MS^n method.

Peak No	RT (min)	$[M-H]^-$ (*m/z*)	Formula $[M-H]^-$	Error (ppm)	MS/MS and MS^3 (*m/z*)[a] (relative abundance %)	Identification [b]
1	2.56	153.0195	$C_7H_5O_4$	0.771	109.0296 (100)	Protocatechuic acid [b]
2	4.64	289.0714	$C_{15}H_{13}O_6$	−1.216	245.0815 (100), 205.0504(36), 179.0349 (13)	(+)-Catechin [b]
3	6.68	167.0353	$C_8H_7O_4$	1.784	152.0122 (72), 123.0459 (100)	Vanillic acid [b]
4	6.95	179.0350	$C_9H_7O_4$	0.436	135.0453 (100)	Caffeic acid [b]
5	9.94	289.0714	$C_{15}H_{13}O_6$	−1.216	245.0815 (100), 205.0504(37), 179.0348 (11)	(−)-Epicatechin [b]
6	10.72	447.0931	$C_{21}H_{19}O_{11}$	−0.39	285.0393 (100)	Cyanidin 3-glucoside [b]
7	12.95	593.1508	$C_{27}H_{29}O_{15}$	−0.629	285.0396 (100)	Cyanidin 3-rutinoside [b]
8	13.91	593.1505	$C_{27}H_{29}O_{15}$	−1.253	575.1396 (19), 503.1189 (30), 485.1071 (6), 473.1085 (100), 455.0979 (6), 413.0864 (2), 383.0771 (17), 353.0663 (35) MS^3: 383.0789 (15), 353.0682 (100)	Apigenin 6,8-di-*C*-hexoside
9	14.67	303.0506	$C_{15}H_{11}O_7$	−1.306	285.0405 (100)	Taxifolin [b]
10	14.88	593.1502	$C_{27}H_{29}O_{15}$	−1.658	575.1400 (10), 503.1189 (28), 485.1076 (4), 473.1083 (100), 455.0987 (4), 413.0869 (2), 383.0767 (18), 353.0663 (37) MS^3: 383.0789 (15), 353.0683 (100)	Apigenin 6,8-di-*C*-hexoside
11	16.85	593.1507	$C_{27}H_{29}O_{15}$	−0.832	503.1207 (6), 473.1089 (41), 431.0980 (71), 341.0664 (8), 311.0558 (100)	Apigenin-*O*-hexoside-*C*-hexoside
12	17.67	449.1087	$C_{21}H_{21}O_{11}$	−0.589	269.0452 (100), 151.0037 (7)	Taxifolin deoxyhexose or isomer
13	17.74	563.1400	$C_{26}H_{27}O_{14}$	−1.099	545.1309 (31), 503.1203 (68), 473.1099 (100), 443.0986 (54), 383.0774 (30), 353.0673 (38)	Apigenin 6-*C*-pentoside-8-*C*-hexoside
14	18.24	447.0932	$C_{21}H_{19}O_{11}$	−0.122	357.0610 (43), 327.0504 (100)	Orientin [b]
15	18.71	563.1403	$C_{26}H_{27}O_{14}$	−0.655	545.1312 (26), 503.1207 (69), 473.1097 (100), 443.0993 (87), 383.0779 (53), 353.0671 (55)	Apigenin 6-*C*-pentoside-8-*C*-hexoside
16	19.42	447.0932	$C_{21}H_{19}O_{11}$	−0.189	429.0824 (18), 357.0613 (70), 327.0508 (100)	Homoorientin [b]
17	19.68	563.1403	$C_{26}H_{27}O_{14}$	−0.655	545.1311 (10), 503.1221 (6), 473.1098 (54), 443.0992 (100), 383.0778 (19), 353.0672 (26)	Apigenin 6-*C*-hexoside-8-*C*-pentoside
18	19.80	593.1505	$C_{27}H_{29}O_{15}$	−1.152	503.1188 (16), 473.1081 (100), 438.5895 (16), 429.0819 (26), 413.0864 (7), 383.0767 (14), 357.0609 (58), 327.0504 (45), 309.0391 (7) MS^3: 327.0525 (100)	Unknown [c]
19	20.30	431.0981	$C_{21}H_{19}O_{10}$	−0.673	341.0661 (6), 311.0556 (100)	Vitexin [b]
20	20.38	593.1503	$C_{27}H_{29}O_{15}$	−1.455	575.1387 (6), 503.1195 (2), 473.1081 (100), 438.5890 (28), 429.0819 (58), 413.0869 (44), 357.0608 (24), 327.0503 (6), 309.0398 (12), 293.0450 (9) MS^3: 327.0524 (100)	Unknown [c]
21	20.47	287.0558	$C_{15}H_{11}O_6$	−1.119	269.0453 (4), 259.0609 (100), 243.0660 (19), 125.0246 (2) MS^3: 241.0517 (16), 215.0724 (100), 173.0618 (29), 151.0047 (13), 125.0252 (58)	(+)-Dihydrokaempferol [b]
22	20.65	593.1491	$C_{27}H_{29}O_{15}$	−3.512	503.1191 (70), 473.1083 (100), 438.5891 (85), 413.0872 (76), 383.0770 (42), 311.0557 (42), 293.0447 (9) MS^3: 383.0792 (100)	Unknown [c]

Table 10 (continued).

Peak No	RT (min)	$[M-H]^-$ (*m/z*)	Formula $[M-H]^-$	Error (ppm)	MS/MS and MS^3 (*m/z*)[a] (relative abundance %)	Identification [b]
23	20.94	563.1399	$C_{26}H_{27}O_{14}$	−1.312	473.1099 (7), 443.0995 (9), 413.0887 (100), 341.0672 (4), 293.0460 (35)	apigenin 8-*C*-(2"-*O*-pentosyl) hexoside
24	21.04	449.1086	$C_{21}H_{21}O_{11}$	−0.856	269.0451 (100), 151.0037 (6)	Isomer of 12
25	21.20	431.0980	$C_{21}H_{19}O_{10}$	−0.881	413.0870 (5), 341.0660 (29), 311.0555 (100)	Isovitexin [b]
26	21.24	449.1086	$C_{21}H_{21}O_{11}$	−0.856	269.0450 (100), 151.0037 (6)	Isomer of 12
27	21.32	593.1504	$C_{27}H_{29}O_{15}$	−1.354	503.1192 (5), 473.1080 (6), 443.0976 (100), 413.0872 (2), 371.0764 (5), 353.0655 (3), 341.0661 (3), 323.0555 (39), 285.0400 (22)	Unknown [c]
28	21.40	287.0557	$C_{15}H_{11}O_6$	−1.572	269.0449 (4), 259.0608 (100), 243.0660 (18), 125.0246 (4) MS^3: 241.0516 (16), 215.0724 (100), 173.0618 (30), 151.0047 (10), 125.0252 (60)	Isomer of 21
29	21.52	461.1086	$C_{22}H_{21}O_{11}$	−0.639	371.0759 (20), 341.0655 (100)	Scoparin
30	21.52	463.0877	$C_{21}H_{19}O_{12}$	−1.186	301.0348 (100)	Quercetin 3-glucoside [b]
31	21.60	609.1456	$C_{27}H_{29}O_{16}$	−0.883	301.0347 (100)	Rutin [b]
32	22.59	593.1504	$C_{27}H_{29}O_{15}$	−1.354	285.0399 (100)	Kaempherol 3-rutinoside [b]
33	22.75	287.0557	$C_{15}H_{11}O_6$	−1.468	151.0037 (100), 135.0454 (3), 125.0245 (5), 107.0136 (1)	Eriodictyol [b]
34	23.62	301.0349	$C_{15}H_9O_7$	−1.548	273.0393 (10), 257.0450 (14), 179.9985 (100), 151.0037 (78), 121.2161 (6), 107.0138 (6)	Quercetin [b]
35	24.00	285.0402	$C_{15}H_9O_6$	−0.952	241.0501 (97), 217.0502 (64), 199.0397 (70), 175.0399 (100), 151.0036 (31), 133.0295 (8)	Luteolin [b]
36	24.86	299.0556	$C_{16}H_{11}O_6$	0.555	284.0315 (100) MS^3: 256.0374 (100)	Chrysoeriol [b]

[a] MS^3 experiments were performed only for peaks 8, 10, 18, 20−22, 28 and 36 from the base peak fragment ion obtained in MS/MS event.
[b] Identification were confirmed by analysis of standards.
[c] Tentative structures are proposed in "General discussion" section for the unknown compounds.

Peaks 12, 24, and 26 presented the same molecular ion at about *m/z* 449.109 $[M - H]^-$ and similar MS/MS spectra with characteristic fragment ions at about *m/z* 269.045 and 151.0037. The molecular formula from the molecular ion and MS/MS fragmentation pattern corresponded to taxifolin deoxyhexose or an isomer. Taxifolin deoxyhexose has already been identified in *E. oleracea* fruit [359,371,381]. Therefore, we identified these three compounds as taxifolin deoxyhexose or isomers.

Several peaks (7, 8, 10, 11, 18, 20, 22, 27, 32) showed molecular ions at about *m/z* 593.15 $[M - H]^-$. Peaks 7 and 32 presented a fragment ion at about *m/z* 285.040 $[M-H-308]^-$ as base peak that corresponded to their aglycone. These compounds were, respectively, characterized as cyanidin 3-rutinoside and kaempferol 3-rutinoside, after comparison with reference compounds. Cyanidin 3-rutinoside is one of the major anthocyanins found in the *E. oleracea* fruit [356,357,374]. Kaempferol 3-rutinoside identification confirmed the tentative identification of a previous study [373]. Peak 10 showed characteristic fragment ions of

vicenin-2, a di-*C*-glucosyl apigenin previously identified in this fruit [420]. Another peak (peak 8) showed very similar MS/MS fragmentation, but we observed the presence of a fragment ion at *m/z* 285.0397 with high abundance (100 %) that could correspond to an aglycone. However, this fragment was considered as coming from another co-eluted compound because in *C*-glycosidic flavonoids, the C–C bond between the sugar and the aglycone is usually not broken, so it was not presented in Table 10. In fact, as seen in Figure 35d, this fragment belongs to the co-eluted cyanidin 3-rutinoside (peak 7). MS^3 spectra obtained by CRM (consecutive reaction monitoring) scan type from the molecular ions $[M-H]^-$ and MS/MS fragment ions $[M-H-120]^-$ of the peaks 8 and 10 (Figure 35e) showed fragment ions at about *m/z* 353.068 and 383.078 for both compounds (Table 10), confirming that they are isomers, but the determination of which one is vicenin-2 was not possible.

Concentrations of the compounds of peaks 11, 18, 20, and 22 were very low. However, peak 11 could be tentatively identified. Accordingly to [421], its MS/MS fragment ion at *m/z* 431.0980 $[M-H-162]^-$ resulted from a loss of a hexoside moiety from *O*-glycosylation on a phenolic hydroxyl. Moreover, typical neutral losses of *C*-glycosyl flavonoids were observed as the ions at *m/z* 503.1207 $[M-H-90]^-$ and *m/z* 473.1089 $[M-H-120]^-$ that characterize a *C*-hexose. Finally, the other ions typify the aglycone: *m/z* 341=[apigenin aglycone or an isomer (270)+71]$^-$ and *m/z* 311=[apigenin aglycone or an isomer (270)+41]$^-$. The compound was thus tentatively identified as apigenin-*O*-hexoside-*C*-hexoside, as apigenin is the only aglycone with this molecular weight identified or present in the flavonoid glycosides in this fruit [373,418]. To the best of our knowledge, this is the first report of an *O*-glycosyl-*C*-glycosylflavone in EOJ. Compounds of peaks 18, 20, and 22 may have two oses with at least one of them *C*-linked to a flavone or flavonol, considering the molecular formula obtained by HRMS analysis and the neutral losses of 90 and 120 Da after MS/MS fragmentation. Fragments found for these peaks (11, 18, 20, and 22) were always present at the beginning, middle and end of the peaks, but with variations in their relative intensities. In these cases, it was difficult to conclude about the purity of the peaks because of the low concentrations of the compounds, which generated poor MS/MS spectra.

Peak 27 could also have two oses with at least one of them *C*-linked to a flavonoid, considering the molecular formula obtained from the molecular ion $[M-H]^-$ and the neutral losses of 90 and 120 Da. Evaluation of the MS/MS spectra obtained at least at three levels (beginning, middle and end) of the peak showed great variability in the relative abundance of

the fragment ion at *m/z* 285.0398, between 6 % at the beginning of the peak and 93 % at its end. Peak 27 should thus be considered as a mixture of compounds.

Peaks 13, 15, 17 and 23 showed a molecular ion at about *m/z* 563.140 $[M - H]^-$. Peaks 13, 15, and 17 showed the same fragment ions after MS/MS experiment (Table 10), characteristic of apigenin *C*-pentoside-*C*-hexoside (or *C*-hexoside-*C*-pentoside) isomers [422,423]. Based on these comparative studies, the peaks 13 and 15 were tentatively identified as apigenin 6-*C*-pentoside-8-*C*-hexoside isomers, and peak 17 as a apigenin 6-*C*-hexoside-8-*C*-pentoside because the ions at about *m/z* 545.131 $[M-H-18]^-$, *m/z* 503.12 $[M-H-60]^-$, and *m/z* 473.110 $[M-H-90]^-$ (base peak) were more abundant for peaks 13 and 15, which is characteristic when a pentose is located at C-6 [422,423]. In addition, the retention times of apigenin 6-*C*-pentoside-8-*C*-hexoside isomers are shorter than those of apigenin 6-*C*-hexoside-8-*C*-pentoside isomers when a C18 column is used [423]. Peak 17 may be the apigenin 6-*C*-glucoside-8-*C*-arabinoside (or an isomer), tentatively identified by Pacheco-Palencia et al. [420], although fragment proportions observed here were different from those observed by these authors. The two apigenin 6-*C*-pentoside-8-*C*-hexoside isomers (peaks 13 and 15) were detected for the first time in EOJ.

For peak 23, MS/MS fragments at *m/z* 293.0460 and 341.0672 allowed the aglycone characterization: *m/z* 341 = [apigenin aglycone or an isomer (270)+71]− and *m/z* 293 = [apigenin aglycone or an isomer (270)+41–18]$^-$. Most likely, the aglycone is apigenin, considering its occurrence in this fruit [373,418]. In addition, the ion at *m/z* 341.0672 characterized the compound as a flavonoid mono-*C*-glycoside. Because its molecular ion $[M-H]^-$ was characteristic of a diglycoside flavonoid, this compound was a *C*-glycosylflavonoid-*O*-glycosylated [423]. The presence of a very abundant fragment ion (base peak) at *m/z* 413.0887 $[M-H-(132+18)]^-$ indicated the presence of a pentose linked to the sugar involved in the *C*-glycosylation. The low abundance of the ions at *m/z* 341.0672 and 443.0995 indicated that the *C*-glycosylation was located at C-8 [423]. Additionally, this last ion $[M-H-120]^-$, alongwith the ion at *m/z* 473.1099 $[M-H-90]^-$, resulted from fragmentation of the sugar moiety of the *C*-linked sugar,with the loss of 120 Da characterizing a hexose. Consequently, the pentose could be attached only at 2″ position of the hexose, because the other positions must be free to produce the neutral loss of 120 Da [421,423]. Therefore, this compound was tentatively identified for the first time in EOJ as an apigenin 8-*C*-(2″-*O*-pentosyl) hexoside. Nevertheless, the relative abundance of the MS/MS fragment ions at the end of the peak significantly changed (data not shown in Table 10), which suggest a co-

elution with another compound. The most important variations were observed for the ion at *m/z* 443.0995, which became the base peak, and for the ion at *m/z* 413.0887, which had its relative intensity reduced to 24 %.

Finally, another anthocyanin was identified as cyanidin 3-glucoside (peak 6, and Table 10) by comparison with the standard. This compound, along with cyanidin 3-rutinoside mentioned before, are the major anthocyanins present in this fruit [356,357,374].

Chromatographic separation improves the selectivity of LC-MS methods. In addition, the use of HRMS with mass tolerance of 5 ppm substantially improves the selectivity of the extracted ion chromatograms by eliminating interferent signals. The selectivity of the proposed UHPLC−LTQ−Orbitrap MS method was evaluated by the analysis of MS/MS spectra obtained at three levels of the peaks (beginning, middle, and end). Product ions as well as their relative abundances were compared with those obtained from standards when available, or they were evaluated within a peak when no standard was available.

The method showed good selectivity for most of the compounds. As discussed above, peak 8 co-eluted with peak 7, but quantification of peak 8 could be performed on one MS/MS ion. Likewise, it was discussed that peaks 23 and 27 probably contain co-eluted compounds because of the significant variations in the relative abundances of their fragment ions observed from MS/MS spectra obtained across the peaks. Furthermore, purities of peaks 11, 18, 20, and 22 were not confirmed because of their low concentrations, which generated poor MS/MS spectra. Finally, peaks 24 and 26 were not fully separated. Therefore, the sum of both compounds was quantified. All of these peaks for which the method was not totally selective are only minor compounds.

3.3.3.2. Response function and accuracy

Different regression models were tested, such as linear, quadratic (weighted or unweighted), with or without transformations. Total error (systematic + random error) was the main decision criterion for our validation process. The suitability of the different models was assessed by plotting the accuracy profiles using 90 % β-expectation tolerance intervals and ±30 % acceptance limits, as frequently used in methods for biological matrices [424,425]. According to the results obtained, regression models in the matrix were selected for the quantification. For isovitexin, homoorientin, rutin, (+)-catechin, (+)-dihydrokaempferol, and quercetin, calibration using a weighted ($1/X^2$) quadratic regression was chosen, whereas for

eriodictyol, chrysoeriol, and quercetin 3-glucoside, weighted (1/X) quadratic regression was selected. For kaempferol 3-rutinoside and luteolin, quadratic regression was chosen. Finally, linear regression after logarithm transformation was chosen for orientin. With these calibration models, all concentrations analyzed gave results within the acceptance limits, except the lowest one for some compounds and the two lowest ones for orientin and homoorientin. The validated range for all compounds is presented in Table 9. Even if the two lowest concentrations for these last two compounds were not validated, the quantification of real samples was not compromised because these compounds are the major NAF in *E. oleracea* fruits [359] with concentrations within the validated range. Figure 37 shows some examples of accuracy profiles obtained from different regression models in the matrix and without matrix. In this figure, it can also be observed that improved accuracy profiles were obtained with a calibration in the matrix compared with a calibration without matrix. In fact, as a matrix effect is a very frequent phenomenon in LC-MS methods, calibration in the matrix has already been used to improve accuracy of the quantifications [426]. Accuracy values of the evaluated compounds are summarized in Table 9. The LC-MS method proposed in this work is the first fully validated method for NAF quantification and is the first that evaluated a calibration in the matrix for samples derived from EOJ.

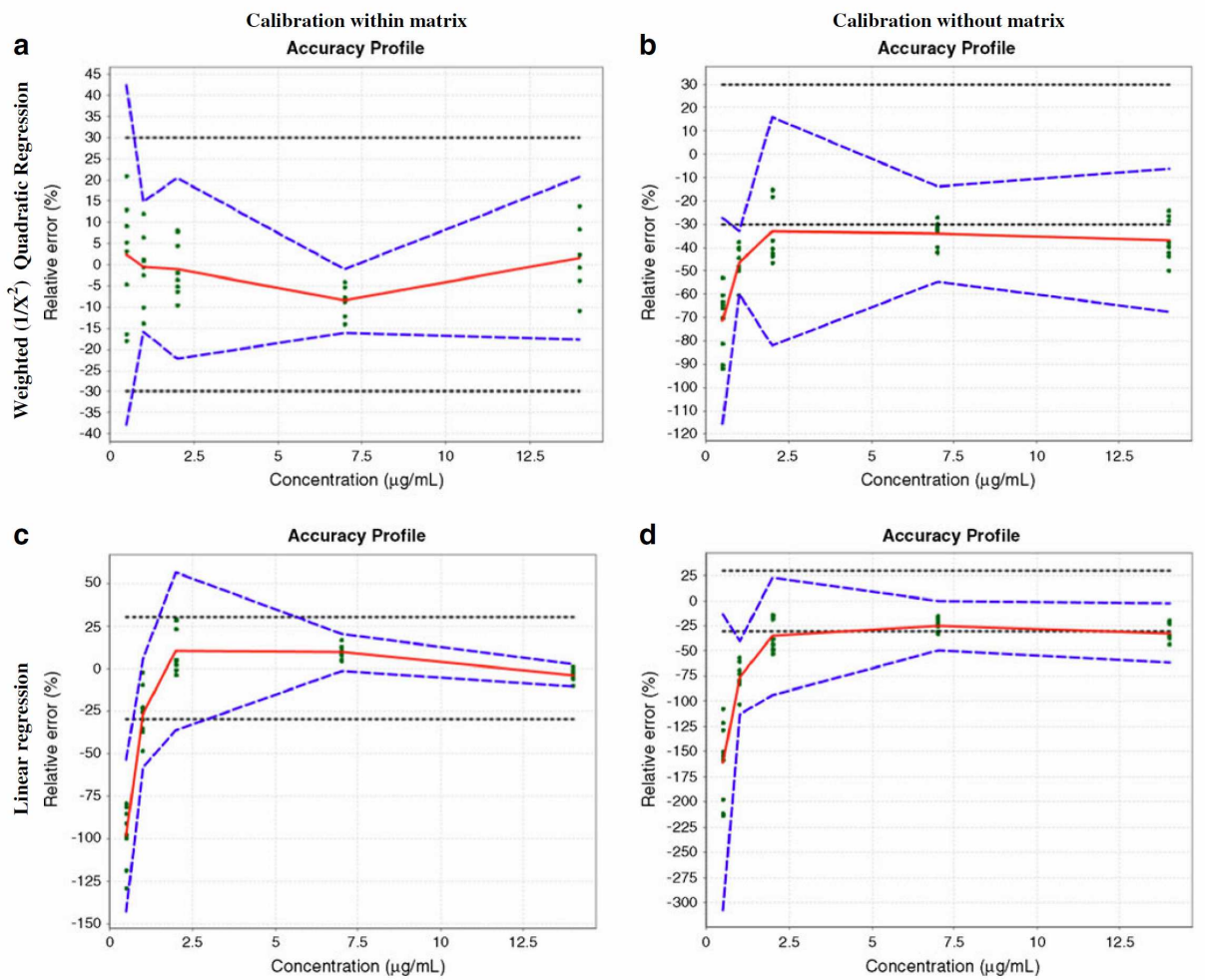

Figure 37 Rutin accuracy profiles in relative values for different regression models using 5-point calibrations. (a) Weighted ($1/X^2$) quadratic regression in the matrix (methanolic extract) and (b) without matrix, (c) linear regression in the matrix, and (d) without matrix. The continuous line represents the relative bias, the dashed lines the 90 % β-expectation tolerance limits, and the dotted lines the ±30 % acceptance limits.

3.3.3.3. Trueness, precision, and linearity

The values obtained for trueness, precision, and linearity are also summarized in Table 9. Trueness expressed in terms of relative bias was inferior to 10 % for all compounds in the validated range (except for luteolin (14.8 %) and orientin (−12.39 %)), which showed the good trueness of the method. The precision was evaluated at two levels, the repeatability and intermediate precision, and their values were expressed in terms of relative standard deviation. The repeatability and intermediate precision for all compounds were very good, and inferior to 13 % in the validated range. Values of repeatability were very close to the values of intermediate precision for a concentration level, which indicated that the effect of the series did not provide significant additional variability [374].

The linearity is the ability within a definite range to obtain results directly proportional to the concentration of the analyte. The concentrations of the validation standards were back-calculated from the calibration curve. A linear regression model was fitted on the back-calculated concentrations as a function of the introduced concentrations. The intercept, the slope, and the coefficient of determination of the equations obtained for all compounds are presented in Table 9. The slopes and R^2 values close to 1 can be good indicators to demonstrate the linearity of the method. Alternatively, the linearity was also demonstrated by the fact that the absolute 90 % *β*-expectation tolerance limits were within the absolute acceptance limits in the validated dosing range [427–429].

3.3.3.4. Limits of detection and of quantification

The LOD were calculated from the residual standard deviation and the slope of the calibration curve. The results obtained are presented in Table 9. The lower and upper limits of quantification [(LLOQ) and (ULOQ)] were, respectively, obtained by calculating the lowest and highest concentration of the targeted substance that can be assayed under the experimental conditions for which the 90 % *β*-expectation limits remain inside the acceptance limits. The LLOQ and ULOQ for all compounds are shown in Table 9.

3.3.4. Application of the quantification method to lyophilized juice samples of E. oleracea *fruits*

E. oleracea fruits were provided by three suppliers (S1, S2, and S3) of Pará state in Brazil. Fruits were processed to juice, then the juices were pasteurized (80°C/12min (P1), or 90°C/2min (P2)) or not, and their phenolic compounds extracted and analyzed in triplicate as described in the Experimental section. Calibration curves in the matrix were applied for the quantification of the major NAF (12 compounds) for which the method was validated, and the results were expressed in mg/100 g dry matter of the lyophilized juice (non-defatted material). For the other NAF, the quantification was expressed in equivalents (Table 11 shows the compounds selected for the equivalence). The peaks 11, 18, 20, 22, 23, and 27 for which selectivity was not obtained, were quantitatively estimated but they were <LLOQ. Peaks 24 and 26 were quantified together as no complete separation was obtained. The concentrations obtained for each of the three suppliers are presented in Table 11. Regarding the not pasteurized samples (P0), we observed in general that their NAF profiles were similar

between the suppliers. The higher quantitative differences were observed for the sample from S1, which contained less total NAF as a consequency of less major compounds. In addition, another remarkable difference was the higher concentrations of (+)-catechin and peaks 24+26 obtained for the sample from S3. On the other hand, quercetin and quercetin 3-glucoside were under LLOQ for this sample. Although the fruits were harvested in the same period (February 2012), some differences between the different suppliers may be expected partly because of pedological factors, but orientin and homoorientin showed the highest concentrations for all suppliers. As reported by Pacheco-Palencia et al. [359], orientin and homorientin accounted for over 50 % of the total flavonoid concentration in *E. oleracea* fruits (58 %, 61 %, and 60 % for the samples from S1, S2, and S3, respectively). These concentrations were markedly higher than those obtained by Gordon et al. [353] in ripe fruits (11 and 3 mg/100 g dry matter, respectively), most likely because of the different extraction procedures used. The pedological and climatic factors can however not be neglected in the explanation for these differences. It is interesting to note that taxifolin deoxyhexose (peak 12) showed high concentrations, a little lower than orientin, whereas in Pacheco-Palencia et al. [359], this compound was much less concentrated than orientin. Concentrations of chrysoeriol, vitexin, and isovitexin were in the same order than those obtained by Gordon et al. [353], whereas taxifolin and luteolin were under the LLOQ in our quantifications. Vanillic acid was present in traces and the sum of the concentrations of protocatechuic acid and caffeic acid was estimated (data not shown) to be <8 % of the total NAF for the three suppliers. To the best of our knowledge, quercetin and (+)-dihydrokaempferol were quantified for the first time in this work.

It should be interesting to analyze a larger number of samples and to verify if the geographical origin and/or the pedological conditions could allow justifying these differences and being utilized in the future to descrimine their origins.

Table 11 Contents of non-anthocyanin polyphenols of juices of *Euterpe oleracea* pasteurized at different conditions in mg/100 ± standard deviation (n = 3) g dry matter.

Compounds [a]/Supplier	Thermal treatment		
Supplier 1	**P0 (not pasteurized)**	**P1 (80°C/12 min)**	**P2 (90°C/2 min)**
(+)-Catechin	3.05 ± 0.07	3.69 ± 0.05	3.31 ± 0.16[e]
(−)-Epicatechin [b]	3.25 ± 0.09	3.49 ± 0.10	3.39 ± 0.18[e]
Quercetin 3-glucoside	1.33 ± 0.03	1.34 ± 0.02[e]	1.29 ± 0.07[e]
Rutin	3.61 ± 0.06	3.53 ± 0.02[e]	3.27 ± 0.20
Orientin	35.72 ± 0.42	35.02 ± 0.71[e]	33.78 ± 1.62[e]
Homoorientin	48.82 ± 0.98	44.83 ± 1.30	39.21 ± 1.80
Vitexin [c]	2.99 ± 0.04	2.98 ± 0.05[e]	2.93 ± 0.14[e]
Isovitexin	3.71 ± 0.10	3.63 ± 0.10[e]	3.37 ± 0.12
Quercetin	1.77 ± 0.03	1.26 ± 0.05	1.15 ± 0.04
Chrysoeriol	0.69 ± 0.04	0.75 ± 0.02[e]	0.72 ± 0.05[e]
(+)-Dihydrokaempferol	2.18 ± 0.02	1.70 ± 0.03	1.49 ± 0.08
Peak 12 [d]	29.81 ± 0.35	30.61 ± 1.01[e]	29.09 ± 2.11[e]
Peak 24 + 26 [d]	3.79 ± 0.06	4.92 ± 0.12	4.94 ± 0.26
Scoparin [c]	2.56 ± 0.04	2.51 ± 0.05[e]	2.38 ± 0.10
Total	*143.33 ± 1.58*	*140.25 ± 3.55[e]*	*130.32 ± 6.88*
Supplier 2			
(+)-Catechin	2.77 ± 0.06	3.35 ± 0.07	3.45 ± 0.26
(−)-Epicatechin [b]	2.57 ± 0.07	2.91 ± 0.02	3.21 ± 0.14
Quercetin 3-glucoside	1.57 ± 0.04	1.47 ± 0.05[e]	1.55 ± 0.08[e]
Rutin	3.95 ± 0.07	4.21 ± 0.19[e]	4.54 ± 0.22
Orientin	53.93 ± 0.59	53.56 ± 0.48[e]	54.98 ± 1.95[e]
Homoorientin	64.60 ± 2.34	62.62 ± 1.25[e]	64.82 ± 3.55[e]
Vitexin [c]	5.71 ± 0.08	5.53 ± 0.15[e]	5.54 ± 0.31[e]
Isovitexin	6.37 ± 0.24	6.06 ± 0.14[e]	6.11 ± 0.33[e]
Quercetin	1.52 ± 0.07	1.42 ± 0.03[e]	1.48 ± 0.05[e]
Chrysoeriol	1.03 ± 0.03	1.36 ± 0.05	1.39 ± 0.08
(+)-Dihydrokaempferol	1.72 ± 0.05	1.78 ± 0.05[e]	2.06 ± 0.11
Peak 12 [d]	37.78 ± 1.13	37.01 ± 0.74[e]	38.71 ± 2.95[e]
Peak 24 + 26 [d]	5.67 ± 0.13	6.88 ± 0.19	7.52 ± 0.35
Scoparin [c]	4.71 ± 0.12	4.38 ± 0.13	4.50 ± 0.20[e]
Total	*193.97 ± 3.97*	*192.54 ± 2.48[e]*	*199.86 ± 10.34[e]*
Supplier 3			
(+)-Catechin	8.14 ± 0.80	7.52 ± 0.38[e]	6.26 ± 0.14
(−)-Epicatechin [b]	4.43 ± 0.28	4.07 ± 0.17[e]	3.41 ± 0.17
Quercetin 3-glucoside	nq	nq	nq
Rutin	3.07 ± 0.25	3.00 ± 0.15[e]	2.96 ± 0.05[e]
Orientin	55.19 ± 0.76	53.16 ± 0.79	53.99 ± 1.09[e]
Homoorientin	71.56 ± 5.81	61.26 ± 3.97[e]	61.22 ± 1.19
Vitexin [c]	6.26 ± 0.48	5.98 ± 0.33[e]	5.86 ± 0.21[e]
Isovitexin	7.07 ± 0.53	6.47 ± 0.42[e]	6.35 ± 0.25[e]
Quercetin	nq	nq	nq
Chrysoeriol	0.99 ± 0.07	1.24 ± 0.06	1.44 ± 0.03
(+)-Dihydrokaempferol	1.96 ± 0.14	1.65 ± 0.10	2.38 ± 0.05
Peak 12 [d]	38.24 ± 0.96	35.23 ± 2.08[e]	33.80 ± 1.46
Peak 24 + 26 [d]	8.32 ± 0.67	9.25 ± 0.51[e]	9.02 ± 0.35[e]
Scoparin [c]	4.38 ± 0.30	3.98 ± 0.17[e]	3.97 ± 0.07[e]
Total	*209.67 ± 8.43*	*192.81 ± 7.74[e]*	*190.67 ± 1.76*

[a] Peaks 8–11, 13, 15, 17, 18, 20, 22, 23, 27, 28, 32, 33, 35 of Table 10 were <LLOQ.
[b] Concentration estimated in equivalents of (+)-catechin, [c] isovitexin, and [d] rutin.
[e] No significant differences (p>0.05) were observed as compared with P0 treatment values.
Peak 12, 24, and 26 are described in Table 10 and correspond to taxifolin deoxyhexose or isomers.
nq, unquantifiable (<LLOQ).

Pasteurization before commercialization is supposed to improve polyphenols stability over time. Indeed, this process induces the inactivation (by denaturation) of a significant proportion of the polyphenoloxydase present in the juice. Additionally, this treatment also promotes a decrease of the microbial load, which also produces enzymes that degrade the phenolic compounds. However, this thermal treatment can also contribute to the degradation of these compounds [359]. To analyse the effect of pasteurization on NAF contents, aliquots of the P0 samples were pasteurized using two different treatments and analyzed. By comparing the total NAF content, before and after treatment, we can observe in most of the cases a small (<10%) decrease. The only exception are the samples from S2 where we observe no significant difference (p>0.05). Pacheco-Palencia et al. [359] also observed the absence of difference after treatment at 80°C for ten minutes. Loss of polyphenols may be explained by their unstability at high temperatures. Nevertheless, when each individual constituent is analyzed, the effet of thermal treatment may differ according to the sample and the compound. The concentration of (+)-catechin and (−)-epicatechin increased for S1 and S2 when submitted to a thermal treatment. One possible explanation for this is that some proanthocyanidins (polymeric forms containing these flavan 3-ols found in açai [381]) have partially degraded with heat, producing these monomers. However, proanthocyanidins were not analyzed nor quantified in our method, because they were not solubilized in the condition we used or because they eluted during the washing gradient of the C18 column, hindering their identification, because at these conditions all other apolar compounds, including interferents are eluted [430]. Proanthocyanidins can be very well separated using normal phase chromatographic columns (polar stationary phase) [381,430]. For S3, these increases were not observed; perhaps because this sample was poor in proanthocyanidins. In [359], the concentrations of all twenty non-anthocyanin polyphenols, including (+)-catechin and (−)-epicatechin, remained constant after treatment. We also noted that the concentrations of chrysoeriol (particularly in S2 and S3), and the sum of peaks 24+26 (particularly in S1 and S2) also increased when heat treated. However, we could not propose any explanation for these increases considering the compounds we identified in the extract.

Other compounds were almost stable, such as quercetin 3-glucoside, rutin (in samples S1/P1, S2/ P1 and S3), orientin, homoorientin (in S2 and S3), vitexin, isovitexin (in S1/P1, S2 and S3), peak 12 (except S3/P3) and scoparin, while the remaining ones usually decreased or had different behaviors according to the sample.

3.4. Conclusions

The first validated UHPLC−LTQ−Orbitrap MS method for the quantification of 12 NAF in EOJ is described. The method was selective and gave good estimators of linearity, accuracy, trueness, and precision. Calibrations in the matrix were used for quantifications and showed better accuracy profiles in comparison to calibrations without matrix. The applicability of the method was demonstrated on real samples of juice of *E. oleracea* fruits from different suppliers, which were compared in terms of content of NAF, some of them being quantified for the first time. In general, the juices non pasteurized showed similar NAF profiles. After thermal treatment, these juices showed a small decrease (<10%) of the total NAF. Nevertheless, the effect of thermal treatment on the individual constituent may differ according to the sample. The optimization of the dissolution media (40 % methanol in water) for the standards and extracts was shown to improve the sensitivity of the method. Extraction time optimization was performed along with evaluation of recovery rates. The chromatographic separation was improved to quantification purposes and allowed the separation of several isomer compounds, including the major ones. In addition, eriodictyol was identified for the first time in this fruit, along with five new compounds for which the identification was tentatively proposed but without the identity of the attached sugars. Finally, tentative structures were also proposed for two groups of 2 and 3 compounds, which were isomers of apigenin 6,8-di-*C*-hexoside and taxifolin deoxyhexose, respectively.

Acknowledgments

The authors thank very much Professor J.-L. Habib-Jiwan for his rich scientific orientation (*in memoriam*), Professor Giulio Muccioli, Julien Masquelier (UCL/LDRI/BPBL), Dr. Marie-France Hérent (UCL/LDRI/GNOS andMASSMET platform), and Gabrielle Chataigné for their kind helpwith LC-MS experiments, Dr. Emmanuelle Lautié from UCL/LDRI/GNOS for her kind scientific and technical advices, Marie-Christine Fayt, Jean Paul Vanhelleputte, and Ramazan Colak for their technical support in the LC-MS system. Dr. Vincent Baeten from CRA-W who kindly donated some commercial standards is acknowledged. ADRI-UCL is acknowledged for financial support to the first author, Belgian National Fund for Scientific Research (FNRS) (FRFC 2.4555.08), the Special Fund for Research (FSR), and the faculty of medicine of UCL for their financial support for the acquisition of the LTQ−Orbitrap XL, the program PIC of the Coopération Universitaire au Développement (CUD), FAPESPA and CNPq (Brazil) for financial support on this research.

Financial support from theWalloon Region of Belgium is gratefully acknowledged for the funding of E.R. with the 0CWALity convention funds 1217614 (iGUARANTEE).

General discussion

The general context of this thesis is a collaboration between the Université catholique de Louvain and the Universidade Federal do Pará (UFPA) in Brazil, from a projet (PIC) financiated by the Commission Universitaire pour le Développment (CUD, Belgium). The main objective of the PIC is to give added value to different plant products from the Andean and Amazonian biodiversity, through a better knowledge on their bioactive compounds, for a sustainable regional development. Several approaches have been formulated and performed to achieve this objective; this thesis is one of them.

We chose to study the fruits and juice of *E. oleracea* palm, because of their economic importance in the development of the Amazon region, where these fruits are very abundant. In the last two decades, they became an important product of exportation. The Pará state, where UFPA is located, is the biggest producer (95%) of these fruits in Brazil. They have gained much attention principally due to their high content in antioxidants, mainly phenolic compounds. The increase of the commercialization of the fruits has directly contributed to the improvement of the economy of the cooperatives of the region. These cooperatives involve the local inhabitants to harvest and process the fruits to juice. Consequently the improvement of the life conditions of the local inhabitants occurred. Recently, the collaborations between academic, commercial and governmental sectors have been intensified to improve the products from the fruits, mainly juices, and to develop new products as purified extracts rich in phenolic compounds, derived from the fruits, in order to improve the economy [355]. This improvement also contributes to the preservation of the *E. oleracea* palms. Their abundant presence along the rivers of the Amazonia estuary is very important to the equilibrium of the ecosystem in the region. Another export product from the palm is the palm heart. In order to obtain this last raw material, the palm has to be sacrificed. Nowadays, the exploitation of the fruits has become more cost effective and more intense than that of the palm heart. The exploitation of *E. oleracea* fruits is an example of sustainable extractivism in the Amazon forest [356] and it has been shown to be closely related to the development of the Amazon region.

Currently, there is a need for analytical methods and scientific collaborations between academic and local private sectors to support studies aiming (1) at understanding the relationship between the phenolic compositon and the biological activities of samples derived from fruits of *E. oleracea*, (2) at determining optimal conditions of harvest, extraction, and purification of extracts and (3) at evaluating the stability of juices over time in function of different processes. The objectives of this thesis were thus to develop and validate analytical

methods for the identification and quantification of phenolic compounds of fruit extracts and juices of *E. oleracea*, in order to give added value to these raw materials, to improve the collaboration between academic and private sectors of the Amazon region, and to contribute to the quality control of these products. Consequently, they will contribute to the regional development. For this purpose, an UHPLC−PDA−LTQ−Orbitrap MS system was fundamental, because of its great potentialities in identification and quantification of compounds. The results presented in this work will be discussed in the two next sections.

1. A rapid validated UHPLC-PDA method for major anthocyanin quantification from *Euterpe oleracea* fruit extracts

Industries, away from the Amazon region, work mainly with the pasteurized juice, which is more stable and easy to be processed for further formulation. On the other hand, local producers and research institutes of the Amazon region are close to the harvest zone, turning possible to analyze fresh fruits. Additionally, the juice requires processing for its production. Therefore, fruits were chosen as raw material for this study. As the anthocyanins are the major compounds and those that give the highest economic value to the fruits, we decided to focus first on them. Because of their high concentrations, both DAD and MS detections provide high signal-to-noise ratios. The DAD detection was chosen because it is less expensive, and has fewer steps to be optimized for the analysis. Additionally, as predicted at the beginning of the thesis, an UHPLC-DAD system, which is similar to the one used in this work, was recently acquired by the partner laboratory in UFPA.

The first problem we had to face during the development of the extraction procedure concerned the stability of the anthocyanins in the extracts from fruits. It is known that their stability is affected by several factors, the most important being pH, storage temperature, chemical structure, light, oxygen, and enzymes. The most common degradation products are aglycones, phenolic acids, and other small aromatic compounds, such as aldehydes [431]. Furthermore, it has been shown that the structure of the anthocyanin is also an important factor, for example diglycosides are more stable than monoglycosides. During the development of our procedure, we observed that a loss of anthocyanin heterosides was mainly observed during the evaporation process of the extract obtained from the fruits, with the appearance in the chromatograms of cyanidin (aglycone) which was not detected in açai samples [359]. This agycone was detected when evaporation was realised under reduced pressure at 40°C for 2.5 hours. After a short evaporation to eliminate the volatile solvents of the anthocyanin fraction and further lyophilisation, similar chromatograms were observed. So we had to optimize the pressure, rotational speed, sample volume and temperature to reduce, as much as possible, the degradation and decreased the evaporation time to 1.5h, necessary to eliminate the water from the extracts. In this condition, the cyanidin aglycone was no more observed in the chromatograms. Even in this optimized condition, the recovery of the procedure showed that the anthocyanins were partly degraded: as could be observed in Chapter 2 (Results section), the recovery of the SPE procedure for cyanidin 3-glucoside and cyanidin 3-rutinoside were 58.7% ± 4.9 and 74.6% ± 3.6, respectively. These values are

consistent with the known stability of anthocyanins i.e. cyanidin 3-rutinoside is more thermostable than cyanidin 3-glucoside [359].

Developing and validating an analytical method may seem easy, but in addition to the finding of a method allowing the separation of the peaks and the best extraction and evaporation procedures, we had to face other problems to obtain acceptable results. During the development of the method of anthocyanin separation, using the chromatographic column described in Chapter 2 and in Table 12 (column A), we observed variations in the analytical responses in function of the water/methanol ratios of the solution (having 1% of formic acid) used for the sample solubilization. When we increased the percentage of methanol from 25% up to 90%, the peak areas of the major anthocyanins (cyanidin 3-glucoside and cyanidin 3-rutinoside) were reduced. Additionally, we observed with the increasing of the methanol percentage, an increase of the "solvent peak" at the beginning of the chromatogram (peak C in Figure 38). MS and MS/MS experiments showed that this peak contained cyanidin 3-glucoside and cyanidin 3-rutinoside, confirming that a fraction of the anthocyanins were early eluted.

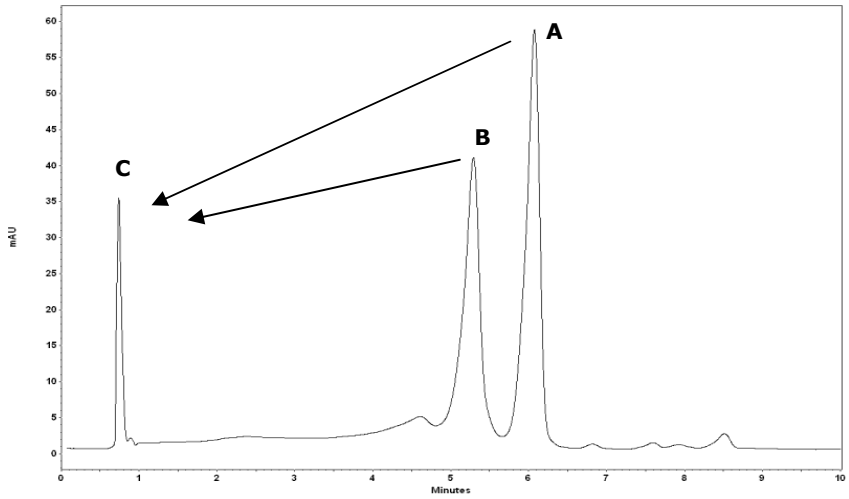

Figure 38 Chromatogram at 520 nm of a methanolic extract of *E. oleracea* fruits, solubilized in water/methanol/HCOOH (9/90/1, v/v). A, cyanidin 3-rutinoside; B, cyanidin 3-glucoside; and C, a mixture of A and B.

When the samples were solubilized in a mixture of water/acetonitrile/formic acid (90/5/5), with an elution strength corresponding to the initial conditions of the elution gradient, the solvent peak did not contain anthocyanins. In addition, we also observed an increase of the areas of peaks A and B. Nevertheless, the samples were not totally solubilized

in these conditions. Therefore, methanol was added and the final composition of the solubilization solution was defined as methanol/acetonitrile/water/formic acid (15/5/75.25/4.75). A chromatogram obtained from samples solubilized in this solution is shown in Figure 29 of Chapter 2. We observed that different experimental conditions were used in the literature (reversed-phase columns, initial gradient, etc.) as well as different solubilisation media for solubilisation of açai anthocyanin-rich extracts before analysis. In three publications, a high "solvent peak" is observed with methanol/water/acetic acid (85/15/0.5) [381] and methanol/5% formic acid in water (15/85) [358,407] as solubilising solutions, but no MS analysis was performed on the peak. In another study this phenomenon was not observed and it was reported that the use of a methanol/water/formic acid (70/29.9/0.1) solubilization solution improved peak shape [432]. These observations demonstrate the need for optmization of this step.

It is known that the use of a sample solubilisation solution containing an organic solvent at a very different proportion than in the aqueous mobile phase can induce peak shape deterioration and split peaks in reversed-phase HPLC [433,434]. However, in our case, we observed not only peak distortions but also the elution of a non-retained fraction of the anthocyanins in the "solvent peak". A similar phenomenon was not discussed in the literature. We wondered if this could be explained by a mass and/or volume overload of the column [23]. When less concentrated samples were injected, the phenomenon illustrated in Figure 38 was also observed, demonstrating that it was not due to a mass overload in the column. We then checked for a volume overload. There are three injection modes in our HPLC system: "full loop", "no waste", and "partial loop". For the first one, the volume injected corresponds to the volume of the loop of injection, that were of 5µL for the A, B, and C columns (Table 12) and of 25µL for the D and E columns. For the two other injection modes, the injection volume is inferior to the loop volume, and the remaining volume is completed with the solvent of the wash bottle of the HPLC system. For A, B, C and D columns, the "peak C" was not observed in "partial" and "no waste" injection modes when the solution in the wash bottle was the mobile phase (at the initial conditions of the elution gradient), but the problem was observed when this solution was 100% methanol, confirming that the high volumes of methanol were responsible for the phenomenon observed in these small diameter columns.

Table 12 Columns used during development of the UHPLC−PDA method.

Column	Producer	Column type	Endcapped	Particle size (µm)	Dimension (mm)
A	Waters	UHPLC HSS C18	yes	1.8	2.1 x 100
B	Thermo scientific	UHPLC Hypersil GOLD C18	yes	1.9	2.1 x 100
C	Thermo scientific	UHPLC Hypersil GOLD C8	yes	1.9	2.1 x 100
D	Phenomenex	HPLC Gemini C18	yes	3	2 x 150
E	Merck	HPLC Lichrospher C18	yes	5	4 x 250

A good chromatogram was obtained using the column E even when the samples were solubilized with water/methanol/formic acid, 9/90/1 (injection volume 25µL, in full loop mode, and 10µL in partial loop mode, using methanol in the wash bottle). This may be explained by the higher diameter of this column [23]. In fact, it seems that the relatively high volumes of methanol in the injected solution elutes a fraction of the anthocyanins before being completely mixed with the mobile phase (Peak C in Figure 38), because of the small diameter of the column and the low mobile phase volume. In the literature, the injection volume is frequently up to 5µL for columns with the same dimensions as column A [435–437]. However, each method has its specifities. In our case, it was demonstraded that the composition of the solubilisation solution needed to be optimized to use 5µL as injection volume. The column E was not used for this work, because of several reasons: high run times, flow rate (approximately of 1.5mL/min) incompatible with ESI source when no split is used, not stable at pH<2, etc. The selected column (column A) has high tolerance to low pH (pH range between 1 and 8), as our mobile phase needed to have a pH of 1.8.

Concomitantly to the publication of the article corresponding to Chapter 2, another work was also published on a validated method for the quantification of anthocyanins from açai dietary supplement raw materials [432]. It used a LC-HRMS method with a Q-TOF as mass spectrometer and a UHPLC C18 column (ZORBAX Eclipse plus C18, 1.8µL, 2.1 x 100mm). In this work the validation experiments were also performed for the major anthocyanins (cyanidin 3-glucoside and cyanidin 3-rutinoside). The solubilisation solution was a mixture of methanol/water/formic acid (70/29.1/0.1), giving the best peak shapes and the samples were injected at a volume of 10µL. The phenomenon illustrated in Figure 38 was not observed. The total run time of this method was 35min and the retention times of cyanidin 3-glucoside and cyanidin 3-rutinoside, 9.65min and 9.81min, respectively. The total run time of our method was significantly lower (only 17min) as well as the retention times of the compounds, 5.19min and 6.01min, respectively. The trueness and selectivity validation

criteria were not evaluated in the other method. LOD and LOQ were defined as the signal-to-noise ratio equal to 3 and 10, respectively, from the analysis of diluted standard solutions. The LOQ values were 0.24 μg/mL and 0.12μg/mL for cyanidin 3-glucoside and cyanidin 3-rutinoside, respectively, which were lower than those obtained in our work of approximately 1 μg/mL. HRMS detection generally has higher sensitivity than DAD detection, which was used in our work. However, in the other work, the accuracy was not evaluated for the LOQ [375], on the contrary to our work. In this other work, the accuracy and precision of the method were determined only for one concentration level of the dosing range. The accuracy was evaluated by recovery experiments and ranged between 91% and 109% for cyanidin 3-glucoside and between 91% and 104% for cyanidin 3-rutinoside, which corresponded to errors < ±10% in relation the spiked concentration. In our work, five concentration levels of the dosing range were evaluated and their β-expectation tolerance limits were < ±10% for both compounds, except for the lowest concentration level that were < ±21% for cyanidin 3-glucoside and < ±15% for cyanidin 3-rutinoside (Table 7, Chapter 2). In terms of precision (repeatability and intermediate precision) the other work reached values <11% whereas in our work they were <5%.

Different qualitative profiles of the major anthocyanins in samples derived from *E. oleracea* fruits have been found in the literature (Table 13). The samples analyzed were very diversified: fruits, commercial juice, non commercial juice, powders obtained from different processing methods, etc., and in many cases, the works did not describe in details the procedures of processing used by the suppliers for the production of the samples. In our work, the major anthocyanins were cyanidin 3-glucoside and cyanidin 3-rutinoside, in accordance with the majority of the works shown in Table 13. The discrepancy of some results could be explained by differences in the maturity stage of the fruits, adulteration of the original product, chemical changes during processing, etc. In our work, the samples were of defined maturity stage and harvest location, they were not processed to juice and the processing was controlled. Therefore, the profile of the major anthocyanins described in the present work should be more authentic.

Table 13 Major anthocyanins found in samples derived from *E. oleracea* fruits.

Major anthocyanins	Samples	References
Cyanidin 3-arabinoside [a] Cyanidin 3-arabinosylarabinoside [a]	Juice	[401]
Cyanidin 3-glucoside	Juice	[438]
Cyanidin 3-rutinoside	Juice	[407]
Peonidin 3-(6"-malonyl)glucoside [a] Cyanidin 3-rutinoside, Delphinidin 3-(6"-acetoyl)glucoside [a] Cyanidin 3-glucoside	powder	[370]
Cyanidin 3-rutinoside Cyanidin 3-glucoside	juice	[286,351,358]
Cyanidin 3-rutinoside Cyanidin 3-glucoside	pulp	[359,371]
Cyanidin 3-rutinoside Cyanidin 3-glucoside	powder	[381,432]
Cyanidin 3-rutinoside Cyanidin 3-glucoside	Fruits	[350,357]

[a] These compounds were reported only in the cited references.

As discussed in a section 1.2.4 (Bioavailability of phenolic compounds), anthocyanin heterosides may be absorbed in the gastrointestinal tract in their unchanged form, as conjugated compounds (phase II metabolism), as aglycones or as phenolic acids and aromatic [103,439] so they can contribute to several functional properties of berries, such as antioxidant, anti-inflammatory, anticancer and neuroprotective [440]. For example, among numerous publications, we can quote the work of Tsuda et al. [441] who reported the antioxidant activity of cyanidin 3-glucoside and cyanidin, using defferent methods: linoleic acid autoxidation, and liposome, rabbit erythrocyte membrane, and rat liver microsome oxidation systems. Cyanidin had a stronger activity than cyanidin 3-glucoside. Another work demonstrated that cyanidin 3-glucoside can increase the oxidation resistance of the serum to lipid peroxidation in rats and suggested that this compound acts as a potent antioxidant *in vivo* when acute oxidative stress is encountered [442]. In fact, an increase of the antioxidant activity of plasma in human studies was observed after the intake of açai juice [1,128], which suggests a protective effect against cardiovascular diseases. In these studies, the major anthocyanins of the juice were the same than those observed in the present work. Their antioxidant activities may also explain anti-inflammatory and chemopreventive effects [440].

Concerning anticancer activities, in a recent work the effects and the mechanisms of cyanidin-3-rutinoside activity on several leukaemia and lymphoma cell lines was studied *in vitro* [443]. Cyanidin-3-rutinoside induced apoptosis in a dose- and time-dependent manner (About 50% of the cells became apoptotic within 18 h when 50 μM of the compound was applied), producing the accumulation of peroxides and reactive oxygen species (ROS)-dependent activation of p38 mitogen-activated protein kinase (MAPK) and c-Jun N-terminal kinase (JNK), which contributed to cell death. Notably, cyanidin-3-rutinoside treatment did not lead to increased ROS accumulation in normal human peripheral blood mononuclear cells and had no cytotoxic effects on these cells.

Protocatechuic acid is one of the catabolites derived from colonic microbial degradation of cyanidin-*O*-glycosides, including cyanidin 3-glucoside and cyanidin 3-rutinoside [444]. Yip et al. [445] reported cytotoxicity of protocatechuic acid against HepG2 hepatocellular carcinoma cells in dose-dependent manner (IC_{50} = 60 μM). This study also showed that the cytotoxic effect might be mediated via sustained phosphorylation and activation of JNK and p38 MAPK. Further studies are nevertheless necessary to assess the potential of these molecules as anticancer agents.

In addition to major compounds, an article reported the presence of two non identified chromatographic peaks eluting before cyanidin 3-glucoside in a partially purified anthocyanins extract from *E. oleracea* juice, using a HPLC-PDA-MS/MS and a HPLC C18 column [358]. In our work, we also detected two minor anthocyanins eluting before cyanidin 3-glucoside from a crude extract and we tentatively identified them as cyanidin-di-*O*-glycosides. This identification was possible because of our analytical tool (UHPLC−PDA−LTQ−Orbitrap) that improves the selectivity and the sensitivity as compared with the one used in [358].

As discussed in Chapter 2, the sum of the concentrations of cyanidin 3-glucoside and cyanidin 3-rutinoside obtained in the present work (between 488 and 583mg/kg fruits, approximately) were inferior to the sum of the same compounds obtained by another work (800 and 1200 mg/kg fruits) [357]. In both works, the samples corresponded to a same region and a same maturity stage. Nevertheless the harvesting were 17 km distant from each other in the last reference. The concentration of anthocyanins seems thus to be highly dependent of specific conditions. Because of these variations, it is necessary to have validated quantitative methods for the standardization of the fruits and derived products and for the evaluation of the

different locations of harvest. In fact, the region where the samples were harvested is a zone of high production.

The PIC project, in collaboration with governmental institutions in Brazil, has also the objective to contribute to the improvement of norms of product quality. The qualitative and quantitative profiles for *E. oleracea* fruits, obtained from validated method and authentic products, will contribute to reach this objective.

In the North of Brazil, some research institutes have acquired analytical tools like those used in this work, and have collaborations with the private sector. Our method can be used in the context of these collaborations to improve conditions of processing, to determine periods and locations of harvest, to develop products etc. Nevertheless, in general, the methods used for routine analysis in the Amazon region are less time-consuming and needed less expensive equipments, etc. However, our method can also be used as a reference method to calibrate the routine methods.

On the other hand, producers, having access to sophisticated equipments, and wanting to perform a detailed characterization of their products, can use and adapt our method, in function of their needs. It was discussed in Chapter 2, that only a small percentage of the anthocyanins was found in the ethyl acetate extract (<0.03%), which also showed concentrations close to the lowest concentration level (approximately 2µg/mL). Therefore the step of SPE performed on the ethyl acetate extract can be removed. Analogously, the last extraction procedure with 50% methanol can also be eliminated of the protocol, because 95% of the anthocyanins were found in the methanol extract. The calibrations in the matrix was chosen for the quantification of the major anthocyanins because of the better accuracy profiles observed with this approach, specially for the lower concentration levels, as compared with the profiles obtained with calibrations without matrix (Figure 32, in Chapter 2). However, good accuracy profiles were also obtained for both major compounds with calibrations without matrix, as illustrated in Figure 39, with LLOQ of 1.67µg/mL and 0.97µg/mL for cyanidin 3-glucoside and cyanidin 3-rutinoside, respectively. So this calibration approach can be used for the quantifications in order to simplify the method.

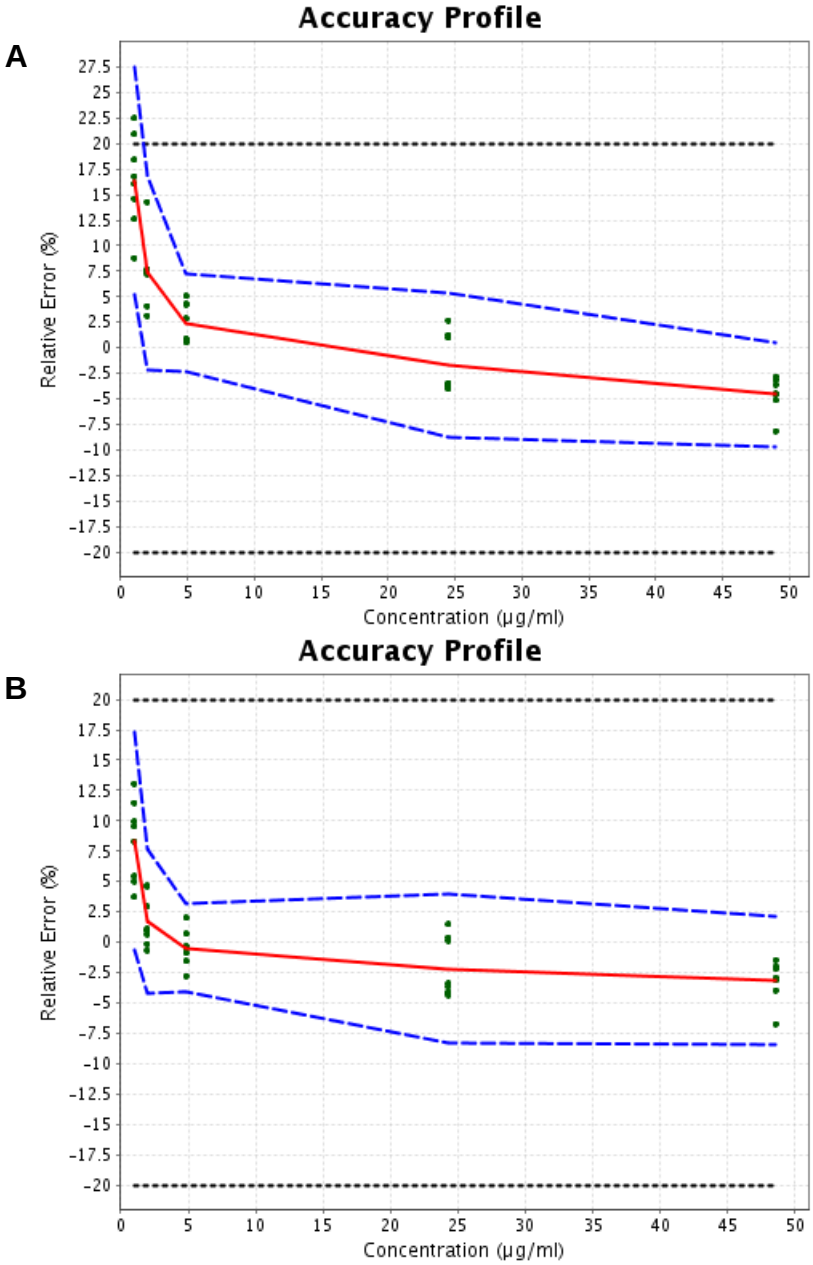

Figure 39 Accuracy profile in relative values obtained by considering Quadratic Regression for cyanidin 3-glucoside **(A)** and by considering Weighted ($1/X^2$) Linear Regression for cyanidin 3-rutinoside **(B)**. Both regression models were fitted using five points calibrations obtained without matrix. The continuous line represents the relative bias, the dashed lines the 95% β-expectation tolerance limits and the dotted lines the ±20% acceptance limits.

Other problems that we had to face were related to sample preparation and transport to Belgium. These difficulties can help future international research projects. The main problems faced were partial loss of the extracts during the flight, difficulties to fully evaporate the solvents from the extracts, and a possible degradation of phenolic compounds in samples. The acquisition of the fruits, the extraction procedures, and the evaporation of the extracts were performed in Brazil, and then, the extracts were sent to Belgium. In Belgium, the

samples were freeze stored and used for the studies on the development and validation of analytical methods, and phenolic characterization. A first set of samples were sent to Belgium in the form of liquid extracts (in acidified methanol and acidified ethyl acetate) in opaque glass tubes. Unfortunately, several samples were partially or fully lost during the flight, probably because of difference of pression between the interior and the exterior of the tubes in the luggage compartment of the plane. The samples were also contaminated with the plastic material of the tube caps used for the transport. Consequently, the quantification of these samples was not suitable to be performed due to the difficulty to relate the phenolic concentration in the extracts with the initial mass of the fruits. Furthemore, the extracts obtained with ethyl acetate were not homogeneous (extracts had red colour, small precipitates, and another phase of white colour, like an emulsion) thus probably the loss of volume was not uniform; moreover the plastic contaminants would hamper the qualitative analysis by LC-MS. Another set of samples was prepared with the same extraction protocol (Extraction and clean-up procedure section in Chapter 2). Some difficulties were found to fully evaporate the extracts due to the limited capacity of the evaporator for high sample volumes. Consequently, each sample was divided in several tubes. However, for the transport, a large number of tubes would not be practical. Therefore, the dried extracts were again solubilised in low volumes and assembled in one tube and again evaporated. Consequently, the extracts were evaporated in several steps. Data we obtained for anthocyanins were generally largely lower than those usually found in the literature and in the Brazilian laboratory, suggesting that the anthocyanins may be degraded. The exact steps responsible for a possible degradation were not fully determined but it is known that anthocyanins are unstable at different conditions, high temperatures, light, presence of oxygen and pH > 7 and some of their degradation products are aglycone compounds (as a result of a deglycosylation) which can be further converted to phenolic acids (e.g. 4-hydroxybenzoic acid from cyanidin aglycone), and polymeric compounds generated by reactions with tannins [377,446]. These degradation products were not detected in the samples. In the case of polymeric compounds, they could be present in the extracts in the form of precipitates; consequently they could be eliminated during filtration and centrifugation procedures. Degradation must have occurred mainly during the evaporation procedures that were performed in several steps, but also during the time that the samples remained in contact with the atmospheric air and light during the sample preparation procedures. In Brazil and in Belgium, the tubes containing extracts were stored hermetically sealed, under N_2 atmosphere, under low temperatures and in the dark, thus probably the degradation did not occur in these steps or was not significant. In addition, the

extracts in solution were always maintained at low pH in which they are more stable [377]. Finally, in order to obtain reliable results, another set of fruits were acquired by the laboratory in Brazil. Another evaporator with higher evaporation efficiency was used for a rapid evaporation time.

We also have to note that it was not possible to determine precisely the recovery of the extraction due to the difficulty to obtain sufficient amounts of standards, and the impossibility to reproduce with standards the behaviour of the anthocyanins in the fruits. As the validation experiments included only the extracts, this method has to be considered as validated for the quantification of anthocyanins from *extracts* and not from *fruits*. In fact, in the fruits, the anthocyanins are stored in the cell vacuoles [38] and during extraction they diffuse into the extraction solution. On the other hand, the pure compounds spiked on the fruits would quickly be solubilized. Consequently, the recovery would be overestimated. In return, it was observed that in the sequential extraction of the anthocyanins, the intermediate extraction with methanol was responsible for approximately 95% of the total amount of quantified anthocyanins, demonstrating the high efficiency of this extraction.

This experience observed with the anthocyanin degradation and loss of samples during transport highlights the crucial importance of the sample preparation and transport in the context of international scientific collaborations. In future projects some concerns should be observed: the different steps of sample preparation need to be as fast as possible in order to reduce the time between the reception of the samples and the final dosage of them. The full optimization of the anthocyanin extraction was not included in the scope of this thesis but should be studied. This would require another project plan and the presence for long periods in Brazil and the thesis was planified to be accomplished entirely in Belgium. For the transport, the extracts need to be dried. In this form, they are more stable and have reduced risk of material loss. The recipients containing samples need to be in opaque glass material and with inert material screw caps, such as Teflon®, avoiding contamination of the samples and reducing the contact of the samples with the light. The recipients can be inserted in a secondary packing to prevent the loss of samples in the case the first recipient is damaged.

To avoid these problems and the transport of samples we hope that the Brazilian partner could acquire an equipment similar to the UHPLC−PDA−LTQ−Orbitrap system and use the developed method to obtain further results and clarify stability problems.

2. Development and validation of an UHPLC−LTQ−Orbitrap MS method for non-anthocyanin flavonoids quantification in *Euterpe oleracea* juice

Due to the high concentration of anthocyanins in *E. oleracea* juice, several phytochemical studies were based in these compounds [286,358,401,432]. However, in the past ten years, some studies have identified several non-anthocyanin polyphenols, that are minor compounds [371,381]. More recently, some studies evaluated the biological activities (mainly antioxidant and anti-inflammatory activities) of non-anthocyanin polyphenols isolated from the pulp [361,404,405]. This group of compounds, thus, has received much attention, and an increasing interest to characterize them has been observed [353,373].

As the juice is also a product of a great interest for the producers of the Amazon region, and easily available in high amounts, we chose it to continue the characterization of the phenolic compounds of açai. In fact, the extracts obtained in the study on the fruits showed low concentrations of non-anthocyanins polyphenols. So we needed higher quantities of extracts for the development and validation of a quantitative method. The relatively high amount of juice acquired from fruits given by different suppliers allowed us to develop this method.

We choose the methanol to extract the non-anthocyanin polyphenols from lyophilized juice, because it is well known that this solvent presents a good efficiency for this type of compounds [375]. We also choose to perform five extraction of 30 minutes to get the best extraction, as shown in Figure 34 of Chapter 3.. This extraction procedure was very different from the one performed to extract the anthocyanins from fruits (Chapter 2), where a sequential extraction was performed using a series of solutions of increasing polarities. In fact, we took into account the particularities of the fruits: on their surface a thin layer of lipids could interfere with the transfer of anthocyanins from the cells to any polar solvent like methanol or water-methanol solutions. Thus, before applying quite polar methanolic extraction, a less polar solvent (ethyl acetate) was used to remove the lipids and other apolar compounds like chlorophylls. A sequential extraction with a quite large range of polarities (from ethyl acetate to water-methanol (50:50)) was also used in order to extract the maximum of anthocyanins, aglycones and mono/disaccharides. So, we performed a total of six extractions of 30 minutes (two extractions for each solvent).

UHPLC methods have the great advantages to perform the chromatographic separation in less time and consequently with less solvent consumption as compared with classical

HPLC methods. Apart from our work, only one method used this technology to analyse non-anthocyanin polyphenols of açai [373]. However, this method was not developed for quantitative purposes, but for fingerprinting and mass profiling of phenolic compounds in raw materials derived from *E. oleracea* fruits. The method proposed in the present work was developed for quantitative purposes. The extraction time was optimized. The sensitivity of the method was improved by the optimization of the solubilisation solution that significantly interfered in the analytical responses of the analytes. Several isomers, including the major compounds, orientin and homoorientin, were baseline-separated in the optimized chromatographic conditions. Mulabagal et al. [373] did not separate these isomers, which is crucial for LC-MS methods. Moreover the present work performed this separation maintaining the same total run time that the last authors. Finally, the quantification was validated. All these steps significantly improved the performance of the method and the reliabity of the results and improved the existing procedures in the analysis of non-anthocyanin phenolics of *E. oleracea* juice. Considering the UHPLC and HPLC methods in the literature for *E. oleracea* juice, the proposed method was the first that was validated for the quantification of these compounds. Moreover, in relation to the conventional HPLC methods, it was significantly less time-consuming and less-solvent consuming. In fact, these other methods have quite long run times, ranging between 50 and 90 min [353,359,371,381,407].

The method we developed allows the simultaneous quantification of twelve non-anthocyanin polyphenols. These compounds are included in different classes of flavonoids, such as flavones, flavonols, flavanones, flavan-3-ols and dihydroflavonols. The quantification of four compounds was performed for the first time in the *E. oleracea* juice ((+)-dihydrokaempferol, quercetin, rutin, and quercetin 3-glucoside). Furthermore, our study allowed the identification of 34 non-anthocyanin phenolics, including the ones tentatively identified. The maximum of characterized compounds in *E. oleracea* fruits and derived products in a same study was 18 [373] and 20 [359]. Evidently, several variables are important in characterization studies, such as the nature of the samples, extraction procedures, sample preparation, sensitivity of the analytical tools, etc. Anyway, our method demonstrated the high complexity of non-anthocyanin polyphenols in *E. oleracea* juice and contributed to its characterization.

Biological activities of the major compounds quantified in the present work (Table 11 in Chapter 3) have already been pointed out. The antioxidant activity of some flavonoids

isolated from *E. oleracea* juice were evaluated *in vitro* [361]. The compounds studied were (+)-dihydrokaempferol, quercetin, chrysoeriol, luteolin (aglycones), orientin, homoorientin and vitexin (*C*-glycosides). In general, the antioxidant activity of the aglycones was higher than that of *C*-glycosides, particularly when compared to orientin and homoorientin (approximately 3-8 times). The same team [404] also evaluated the antioxidant activity of isovitexin, another *C*-glycoside that was also isolated from *E. oleracea* juice. This compound also showed *in vitro* antioxidant activity higher than that of orientin and homoorientin found in the previous citation [361]. In our quantification study, orientin and homoorientin are major compounds in *E. oleracea* juice (Table 11 in Chapter 3), which confirmed the results of other studies [353,359]. Therefore, they have a higher contribution to the antioxidant activity of the *E. oleracea* juice, even if their antioxidant activities are smaller than that of the other minor compounds abovementioned.

(+)-Catechin and (−)-epicatechin as well as their metabolites also demonstrated good *in vitro* antioxidant activity. The *O*-methylated metabolites showed reduced antioxidant activity with respect to the parent compounds. However, they still retained significant radical-scavenging activity at pH 7.4, suggesting that they could also act as potential antioxidants under physiological conditions [447].

The biological activity of scoparin was not much studied. A fraction containing scoparin and other related compounds (flavone *C*-glycosides) was obtained from *Citrus sinensis* (L.) Osbeck juice. This fraction showed good radical scavenging activity towards the $DPPH^{\bullet}$, $ABTS^{\bullet+}$ and $OH^{\bullet}$ radicals, but the contribution of the scoparin activity for the total activity of the fraction was not determined [448].

Homoorientin exhibited selectively good inhibitory activity against thromboxane B2 synthesis [449]. Thromboxane B2, a product of arachidonic acid metabolism, has attracted a great deal of attention as a potential proinflammatory mediator in diseases such as liver cirrhosis, systemic lupus erythematosis and thrombosis. Homoorientin, its isomer (orientin), and related flavone *C*-glycosides (vitexin and isovitexin) were found in their intact form in human plasma after oral ingestion [450].

A number of plant-derived substances including certain flavonoids showed anti-inflammatory properties related to the modulation of NF-κB (see section 1.2.6.). NF-κB is one of the principal inducible transcription factors in mammals and has been shown to play a pivotal role in the mammalian innate immune response and in chronic inflammatory

conditions [451]. NF-κB participates in the control of transcription of over 150 target genes, including the expression of various inflammatory cytokines, chemokines, immunoreceptors, and cell adhesion molecules [452]. Among the major compounds quantified in the present work, quercetin is known as NF-κB modulator. In Nair et al. [453], quercetin (concentration range = 5 and 50 μM) significantly inhibited TNF-α production and gene expression, in a dose-dependent manner in human peripheral blood mononuclear cells, which corresponded to a significant downregulation of NF-κB gene expression for the same concentration range.

Moreover, quercetin, quercetin 3-glucoside and rutin (quercetin 3-rutinoside) showed antiproliferative activities in different cancer cell lines including colon, breast, hepatocellular, and lung cancer. The IC_{50} value of quercetin 3-glucoside ranged between 15 and 25 μM. This compound showed the most potent growth inhibition. The IC_{50} value of quercetin was greater than 80 μM, whereas rutin showed the least potency [454]. Bioavailability of quercetin and quercetin 3-glucoside in their unconjugated forms were analysed in rats [455]. These compounds along with rutin are also absorbed as conjugated metabolites (glucuronides, sulfates and methylated compounds) [456]. Additionally, quercetin 3-glucoside and rutin were also absorbed as aglycone in rats and humans [455,456].

Homoorientin has also showed cytotoxic properties [457]. This compound decreased cell viability of hepatoblastoma cancer cells in a dose- and time-dependent manner. Induction of apoptosis is a main cause for homoorientin-induced cytotoxicity. When cells were exposed to 80 μM of homoorientin for 48 h, approximately 90% of cells showed cell shrinkage and nuclear fragmentation, which were considered to indicate apoptotic cells. This activity is associated with Erk1/2 kinase inhibition and JNK and p38 kinases activation. Considerations about this and other general mechanisms of polyphenol activities were given in section 1.2.7.1. (−)-Epicatechin (30 μM) has also shown *in vitro* cytotoxic properties by inhibiting ERK1/2 phosphorylation and downstream cyclin D1 expression leading to a block in cell cycle progression (Caco-2 cells) [214]. Nevertheless, their potential in cancer treatment/prevention has still to be determined.

Dietary flavonoids have been shown to be potentially beneficial in reversing the course of neuronal and behavioral aging because of their neuroprotective action [458]. This was demonstrated for flavonoids such as rutin and quercetin, which had positive effects on spatial memory impairment and neuronal death induced by repeated cerebral ischemia in rats.

In the literature seven flavonoid *C*-glycosides were already known to occur in açai juice [373,420]: orientin, homoorientin, vitexin, isovitexin, scoparin, schaftoside and vicenin-2. Our work described all the seven compounds, but also five other compounds of this group which were tentatively identified (Table 10 in Chapter 3: peaks 8, 11, 13, 15 and 23). Some additional unknown flavonoid *C*-glycosides were detected in the juice and referred to in Table 10 of Chapter 3. They will be discussed here.

The peaks 18, 20, 22 and 27 (Figure 35, Chapter 3) seem to contain isomer compounds belonging to the group of X"-*O*-glycosyl-*C*-glycosyl flavones and having a molecular ion $[M-H]^-$ at about *m/z* 593.15. This group is characterized by the Z_1^- fragment ion (Figure 40), which is highly abundant, generally the base peak [421,423]. Additionally, the neutral losses between $[M-H]^-$ and Z_1^- characterize the terminal sugar as a hexose (180 amu), a deoxyhexose (164 amu) or a pentose (150 amu).

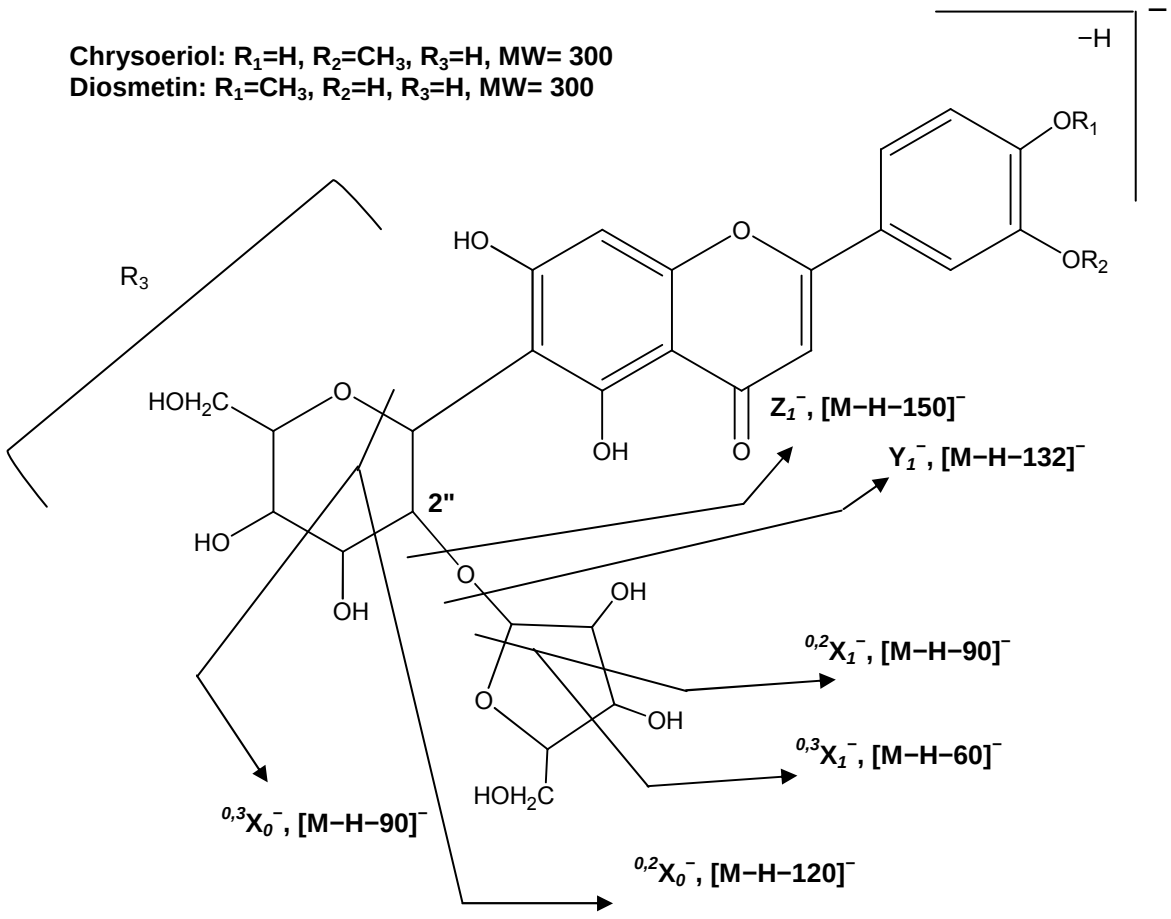

Figure 40 A generic 2"-*O*-pentosyl-6-*C*-hexosyl flavone and its main fragments after MS/MS experiment. For fragment nomenclature, see *1.3.5.3* section (Figure 21). MW: molecular weight.

The Figure 41 shows the MS/MS spectra obtained from these molecular ions at about *m/z* 593.15 $[M-H]^-$ of peaks 27, 22, 20, and 18, referred to in Table 10 of Chapter 3. For the peak 27 (Figure 41A), the fragment ion at *m/z* 443.0976 $[M-H-150]^-$ may correspond to the Z_1^- ion. The neutral loss of 150 u characterizes the terminal sugar as a pentose (Figure 40) [421]. The fragment ions at *m/z* 503.1192 $[M-H-90]^-$ and *m/z* 473.1080 $[M-H-120]^-$ may correspond to the $^{0,3}X_0^-$ and $^{0,2}X_0^-$ fragment ions, respectively (Figure 40) and indicate a *C*-glycosylation by a hexose. The occurrence of these two neutral losses could indicate that the terminal sugar is linked in the 2" position, since the other positions need to be free to produce the neutral loss of 120 u (Figure 40). The fragment ion at *m/z* 353.0656 $[M-H-150-90]^-$ may correspond to the $Z_1^- - 90$ ion, where the loss of 90 u can be attributed to the *C*-hexose. Analogously, the fragment ion at *m/z* 323.0555 $[M-H-150-120]^-$ ($Z_1^- - 120$ ion) confirmed the presence of a *C*-hexose. The Y_1^- fragment ion, illustrated in Figure 40, was observed at very low intensity at *m/z* 461.1074 $[M-H-132]^-$ (not indicated in the Figure 41A). It also characterizes the terminal sugar as a pentose. The presence of a *C*-hexose *O*-linked with a pentose is also in accordance with the fragment ions at *m/z* 371.0764 $[M-H-132-90]^-$ ($Y_1^- - 90$), *m/z* 341.0655 $[M-H-132-120]^-$ ($Y_1^- - 120$), and *m/z* 413.0872 $[M-H-120-60]^-$. From these fragment ions we can deduce that the aglycone has a molecular weight of 300 u as the fragments are found at [421,423]: *m/z* 371 = (aglycone + 71), *m/z* 353 = (aglycone + 71 − 18), *m/z* 341 = (aglycone + 41) and *m/z* 323 = (aglycone +41 − 18). As proposed by Ferreres et al. [421], this value matches with a methyl-luteolin. Nevertheless, it is not possible to determine the position of the methyl group, so the aglycone can be chrysoeriol, diosmetin or another isomer (Figure 40). Due to the occurrence of free chrysoeriol in the juice [353] and of scoparin = chrysoeriol 8-*C*-glucoside [371] it is likely that chrysoeriol is the aglycone, but this has to be proven by NMR. When MS^3 experiment was performed on the fragment ion at *m/z* 443.0976 $[M-H-150]^-$, the only product ion observed was at *m/z* 323.0574 $[M-H-150-120]^-$ (aglycone + 41 – 18). Ions corresponding to "aglycone + 41 – 18" and "aglycone + 71 – 18" are also peculiar for 2"-*O*-pentosyl-6-*C*-hexosyl flavones in MS^3 spectra showing the presence of only one "aglycone +41 – 18" ion or, when both are detected, the "aglycone +41 – 18" ion as the base peak [421]. Other fragmentation patterns could explain some of the ions obtained from MS/MS experiments. For example, the fragment ion at *m/z* 503.1192 $[M-H-90]^-$ can be produced from a neutral loss of 90 u from the terminal pentose to yield the $^{0,2}X_1^-$ ion. The ion at *m/z* 443.0976 can be produced from the sequential neutral losses of 60 u (pentose) and 90 u (hexose). On the basis of these informations, the compound of the peak 27 can be tentatively identified as a 2"-*O*-pentosyl-*C*-hexosyl chrysoeriol.

The fragment ion at *m/z* 285.0399 (Figure 41A) cannot be explained by the proposed structure. The molecular formula obtained by HRMS for this ion was $[C_{15}H_9O_6]^-$ (error = -1.794 ppm). It may correspond to luteolin, kaempferol or another aglycone isomer. However, all other fragments are in accordance with a 300 amu aglycone and as it is a *C*-glycosylated flavonoid, because of the difficulty to break the C-C bond, it is unlikely to find a fragment corresponding to the aglycone [459]. We confirm that fact by analysis of a standard of homoorientin (luteolin-6-*C*-glucoside) using the same experimental conditions than those applied for peak 27 (collision energy at 25%) and observed that the fragment corresponding to the free aglycone (luteolin) had very low intensity, and was not detectable when the standard was analyzed in a concentration similar to the concentration of the peak 27. Therefore, this fragment ion at *m/z* 285.0399 was probably originated from a coeluting compound, most likely an *O*-glycosylated flavonoid, yielding an abundant free aglycone ion. An example of the MS/MS fragmentation pattern of an *O*-glycosylated compound is shown in Figure 42 (kaempferol 3-*O*-rutinoside, peak 32 in Figure 35 of Chapter 3), which is an isomer of the previously identified *C*-glycosylated compound. The MS/MS spectrum obtained from the molecular ion at *m/z* 593.1504 shows as base peak the fragment ion at *m/z* 285.0396, which corresponds to the kaempferol aglycone.

Moreover, when we analyse the MS/MS spectra obtained at the beginning, the middle, and the end of the peak 27, we can observe that the intensity of the fragment ion at *m/z* 285.0399 is significantly more abundant, in absolute terms, at the end of the peak, confirming the co-elution, which occurs mainly at the end of peak 27.

We also have to note that some fragments seem to be present all along the chromatogram and should be considered as “background interferences” in MS/MS spectra, as the ions at about *m/z* 338.9. A MS/MS spectrum at a retention time with no peaks is shown in Figure 41E indicating the presence of the ion at *m/z* 338.9297. The molecular formula of this ion proposed by the Xcalibur® software contains the atom of nitrogen, which does not match with the structure of phenolic compounds.

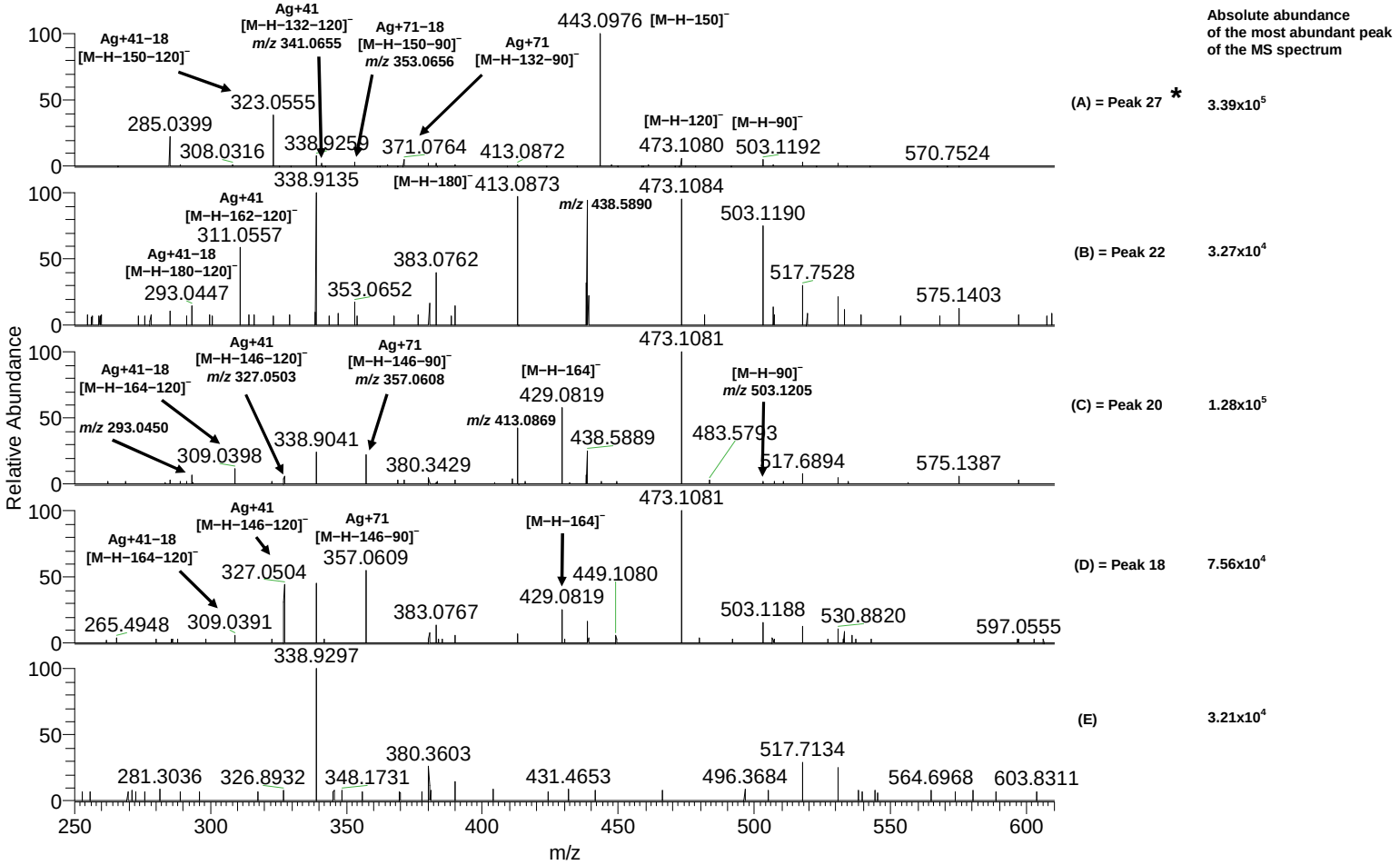

Figure 41 MS/MS spectra of the melecular ions at about *m/z* 593.15 $[M-H]^-$ of the peaks 27 **(A)**, 22 **(B)**, 20 **(C)** and 18 **(D)**, and MS/MS spectrum showing interferents in this analysis **(E)**.

***** The chromatographic peaks are referred to in Table 10 and Figure 35 (Chapter 3).

Ag: means "aglycone" in its neutral form.

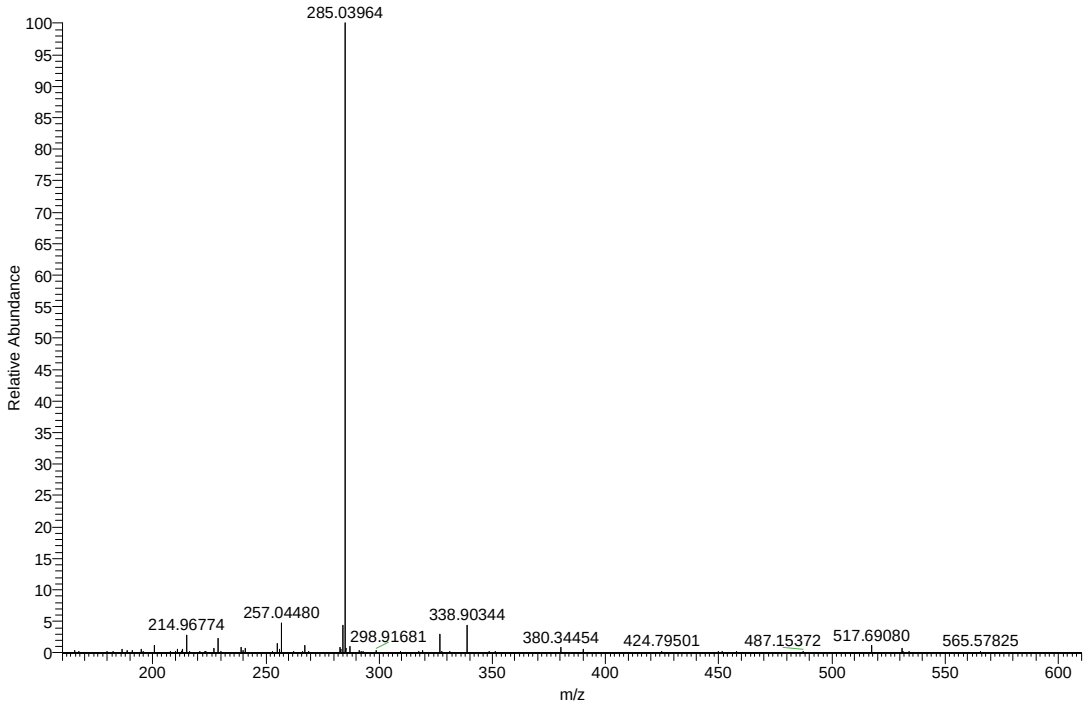

Figure 42 MS/MS spectra from the molecular ion at *m/z* 593.1504 [M−H]−, corresponding to kaempferol 3-rutinoside (peak 32, Figure 35 in Chapter 3).

The MS/MS fragmentation of the molecular ion at *m/z* 593.1491 of peak 22 (Figure 35 in Chapter 3 and Figure 41B) also showed very similar fragment ions than those obtained by Ferreres et al.[421] for *C*-glycosyl flavones *O*-glycosylated on the *C*-linked sugar moiety. The fragment ion at *m/z* 413.0873 $[M-H-180]^-$ could correspond to the Z_1^- ion (Figure 43), where the neutral loss of 180 u may indicate that the terminal sugar is a hexose [421]. The ions at *m/z* 503.1190 $[M-H-90]^-$, *m/z* 473.1084 $[M-H-120]^-$, which correspond to neutral losses of 90 u and 120 u, may characterize the sugar moiety of the *C*-glycosylation as a hexose (Figure 43) and they may suggest that the terminal sugar is linked to the *C*-hexose in the position 2", analogously to the compound of the peak 27. The previous fragment ions can also have additional origins: the neutral loss of 90 u and 120 u, could also involve the terminal hexose. In addition, the ion at *m/z* 413.0873 may be originated from a sequential loss of 2x 90 u, one loss from each hexose. The ion at *m/z* 383.0762 may correspond to a sequential neutral loss of 120 u from the *C*-hexose and 90 u from the terminal hexose or vice-versa. An ion at *m/z* 353.0652 has similar *m/z* value that the one showed for the peak 27. However, for the compound of the peak 22 it could be generated from a sequential neutral loss of 2x 120 u, one from each hexose. As observed by Ferreres et al. [421] the ions at *m/z* 311.0557 ($[M-H-162-120]^-$, aglycone + 41) and *m/z* 293.0447 ($[M-H-180-120]^-$,

aglycone + 41 − 18) (Figure 41B) can be used to characterize the aglycone moiety, as having a molecular weight of 270 Da. It is likely that the aglycone is apigenin because this compound was already found in the form of free aglycone in a methanolic extract of *E. oleracea* fruits [418] and in the structure of *C*-glycosides found in the juice, as vitexin (apigenin-8-*C*-glucoside) and isovitexin (apigenin-6-*C*-glucoside) [353]. Therefore, this compound can be tentatively identified as 2”-*O*-hexosyl-*C*-hexosyl apigenin. The origin of the fragment ion at *m/z* 438.5890 $[M-H-155]^-$ was not found. Its molecular formula proposed by the Xcalibur® software, during data analysis, corresponded to a formula containing nitrogen atoms, which did not match with the structures of flavonoids. This ion was also found for the peaks 18 and 20.

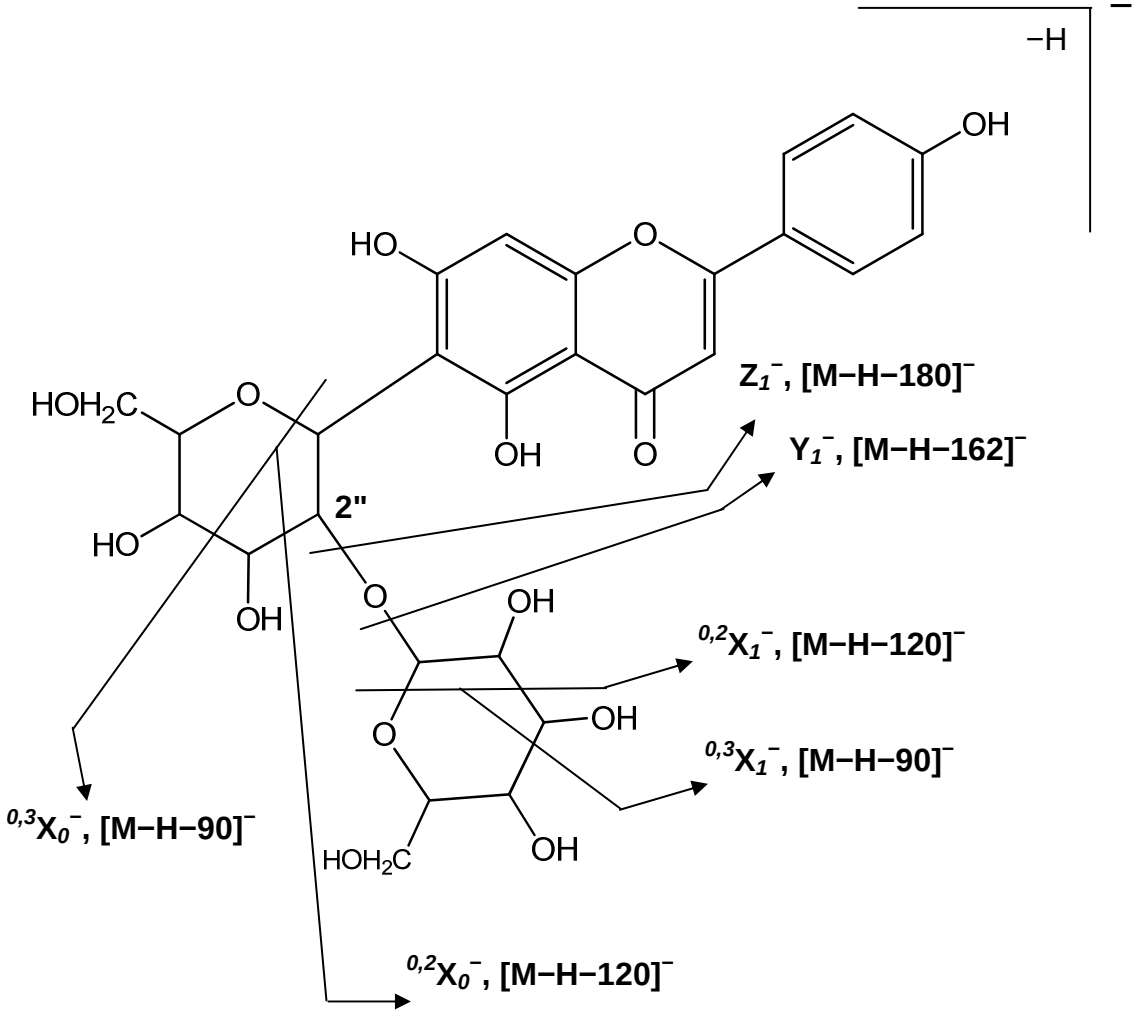

Figure 45 Structure of a generic 2"-*O*-hexosyl-6-*C*-hexosyl apigenin and its main fragments after MS/MS experiment. For fragment nomenclature, see *1.3.5.3* section (Figure 21).

The Peak 20 (Figure 35 in Chapter 3) may contain a mixture of isomer compounds. It showed a molecular ion at *m/z* 593.1503. The fragment ion at *m/z* 429.0819 $[M-H-164]^-$ (Figure 41C) obtained from this molecular ion may correspond to the Z_1^- ion, and characterize the terminal sugar as a deoxyhexose (neutral loss of 164 u) (Figure 44). Analogously to the other compounds previously discussed, the fragment ions at *m/z* 503.1205 $[M-H-90]^-$ and *m/z* 473.1081 $[M-H-120]^-$ may characterize the *C*-linked sugar moiety as a hexose. The ions that characterize the aglycone were formed from the Y_1^- and Z_1^- fragment ions along with neutral losses from the *C*-hexose: the ions at *m/z* 357.0608 may correspond to Y_1^- − 90 (aglycone + 71), and the ion at *m/z* 327.0503 may correspond to the Y_1^- − 120 ion (aglycone + 41). The ion at *m/z* 309.0398 could correspond to the Z_1^- − 120 ion (aglycone + 41 − 18). Therefore, the aglycone has a molecular weight of 286 Da, which may correspond to luteolin, kaempferol or other isomers. Based in these fragments, this peak may contain a 2”-*O*-deoxyhexose-*C*-hexosyl luteolin (or isomer) [421]. On the other hand, the possible origins of the fragment ions at *m/z* 413.0869 and *m/z* 293.0450 were not found for this previous proposed structure. The loss of 180 u (from the ion at *m/z* 413.0869) did not correspond to neutral losses generated from a *C*-hexose and a deoxyhexose. Additionally, the ion at *m/z* 293.0450 could correspond to $[M-H-180-120]^-$ as for the peak 22 and the ion at *m/z* 413.0869 to $[M-H-180]^-$; most probably these fragments come from a co-eluting isomer of the compound of the peak 22.

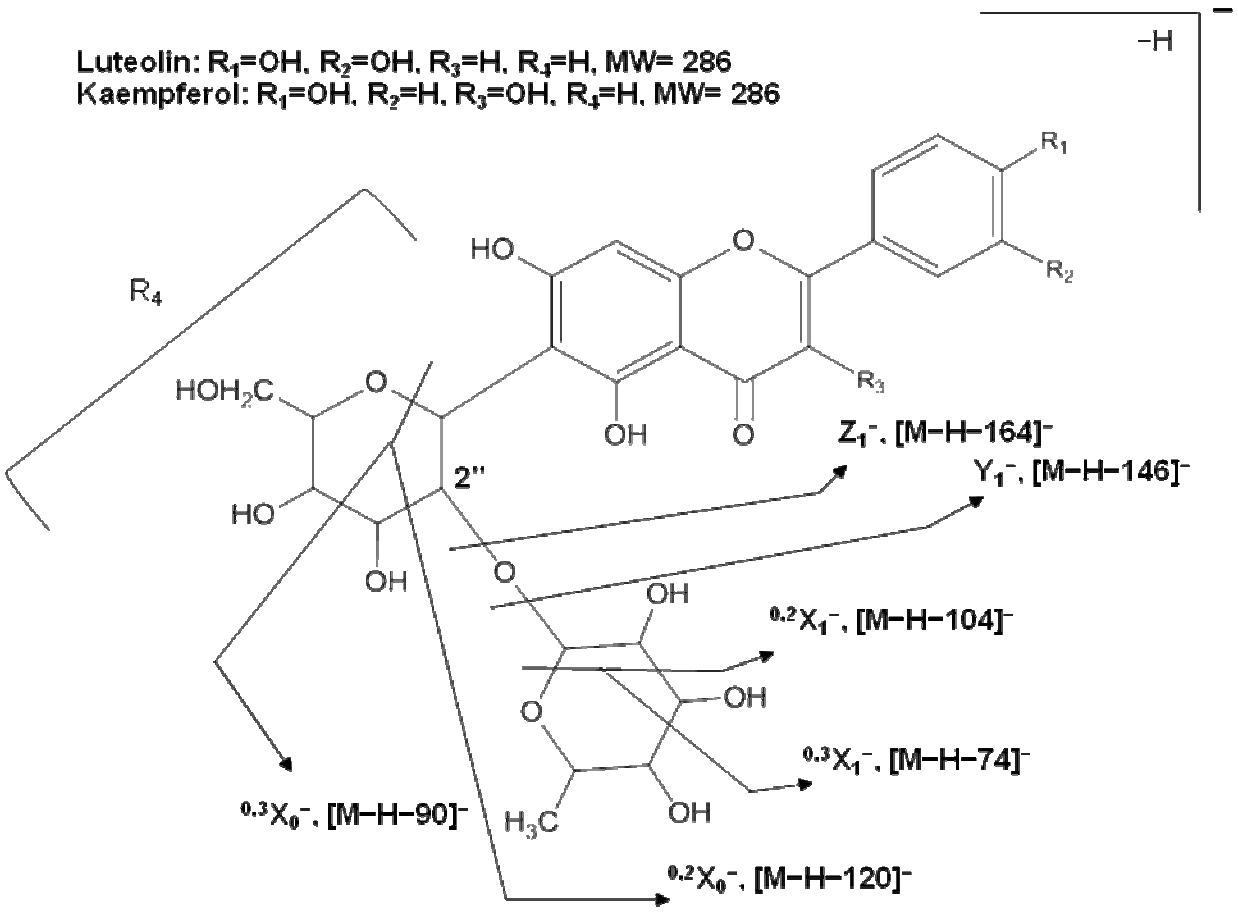

Figure 44 Structure of a generic 2"-*O*-deoxyhexosyl-6-*C*-hexosyl flavones and its main fragments after MS/MS experiment. For fragment nomenclature, see 1.3.5.3 section (Figure 21).

Similarly, the peak 18 seems to contain a mixture of compounds. This peak has in common with the peak 20, the fragment ions at *m/z* 503.1188, *m/z* 473.1081, *m/z* 429.0819, *m/z* 357.0609, *m/z* 327.0504 and *m/z* 309.0391, indicating that this peak also contains a luteolin (or isomer)-(2”-*O*-deoxyhexose)hexoside. However, the possible origins of the fragment ions at *m/z* 413.0864 and at *m/z* 383.0767 were not found for this structure. Both ions were observed for peaks 22 and 27 and were attributed to sequential losses from the sugar moieties corresponding to hexose + hexose (peak 22) and hexose + pentose (peak 27) as previously discussed. Therefore, probably other compound(s) having a hexose or a pentose as terminal sugar can be present in the peak 18. The peaks 27, 22, 20, 18, along with the peak 11 discussed in Chapter 3 showed great variations in terms of relative abundances of the fragments when we compare MS/MS spectra at the beginning, middle and end of the peak. This may be explained by the low concentrations of the compounds and/or by the co-elution

of isomers. It has been observed that this type of isomers (2”-*O*-glycosyl-*C*-glycosyl flavones) have identical fragment ions but different relative abundances [421,423].

To solve this problem, further purification of the extracts will be necessary, for example by SPE-C18, in order to concentrate the compounds, and allow to obtain more informations on fragments and an improvement of the chromatographic separation to separate possible isomers. It is the first time that this type *C*-glysosylated compounds is detected in *E. oleracea* juice.

The Figure 45A illustrates an extracted ion chromatogram of the molecular ion at *m/z* 505.1334 $[M-H]^-$, which shows a chromatographic peak at a retention time of 22.96 min. The molecular ion corresponded to the molecular formula of $[M-H]^- = C_{24}H_{25}O_{12}$ (error = -3.424 ppm). Figure 45B shows a MS/MS spectrum of the molecular ion, obtained from a collision energy of 25%. The fragment ion at *m/z* 343.0817 $[M-H-162]^-$ may correspond to the neutral loss of a hexose, that occurs typically in *O*-glycosylated flavonoids [333]. The fragment ion at *m/z* 490.1111 $[M-H-15]^-$ may correspond to a loss of a methyl group. Sequential losses of a hexose and a methyl group could be responsible for the fragment ion at *m/z* 328.0582 $[M-H-162-15]^-$. Analogously for the fragment ion at *m/z* 313.0349 $[M-H-162-15-15]^-$, with the loss of two methyl groups. The molecular formula obtained from the molecular ion at *m/z* 343.0817 $[M-H-162]^-$ (aglycone moiety) was $C_{18}H_{15}O_7$. The molecular structure of flavonoids has 15 carbons. Therefore, this compound can have three methyl groups in its structure. Nevertheless, it is not possible to know if the methyl group that was lost to generate the ion at *m/z* 490.1111 $[M-H-15]^-$ is different of the other two methyl groups lost from the aglycone moiety. MS^n experiments were performed from the molecular ion (Figure 46). The MS^n spectra presented quite background noise, but the main fragment ions can be observed. The fragment ions indicated in Figure 45 can also be observed in Figure 46. In the MS^4 and MS^5 experiments, a sequential losses of 28 u and 44 u were observed from the fragment ion at *m/z* 313.0367 $[M-H-162-15-15]^-$, that corresponded to the losses of CO and CO_2 groups. These small neutral losses are very common for flavonoid aglycones [332]. The MS^n experiments did not show the loss of a third methyl group. Some reports showed that polymethylated flavonoids (monoglycosylated and aglycones) lost only two methyl groups of the three present in the structure after MS/MS experiments [460,461]. Therefore, this compound can be a trimethoxyflavonoid *O*-glycosylated.

In the present study, ESI in negative ion mode was used. However, ESI in positive ion mode is more sensitive to polymethoxylated flavonoids than ESI in negative ion mode, due to

the reduced number (or absence) of hydroxyl groups in the aglycone [462]. Additionally, the fragmentation pathway in ESI positive ion mode of this type of compounds showed more structural information [462] than the one in negative ion mode. In the present study, the fragments retaining the A or B ring (originated by RDA cleavage on the C ring) that give information about the aglycone moiety were not observed. The same was observed by Parejo et al. [460]. On the other hand, in ESI positive ion mode some compounds showed these fragments in high intensity [462]. Further works can use the positive ion mode to obtain more information on the compound previously discussed. This compound was not yet reported for *E. oleracea* juice/fruits. However a recent study isolated a polymethoxylated flavonoid (not glycosylated) from *E. oleracea* pulp [404]: the 5,4'-dihydroxy-7,3',5'-trimethoxyflavone.

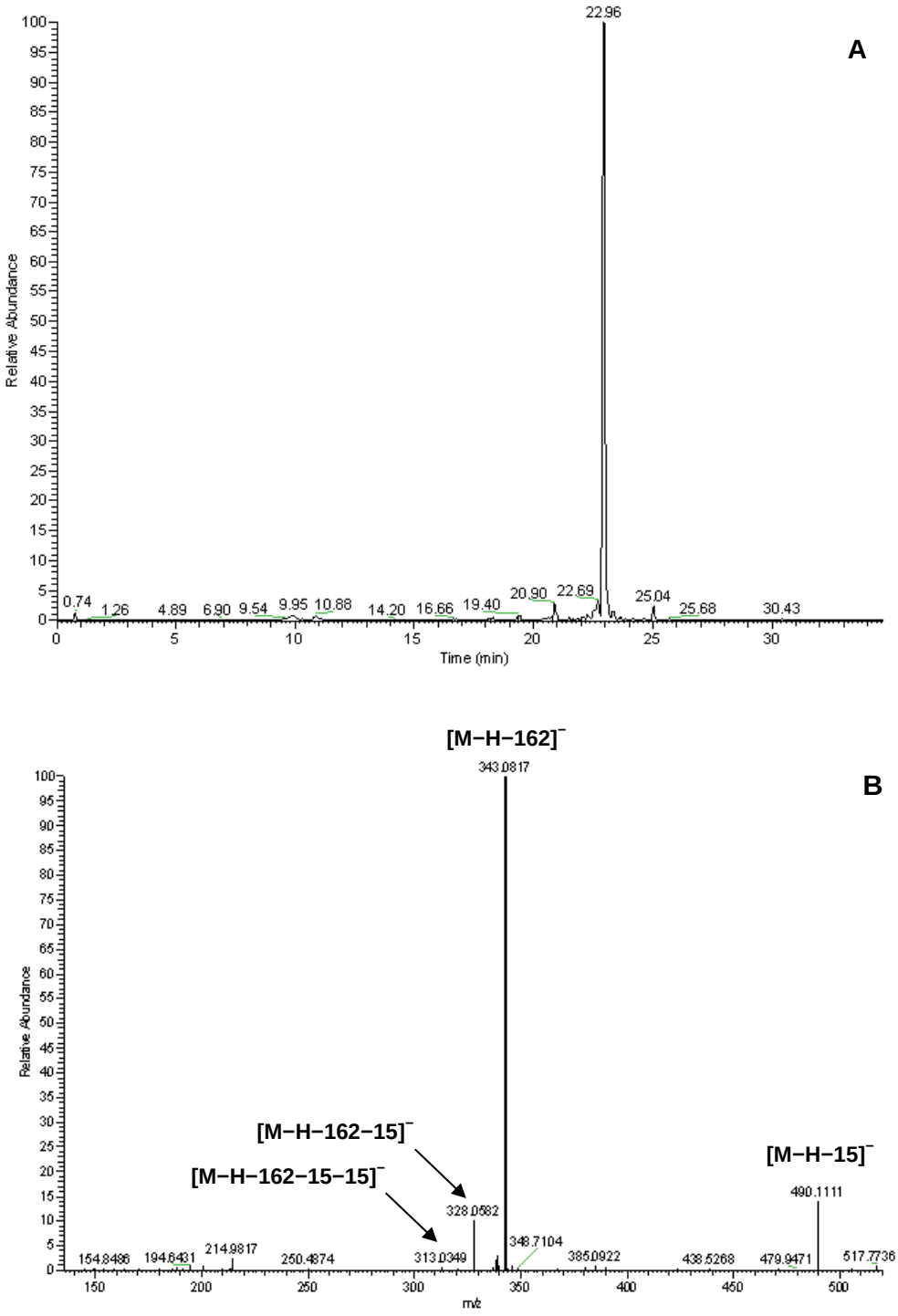

Figure 45 Extracted ion chromatogram of the molecular ion at *m/z* 505.1334 $[M-H]^-$, using a mass extraction window of 5 ppm **(A)**. MS/MS spectrum from the molecular ion **(B)**.

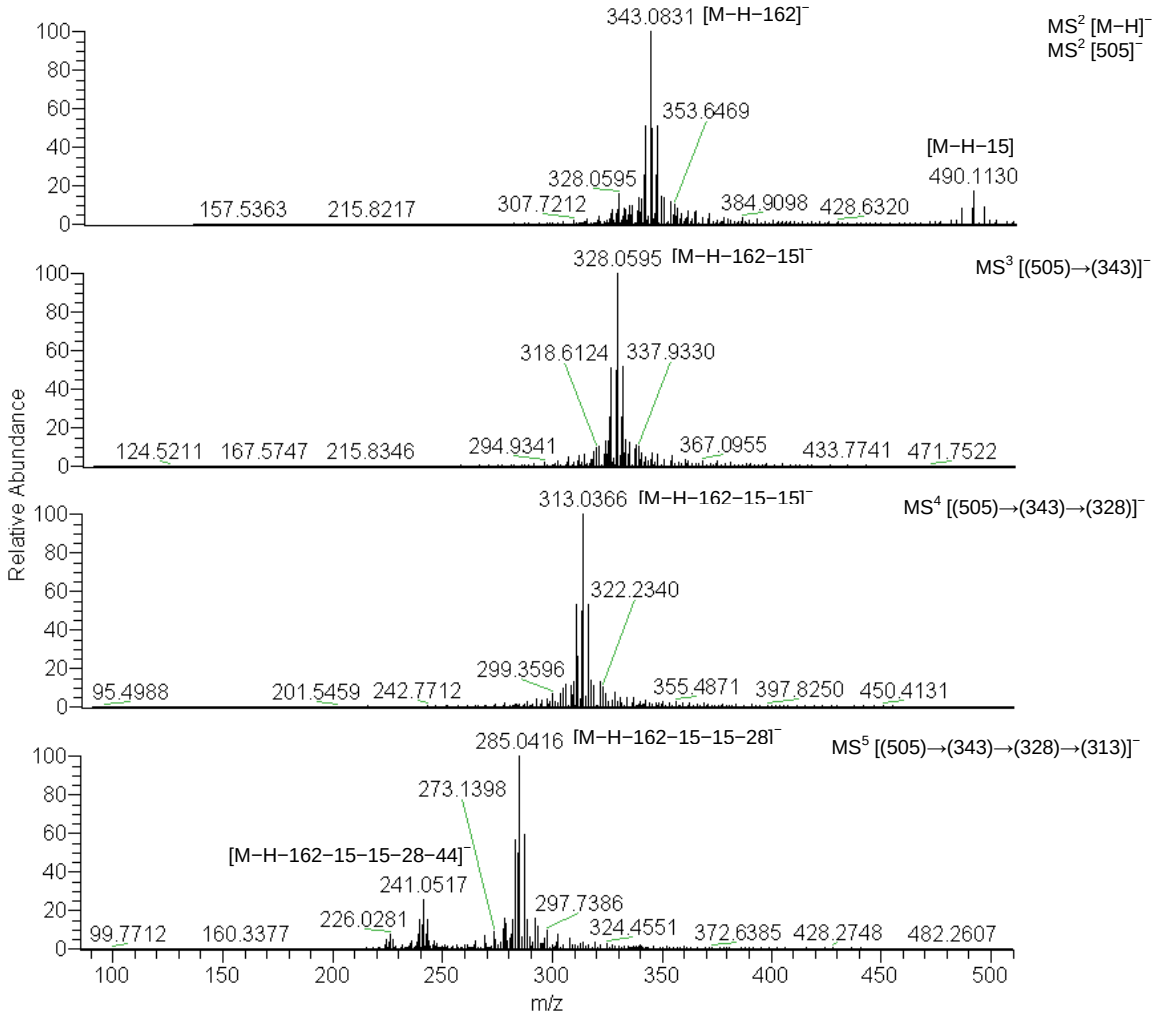

Figure 46 MS^n spectra from the molecular ion at *m/z* 505.1334 $[M-H]^-$.

For the validation of the UHPLC-PDA method for quantification of anthocyanins (Chapter 2), the *β*-expectation tolerance limits and the acceptance limits were set at 95% and ±20, respectively. On the other hand, the validation of the UHPLC-HRMS quantitative method for non-anthocyanin polyphenols was more challenging. These compounds are minor compounds, possess various skeletons and a large range of polarity (different phenolic classes, *O*-glycosylated, *C*-glycosylated, aglycones, etc). Additionally, matrix effect is more observed in MS detection [322]. Therefore we decided to choose other reasonable limits: 90% *β*-expectation tolerance limits and ±30% acceptance limits, as frequently used for the analysis of biological matrices, as plant extracts [463].

For the quantification of non-anthocyanin polyphenols by UHPLC-HRMS, another calibration approach was used as compared to the study on anthocyanins: the internal standard method, which was tested with calibrations in the matrix and without matrix. Considering LC-

MS methods, the use of an internal standard is suitable to compensate possible variations in the ionization of the analytes in the ion source. The isotopically labelled standard is the best choice as internal standard. Nevertheless, they are expensive and not always commercially available. Moreover, in our study that considered several compounds, the use of several internal standards was not possible. Therefore, only one internal standard was chosen as a compromise among all other compounds. Several internal standards candidates were tested, including glycosylated compounds and aglycones. Finally, 7-hydroxyflavone was chosen because it did not show any interference with the signal of the matrix. Several batches of juices were tested. Additionally, it is a synthetic phenolic compound that has rarely been found in foods or plants. Moreover, it is relatively cheap. The validation of the method using only one internal standard was performed to confirm the reliability of the results.

The accuracy profiles (90% β-expectation limits and ±30% acceptance limits) were obtained using calibrations in (or without) the matrix, and with or without the internal standard. From these profiles, a high interference of the matrix in the accuracy of the results was observed. Therefore, it was necessary to use calibration in the matrix. We also noted that for some compounds (kaempferol 3-rutinoside, quercetin 3-glucoside, (+)-dihydrokaempferol, isovitexin, and rutin) calibrations without internal standards showed better accuracy profiles, but for other compounds (eriodictyol, luteolin, chrysoeriol, quercetin, homoorientin, and orientin) the internal standard seemed necessary, wheres for catechin, similar accuracy profiles were obtained with and without internal standard. As we obtained acceptable validation data for the twelve non-anthocyanin flavonoids selected for the study using an internal standard, this calibration method was chosen, it constitutes a compromise.

One of the difficulties to work with multi-component matrix, such as plant and food extracts is that it is rarely possible to use a single sample preparation procedure and a single analytical method to analyse all the classes of compounds present in the samples. In the present study the method could not be validated for the quantification of protocatechuic acid. This compound belongs to the class of phenolic acids. The 90% β-expectation tolerance limits were within the acceptance limits of ±30% only for the highest concentration level. These results were observed for both, a calibration in the matrix using internal standard, and a calibration without matrix using only the analytical response of protocatechuic acid standard (area). These results suggested that for the quantification of phenolic acids another calibration approach is necessary to compensate the variation between the analytical response of the analytes in the samples and the responses obtained from the standards of the calibration

curves. An alternative can be the use of an internal standard corresponding to the class of the phenolic acids. Two other phenolic acids were identified in the juice: vanillic acid and caffeic acid. The concentrations of the three phenolic acids were only estimated based in a calibration in the matrix usind internal standard and the sum of their concentrations were <8% of the total of non-anthocyanin flavonoids quantified. In fact, phenolic acids are minor compounds in relation to anthocyanins and other flavonoids in *E. oleracea* fruits [359]. Nevertheless, higher concentrations of phenolic acids were found generally in unripe and in intermediate maturity stage of the fruits [353]. In further works, the validation of an analytical method for the quantification of phenolic acids can be interesting for the evaluation of these compounds when present in significant concentrations, such as in juices produced from fruits at different maturity stages or harvested in the different regions of harvest.

The twelve compounds for which the method was validated were quantified with their respective standards. In order to reduce the number of standards for the analysis and consequently to reduce the cost of the experiments, the possibility to perform the quantification of the compounds in equivalents was tested. For this purpose, the analytical responses obtained for a compound with the validation standards (three series of experiments) were quantified using the calibration curve of another compound. A correction factor was applied between the response obtained by the corresponding standard of the compound and the candidate standard for the equivalence. From the accuracy profiles obtained, we observed in general that the β-expectation intervals for the different concentration levels were superior to the acceptance limits. Therefore, the equivalence was not possible to quantify accurately the selected compounds. These results demonstrated that the analytical response from LC-MS can be very dependent of the compound, so that for their quantification the use of the corresponding standard is necessary [271]. In addition, for all the compounds evaluated, significantly better accuracy profiles were generally obtained using calibration in the matrix as compared with the calibration without matrix (standards solubilized in solvents), indicating an important matrix effect. In fact, the major drawbacks of LC-MS methods is that they can be compound-dependent and matrix-dependent [271,320]. Therefore, it is necessary to address these problems and validate the method to confirm the reliability of the results.

Finally, the extraction procedures, sample preparation, and UHPLC-HRMS analysis were developed for non-anthocyanins phenolics in juice, thus the anthocyanins were not evaluated. Generally, for anthocyanins quantification, these last steps are performed in more acidified conditions. Therefore, another extraction procedure on the lyophilized juice needs to

be optimized for anthocyanin analysis. The extracts can be analyzed by the UHPLC-PDA method, described in Chapter 2. However, the matrix from lyophilized juice can be different of the matrix from the fruits used to validate that method, giving possible interferences. Additionally the qualitative profile of anthocyanins may be different in the extract from lyophilized juice. Therefore, these possible differences need to be evaluated to demonstrate that the UHPLC-PDA method can be applied for the analysis of the juice maintaining the same selectivity and accuracy. The selectivity of the analysis of the juice extract can be evaluated by LC-MS/MS analysis and the matrix effect by spiking standards in the matrix. This method we developed for anthocyanin quantification in fruit extracts may also be used for the anthocyanin quantification of other açai extracts, provided the selectivity and the matrix effect are analysed. In fact, extracts of this type are already on the market or under development in the frame of our PIC project. Links should be done in the future between chemical composition and biological activities.

Phenolic compounds of açai juice undergo degradation by oxidation but also by the action of the polyphenoloxidase vegetal enzyme and microbial enzymes [351]. Therefore, the pasteurization of the juices should increase the stability of these compounds over time by enzyme denaturation and reduction of microbial content.

Juices pasteurized and not pasteurized from three suppliers (S1, S2, and S3) were analyzed (Table 11 in Chapter 3). For each supplier, three different thermal treatments were performed, as follows: without pasteurization (samples P0); 80°C/12min (sample P1), and 90°C/2min (sample P3). Similarities, but also differences can be observed in all three suppliers. The same compounds were quantified in all samples, except quercetin 3-glucoside and quercetin that were <LLOQ in sample from S3. Orientin and homoorientin remained the major compounds in all samples, followed by the “peak 12” compound, which was tentatively identified as taxifolin deoxyhexose. Nevertheless, the total non-anthocyanin polyphenols concentrations were different between the suppliers: S1 <<S2 <S3, with fewer differences between S2 and S3 except for (−)-epicatechin, (+)-catechin, quercetin, and quercetin 3-glucoside. This may be explained by different factors such as time and place of harvest, maturity of the fruits, and processing to obtain the juices.

In general, a slight reduction (<10%) of the total non-anthocyanins polyphenols concentration was observed after thermal treatments, which can be explained by the unstability of these compounds at high temperatures. Regarding the individual constituents, the effet of thermal treatment may differ according to the sample. Particularly, the

concentration of (+)-catechin and (−)-epicatechin increased for S1 and S2, which can be tentatively explained by the degradation with heat of proanthocyanidins (polymeric forms containing these flavan 3-ols found in açai [381]), producing monomers.

Generally, the major compounds, orientin, homoorientin, and taxifolin deoxyhexose (peak 12), which most contribute to the total non-anthocyanins polyphenols concentration were almost stable. Further studies should evaluate the stability over time of these compounds and of anthocyanins in order to optimize the treatments that promote better conservation of juices.

Conclusions and perspectives

The aims of this thesis were to develop and validate analytical methods for the identification and quantification of phenolic compounds in fruit extracts and juice of *E. oleracea*, in order to improve the added value of these products, and to improve collaborations between the academic and private sectors, and consequently to contribute to the development of the Amazonian region. This fruit was chosen for the study because of its abundance and importance for the local economy. It is part of the alimentary diet of the local inhabitants and has been widely exported, mainly because it is rich in phenolic compounds, which are natural antioxidants. To achieve these objectives, particularly for the identification and the quantification of minor compounds, such as non-anthocyanin polyphenols, the use of equipments that allow reaching a high degree of sensitivity in the analysis and adapted to the analysis of complex matrices was necessary: the UHPLC−PDA−LTQ−Orbitrap.

A detailed characterization of phenolic compounds was performed in fruit extracts and juice of *E. oleracea*. It includes identification and quantification of several phenolic compounds. Two analytical methods were developed in this thesis. First, the anthocyanins were characterized in fruit extracts. An UHPLC-PDA method was for the first time validated for the quantification of the major anthocyanins, cyanidin 3-glucoside and cyanidin 3-rutinoside. The method was validated using β-expectation tolerance limits and acceptance limits of 95% and ± 20%, respectively. A rapid extraction procedure, directly on the fruits, was developed. Seven anthocyanins were chromatographically separated in a short run time under optimized conditions. Two new anthocyanins were for the first time tentatively identified by UHPLC-PDA-HRMS-MS/MS.

The non-anthocyanin polyphenols were characterized in the juice. The sample preparation and a UHPLC-HRMS method were optimized for quantitative purposes. For the first time, a method using these devices was validated for the quantification of these compounds in the juice of *E. oleracea*. The method was validated using β-expectation tolerance limits and acceptance limits of 90% and ± 30%, respectively. The method allowed the simultaneous quantification of twelve compounds of different families of flavonoids. Among them, four compounds were quantified in the juice for the first time. Furthermore, a flavanone (eriodictyol) was identified in the juice and eight other compounds were tentatively identified for the first time. The profiles of the non-anthocyanin polyphenols of juice samples prepared from fruits obtained from different suppliers were similar, demonstrating a potential for the authentication of the juice by a MS fingerprint of the samples. Additionally, several

isomers, including the major compounds, were base-line separated in the optimized chromatographic conditions, allowing their identification and quantification by LC-HRMS.

Considering the two methods, a total of 41 phenolic compounds, including anthocyanins and non-anthocyanin polyphenols, were identified or tentatively identified, demonstrating the high phenolic complexity in the samples (fruit extracts and juice), not yet observed in the literature in these proportions. The HRMS detection used for non-anthocyanin polyphenols was more sensitive than the DAD detection used for anthocyanins, but the major drawbacks found for HRMS were the higher matrix effect as compared to DAD and the need for standards for each class of compounds. Consequently, it is necessary to use calibrations in the matrix for quantification by HRMS.

In terms of general perspectives, the knowledge in development and validation of analytical methods obtained with this thesis, as well as the developed methods themselves, can be very useful to further studies concerning açai polyphenols aiming to contribute to the regional development in the Amazon region. These studies will involve the health and food sector and can include works on biological activities, conservation of the compounds and extracts, authentication of products (in terms of bioactive compounds), development of new products derived from the fruits, etc. Such works, evidently, will contribute to give added values to these fruits and derived products. These perspectives will be briefly described below.

Concretely, this thesis opened perspectives of collaborations between the academic sector in Belgium (UCL) and in Brazil (UFPA) along with the private sector in Brazil, represented by small companies that process the *E. oleracea* fruits. Recently, the investment in scientific research has been improved in Brazil. Specifically in the Amazon region, we can note the creation of research centers to study the Amazon biodiversity, and a most likely acquisition of analytical devices similar to those used in this work, as a LC-PDA-HRMS system. Therefore, after acquisition of this device, the methods developed in the present work will be transferred to Brazil, in collaboration with the partner universities in Belgium (ULg and UCL), so the methods developed in this work could be applied to characterize phenolic compounds of fruits obtained from different conditions, from different harvest regions including zones with different degrees of flooding and different degrees of water salinity. These and many other parameters can influence the phenolic composition of the fruits. Additionally, the fruits are harvested for the commercialization at different maturity stages. During maturation, important morphological differences are observed, the most remarkable

being the intensification of their red color, which suggests that important variations in the phenolic composition occur in the fruits during maturation. Therefore, the application of the methods can help in the improvement of the harvest conditions of the fruits to give the higher desired activity.

The authentication of natural products is a challenge to the food industry and the food regulatory agencies. In the case of açai, the application of the methods developed in this work to several samples (hundreds) can contribute to the establishment of quality norms in terms of potential bioactive compounds.

In this context, the data obtained from the analysis of hundreds of samples could also be correlated with data obtained from methods using less expensive techniques, such as near-infrared spectroscopy (NIR) or ultraviolet-visible spectrophotometry in order to calibrate these methods for routine analysis. For this purpose, it is, in fact, very important to analyse a high number of samples obtained from different origins, maturity stages and harvest periods in order to obtain samples which are representative of the naturally found variability [464]. HPLC-UV methods are also suitable for the analysis of individual compounds. In the case of anthocyanins, this perspective is more interesting, because they have less complex profile in the fruits (two major compounds that correspond to almost the total anthocyanin concentration in the fruits [350]). Additionally, they are present in the mature fruits in high concentrations and are very well analysed by HPLC-UV. On the other hand, most of the non-anthocyanin polyphenols detected in the present work by mass spectrometry could probably not be quantified by UV detectior because of its lower selectivity and sensitivity.

The methods can be adapted to analyze other commercial phenolic extracts derived from the fruits and juices of *E. oleracea*, commercialized by small companies in the region. The production of purified extracts rich in phenolic compounds is an initiative to add value to products of the region. In function of the procedures of purification, fractions of different phenolic profiles are obtained, which could be analysed by the adapted methods we developed. Therefore, the application of the methods will contribute to the development of new products and to the improvement of their quality.

Additionally, some fractions of extracts discussed above have been tested in relation to their biological activities, in the context of other scientific collaborations. Their complete phenolic characterization will be useful to understand their biological effects, in relation to their composition. It would also, in that context, be interesting to use or develop standard

biological methods (such as ORAC) to compare the biological activities and potential of these different fractions or extracts on different health problems or diseases. These studies could include, for example, the measurement of the antioxidant activity, or the monitoring of pro-inflammatory mediators (IL-4, IL-13, etc) [465] in human plasma before and after the intake of açai extracts.

The identification and quantification works were performed on fruit/juice extracts, but could be used as models for the development and validation for the analysis of samples derived from cell models, animal and human studies, such as plasma, faeces and urine. This is of crucial importance for studies of absorption, biotransformation, bioavailability and elimination of phenolic compounds of *E. oleracea* fruits. For these analyses, new developments will be necessary because these samples contain phenolic compounds metabolites (glucuronides, sulphates, methylated, etc.) and hydrolysis products (aglycones). Consequently, some modifications of the methods developed here need to be made, e.g. the adaptation of chromatographic separation, the use of other internal standards, the use of clean-up procedures of extracts derived from the samples, etc. Additionally, the matrix effect has also to be evaluated. These methods will contribute to a better knowledge on the pharmacokinetic of açai polyphenols and their biological activities.

The juices undergo different treatments during processing, such as pasteurization, in order to improve the stability of the products over time. These treatments have a direct impact on the phenolic composition of the juices. Our results have shown that in general the total non-anthocyanin polyphenols decreased (<10%) after pasteurization, whereas for the individual constituents, the effect of the thermal treatment may differ according to the sample. Stability studies of the phenolic compounds from juices that underwent different treatments will contribute to optimize treatment conditions in order to better preserve the phenolic composition, and will improve the knowledge about the stability of these compounds.

Recently, it was demonstrated that some açai polyphenols (four compounds were evaluated) undergo a time dependent logarithmic decrease during the transport (closed system) of the fruits from the harvest zone to the cities [466]. Indeed, the fruits contain a high bacterial load (microorganisms naturally present in the forest environment and other acquired during de transport in boats). Therefore, depending on the transport conditions (closed or open systems), spontaneous fermentation processes occur more intensely due to the microbiological action and contribute to the degradation of the polyphenols. The methods

developed here will be useful for the evaluation of compounds in order to improve the preservation of polyphenols, and particularly those that will show better health potential.

More specifically, an extraction procedure should be developed for the anthocyanins from lyophilized juices. This procedure needs to use more acidified conditions, mainly in order to preserve the anthocyanins, which are more stable in these conditions. The extracts produced from this procedure could be analyzed by the UHPLC-PDA method developed for the anthocyanins of extracts obtained from the fruits. Nevertheless, before that, the selectivity and accuracy of the method have to be evaluated for this new matrix.

The method for non-anthocyanin polyphenol quantification was not validated for the quantification of phenolic acids, but a further validation could be interesting particularly for unripe fruits or juices extracted from them. Our results also show that further identification studies should be performed on the non-anthocyanin compounds to confirm the structures we proposed from our LC-HRMS/MS/MS method, and on the chromatographic peaks that probably contain other co-eluting phenolic compounds.

As general conclusion, the Amazon region has an enormous potential to provide foods rich in bioactive compounds. Mainly due to their high phenolic content, the commercialization of *Euterpe oleracea* fruits has been greatly expanded. This work allowed an increase of the knowledge about the phenolic composition of fruits and juice of *E. oleracea*, which represents a potential added value to these products. Moreover, the methods developed and validated in this work can contribute to the development of the Amazon region, by providing a detailed and reliable phenolic characterization of fruits and juices in studies of improvement of the quality of these products.

References

[1] C.M.G. Bichara, H. Rogez, In: Yahia, EM (ed) Postharvest biology and technology of tropical and subtropical fruits, 2, 1st edn. Woodhead Publishing Limited, Cambridge, in: 1st ed., Woodhead Pub., Cambridge, 2011.
[2] International Organization for Standardization (ISO), ISO 5725 parts 1–6, Accuracy (Trueness and Precision) of Measurement Methods and Results, Geneva, 1994.
[3] US Department of Health and Human Services, US Food and Drug Administration (FDA), Center for Drug Evaluation and Research (CDER), Center for Biologics Evaluation and Research (CBER), Guidance for Industry: Bioanalytical Method Validation, Rockville, 2001.
[4] Eurachem, The Fitness for Purpose of Analytical Methods, Teddington, 1998.
[5] International Organization for Standardization (ISO), ISO/CEI 17025: General Requirements for the Competence of Testing and calibration Laboratories, Geneva, 2005.
[6] P. Hubert, J.-J. Nguyen-Huu, B. Boulanger, E. Chapuzet, P. Chiap, N. Cohen, et al., Harmonization of strategies for the validation of quantitative analytical procedures: A SFSTP proposal—part I, J. Pharm. Biomed. Anal. 36 (2004) 579–586.
[7] M. Rafamantanana, Mise au point et validation de méthodes analytiques pour le contrôle de qualité de plantes médicinales malgaches et la mise en place de cultures locales, Université catholique de Louvain, 2012.
[8] Association of Official Analytical Chemists (AOAC), Official Methods of Analysis, 15th ed., AOAC, Arlington, VA, 1990.
[9] Food and Drug Administration, Guidance for Industry (draft), Analytical Procedures and Methods Validation, 2000.
[10] Food and Drug Administration, International Conference on Harmonization, Definitions and Terminology, Fed. Regist. 60 (1995) 11260–11262.
[11] Food and Drug Administration, International Conference on Harmonization, Methodology, Fed. Regist. 62 (1997) 27463–27467.
[12] International Conference on Harmonization of Technical Requirements for Registration of Pharmaceuticals for Human Use, ICH Q2(R1) Validation of Analytical Procedures: Text and Methodology, 2005.
[13] P. Hubert, J.-J. Nguyen-Huu, B. Boulanger, E. Chapuzet, P. Chiap, N. Cohen, et al., Harmonization of strategies for the validation of quantitative analytical procedures: A SFSTP proposal—part II, J. Pharm. Biomed. Anal. 45 (2007) 70–81.
[14] P. Hubert, J.-J. Nguyen-Huu, B. Boulanger, E. Chapuzet, N. Cohen, P.-A. Compagnon, et al., Harmonization of strategies for the validation of quantitative analytical procedures: A SFSTP proposal—part III, J. Pharm. Biomed. Anal. 45 (2007) 82–96.
[15] P. Araujo, Key aspects of analytical method validation and linearity evaluation, J. Chromatogr. B. 877 (2009) 2224–2234.
[16] E. Rozet, A. Ceccato, C. Hubert, E. Ziemons, R. Oprean, S. Rudaz, et al., Analysis of recent pharmaceutical regulatory documents on analytical method validation, J. Chromatogr. A. 1158 (2007) 111–125.
[17] Ph. Hubert, J.J. Nguyen-Huu, B. Boulanger, E. Chapuzet, P. Chiap, N. Cohen, P.A. Compagnon, W. Dewé, M. Feinberg, M. Lallier, M. Laurentie, N. Mercie, G. Muzard, C. Nivet, L. Valat, Validation des procédures analytiques quantitatives: harmonisation des démarches, STP PHARMA Prat. 13 (2003) 101–138.
[18] P. Hubert, J.-J. Nguyen-Huu, B. Boulanger, E. Chapuzet, N. Cohen, P.-A. Compagnon, et al., Harmonization of strategies for the validation of quantitative analytical procedures: A SFSTP proposal - Part IV. Examples of application, J. Pharm. Biomed. Anal. 48 (2008) 760–771.
[19] J. Vessman, R.I. Stefan, J.F. van Staden, K. Danzer, W. Lindner, D.T. Burns, et al., Selectivity in analytical chemistry (IUPAC Recommendations 2001), Pure Appl. Chem. 73

(2001) 1381–1386.
[20] WELAC Guidance Documents WG D2, Eurachem/Western European Laboratory Accreditation Cooperation (WELAC) Chemistry, Teddington, UK, first ed., 1993., (n.d.).
[21] International Union of Pure and Applied Chemistry, Compendium of chemical terminology: IUPAC recommendations, 2nd ed, Blackwell Science, Oxford [England]□; Malden, MA, USA, 1997.
[22] E. Rozet, A. Ceccato, C. Hubert, E. Ziemons, R. Oprean, S. Rudaz, et al., Analysis of recent pharmaceutical regulatory documents on analytical method validation, J. Chromatogr. A. 1158 (2007) 111–125.
[23] L.R. Snyder, Introduction to modern liquid chromatography, 3rd ed, Wiley, Hoboken, N.J, 2010.
[24] L. Nováková, Z. Spáčil, M. Seifrtová, L. Opletal, P. Solich, Rapid qualitative and quantitative ultra high performance liquid chromatography method for simultaneous analysis of twenty nine common phenolic compounds of various structures, Talanta. 80 (2010) 1970–1979.
[25] E. Lautié, E. Rozet, P. Hubert, J. Quetin Leclercq, Quantification of rotenone in seeds of different species of yam bean (Pachyrhizus sp.) by a SPE HPLC–UV method, Food Chem. 131 (2012) 1531–1538.
[26] M.H. Rafamantanana, E. Rozet, G.E. Raoelison, K. Cheuk, S.U. Ratsimamanga, P. Hubert, et al., An improved HPLC-UV method for the simultaneous quantification of triterpenic glycosides and aglycones in leaves of Centella asiatica (L.) Urb (APIACEAE), J. Chromatogr. B. 877 (2009) 2396–2402.
[27] Comission Directive 2002/63/EC, L187/30 establishing Community methods of sampling for the official control of pesticides residues in and on products of plant and animal origin and repealing directive 79/700/EEC., (n.d.).
[28] E. Rozet, R.D. Marini, E. Ziemons, B. Boulanger, P. Hubert, Advances in validation, risk and uncertainty assessment of bioanalytical methods, J. Pharm. Biomed. Anal. 55 (2011) 848–858.
[29] G. Martin, F. Mansion, V. Houbart, P. Paquet, A. Rorive, P. Chiap, et al., Pre-study and in-study validation of a SPE-LC–MS–MS method for the determination of 5-S-cysteinyldopa, a melanoma biomarker, in human plasma, Talanta. 84 (2011) 280–286.
[30] B. Streel, A. Ceccato, R. Klinkenberg, P. Hubert, Validation of a liquid chromatographic-tandem mass spectrometric method for the determination of loperamide in human plasma, J. Chromatogr. B. 814 (2005) 263–273.
[31] D. Hoffman, R. Kringle, Two-Sided Tolerance Intervals for Balanced and Unbalanced Random Effects Models, J. Biopharm. Stat. 15 (2005) 283–293.
[32] F.T. Peters, O.H. Drummer, F. Musshoff, Validation of new methods, Forensic Sci. Int. 165 (2007) 216–224.
[33] J. Ermer, J.H.M. Miller, Practical Method Validation in Pharmaceutical Analysis, Wiley-VCH, Weinheim, 2005.
[34] N. Ansermot, M. Brawand-Amey, C.B. Eap, Simultaneous quantification of selective serotonin reuptake inhibitors and metabolites in human plasma by liquid chromatography–electrospray mass spectrometry for therapeutic drug monitoring, J. Chromatogr. B. 885-886 (2012) 117–130.
[35] M.A. Bimazubute, E. Rozet, I. Dizier, P. Gustin, P. Hubert, J. Crommen, et al., Liquid chromatographic determination of enrofloxacin in nasal secretions and plasma of healthy pigs using restricted access material for on-line sample clean-up, J. Chromatogr. A. 1189 (2008) 456–466.
[36] B. Boulanger, W. Dewé, A. Gilbert, B. Govaerts, M. Maumy-Bertrand, Risk management for analytical methods based on the total error concept: Conciliating the

objectives of the pre-study and in-study validation phases, Chemom. Intell. Lab. Syst. 86 (2007) 198–207.
[37] R.W. Mee, β-Expectation and β-Content Tolerance Limits for Balanced One-Way ANOVA Random Model, Technometrics. 26 (1984) 251–254.
[38] J. Bruneton, Pharmacognosie, phytochimie, plantes médicinales, Éd. Tec & doc; Éd. médicales internationales, Paris; Cachan, 2009.
[39] M. Clifford, A nomenclature for phenols with special reference to tea, Crit. Rev. Food Sci. Nutr. 41 (2001) 393–397.
[40] Flavonoids: chemistry, biochemistry, and applications, CRC, Taylor & Francis, Boca Raton, FL, 2006.
[41] V.I. Popa, M. Dumitru, I. Volf, N. Anghel, Lignin and polyphenols as allelochemicals, Ind. Crops Prod. 27 (2008) 144–149.
[42] C. Alasalvar, J.M. Grigor, D. Zhang, P.C. Quantick, F. Shahidi, Comparison of Volatiles, Phenolics, Sugars, Antioxidant Vitamins, and Sensory Quality of Different Colored Carrot Varieties, J. Agric. Food Chem. 49 (2001) 1410–1416.
[43] L. Gennaro, C. Leonardi, F. Esposito, M. Salucci, G. Maiani, G. Quaglia, et al., Flavonoid and Carbohydrate Contents in Tropea Red Onions: Effects of Homelike Peeling and Storage, J. Agric. Food Chem. 50 (2002) 1904–1910.
[44] H. Rogez, D.R. Pompeu, S.N.T. Akwie, Y. Larondelle, Sigmoidal kinetics of anthocyanin accumulation during fruit ripening: A comparison between açai fruits (Euterpe oleracea) and other anthocyanin-rich fruits, J. Food Compos. Anal. 24 (2011) 796–800.
[45] M. Naczk, F. Shahidi, Phenolics in cereals, fruits and vegetables: Occurrence, extraction and analysis, J. Pharm. Biomed. Anal. 41 (2006) 1523–1542.
[46] H. Wu, X. Liang, Y. Fang, X. Qin, Y. Zhang, J. Liu, Resveratrol inhibits hypoxia-induced metastasis potential enhancement by restricting hypoxia-induced factor-1α expression in colon carcinoma cells, Biomed. Pharmacother. 62 (2008) 613–621.
[47] H. Schroeter, C. Heiss, J. Balzer, P. Kleinbongard, C.L. Keen, N.K. Hollenberg, et al., (–)-Epicatechin mediates beneficial effects of flavanol-rich cocoa on vascular function in humans, Proc. Natl. Acad. Sci. U. S. A. 103 (2006) 1024–1029.
[48] F. Perez-Vizcaino, J. Duarte, R. Jimenez, C. Santos-Buelga, A. Osuna, Antihypertensive effects of the flavonoid quercetin, Pharmacol. Rep. 61 (2009) 67–75.
[49] V. Mulabagal, A.I. Calderón, Liquid chromatography/mass spectrometry based fingerprinting analysis and mass profiling of Euterpe oleracea (açaí) dietary supplement raw materials, Food Chem. 134 (2012) 1156–1164.
[50] A.G.V. Costa, D.F. Garcia-Diaz, P. Jimenez, P.I. Silva, Bioactive compounds and health benefits of exotic tropical red–black berries, J. Funct. Foods. 5 (2013) 539–549.
[51] J.F. Ayala-Zavala, V. Vega-Vega, C. Rosas-Domínguez, H. Palafox-Carlos, J.A. Villa-Rodriguez, M.W. Siddiqui, et al., Agro-industrial potential of exotic fruit byproducts as a source of food additives, Food Res. Int. 44 (2011) 1866–1874.
[52] E.M. Silva, J.N.S. Souza, H. Rogez, J.F. Rees, Y. Larondelle, Antioxidant activities and polyphenolic contents of fifteen selected plant species from the Amazonian region, Food Chem. 101 (2006) 1012–1018.
[53] J.N.S. Souza, E.M. Silva, A. Loir, J.-F. Rees, H. Rogez, Y. Larondelle, Antioxidant capacity of four polyphenol-rich Amazonian plant extracts: A correlation study using chemical and biological in vitro assays, Food Chem. 106 (2008) 331–339.
[54] C.M. André, M. Oufir, L. Hoffmann, J.-F. Hausman, H. Rogez, Y. Larondelle, et al., Influence of environment and genotype on polyphenol compounds and in vitro antioxidant capacity of native Andean potatoes (Solanum tuberosum L.), J. Food Compos. Anal. 22 (2009) 517–524.
[55] E.M. Silva, D.R. Pompeu, Y. Larondelle, H. Rogez, Optimisation of the adsorption of

polyphenols from Inga edulis leaves on macroporous resins using an experimental design methodology, Sep. Purif. Technol. 53 (2007) 274–280.
[56] D.R. Pompeu, E.M. Silva, H. Rogez, Optimisation of the solvent extraction of phenolic antioxidants from fruits of Euterpe oleracea using Response Surface Methodology, Bioresour. Technol. 100 (2009) 6076–6082.
[57] R. Chirinos, H. Rogez, D. Campos, R. Pedreschi, Y. Larondelle, Optimization of extraction conditions of antioxidant phenolic compounds from mashua (Tropaeolum tuberosum Ruíz & Pavón) tubers, Sep. Purif. Technol. 55 (2007) 217–225.
[58] R. Llorach, A. Gil-Izquierdo, F. Ferreres, F.A. Tomás-Barberán, HPLC-DAD-MS/MS ESI Characterization of Unusual Highly Glycosylated Acylated Flavonoids from Cauliflower (*Brassica oleracea* L. *v* ar. *botrytis*) Agroindustrial Byproducts, J. Agric. Food Chem. 51 (2003) 3895–3899.
[59] X. Wu, R.L. Prior, Systematic Identification and Characterization of Anthocyanins by HPLC-ESI-MS/MS in Common Foods in the United States: Fruits and Berries, J. Agric. Food Chem. 53 (2005) 2589–2599.
[60] A. Chandra, J. Rana, Y. Li, Separation, Identification, Quantification, and Method Validation of Anthocyanins in Botanical Supplement Raw Materials by HPLC and HPLC−MS, J. Agric. Food Chem. 49 (2001) 3515–3521.
[61] J. Bruneton, Pharmacognosie, phytochimie, plantes médicinales, Éd. Tec & Doc; Éd. médicales internationales, Paris; Cachan, 2009.
[62] P.M. Dewick, Medicinal Natural Products: A Biosynthetic Approach, Second Edition, 2001.
[63] V. Tzin, G. Galili, New Insights into the Shikimate and Aromatic Amino Acids Biosynthesis Pathways in Plants, Mol. Plant. 3 (2010) 956–972.
[64] T. Vogt, Phenylpropanoid Biosynthesis, Mol. Plant. 3 (2009) 2–20.
[65] T. Tohge, M. Watanabe, R. Hoefgen, A.R. Fernie, Shikimate and Phenylalanine Biosynthesis in the Green Lineage, Front. Plant Sci. 4 (2013).
[66] I. Abe, Y. Utsumi, S. Oguro, H. Morita, Y. Sano, H. Noguchi, A Plant Type III Polyketide Synthase that Produces Pentaketide Chromone, J. Am. Chem. Soc. 127 (2005) 1362–1363.
[67] I.A.M. Abdel-Rahman, T. Beuerle, L. Ernst, A.M. Abdel-Baky, E.E.-D.K. Desoky, A.S. Ahmed, et al., In vitro formation of the anthranoid scaffold by cell-free extracts from yeast-extract-treated Cassia bicapsularis cell cultures, Phytochemistry. 88 (2013) 15–24.
[68] G. Castellano, J.L. González-Santander, A. Lara, F. Torrens, Classification of flavonoid compounds by using entropy of information theory, Phytochemistry. (n.d.).
[69] I.J. Flores-Sanchez, R. Verpoorte, Plant Polyketide Synthases: A fascinating group of enzymes, Plant Physiol. Biochem. 47 (2009) 167–174.
[70] R.J. Robbins, Phenolic Acids in Foods: An Overview of Analytical Methodology, J. Agric. Food Chem. 51 (2003) 2866–2887.
[71] K. Herrmann, The Shikimate Pathway: Early Steps in the Biosynthesis of Aromatic Compounds., Plant Cell. 7 (1995) 907–919.
[72] A.R. Knaggs, A.R. Knaggs, A.R. Knaggs, The biosynthesis of shikimate metabolites, Nat. Prod. Rep. 16 (1999) 525–560.
[73] H. Maeda, N. Dudareva, The Shikimate Pathway and Aromatic Amino Acid Biosynthesis in Plants, Annu. Rev. Plant Biol. 63 (2012) 73–105.
[74] A.-M. Boudet, Lignins and lignification: Selected issues, Plant Physiol. Biochem. 38 (2000) 81–96.
[75] M.J. MacDonald, G.B. D'Cunha, A modern view of phenylalanine ammonia lyase, Biochem. Cell Biol. 85 (2007) 273–282.
[76] K. Saito, K. Yonekura-Sakakibara, R. Nakabayashi, Y. Higashi, M. Yamazaki, T.

Tohge, et al., The flavonoid biosynthetic pathway in Arabidopsis: Structural and genetic diversity, Plant Physiol. Biochem. (n.d.).
[77] A.C. Neish, Formation of m- and p-coumaric acids by enzymatic deamination of the corresponding isomers of tyrosine, Phytochemistry. 1 (1961) 1–24.
[78] K. Hamada, T. Nishida, K. Yamauchi, K. Fukushima, R. Kondo, Y. Tsutsumi, 4-Coumarate:coenzyme A ligase in black locust (Robinia pseudoacacia) catalyses the conversion of sinapate to sinapoyl-CoA, J. Plant Res. 117 (2004).
[79] S.Z. el-Basyouni, D. Chen, R.K. Ibrahim, A.C. Neish, G.H.N. Towers, The biosynthesis of hydroxybenzoic acids in higher plants, Phytochemistry. 3 (1964) 485–492.
[80] R.M. Muir, A.M. Ibáñez, S.L. Uratsu, E.S. Ingham, C.A. Leslie, G.H. McGranahan, et al., Mechanism of gallic acid biosynthesis in bacteria (Escherichia coli) and walnut (Juglans regia), Plant Mol. Biol. 75 (2011) 555–565.
[81] C. Garcion, A. Lohmann, E. Lamodiere, J. Catinot, A. Buchala, P. Doermann, et al., Characterization and Biological Function of the ISOCHORISMATE SYNTHASE2 Gene of Arabidopsis, PLANT Physiol. 147 (2008) 1279–1287.
[82] H. Sawada, I.-S. Shim, K. Usui, Induction of benzoic acid 2-hydroxylase and salicylic acid biosynthesis—Modulation by salt stress in rice seedlings, Plant Sci. 171 (2006) 263–270.
[83] A.V. Qualley, J.R. Widhalm, F. Adebesin, C.M. Kish, N. Dudareva, Completion of the core β-oxidative pathway of benzoic acid biosynthesis in plants, Proc. Natl. Acad. Sci. 109 (2012) 16383–16388.
[84] E. Wollenweber, On the occurrence of acylated flavonoid aglycones, Phytochemistry. 24 (1985) 1493–1494.
[85] F. Sosulski, K. Krygier, L. Hogge, Free, esterified, and insoluble-bound phenolic acids. 3. Composition of phenolic acids in cereal and potato flours, J. Agric. Food Chem. 30 (1982) 337–340.
[86] A. Renger, H. Steinhart, Ferulic acid dehydrodimers as structural elements in cereal dietary fibre, Eur. Food Res. Technol. 211 (2000) 422–428.
[87] K. Saito, K. Yonekura-Sakakibara, R. Nakabayashi, Y. Higashi, M. Yamazaki, T. Tohge, et al., The flavonoid biosynthetic pathway in Arabidopsis: Structural and genetic diversity, Plant Physiol. Biochem. PPB Soc. Francaise Physiol. Veg. (2013).
[88] I.J. Flores-Sanchez, R. Verpoorte, Plant Polyketide Synthases: A fascinating group of enzymes, Plant Physiol. Biochem. 47 (2009) 167–174.
[89] J.-L. Ferrer, M.B. Austin, C. Stewart Jr, J.P. Noel, Structure and function of enzymes involved in the biosynthesis of phenylpropanoids, Plant Physiol. Biochem. PPB Société Fr. Physiol. Végétale. 46 (2008) 356–370.
[90] K.M. Olsen, A. Hehn, H. Jugdé, R. Slimestad, R. Larbat, F. Bourgaud, et al., Identification and characterisation of CYP75A31, a new flavonoid 3’5’-hydroxylase, isolated from Solanum lycopersicum, BMC Plant Biol. 10 (2010) 21.
[91] M. Bredebach, U. Matern, S. Martens, Three 2-oxoglutarate-dependent dioxygenase activities of Equisetum arvense L. forming flavone and flavonol from (2S)-naringenin, Phytochemistry. 72 (2011) 557–563.
[92] L. Lepiniec, I. Debeaujon, J.-M. Routaboul, A. Baudry, L. Pourcel, N. Nesi, et al., GENETICS AND BIOCHEMISTRY OF SEED FLAVONOIDS, Annu. Rev. Plant Biol. 57 (2006) 405–430.
[93] F. Ferreres, R. Llorach, A. Gil-Izquierdo, Characterization of the interglycosidic linkage in di-, tri-, tetra- and pentaglycosylated flavonoids and differentiation of positional isomers by liquid chromatography/electrospray ionization tandem mass spectrometry, J. Mass Spectrom. 39 (2004) 312–321.
[94] M. Brazier-Hicks, K.M. Evans, M.C. Gershater, H. Puschmann, P.G. Steel, R. Edwards, The C-Glycosylation of Flavonoids in Cereals, J. Biol. Chem. 284 (2009) 17926–

17934.
[95] Y. Du, H. Chu, I.K. Chu, C. Lo, CYP93G2 is a flavanone 2-hydroxylase required for C-glycosylflavone biosynthesis in rice, Plant Physiol. 154 (2010) 324–333.
[96] N. Balasundram, K. Sundram, S. Samman, Phenolic compounds in plants and agri-industrial by-products: Antioxidant activity, occurrence, and potential uses, Food Chem. 99 (2006) 191–203.
[97] B.A. Bohm, Introduction to flavonoids, Harwood Academic Publishers, Amsterdam, 1998.
[98] J. Fleschhut, F. Kratzer, G. Rechkemmer, S.E. Kulling, Stability and biotransformation of various dietary anthocyanins in vitro, Eur. J. Nutr. 45 (2005) 7–18.
[99] F.H. Quina, P.F. Moreira, C. Vautier-Giongo, D. Rettori, R.F. Rodrigues, A.A. Freitas, et al., Photochemistry of anthocyanins and their biological role in plant tissues, Pure Appl. Chem. 81 (2009) 1687–1694.
[100] A. Castañeda-Ovando, M. de L. Pacheco-Hernández, M.E. Páez-Hernández, J.A. Rodríguez, C.A. Galán-Vidal, Chemical studies of anthocyanins: A review, Food Chem. 113 (2009) 859–871.
[101] S.R. Mallery, D.E. Budendorf, M.P. Larsen, P. Pei, M. Tong, A.S. Holpuch, et al., Effects of human oral mucosal tissue, saliva, and oral microflora on intraoral metabolism and bioactivation of black raspberry anthocyanins, Cancer Prev. Res. Phila. Pa. 4 (2011) 1209–1221.
[102] T. Walle, A.M. Browning, L.L. Steed, S.G. Reed, U.K. Walle, Flavonoid glucosides are hydrolyzed and thus activated in the oral cavity in humans, J. Nutr. 135 (2005) 48–52.
[103] I. Fernandes, A. Faria, C. Calhau, V. de Freitas, N. Mateus, Bioavailability of anthocyanins and derivatives, J. Funct. Foods. (n.d.).
[104] S. Talavéra, C. Felgines, O. Texier, C. Besson, J.-L. Lamaison, C. Rémésy, Anthocyanins are efficiently absorbed from the stomach in anesthetized rats, J. Nutr. 133 (2003) 4178–4182.
[105] C. Felgines, O. Texier, C. Besson, B. Lyan, J.-L. Lamaison, A. Scalbert, Strawberry pelargonidin glycosides are excreted in urine as intact glycosides and glucuronidated pelargonidin derivatives in rats, Br. J. Nutr. 98 (2007) 1126–1131.
[106] V. Crespy, C. Morand, C. Besson, C. Manach, C. Demigne, C. Remesy, Quercetin, but not its glycosides, is absorbed from the rat stomach, J. Agric. Food Chem. 50 (2002) 618–621.
[107] Y. Konishi, Z. Zhao, M. Shimizu, Phenolic Acids Are Absorbed from the Rat Stomach with Different Absorption Rates, J. Agric. Food Chem. 54 (2006) 7539–7543.
[108] S.A. Eraly, K.T. Bush, R.V. Sampogna, V. Bhatnagar, S.K. Nigam, The Molecular Pharmacology of Organic Anion Transporters: from DNA to FDA?, Mol. Pharmacol. 65 (2004) 479–487.
[109] C.K. Garcia, M.S. Brown, R.K. Pathak, J.L. Goldstein, cDNA Cloning of MCT2, a Second Monocarboxylate Transporter Expressed in Different Cells than MCT1, J. Biol. Chem. 270 (1995) 1843–1849.
[110] T. Yoshikawa, R. Inoue, M. Matsumoto, T. Yajima, K. Ushida, T. Iwanaga, Comparative expression of hexose transporters (SGLT1, GLUT1, GLUT2 and GLUT5) throughout the mouse gastrointestinal tract, Histochem. Cell Biol. 135 (2011) 183–194.
[111] A.J. Day, F.J. Cañada, J.C. Díaz, P.A. Kroon, R. Mclauchlan, C.B. Faulds, et al., Dietary flavonoid and isoflavone glycosides are hydrolysed by the lactase site of lactase phlorizin hydrolase, FEBS Lett. 468 (2000) 166–170.
[112] J.M. Gee, M.S. DuPont, A.J. Day, G.W. Plumb, G. Williamson, I.T. Johnson, Intestinal transport of quercetin glycosides in rats involves both deglycosylation and interaction with the hexose transport pathway, J. Nutr. 130 (2000) 2765–2771.

[113] A. Faria, D. Pestana, J. Azevedo, F. Martel, V. de Freitas, I. Azevedo, et al., Absorption of anthocyanins through intestinal epithelial cells – Putative involvement of GLUT2, Mol. Nutr. Food Res. 53 (2009) 1430–1437.
[114] S. Manzano, G. Williamson, Polyphenols and phenolic acids from strawberry and apple decrease glucose uptake and transport by human intestinal Caco-2 cells, Mol. Nutr. Food Res. 54 (2010) 1773–1780.
[115] K. van de Wetering, A. Burkon, W. Feddema, A. Bot, H. de Jonge, V. Somoza, et al., Intestinal breast cancer resistance protein (BCRP)/Bcrp1 and multidrug resistance protein 3 (MRP3)/Mrp3 are involved in the pharmacokinetics of resveratrol, Mol. Pharmacol. 75 (2009) 876–885.
[116] J. Chen, S. Wang, X. Jia, S. Bajimaya, H. Lin, V.H. Tam, et al., Disposition of flavonoids via recycling: comparison of intestinal versus hepatic disposition, Drug Metab. Dispos. Biol. Fate Chem. 33 (2005) 1777–1784.
[117] T. Miyazawa, K. Nakagawa, M. Kudo, K. Muraishi, K. Someya, Direct Intestinal Absorption of Red Fruit Anthocyanins, Cyanidin-3-glucoside and Cyanidin-3,5-diglucoside, into Rats and Humans, J. Agric. Food Chem. 47 (1999) 1083–1091.
[118] K. Kahle, M. Kraus, W. Scheppach, M. Ackermann, F. Ridder, E. Richling, Studies on apple and blueberry fruit constituents: do the polyphenols reach the colon after ingestion?, Mol. Nutr. Food Res. 50 (2006) 418–423.
[119] S. Roowi, A. Stalmach, W. Mullen, M.E.J. Lean, C.A. Edwards, A. Crozier, Green tea flavan-3-ols: colonic degradation and urinary excretion of catabolites by humans, J. Agric. Food Chem. 58 (2010) 1296–1304.
[120] D. Del Rio, A. Rodriguez-Mateos, J.P.E. Spencer, M. Tognolini, G. Borges, A. Crozier, Dietary (Poly)phenolics in Human Health: Structures, Bioavailability, and Evidence of Protective Effects Against Chronic Diseases, Antioxid. Redox Signal. 18 (2013) 1818–1892.
[121] W. Kalt, J.B. Blumberg, J.E. McDonald, M.R. Vinqvist-Tymchuk, S.A.E. Fillmore, B.A. Graf, et al., Identification of anthocyanins in the liver, eye, and brain of blueberry-fed pigs, J. Agric. Food Chem. 56 (2008) 705–712.
[122] C. Felgines, O. Texier, P. Garcin, C. Besson, J.-L. Lamaison, A. Scalbert, Tissue distribution of anthocyanins in rats fed a blackberry anthocyanin-enriched diet, Mol. Nutr. Food Res. 53 (2009) 1098–1103.
[123] A. Ishisaka, S. Ichikawa, H. Sakakibara, M.K. Piskula, T. Nakamura, Y. Kato, et al., Accumulation of orally administered quercetin in brain tissue and its antioxidative effects in rats, Free Radic. Biol. Med. 51 (2011) 1329–1336.
[124] M. Suganuma, S. Okabe, M. Oniyama, Y. Tada, H. Ito, H. Fujiki, Wide distribution of [3H](-)-epigallocatechin gallate, a cancer preventive tea polyphenol, in mouse tissue., Carcinogenesis. 19 (1998) 1771–1776.
[125] K.O. Chu, C.C. Wang, C.Y. Chu, K.W. Choy, C.P. Pang, M.S. Rogers, Uptake and distribution of catechins in fetal organs following in utero exposure in rats, Hum. Reprod. Oxf. Engl. 22 (2007) 280–287.
[126] L. Ziberna, S. Fornasaro, J. Čvorović, F. Tramer, S. Passamonti, Chapter 37 - Bioavailability of Flavonoids: The Role of Cell Membrane Transporters, in: R.R. Watson, V.R. Preedy, S. Zibadi (Eds.), Polyphenols Hum. Health Dis., Academic Press, San Diego, 2014: pp. 489–511.
[127] T. Frank, M. Netzel, G. Strass, R. Bitsch, I. Bitsch, Bioavailability of anthocyanidin-3-glucosides following consumption of red wine and red grape juice, Can. J. Physiol. Pharmacol. 81 (2003) 423–435.
[128] S.U. Mertens-Talcott, J. Rios, P. Jilma-Stohlawetz, L.A. Pacheco-Palencia, B. Meibohm, S.T. Talcott, et al., Pharmacokinetics of Anthocyanins and Antioxidant Effects

after the Consumption of Anthocyanin-Rich Açai Juice and Pulp (Euterpe oleracea Mart.) in Human Healthy Volunteers, J. Agric. Food Chem. 56 (2008) 7796–7802.
[129] L.T. Bloedon, A. Robert Jeffcoat, W. Lopaczynski, M.J. Schell, T.M. Black, K.J. Dix, et al., Safety and pharmacokinetics of purified soy isoflavones: Single-dose administration to postmenopausal women, Am. J. Clin. Nutr. 76 (2002) 1126–1137.
[130] P.E. Milbury, J.A. Vita, J.B. Blumberg, Anthocyanins are Bioavailable in Humans following an Acute Dose of Cranberry Juice, J. Nutr. 140 (2010) 1099–1104.
[131] M.-J. Lee, J.D. Lambert, S. Prabhu, X. Meng, H. Lu, P. Maliakal, et al., Delivery of Tea Polyphenols to the Oral Cavity by Green Tea Leaves and Black Tea Extract, Cancer Epidemiol. Biomarkers Prev. 13 (2004) 132–137.
[132] A. Tsuji, Small Molecular Drug Transfer across the Blood-Brain Barrier via Carrier-Mediated Transport Systems, NeuroRX. 2 (2005) 54–62.
[133] J. Terao, K. Murota, Y. Kawai, Conjugated quercetin glucuronides as bioactive metabolites and precursors of aglyconein vivo, Food Funct. 2 (2011) 11–17.
[134] E. Kurin, A.G. Atanasov, O. Donath, E.H. Heiss, V.M. Dirsch, M. Nagy, Synergy study of the inhibitory potential of red wine polyphenols on vascular smooth muscle cell proliferation, Planta Med. 78 (2012) 772–778.
[135] S.K. Nicholson, G.A. Tucker, J.M. Brameld, Effects of dietary polyphenols on gene expression in human vascular endothelial cells, Proc. Nutr. Soc. 67 (2008) 42–47.
[136] L. Ziberna, F. Tramer, S. Moze, U. Vrhovsek, F. Mattivi, S. Passamonti, Transport and bioactivity of cyanidin 3-glucoside into the vascular endothelium, Free Radic. Biol. Med. 52 (2012) 1750–1759.
[137] S.M. Bornsek, L. Ziberna, T. Polak, A. Vanzo, N.P. Ulrih, V. Abram, et al., Bilberry and blueberry anthocyanins act as powerful intracellular antioxidants in mammalian cells, Food Chem. 134 (2012) 1878–1884.
[138] V. Benetou, P. Orfanos, P. Lagiou, D. Trichopoulos, P. Boffetta, A. Trichopoulou, Vegetables and Fruits in Relation to Cancer Risk: Evidence from the Greek EPIC Cohort Study, Cancer Epidemiol. Biomarkers Prev. 17 (2008) 387–392.
[139] L. Dauchet, P. Amouyel, S. Hercberg, J. Dallongeville, Fruit and vegetable consumption and risk of coronary heart disease: a meta-analysis of cohort studies, J. Nutr. 136 (2006) 2588–2593.
[140] K. Beking, A. Vieira, Flavonoid intake and disability-adjusted life years due to Alzheimer's and related dementias: a population-based study involving twenty-three developed countries, Public Health Nutr. 13 (2010) 1403–1409.
[141] M. Michalska, A. Gluba, D.P. Mikhailidis, P. Nowak, A. Bielecka-Dabrowa, J. Rysz, et al., The role of polyphenols in cardiovascular disease, Med. Sci. Monit. Int. Med. J. Exp. Clin. Res. 16 (2010) RA110–119.
[142] C. Ramassamy, Emerging role of polyphenolic compounds in the treatment of neurodegenerative diseases: a review of their intracellular targets, Eur. J. Pharmacol. 545 (2006) 51–64.
[143] S. Renaud, M. de Lorgeril, Wine, alcohol, platelets, and the French paradox for coronary heart disease, The Lancet. 339 (1992) 1523–1526.
[144] E.. Frankel, J.. German, J.. Kinsella, E. Parks, J. Kanner, Inhibition of oxidation of human low-density lipoprotein by phenolic substances in red wine, The Lancet. 341 (1993) 454–457.
[145] M. Leopoldini, N. Russo, M. Toscano, The molecular basis of working mechanism of natural polyphenolic antioxidants, Food Chem. 125 (2011) 288–306.
[146] P.A. Grace, Ischaemia-reperfusion injury, Br. J. Surg. 81 (1994) 637–647.
[147] B. Halliwell, How to characterize an antioxidant: an update, Biochem. Soc. Symp. 61 (1995) 73–101.

[148] H. de Groot, Reactive oxygen species in tissue injury, Hepatogastroenterology. 41 (1994) 328–332.
[149] G. Di Carlo, N. Mascolo, A.A. Izzo, F. Capasso, Flavonoids: Old and new aspects of a class of natural therapeutic drugs, Life Sci. 65 (1999) 337–353.
[150] S. Kuntz, U. Wenzel, H. Daniel, Comparative analysis of the effects of flavonoids on proliferation, cytotoxicity, and apoptosis in human colon cancer cell lines, Eur. J. Nutr. 38 (1999) 133–142.
[151] P. Cos, L. Ying, M. Calomme, J.P. Hu, K. Cimanga, B. Van Poel, et al., Structure−Activity Relationship and Classification of Flavonoids as Inhibitors of Xanthine Oxidase and Superoxide Scavengers, J. Nat. Prod. 61 (1998) 71–76.
[152] J.B. Schulz, J. Lindenau, J. Seyfried, J. Dichgans, Glutathione, oxidative stress and neurodegeneration, Eur. J. Biochem. 267 (2000) 4904–4911.
[153] R.L. Prior, H. Hoang, L. Gu, X. Wu, M. Bacchiocca, L. Howard, et al., Assays for Hydrophilic and Lipophilic Antioxidant Capacity (oxygen radical absorbance capacity (ORACFL)) of Plasma and Other Biological and Food Samples, J. Agric. Food Chem. 51 (2003) 3273–3279.
[154] G. Cao, R.L. Prior, Measurement of oxygen radical absorbance capacity in biological samples, Methods Enzymol. 299 (1999) 50–62.
[155] R.L. Prior, X. Wu, K. Schaich, Standardized methods for the determination of antioxidant capacity and phenolics in foods and dietary supplements, J. Agric. Food Chem. 53 (2005) 4290–4302.
[156] C. Nathan, Points of control in inflammation, Nature. 420 (2002) 846–852.
[157] G.M. Barton, A calculated response: control of inflammation by the innate immune system, J. Clin. Invest. 118 (2008) 413–420.
[158] P.S. Haddad, G.A. Azar, S. Groom, M. Boivin, Natural health products, modulation of immune function and prevention of chronic diseases, Evid.-Based Complement. Altern. Med. ECAM. 2 (2005) 513–520.
[159] A. García-Lafuente, E. Guillamón, A. Villares, M.A. Rostagno, J.A. Martínez, Flavonoids as anti-inflammatory agents: implications in cancer and cardiovascular disease, Inflamm. Res. 58 (2009) 537–552.
[160] A.E. Rotelli, T. Guardia, A.O. Juárez, N.E. de la Rocha, L.E. Pelzer, Comparative study of flavonoids in experimental models of inflammation, Pharmacol. Res. Off. J. Ital. Pharmacol. Soc. 48 (2003) 601–606.
[161] L. Wang, Y.-C. Tu, T.-W. Lian, J.-T. Hung, J.-H. Yen, M.-J. Wu, Distinctive antioxidant and antiinflammatory effects of flavonols, J. Agric. Food Chem. 54 (2006) 9798–9804.
[162] C.A. Jolly, Diet manipulation and prevention of aging, cancer and autoimmune disease, Curr. Opin. Clin. Nutr. Metab. Care. 8 (2005) 382–387.
[163] K.W. Hance, C.J. Rogers, S.D. Hursting, J.W. Greiner, Combination of physical activity, nutrition, or other metabolic factors and vaccine response, Front. Biosci. J. Virtual Libr. 12 (2007) 4997–5029.
[164] J.J. Volman, J.D. Ramakers, J. Plat, Dietary modulation of immune function by beta-glucans, Physiol. Behav. 94 (2008) 276–284.
[165] E. Middleton Jr, C. Kandaswami, T.C. Theoharides, The effects of plant flavonoids on mammalian cells: implications for inflammation, heart disease, and cancer, Pharmacol. Rev. 52 (2000) 673–751.
[166] C.E. Rudd, CD4, CD8 and the TCR-CD3 complex: a novel class of protein-tyrosine kinase receptor, Immunol. Today. 11 (1990) 400–406.
[167] M.A. Campbell, B.M. Sefton, Protein tyrosine phosphorylation is induced in murine B lymphocytes in response to stimulation with anti-immunoglobulin, EMBO J. 9 (1990)

2125–2131.
[168] Y. Geng, B. Zhang, M. Lotz, Protein tyrosine kinase activation is required for lipopolysaccharide induction of cytokines in human blood monocytes, J. Immunol. Baltim. Md 1950. 151 (1993) 6692–6700.
[169] J.P. Bennett, B.D. Gomperts, E. Wollenweber, Inhibitory effects of natural flavonoids on secretion from mast cells and neutrophils, Arzneimittelforschung. 31 (1981) 433–437.
[170] G. Berton, C. Schneider, D. Romeo, Inhibition by quercetin of activation of polymorphonuclear leucocyte functions. Stimulus-specific effects, Biochim. Biophys. Acta. 595 (1980) 47–55.
[171] A. Kanashiro, J.G. Souza, L.M. Kabeya, A.E.C.S. Azzolini, Y.M. Lucisano-Valim, Elastase release by stimulated neutrophils inhibited by flavonoids: importance of the catechol group, Z. Für Naturforschung C J. Biosci. 62 (2007) 357–361.
[172] B. Gil, M.J. Sanz, M.C. Terencio, R. Gunasegaran, M. Payá, M.J. Alcaraz, Morelloflavone, a novel biflavonoid inhibitor of human secretory phospholipase A2 with anti-inflammatory activity, Biochem. Pharmacol. 53 (1997) 733–740.
[173] H.W. Chang, S.H. Baek, K.W. Chung, K.H. Son, H.P. Kim, S.S. Kang, Inactivation of phospholipase A2 by naturally occurring biflavonoid, ochnaflavone, Biochem. Biophys. Res. Commun. 205 (1994) 843–849.
[174] Y.S. Chi, H.G. Jong, K.H. Son, H.W. Chang, S.S. Kang, H.P. Kim, Effects of naturally occurring prenylated flavonoids on enzymes metabolizing arachidonic acid: cyclooxygenases and lipoxygenases, Biochem. Pharmacol. 62 (2001) 1185–1191.
[175] B.S. Cheon, Y.H. Kim, K.S. Son, H.W. Chang, S.S. Kang, H.P. Kim, Effects of prenylated flavonoids and biflavonoids on lipopolysaccharide-induced nitric oxide production from the mouse macrophage cell line RAW 264.7, Planta Med. 66 (2000) 596–600.
[176] H. Kobuchi, F. Virgili, L. Packer, Assay of inducible form of nitric oxide synthase activity: effect of flavonoids and plant extracts, Methods Enzymol. 301 (1999) 504–513.
[177] P.N. Paradkar, P.S. Blum, M.A. Berhow, H. Baumann, S.-M. Kuo, Dietary isoflavones suppress endotoxin-induced inflammatory reaction in liver and intestine, Cancer Lett. 215 (2004) 21–28.
[178] X.W. Chen, S.C. Garner, J.J.B. Anderson, Isoflavones regulate interleukin-6 and osteoprotegerin synthesis during osteoblast cell differentiation via an estrogen-receptor-dependent pathway, Biochem. Biophys. Res. Commun. 295 (2002) 417–422.
[179] S.-Z. Ding, C.-H. Cho, S.-K. Lam, REGULATION OF INTERLEUKIN 6 PRODUCTION IN A HUMAN GASTRIC EPITHELIAL CELL LINE MKN-28, Cytokine. 12 (2000) 1129–1135.
[180] A. Xagorari, A. Papapetropoulos, A. Mauromatis, M. Economou, T. Fotsis, C. Roussos, Luteolin inhibits an endotoxin-stimulated phosphorylation cascade and proinflammatory cytokine production in macrophages, J. Pharmacol. Exp. Ther. 296 (2001) 181–187.
[181] C. Santangelo, R. Varì, B. Scazzocchio, R. Di Benedetto, C. Filesi, R. Masella, Polyphenols, intracellular signalling and inflammation, Ann. DellIstituto Super. Sanità. 43 (2007) 394–405.
[182] Y.C. Liang, Y.T. Huang, S.H. Tsai, S.Y. Lin-Shiau, C.F. Chen, J.K. Lin, Suppression of inducible cyclooxygenase and inducible nitric oxide synthase by apigenin and related flavonoids in mouse macrophages, Carcinogenesis. 20 (1999) 1945–1952.
[183] M. Mutoh, M. Takahashi, K. Fukuda, H. Komatsu, T. Enya, Y. Matsushima-Hibiya, et al., Suppression by flavonoids of cyclooxygenase-2 promoter-dependent transcriptional activity in colon cancer cells: structure-activity relationship, Jpn. J. Cancer Res. Gann. 91 (2000) 686–691.
[184] C.-Y. Chen, W.-H. Peng, K.-D. Tsai, S.-L. Hsu, Luteolin suppresses inflammation-

associated gene expression by blocking NF-κB and AP-1 activation pathway in mouse alveolar macrophages, Life Sci. 81 (2007) 1602–1614.
[185] F. Sheu, H.H. Lai, G.C. Yen, Suppression effect of soy isoflavones on nitric oxide production in RAW 264.7 macrophages, J. Agric. Food Chem. 49 (2001) 1767–1772.
[186] G. Autore, L. Rastrelli, M.R. Lauro, S. Marzocco, R. Sorrentino, U. Sorrentino, et al., Inhibition of nitric oxide synthase expression by a methanolic extract of Crescentia alata and its derived flavonols, Life Sci. 70 (2001) 523–534.
[187] M. Hämäläinen, R. Nieminen, P. Vuorela, M. Heinonen, E. Moilanen, Anti-Inflammatory Effects of Flavonoids: Genistein, Kaempferol, Quercetin, and Daidzein Inhibit STAT-1 and NF-κB Activations, Whereas Flavone, Isorhamnetin, Naringenin, and Pelargonidin Inhibit only NF-κB Activation along with Their Inhibitory Effect on iNOS Expression and NO Production in Activated Macrophages, Mediators Inflamm. 2007 (2007) 1–10.
[188] H.P. Kim, K.H. Son, H.W. Chang, S.S. Kang, Anti-inflammatory plant flavonoids and cellular action mechanisms, J. Pharmacol. Sci. 96 (2004) 229–245.
[189] C. Dong, R.J. Davis, R.A. Flavell, MAP kinases in the immune response, Annu. Rev. Immunol. 20 (2002) 55–72.
[190] A. Xagorari, C. Roussos, A. Papapetropoulos, Inhibition of LPS-stimulated pathways in macrophages by the flavonoid luteolin, Br. J. Pharmacol. 136 (2002) 1058–1064.
[191] S.-Y. Cho, S.-J. Park, M.-J. Kwon, T.-S. Jeong, S.-H. Bok, W.-Y. Choi, et al., Quercetin suppresses proinflammatory cytokines production through MAP kinases andNF-kappaB pathway in lipopolysaccharide-stimulated macrophage, Mol. Cell. Biochem. 243 (2003) 153–160.
[192] P.J. Barnes, M. Karin, Nuclear factor-kappaB: a pivotal transcription factor in chronic inflammatory diseases, N. Engl. J. Med. 336 (1997) 1066–1071.
[193] E. Park, S. Kum, C. Wang, S.Y. Park, B.S. Kim, G. Schuller-Levis, Anti-inflammatory activity of herbal medicines: inhibition of nitric oxide production and tumor necrosis factor-alpha secretion in an activated macrophage-like cell line, Am. J. Chin. Med. 33 (2005) 415–424.
[194] A. Kotanidou, A. Xagorari, E. Bagli, P. Kitsanta, T. Fotsis, A. Papapetropoulos, et al., Luteolin reduces lipopolysaccharide-induced lethal toxicity and expression of proinflammatory molecules in mice, Am. J. Respir. Crit. Care Med. 165 (2002) 818–823.
[195] V.L. Roger, A.S. Go, D.M. Lloyd-Jones, E.J. Benjamin, J.D. Berry, W.B. Borden, et al., Executive Summary: Heart Disease and Stroke Statistics—2012 Update A Report From the American Heart Association, Circulation. 125 (2012) 188–197.
[196] WHO | Cancer, WHO. (n.d.).
[197] L.M. de Lau, M.M. Breteler, Epidemiology of Parkinson's disease, Lancet Neurol. 5 (2006) 525–535.
[198] D. Hanahan, R.A. Weinberg, The hallmarks of cancer, Cell. 100 (2000) 57–70.
[199] W. Guo, E. Kong, M. Meydani, Dietary Polyphenols, Inflammation, and Cancer, Nutr. Cancer. 61 (2009) 807–810.
[200] C.S. Yang, J.M. Landau, M.T. Huang, H.L. Newmark, Inhibition of carcinogenesis by dietary polyphenolic compounds, Annu. Rev. Nutr. 21 (2001) 381–406.
[201] C.A. González, G. Pera, A. Agudo, H.B. Bueno-de-Mesquita, M. Ceroti, H. Boeing, et al., Fruit and vegetable intake and the risk of stomach and oesophagus adenocarcinoma in the European Prospective Investigation into Cancer and Nutrition (EPIC–EURGAST), Int. J. Cancer. 118 (2006) 2559–2566.
[202] U. Nöthlings, S.P. Murphy, L.R. Wilkens, B.E. Henderson, L.N. Kolonel, Flavonols and Pancreatic Cancer Risk The Multiethnic Cohort Study, Am. J. Epidemiol. 166 (2007) 924–931.

[203] N. Khan, F. Afaq, M. Saleem, N. Ahmad, H. Mukhtar, Targeting multiple signaling pathways by green tea polyphenol (-)-epigallocatechin-3-gallate, Cancer Res. 66 (2006) 2500–2505.
[204] G. Corona, M. Deiana, A. Incani, D. Vauzour, M.A. Dessì, J.P.E. Spencer, Hydroxytyrosol inhibits the proliferation of human colon adenocarcinoma cells through inhibition of ERK1/2 and cyclin D1, Mol. Nutr. Food Res. 53 (2009) 897–903.
[205] R. Fabiani, A. De Bartolomeo, P. Rosignoli, M. Servili, G.F. Montedoro, G. Morozzi, Cancer chemoprevention by hydroxytyrosol isolated from virgin olive oil through G1 cell cycle arrest and apoptosis, Eur. J. Cancer Prev. Off. J. Eur. Cancer Prev. Organ. ECP. 11 (2002) 351–358.
[206] S.C. Forester, A.L. Waterhouse, Gut metabolites of anthocyanins, gallic acid, 3-O-methylgallic acid, and 2,4,6-trihydroxybenzaldehyde, inhibit cell proliferation of Caco-2 cells, J. Agric. Food Chem. 58 (2010) 5320–5327.
[207] S.G. Khan, S.K. Katiyar, R. Agarwal, H. Mukhtar, Enhancement of antioxidant and phase II enzymes by oral feeding of green tea polyphenols in drinking water to SKH-1 hairless mice: possible role in cancer chemoprevention, Cancer Res. 52 (1992) 4050–4052.
[208] S. Ramos, Cancer chemoprevention and chemotherapy: dietary polyphenols and signalling pathways, Mol. Nutr. Food Res. 52 (2008) 507–526.
[209] W. Wang, X. Wang, L. Peng, Q. Deng, Y. Liang, H. Qing, et al., CD24-dependent MAPK pathway activation is required for colorectal cancer cell proliferation, Cancer Sci. 101 (2010) 112–119.
[210] A. García-Lafuente, E. Guillamón, A. Villares, M.A. Rostagno, J.A. Martínez, Flavonoids as anti-inflammatory agents: implications in cancer and cardiovascular disease, Inflamm. Res. 58 (2009) 537–552.
[211] J.S. Sebolt-Leopold, R. Herrera, Targeting the mitogen-activated protein kinase cascade to treat cancer, Nat. Rev. Cancer. 4 (2004) 937–947.
[212] C. Tsatsanis, A. Androulidaki, M. Venihaki, A.N. Margioris, Signalling networks regulating cyclooxygenase-2, Int. J. Biochem. Cell Biol. 38 (2006) 1654–1661.
[213] G. Corona, M. Deiana, A. Incani, D. Vauzour, M.A. Dessì, J.P.E. Spencer, Inhibition of p38/CREB phosphorylation and COX-2 expression by olive oil polyphenols underlies their anti-proliferative effects, Biochem. Biophys. Res. Commun. 362 (2007) 606–611.
[214] S.Y.H. Lee, B. Munerol, S. Pollard, K.A. Youdim, A.S. Pannala, G.G.C. Kuhnle, et al., The reaction of flavanols with nitrous acid protects against N-nitrosamine formation and leads to the formation of nitroso derivatives which inhibit cancer cell growth, Free Radic. Biol. Med. 40 (2006) 323–334.
[215] V.M. Adhami, A. Malik, N. Zaman, S. Sarfaraz, I.A. Siddiqui, D.N. Syed, et al., Combined inhibitory effects of green tea polyphenols and selective cyclooxygenase-2 inhibitors on the growth of human prostate cancer cells both in vitro and in vivo, Clin. Cancer Res. Off. J. Am. Assoc. Cancer Res. 13 (2007) 1611–1619.
[216] S. Banerjee, S. Manna, S. Mukherjee, D. Pal, C.K. Panda, S. Das, Black tea polyphenols restrict benzopyrene-induced mouse lung cancer progression through inhibition of Cox-2 and induction of caspase-3 expression, Asian Pac. J. Cancer Prev. APJCP. 7 (2006) 661–666.
[217] S. Chell, A. Kaidi, A. Kadi, A.C. Williams, C. Paraskeva, Mediators of PGE2 synthesis and signalling downstream of COX-2 represent potential targets for the prevention/treatment of colorectal cancer, Biochim. Biophys. Acta. 1766 (2006) 104–119.
[218] N.P. Seeram, Y. Zhang, M.G. Nair, Inhibition of Proliferation of Human Cancer Cells and Cyclooxygenase Enzymes by Anthocyanidins and Catechins, Nutr. Cancer. 46 (2003) 101–106.
[219] Y. Zhang, S.K. Vareed, M.G. Nair, Human tumor cell growth inhibition by nontoxic

anthocyanidins, the pigments in fruits and vegetables, Life Sci. 76 (2005) 1465–1472.
[220] D. Vauzour, A. Rodriguez-Mateos, G. Corona, M.J. Oruna-Concha, J.P.E. Spencer, Polyphenols and Human Health: Prevention of Disease and Mechanisms of Action, Nutrients. 2 (2010) 1106–1131.
[221] J.W.J. van Heijst, H.W.M. Niessen, K. Hoekman, C.G. Schalkwijk, Advanced glycation end products in human cancer tissues: detection of Nepsilon-(carboxymethyl)lysine and argpyrimidine, Ann. N. Y. Acad. Sci. 1043 (2005) 725–733.
[222] C.-Y. Lo, S. Li, D. Tan, M.-H. Pan, S. Sang, C.-T. Ho, Trapping reactions of reactive carbonyl species with tea polyphenols in simulated physiological conditions, Mol. Nutr. Food Res. 50 (2006) 1118–1128.
[223] T. Kiho, S. Usui, K. Hirano, K. Aizawa, T. Inakuma, Tomato paste fraction inhibiting the formation of advanced glycation end-products, Biosci. Biotechnol. Biochem. 68 (2004) 200–205.
[224] H. Kuniyasu, N. Oue, A. Wakikawa, H. Shigeishi, N. Matsutani, K. Kuraoka, et al., Expression of receptors for advanced glycation end-products (RAGE) is closely associated with the invasive and metastatic activity of gastric cancer, J. Pathol. 196 (2002) 163–170.
[225] M. Takada, Y. Ku, H. Toyama, Y. Suzuki, Y. Kuroda, Suppressive effects of tea polyphenol and conformational changes with receptor for advanced glycation end products (RAGE) expression in human hepatoma cells, Hepatogastroenterology. 49 (2002) 928–931.
[226] J.A. Ambrose, R.S. Barua, The pathophysiology of cigarette smoking and cardiovascular disease: an update, J. Am. Coll. Cardiol. 43 (2004) 1731–1737.
[227] M. Tanasescu, M.F. Leitzmann, E.B. Rimm, W.C. Willett, M.J. Stampfer, F.B. Hu, Exercise type and intensity in relation to coronary heart disease in men, JAMA J. Am. Med. Assoc. 288 (2002) 1994–2000.
[228] F.L. Crowe, A.W. Roddam, T.J. Key, P.N. Appleby, K. Overvad, M.U. Jakobsen, et al., Fruit and vegetable intake and mortality from ischaemic heart disease: results from the European Prospective Investigation into Cancer and Nutrition (EPIC)-Heart study, Eur. Heart J. 32 (2011) 1235–1243.
[229] F.J. He, C.A. Nowson, M. Lucas, G.A. MacGregor, Increased consumption of fruit and vegetables is related to a reduced risk of coronary heart disease: meta-analysis of cohort studies, J. Hum. Hypertens. 21 (2007) 717–728.
[230] P.J. Mink, C.G. Scrafford, L.M. Barraj, L. Harnack, C.-P. Hong, J.A. Nettleton, et al., Flavonoid intake and cardiovascular disease mortality: a prospective study in postmenopausal women, Am. J. Clin. Nutr. 85 (2007) 895–909.
[231] A. Basu, M. Du, M.J. Leyva, K. Sanchez, N.M. Betts, M. Wu, et al., Blueberries decrease cardiovascular risk factors in obese men and women with metabolic syndrome, J. Nutr. 140 (2010) 1582–1587.
[232] D.L. McKay, C.-Y.O. Chen, E. Saltzman, J.B. Blumberg, Hibiscus sabdariffa L. tea (tisane) lowers blood pressure in prehypertensive and mildly hypertensive adults, J. Nutr. 140 (2010) 298–303.
[233] M. Naruszewicz, I. Laniewska, B. Millo, M. Dłużniewski, Combination therapy of statin with flavonoids rich extract from chokeberry fruits enhanced reduction in cardiovascular risk markers in patients after myocardial infraction (MI), Atherosclerosis. 194 (2007) e179–184.
[234] Y.K. Park, J.-S. Kim, M.-H. Kang, Concord grape juice supplementation reduces blood pressure in Korean hypertensive men: double-blind, placebo controlled intervention trial, BioFactors Oxf. Engl. 22 (2004) 145–147.
[235] Y. Zhu, M. Xia, Y. Yang, F. Liu, Z. Li, Y. Hao, et al., Purified anthocyanin supplementation improves endothelial function via NO-cGMP activation in hypercholesterolemic individuals, Clin. Chem. 57 (2011) 1524–1533.

[236] M.M. Dohadwala, M. Holbrook, N.M. Hamburg, S.M. Shenouda, W.B. Chung, M. Titas, et al., Effects of cranberry juice consumption on vascular function in patients with coronary artery disease, Am. J. Clin. Nutr. 93 (2011) 934–940.
[237] A.R. Albers, S. Varghese, O. Vitseva, J.A. Vita, J.E. Freedman, The antiinflammatory effects of purple grape juice consumption in subjects with stable coronary artery disease, Arterioscler. Thromb. Vasc. Biol. 24 (2004) e179–180.
[238] I. Erlund, R. Koli, G. Alfthan, J. Marniemi, P. Puukka, P. Mustonen, et al., Favorable effects of berry consumption on platelet function, blood pressure, and HDL cholesterol, Am. J. Clin. Nutr. 87 (2008) 323–331.
[239] M.M. Appeldoorn, D.P. Venema, T.H.F. Peters, M.E. Koenen, I.C.W. Arts, J.-P. Vincken, et al., Some phenolic compounds increase the nitric oxide level in endothelial cells in vitro, J. Agric. Food Chem. 57 (2009) 7693–7699.
[240] J.F. Leikert, T.R. Räthel, P. Wohlfart, V. Cheynier, A.M. Vollmar, V.M. Dirsch, Red wine polyphenols enhance endothelial nitric oxide synthase expression and subsequent nitric oxide release from endothelial cells, Circulation. 106 (2002) 1614–1617.
[241] M. Lorenz, S. Wessler, E. Follmann, W. Michaelis, T. Düsterhöft, G. Baumann, et al., A constituent of green tea, epigallocatechin-3-gallate, activates endothelial nitric oxide synthase by a phosphatidylinositol-3-OH-kinase-, cAMP-dependent protein kinase-, and Akt-dependent pathway and leads to endothelial-dependent vasorelaxation, J. Biol. Chem. 279 (2004) 6190–6195.
[242] J.-C. Stoclet, T. Chataigneau, M. Ndiaye, M.-H. Oak, J. El Bedoui, M. Chataigneau, et al., Vascular protection by dietary polyphenols, Eur. J. Pharmacol. 500 (2004) 299–313.
[243] T. Wallerath, G. Deckert, T. Ternes, H. Anderson, H. Li, K. Witte, et al., Resveratrol, a polyphenolic phytoalexin present in red wine, enhances expression and activity of endothelial nitric oxide synthase, Circulation. 106 (2002) 1652–1658.
[244] S.-M. Huang, C.-H. Wu, G.-C. Yen, Effects of flavonoids on the expression of the pro-inflammatory response in human monocytes induced by ligation of the receptor for AGEs, Mol. Nutr. Food Res. 50 (2006) 1129–1139.
[245] J.M. Kim, E.K. Lee, D.H. Kim, B.P. Yu, H.Y. Chung, Kaempferol modulates pro-inflammatory NF-kappaB activation by suppressing advanced glycation endproducts-induced NADPH oxidase, Age Dordr. Neth. 32 (2010) 197–208.
[246] I. Wiswedel, D. Hirsch, S. Kropf, M. Gruening, E. Pfister, T. Schewe, et al., Flavanol-rich cocoa drink lowers plasma F(2)-isoprostane concentrations in humans, Free Radic. Biol. Med. 37 (2004) 411–421.
[247] Y. Steffen, C. Gruber, T. Schewe, H. Sies, Mono-O-methylated flavanols and other flavonoids as inhibitors of endothelial NADPH oxidase, Arch. Biochem. Biophys. 469 (2008) 209–219.
[248] K.A. Jellinger, Cell death mechanisms in neurodegeneration, J. Cell. Mol. Med. 5 (2001) 1–17.
[249] J. Lindsay, D. Laurin, R. Verreault, R. Hébert, B. Helliwell, G.B. Hill, et al., Risk factors for Alzheimer's disease: a prospective analysis from the Canadian Study of Health and Aging, Am. J. Epidemiol. 156 (2002) 445–453.
[250] J.M. Orgogozo, J.F. Dartigues, S. Lafont, L. Letenneur, D. Commenges, R. Salamon, et al., Wine consumption and dementia in the elderly: a prospective community study in the Bordeaux area, Rev. Neurol. (Paris). 153 (1997) 185–192.
[251] D. Commenges, V. Scotet, S. Renaud, H. Jacqmin-Gadda, P. Barberger-Gateau, J.F. Dartigues, Intake of flavonoids and risk of dementia, Eur. J. Epidemiol. 16 (2000) 357–363.
[252] J.P.E. Spencer, The impact of fruit flavonoids on memory and cognition, Br. J. Nutr. 104 Suppl 3 (2010) S40–47.
[253] K.A. Youdim, M.Z. Qaiser, D.J. Begley, C.A. Rice-Evans, N.J. Abbott, Flavonoid

permeability across an in situ model of the blood-brain barrier, Free Radic. Biol. Med. 36 (2004) 592–604.
[254] S. Passamonti, U. Vrhovsek, A. Vanzo, F. Mattivi, Fast access of some grape pigments to the brain, J. Agric. Food Chem. 53 (2005) 7029–7034.
[255] K.A. Youdim, J.A. Joseph, A possible emerging role of phytochemicals in improving age-related neurological dysfunctions: a multiplicity of effects, Free Radic. Biol. Med. 30 (2001) 583–594.
[256] O. Inanami, Y. Watanabe, B. Syuto, M. Nakano, M. Tsuji, M. Kuwabara, Oral administration of (-)catechin protects against ischemia-reperfusion-induced neuronal death in the gerbil, Free Radic. Res. 29 (1998) 359–365.
[257] J. Joseph, G. Cole, E. Head, D. Ingram, Nutrition, Brain Aging, and Neurodegeneration, J. Neurosci. 29 (2009) 12795–12801.
[258] S. Bastianetto, W.H. Zheng, R. Quirion, The Ginkgo biloba extract (EGb 761) protects and rescues hippocampal cells against nitric oxide-induced toxicity: involvement of its flavonoid constituents and protein kinase C, J. Neurochem. 74 (2000) 2268–2277.
[259] D. Vauzour, K. Vafeiadou, G. Corona, S.E. Pollard, X. Tzounis, J.P.E. Spencer, Champagne wine polyphenols protect primary cortical neurons against peroxynitrite-induced injury, J. Agric. Food Chem. 55 (2007) 2854–2860.
[260] J.P.E. Spencer, Food for thought: the role of dietary flavonoids in enhancing human memory, learning and neuro-cognitive performance, Proc. Nutr. Soc. 67 (2008) 238–252.
[261] D. Vauzour, K. Vafeiadou, C. Rice-Evans, R.J. Williams, J.P.E. Spencer, Activation of pro-survival Akt and ERK1/2 signalling pathways underlie the anti-apoptotic effects of flavanones in cortical neurons, J. Neurochem. 103 (2007) 1355–1367.
[262] J.P.E. Spencer, The interactions of flavonoids within neuronal signalling pathways, Genes Nutr. 2 (2007) 257–273.
[263] Q. Shan, J. Lu, Y. Zheng, J. Li, Z. Zhou, B. Hu, et al., Purple sweet potato color ameliorates cognition deficits and attenuates oxidative damage and inflammation in aging mouse brain induced by d-galactose, J. Biomed. Biotechnol. 2009 (2009) 564737.
[264] N.R. Bhat, D.L. Feinstein, Q. Shen, A.N. Bhat, p38 MAPK-mediated transcriptional activation of inducible nitric-oxide synthase in glial cells. Roles of nuclear factors, nuclear factor kappa B, cAMP response element-binding protein, CCAAT/enhancer-binding protein-beta, and activating transcription factor-2, J. Biol. Chem. 277 (2002) 29584–29592.
[265] S. Lee, K.-W. Lee, Protective effect of (-)-epigallocatechin gallate against advanced glycation endproducts-induced injury in neuronal cells, Biol. Pharm. Bull. 30 (2007) 1369–1373.
[266] E. Verzelloni, C. Pellacani, D. Tagliazucchi, S. Tagliaferri, L. Calani, L.G. Costa, et al., Antiglycative and neuroprotective activity of colon-derived polyphenol catabolites, Mol. Nutr. Food Res. 55 (2011) S35–S43.
[267] I. Ignat, I. Volf, V.I. Popa, A critical review of methods for characterisation of polyphenolic compounds in fruits and vegetables, Food Chem. 126 (2011) 1821–1835.
[268] K. Robards, Strategies for the determination of bioactive phenols in plants, fruit and vegetables, J. Chromatogr. A. 1000 (2003) 657–691.
[269] M. Naczk, F. Shahidi, Extraction and analysis of phenolics in food, J. Chromatogr. A. 1054 (2004) 95–111.
[270] J. Valls, S. Millán, M.P. Martí, E. Borràs, L. Arola, Advanced separation methods of food anthocyanins, isoflavones and flavanols, J. Chromatogr. A. 1216 (2009) 7143–7172.
[271] M.-J. Motilva, A. Serra, A. Macià, Analysis of food polyphenols by ultra high-performance liquid chromatography coupled to mass spectrometry: An overview, J. Chromatogr. A. 1292 (2013) 66–82.
[272] L. Nováková, Challenges in the development of bioanalytical liquid chromatography–

mass spectrometry method with emphasis on fast analysis, J. Chromatogr. A. 1292 (2013) 25–37.
[273] D. Guillarme, C. Casetta, C. Bicchi, J.-L. Veuthey, High throughput qualitative analysis of polyphenols in tea samples by ultra-high pressure liquid chromatography coupled to UV and mass spectrometry detectors, J. Chromatogr. A. 1217 (2010) 6882–6890.
[274] L.-Z. Lin, J. Sun, P. Chen, J. Harnly, UHPLC-PDA-ESI/HRMS/MS ^{n} Analysis of Anthocyanins, Flavonol Glycosides, and Hydroxycinnamic Acid Derivatives in Red Mustard Greens (Brassica juncea Coss Variety), J. Agric. Food Chem. 59 (2011) 12059–12072.
[275] L. Nováková, Z. Spáčil, M. Seifrtová, L. Opletal, P. Solich, Rapid qualitative and quantitative ultra high performance liquid chromatography method for simultaneous analysis of twenty nine common phenolic compounds of various structures, Talanta. 80 (2010) 1970–1979.
[276] S.N. Jimenez-Garcia, R.G. Guevara-Gonzalez, R. Miranda-Lopez, A.A. Feregrino-Perez, I. Torres-Pacheco, M.A. Vazquez-Cruz, Functional properties and quality characteristics of bioactive compounds in berries: Biochemistry, biotechnology, and genomics, Food Res. Int. (n.d.).
[277] R.J. Robbins, Phenolic Acids in Foods: An Overview of Analytical Methodology, J. Agric. Food Chem. 51 (2003) 2866–2887.
[278] H.M. Merken, G.R. Beecher, Measurement of Food Flavonoids by High-Performance Liquid Chromatography: A Review, J. Agric. Food Chem. 48 (2000) 577–599.
[279] K. Robards, P.D. Prenzler, G. Tucker, P. Swatsitang, W. Glover, Phenolic compounds and their role in oxidative processes in fruits, Food Chem. 66 (1999) 401–436.
[280] E. de Hoffmann, Mass spectrometry: principles and applications, 3rd ed, J. Wiley, Chichester, West Sussex, England□; Hoboken, NJ, 2007.
[281] D. Steinmann, M. Ganzera, Recent advances on HPLC/MS in medicinal plant analysis, J. Pharm. Biomed. Anal. 55 (2011) 744–757.
[282] S. Banerjee, S. Mazumdar, Electrospray Ionization Mass Spectrometry: A Technique to Access the Information beyond the Molecular Weight of the Analyte, Int. J. Anal. Chem. 2012 (2012) 1–40.
[283] LTQ Orbitrap Operations Training Course, (n.d.).
[284] H. Wu, J. Guo, S. Chen, X. Liu, Y. Zhou, X. Zhang, et al., Recent developments in qualitative and quantitative analysis of phytochemical constituents and their metabolites using liquid chromatography–mass spectrometry, J. Pharm. Biomed. Anal. 72 (2013) 267–291.
[285] J. Bernal, J.A. Mendiola, E. Ibáñez, A. Cifuentes, Advanced analysis of nutraceuticals, J. Pharm. Biomed. Anal. 55 (2011) 758–774.
[286] R. Lichtenthäler, R.B. Rodrigues, J.G.S. Maia, M. Papagiannopoulos, H. Fabricius, F. Marx, Total oxidant scavenging capacities of *Euterpe oleracea* Mart. (Açaí) fruits, Int. J. Food Sci. Nutr. 56 (2005) 53–64.
[287] J.-B. Peng, H.-M. Jia, Y.-T. Liu, H.-W. Zhang, S. Dong, Z.-M. Zou, Qualitative and quantitative characterization of chemical constituents in Xin-Ke-Shu preparations by liquid chromatography coupled with a LTQ Orbitrap mass spectrometer, J. Pharm. Biomed. Anal. 55 (2011) 984–995.
[288] A. Božović, V. Kulasingam, Quantitative mass spectrometry-based assay development and validation: From small molecules to proteins, Clin. Biochem. 46 (2013) 444–455.
[289] Handbook of food analysis instruments, CRC Press, Boca Raton, FL, 2009.
[290] P. Kebarle, U.H. Verkerk, Electrospray: From ions in solution to ions in the gas phase, what we know now, Mass Spectrom. Rev. 28 (2009) 898–917.
[291] W. Zhu, Y. Yuan, P. Zhou, L. Zeng, H. Wang, L. Tang, et al., The Expanding Role of Electrospray Ionization Mass Spectrometry for Probing Reactive Intermediates in Solution,

Molecules. 17 (2012) 11507–11537.
[292] S.J. Gaskell, Electrospray: Principles and Practice, J. Mass Spectrom. 32 (1997) 677–688.
[293] Y.-Q. Xia, J. Lau, T. Olah, M. Jemal, Targeted quantitative bioanalysis in plasma using liquid chromatography/high-resolution accurate mass spectrometry: an evaluation of global selectivity as a function of mass resolving power and extraction window, with comparison of centroid and profile mo, Rapid Commun. Mass Spectrom. 25 (2011) 2863–2878.
[294] S. Forcisi, F. Moritz, B. Kanawati, D. Tziotis, R. Lehmann, P. Schmitt-Kopplin, Liquid chromatography–mass spectrometry in metabolomics research: Mass analyzers in ultra high pressure liquid chromatography coupling, J. Chromatogr. A. 1292 (2013) 51–65.
[295] M. Holčapek, R. Jirásko, M. Lísa, Recent developments in liquid chromatography–mass spectrometry and related techniques, J. Chromatogr. A. 1259 (2012) 3–15.
[296] O. Núñez, H. Gallart-Ayala, C.P.B. Martins, P. Lucci, R. Busquets, State-of-the-art in fast liquid chromatography–mass spectrometry for bio-analytical applications, J. Chromatogr. B. 927 (2013) 3–21.
[297] M. Rodriguez-Aller, R. Gurny, J.-L. Veuthey, D. Guillarme, Coupling ultra high-pressure liquid chromatography with mass spectrometry: Constraints and possible applications, J. Chromatogr. A. 1292 (2013) 2–18.
[298] O.D. Sparkman, Mass spectrometry desk reference, 1st ed, Global View Pub, Pittsburgh, Pa, 2000.
[299] Q. Hu, R.J. Noll, H. Li, A. Makarov, M. Hardman, R. Graham Cooks, The Orbitrap: a new mass spectrometer, J. Mass Spectrom. 40 (2005) 430–443.
[300] R.H. Perry, R.G. Cooks, R.J. Noll, Orbitrap mass spectrometry: Instrumentation, ion motion and applications, Mass Spectrom. Rev. 27 (2008) 661–699.
[301] M. Scigelova, M. Hornshaw, A. Giannakopulos, A. Makarov, Fourier Transform Mass Spectrometry, Mol. Cell. Proteomics. 10 (2011) M111.009431–M111.009431.
[302] M. Hardman, A.A. Makarov, Interfacing the Orbitrap Mass Analyzer to an Electrospray Ion Source, Anal. Chem. 75 (2003) 1699–1705.
[303] A. Makarov, M. Scigelova, Coupling liquid chromatography to Orbitrap mass spectrometry, J. Chromatogr. A. 1217 (2010) 3938–3945.
[304] D.W. Koppenaal, C.J. Barinaga, M.B. Denton, R.P. Sperline, G.M. Hieftje, G.D. Schilling, et al., MS Detectors, Anal. Chem. 77 (2005) 418 A–427 A.
[305] C. Dass, Fundamentals of contemporary mass spectrometry, Wiley-Interscience, Hoboken, N.J, 2007.
[306] Thermo electron corporation, LTQ XL Hardware manual, (2006).
[307] I.J. Amster, Fourier Transform Mass Spectrometry, J. Mass Spectrom. 31 (1996) 1325–1337.
[308] K.K. Murray, R.K. Boyd, M.N. Eberlin, G.J. Langley, L. Li, Y. Naito, Definitions of terms relating to mass spectrometry (IUPAC Recommendations 2013), Pure Appl. Chem. 85 (2013) 1515–1609.
[309] B. Abad-García, L.A. Berrueta, S. Garmón-Lobato, B. Gallo, F. Vicente, A general analytical strategy for the characterization of phenolic compounds in fruit juices by high-performance liquid chromatography with diode array detection coupled to electrospray ionization and triple quadrupole mass spectrometry, J. Chromatogr. A. 1216 (2009) 5398–5415.
[310] E. Werner, J.-F. Heilier, C. Ducruix, E. Ezan, C. Junot, J.-C. Tabet, Mass spectrometry for the identification of the discriminating signals from metabolomics: Current status and future trends, J. Chromatogr. B. 871 (2008) 143–163.
[311] F. Cuyckens, M. Claeys, Optimization of a liquid chromatography method based on

simultaneous electrospray ionization mass spectrometric and ultraviolet photodiode array detection for analysis of flavonoid glycosides, Rapid Commun. Mass Spectrom. 16 (2002) 2341–2348.
[312] F. Cuyckens, M. Claeys, Mass spectrometry in the structural analysis of flavonoids, J. Mass Spectrom. 39 (2004) 1–15.
[313] M. Suárez, A. Macià, M.-P. Romero, M.-J. Motilva, Improved liquid chromatography tandem mass spectrometry method for the determination of phenolic compounds in virgin olive oil, J. Chromatogr. A. 1214 (2008) 90–99.
[314] K.K. Murray, Glossary of terms for separations coupled to mass spectrometry, J. Chromatogr. A. 1217 (2010) 3922–3928.
[315] K.P. Bateman, M. Kellmann, H. Muenster, R. Papp, L. Taylor, Quantitative-qualitative data acquisition using a benchtop orbitrap mass spectrometer, J. Am. Soc. Mass Spectrom. 20 (2009) 1441–1450.
[316] G.C. Kite, E.R. Rowe, G.P. Lewis, N.C. Veitch, Acylated flavonol tri- and tetraglycosides in the flavonoid metabolome of Cladrastis kentukea (Leguminosae), Phytochemistry. 72 (2011) 372–384.
[317] X. Qiu, J. Zhang, Z. Huang, D. Zhu, W. Xu, Profiling of phenolic constituents in Polygonum multiflorum Thunb. by combination of ultra-high-pressure liquid chromatography with linear ion trap-Orbitrap mass spectrometry, J. Chromatogr. A. 1292 (2013) 121–131.
[318] J.-B. Peng, H.-M. Jia, Y.-T. Liu, H.-W. Zhang, S. Dong, Z.-M. Zou, Qualitative and quantitative characterization of chemical constituents in Xin-Ke-Shu preparations by liquid chromatography coupled with a LTQ Orbitrap mass spectrometer, J. Pharm. Biomed. Anal. 55 (2011) 984–995.
[319] X. Li, Y. Zhang, X. Zeng, L. Yang, Y. Deng, Chemical profiling of bioactive constituents in Sarcandra glabra and its preparations using ultra-high-pressure liquid chromatography coupled with LTQ Orbitrap mass spectrometry: Constituents in Sarcandra glabra by UPLC LTQ Orbitrap, Rapid Commun. Mass Spectrom. 25 (2011) 2439–2447.
[320] G. Glauser, N. Veyrat, B. Rochat, J.-L. Wolfender, T.C.J. Turlings, Ultra-high pressure liquid chromatography–mass spectrometry for plant metabolomics: A systematic comparison of high-resolution quadrupole-time-of-flight and single stage Orbitrap mass spectrometers, J. Chromatogr. A. 1292 (2013) 151–159.
[321] H. Trufelli, P. Palma, G. Famiglini, A. Cappiello, An overview of matrix effects in liquid chromatography-mass spectrometry, Mass Spectrom. Rev. 30 (2011) 491–509.
[322] B.K. Matuszewski, M.L. Constanzer, C.M. Chavez-Eng, Strategies for the Assessment of Matrix Effect in Quantitative Bioanalytical Methods Based on HPLC−MS/MS, Anal. Chem. 75 (2003) 3019–3030.
[323] E.A. Prokudina, L. Havlíček, N. Al-Maharik, O. Lapčík, M. Strnad, J. Gruz, Rapid UPLC–ESI–MS/MS method for the analysis of isoflavonoids and other phenylpropanoids, J. Food Compos. Anal. 26 (2012) 36–42.
[324] J. Gruz, O. Novák, M. Strnad, Rapid analysis of phenolic acids in beverages by UPLC–MS/MS, Food Chem. 111 (2008) 789–794.
[325] J. Kang, L.A. Hick, W.E. Price, Using calibration approaches to compensate for remaining matrix effects in quantitative liquid chromatography/electrospray ionization multistage mass spectrometric analysis of phytoestrogens in aqueous environmental samples, Rapid Commun. Mass Spectrom. 21 (2007) 4065–4072.
[326] M. Suárez, A. Macià, M.-P. Romero, M.-J. Motilva, Improved liquid chromatography tandem mass spectrometry method for the determination of phenolic compounds in virgin olive oil, J. Chromatogr. A. 1214 (2008) 90–99.
[327] N. Ortega, A. Macià, M.-P. Romero, E. Trullols, J.-R. Morello, N. Anglès, et al., Rapid Determination of Phenolic Compounds and Alkaloids of Carob Flour by Improved

Liquid Chromatography Tandem Mass Spectrometry, J. Agric. Food Chem. 57 (2009) 7239–7244.
[328] M. Gómez-Romero, G. Zurek, B. Schneider, C. Baessmann, A. Segura-Carretero, A. Fernández-Gutiérrez, Automated identification of phenolics in plant-derived foods by using library search approach, Food Chem. 124 (2011) 379–386.
[329] Y.L. Ma, Q.M. Li, H. Van den Heuvel, M. Claeys, Characterization of flavone and flavonol aglycones by collision-induced dissociation tandem mass spectrometry, Rapid Commun. Mass Spectrom. 11 (1997) 1357–1364.
[330] B. Domon, C.E. Costello, A systematic nomenclature for carbohydrate fragmentations in FAB-MS/MS spectra of glycoconjugates, Glycoconj. J. 5 (1988) 397–409.
[331] V. Vukics, A. Guttman, Structural characterization of flavonoid glycosides by multi-stage mass spectrometry, Mass Spectrom. Rev. (2008) n/a–n/a.
[332] N. Fabre, I. Rustan, E. de Hoffmann, J. Quetin-Leclercq, Determination of flavone, flavonol, and flavanone aglycones by negative ion liquid chromatography electrospray ion trap mass spectrometry, J. Am. Soc. Mass Spectrom. 12 (2001) 707–715.
[333] F. Cuyckens, M. Claeys, Mass spectrometry in the structural analysis of flavonoids, J. Mass Spectrom. 39 (2004) 1–15.
[334] N. Fabre, I. Rustan, E. de Hoffmann, J. Quetin-Leclercq, Determination of flavone, flavonol, and flavanone aglycones by negative ion liquid chromatography electrospray ion trap mass spectrometry, J. Am. Soc. Mass Spectrom. 12 (2001) 707–715.
[335] E. de Rijke, P. Out, W.M.A. Niessen, F. Ariese, C. Gooijer, U.A.T. Brinkman, Analytical separation and detection methods for flavonoids, J. Chromatogr. A. 1112 (2006) 31–63.
[336] U. Justesen, Collision-induced fragmentation of deprotonated methoxylated flavonoids, obtained by electrospray ionization mass spectrometry, J. Mass Spectrom. JMS. 36 (2001) 169–178.
[337] R.E. March, E.G. Lewars, C.J. Stadey, X.-S. Miao, X. Zhao, C.D. Metcalfe, A comparison of flavonoid glycosides by electrospray tandem mass spectrometry, Int. J. Mass Spectrom. 248 (2006) 61–85.
[338] F. Ferreres, R. Llorach, A. Gil-Izquierdo, Characterization of the interglycosidic linkage in di-, tri-, tetra- and pentaglycosylated flavonoids and differentiation of positional isomers by liquid chromatography/electrospray ionization tandem mass spectrometry, J. Mass Spectrom. 39 (2004) 312–321.
[339] F. Ferreres, B.M. Silva, P.B. Andrade, R.M. Seabra, M.A. Ferreira, Approach to the study of C-glycosyl flavones by ion trap HPLC-PAD-ESI/MS/MS: application to seeds of quince (Cydonia oblonga), Phytochem. Anal. PCA. 14 (2003) 352–359.
[340] F. Ferreres, R.F. Gonçalves, A. Gil-Izquierdo, P. Valentão, A.M.S. Silva, J.B. Silva, et al., Further Knowledge on the Phenolic Profile of *Colocasia esculenta* (L.) Shott, J. Agric. Food Chem. 60 (2012) 7005–7015.
[341] F. Ferreres, A. Gil-Izquierdo, P.B. Andrade, P. Valentão, F.A. Tomás-Barberán, Characterization of C-glycosyl flavones O-glycosylated by liquid chromatography–tandem mass spectrometry, J. Chromatogr. A. 1161 (2007) 214–223.
[342] F. Ferreres, P.B. Andrade, P. Valentão, A. Gil-Izquierdo, Further knowledge on barley (Hordeum vulgare L.) leaves O-glycosyl-C-glycosyl flavones by liquid chromatography-UV diode-array detection-electrospray ionisation mass spectrometry, J. Chromatogr. A. 1182 (2008) 56–64.
[343] J.S. Barnes, K.A. Schug, Structural characterization of cyanidin-3,5-diglucoside and pelargonidin-3,5-diglucoside anthocyanins: Multi-dimensional fragmentation pathways using high performance liquid chromatography-electrospray ionization-ion trap-time of flight mass spectrometry, Int. J. Mass Spectrom. 308 (2011) 71–80.

[344] M.C. Oliveira, P. Esperança, M.A. Almoster Ferreira, Characterisation of anthocyanidins by electrospray ionisation and collision-induced dissociation tandem mass spectrometry, Rapid Commun. Mass Spectrom. 15 (2001) 1525–1532.
[345] A. Piovan, R. Filippini, D. Favretto, Characterization of the anthocyanins of Catharanthus roseus (L.) G. Don in vivo and in vitro by electrospray ionization ion trap mass spectrometry, Rapid Commun. Mass Spectrom. 12 (1998) 361–367.
[346] X. Wu, R.L. Prior, Systematic Identification and Characterization of Anthocyanins by HPLC-ESI-MS/MS in Common Foods in the United States: Fruits and Berries, J. Agric. Food Chem. 53 (2005) 2589–2599.
[347] M.M. Giusti, L.E. Rodríguez-Saona, D. Griffin, R.E. Wrolstad, Electrospray and tandem mass spectroscopy as tools for anthocyanin characterization, J. Agric. Food Chem. 47 (1999) 4657–4664.
[348] A. Vallverdú-Queralt, O. Jáuregui, A. Medina-Remón, C. Andrés-Lacueva, R.M. Lamuela-Raventós, Improved characterization of tomato polyphenols using liquid chromatography/electrospray ionization linear ion trap quadrupole Orbitrap mass spectrometry and liquid chromatography/electrospray ionization tandem mass spectrometry, Rapid Commun. Mass Spectrom. 24 (2010) 2986–2992.
[349] M. Heinrich, T. Dhanji, I. Casselman, Açai (Euterpe oleracea Mart.)—A phytochemical and pharmacological assessment of the species' health claims, Phytochem. Lett. 4 (2011) 10–21.
[350] D.R. Pompeu, E.M. Silva, H. Rogez, Optimisation of the solvent extraction of phenolic antioxidants from fruits of *Euterpe oleracea* using Response Surface Methodology, Bioresour. Technol. 100 (2009) 6076–6082.
[351] H. Rogez, Açai: preparo, composição e Melhoramento da Conservação, EDUFPA, Belém, 2000.
[352] M. Heinrich, T. Dhanji, I. Casselman, Açai (*Euterpe oleracea* Mart.)—A phytochemical and pharmacological assessment of the species' health claims, Phytochem. Lett. 4 (2011) 10–21.
[353] A. Gordon, A.P.G. Cruz, L.M.C. Cabral, S.C. de Freitas, C.M.A.D. Taxi, C.M. Donangelo, et al., Chemical characterization and evaluation of antioxidant properties of Açaí fruits (*Euterpe oleraceae* Mart.) during ripening, Food Chem. 133 (2012) 256–263.
[354] R.B. Rodrigues, R. Lichtenthäler, B.F. Zimmermann, M. Papagiannopoulos, H. Fabricius, F. Marx, et al., Total oxidant scavenging capacity of Euterpe oleracea Mart. (açaí) seeds and identification of their polyphenolic compounds, J. Agric. Food Chem. 54 (2006) 4162–4167.
[355] A.A.D. Meirelles, H. Rogez, Tendências do mercado do açaí, Rev. Amaz. 17 (n.d.) 73–75.
[356] R.E. Smith, J. Eaker, K. Tran, C. Smith, D.M. Monroe, E.M.S. Menezes, et al., Proposed Benchmark Methods for Analyzing Açaí (*Euterpe oleraceae* Mart.), Nat. Prod. J. 2 (2012) 76–85.
[357] H. Rogez, D.R. Pompeu, S.N.T. Akwie, Y. Larondelle, Sigmoidal kinetics of anthocyanin accumulation during fruit ripening: A comparison between açai fruits (*Euterpe oleracea*) and other anthocyanin-rich fruits, J. Food Compos. Anal. 24 (2011) 796–800.
[358] V. Vera de Rosso, S. Hillebrand, E. Cuevas Montilla, F.O. Bobbio, P. Winterhalter, A.Z. Mercadante, Determination of anthocyanins from acerola (Malpighia emarginata DC.) and açai (Euterpe oleracea Mart.) by HPLC–PDA–MS/MS, J. Food Compos. Anal. 21 (2008) 291–299.
[359] L.A. Pacheco-Palencia, C.E. Duncan, S.T. Talcott, Phytochemical composition and thermal stability of two commercial açai species, *Euterpe oleracea* and *Euterpe precatoria*, Food Chem. 115 (2009) 1199–1205.

[360] A.G. Schauss, X. Wu, R.L. Prior, B. Ou, D. Huang, J. Owens, et al., Antioxidant Capacity and Other Bioactivities of the Freeze-Dried Amazonian Palm Berry, *Euterpe oleraceae* Mart. (Acai), J. Agric. Food Chem. 54 (2006) 8604–8610.
[361] J. Kang, Z. Li, T. Wu, G.S. Jensen, A.G. Schauss, X. Wu, Anti-oxidant capacities of flavonoid compounds isolated from acai pulp (*Euterpe oleracea* Mart.), Food Chem. 122 (2010) 610–617.
[362] I.C.W. Arts, P.C.H. Hollman, Polyphenols and disease risk in epidemiologic studies, Am. J. Clin. Nutr. 81 (2005) 317S–325S.
[363] P.J. Mink, C.G. Scrafford, L.M. Barraj, L. Harnack, C.-P. Hong, J.A. Nettleton, et al., Flavonoid intake and cardiovascular disease mortality: a prospective study in postmenopausal women, Am. J. Clin. Nutr. 85 (2007) 895–909.
[364] C.D. Kay, L. Hooper, P.A. Kroon, E.B. Rimm, A. Cassidy, Relative impact of flavonoid composition, dose and structure on vascular function: a systematic review of randomised controlled trials of flavonoid-rich food products, Mol. Nutr. Food Res. 56 (2012) 1605–1616.
[365] A. Cassidy, K.J. Mukamal, L. Liu, M. Franz, A.H. Eliassen, E.B. Rimm, High Anthocyanin Intake Is Associated With a Reduced Risk of Myocardial Infarction in Young and Middle-Aged Women, Circulation. 127 (2013) 188–196.
[366] P. Lagiou, E. Samoli, A. Lagiou, A. Tzonou, A. Kalandidi, J. Peterson, et al., Intake of specific flavonoid classes and coronary heart disease--a case-control study in Greece, Eur. J. Clin. Nutr. 58 (2004) 1643–1648.
[367] Bastos C. T. R. M., Souza J. N. S., Larondelle Y., Rogez H., Excretion of açai (Euterpe oleracea) anthocyanins in human urine. In ICPH2007 – 3rd International Conference on Polyphenols and Health, in: Kyoto, Japan., 2007.
[368] S.U. Mertens-Talcott, J. Rios, P. Jilma-Stohlawetz, L.A. Pacheco-Palencia, B. Meibohm, S.T. Talcott, et al., Pharmacokinetics of anthocyanins and antioxidant effects after the consumption of anthocyanin-rich acai juice and pulp (Euterpe oleracea Mart.) in human healthy volunteers, J. Agric. Food Chem. 56 (2008) 7796–7802.
[369] G.D. Noratto, G. Angel-Morales, S.T. Talcott, S.U. Mertens-Talcott, Polyphenolics from açaí (Euterpe oleracea Mart.) and red muscadine grape (Vitis rotundifolia) protect human umbilical vascular Endothelial cells (HUVEC) from glucose- and lipopolysaccharide (LPS)-induced inflammation and target microRNA-126, J. Agric. Food Chem. 59 (2011) 7999–8012.
[370] S. Hogan, H. Chung, L. Zhang, J. Li, Y. Lee, Y. Dai, et al., Antiproliferative and antioxidant properties of anthocyanin-rich extract from açai, Food Chem. 118 (2010) 208–214.
[371] S. Gallori, A.R. Bilia, M.C. Bergonzi, W.L.R. Barbosa, F.F. Vincieri, Polyphenolic Constituents of Fruit Pulp of *Euterpe oleracea* Mart. (Açai palm), Chromatographia. 59 (2004) 739–743.
[372] L. Pachecopalencia, P. Hawken, S. Talcott, Juice matrix composition and ascorbic acid fortification effects on the phytochemical, antioxidant and pigment stability of açai (Euterpe oleracea Mart.), Food Chem. 105 (2007) 28–35.
[373] V. Mulabagal, A.I. Calderón, Liquid chromatography/mass spectrometry based fingerprinting analysis and mass profiling of *Euterpe oleracea* (açaí) dietary supplement raw materials, Food Chem. 134 (2012) 1156–1164.
[374] A.L.S. Dias, E. Rozet, G. Chataigné, A.C. Oliveira, C.A.S. Rabelo, P. Hubert, et al., A rapid validated UHPLC–PDA method for anthocyanins quantification from *Euterpe oleracea* fruits, J. Chromatogr. B. 907 (2012) 108–116.
[375] V. Mulabagal, W.J. Keller, A.I. Calderón, Quantitative analysis of anthocyanins in *Euterpe oleracea* (açaí) dietary supplement raw materials and capsules by Q-TOF liquid

chromatography/mass spectrometry, Pharm. Biol. 50 (2012) 1289–1296.
[376] M.N. Clifford, Anthocyanins – nature, occurrence and dietary burden, J. Sci. Food Agric. 80 (2000) 1063–1072.
[377] A. Castañeda-Ovando, M. de L. Pacheco-Hernández, M.E. Páez-Hernández, J.A. Rodríguez, C.A. Galán-Vidal, Chemical studies of anthocyanins: A review, Food Chem. 113 (2009) 859–871.
[378] J.F. Ayala-Zavala, V. Vega-Vega, C. Rosas-Domínguez, H. Palafox-Carlos, J.A. Villa-Rodriguez, M.W. Siddiqui, et al., Agro-industrial potential of exotic fruit byproducts as a source of food additives, Food Res. Int. 44 (2011) 1866–1874.
[379] A. Szajdek, E.J. Borowska, Bioactive Compounds and Health-Promoting Properties of Berry Fruits: A Review, Plant Foods Hum. Nutr. 63 (2008) 147–156.
[380] M. Iaderoza, V.L.S. Baldini, I.D.S. Draetta, M.L.A. Bovi, Anthocyanins from fruits of açai (Euterpe oleracea Mart.) and jucara (Euterpe edulis Mart.), Trop Sci. 32 (1992) 41–46.
[381] A.G. Schauss, X. Wu, R.L. Prior, B. Ou, D. Patel, D. Huang, et al., Phytochemical and Nutrient Composition of the Freeze-Dried Amazonian Palm Berry, *Euterpe oleraceae* Mart. (Acai), J. Agric. Food Chem. 54 (2006) 8598–8603.
[382] A.G. Schauss, X. Wu, R.L. Prior, B. Ou, D. Huang, J. Owens, et al., Antioxidant Capacity and Other Bioactivities of the Freeze-Dried Amazonian Palm Berry, Euterpe oleraceae Mart. (Acai), J. Agric. Food Chem. 54 (2006) 8604–8610.
[383] P. Hubert, J.-J. Nguyen-Huu, B. Boulanger, E. Chapuzet, P. Chiap, N. Cohen, et al., Harmonization of strategies for the validation of quantitative analytical procedures: A SFSTP proposal—part I, J. Pharm. Biomed. Anal. 36 (2004) 579–586.
[384] A.C.M.S. Gouvêa, M.C.P. de Araujo, D.F. Schulz, S. Pacheco, R.L. de O. Godoy, L.M.C. Cabral, Anthocyanins standards (cyanidin-3-O-glucoside and cyanidin-3-O-rutinoside) isolation from freeze-dried açaí (Euterpe oleraceae Mart.) by HPLC, Food Sci. Technol. Camp. 32 (2012) 43–46.
[385] B. Avula, Y. Wang, T. Smillie, I. Khan, Extraction and Analysis of Anthocyanins from Acai (Euterpe oleracea Mart.) Berries and Dietary Supplements using UPLC and HPLC Methods, Planta Med. 76 (2010).
[386] D. Guillarme, J. Ruta, S. Rudaz, J.-L. Veuthey, New trends in fast and high-resolution liquid chromatography: a critical comparison of existing approaches, Anal. Bioanal. Chem. 397 (2010) 1069–1082.
[387] M.-P. Martí, A. Pantaleón, A. Rozek, A. Soler, J. Valls, A. Macià, et al., Rapid analysis of procyanidins and anthocyanins in plasma by microelution SPE and ultra-HPLC, J. Sep. Sci. 33 (2010) 2841–2853.
[388] Y. Nakamura, H. Matsumoto, M. Morifuji, H. Iida, Y. Takeuchi, Development and Validation of a Liquid Chromatography Tandem Mass Spectrometry Method for Simultaneous Determination of Four Anthocyanins in Human Plasma after Black Currant Anthocyanins Ingestion, J. Agric. Food Chem. 58 (2010) 1174–1179.
[389] A. Serra, A. Macià, M.-P. Romero, C. Piñol, M.-J. Motilva, Rapid methods to determine procyanidins, anthocyanins, theobromine and caffeine in rat tissues by liquid chromatography-tandem mass spectrometry, J. Chromatogr. B. 879 (2011) 1519–1528.
[390] K. Nagy, K. Redeuil, R. Bertholet, H. Steiling, M. Kussmann, Quantification of Anthocyanins and Flavonols in Milk-Based Food Products by Ultra Performance Liquid Chromatography−Tandem Mass Spectrometry, Anal. Chem. 81 (2009) 6347–6356.
[391] S. Muñoz, M. Mestres, O. Busto, J. Guasch, Determination of some flavan-3-ols and anthocyanins in red grape seed and skin extracts by HPLC-DAD: Validation study and response comparison of different standards, Anal. Chim. Acta. 628 (2008) 104–110.
[392] B.K. Matuszewski, M.L. Constanzer, C.M. Chavez-Eng, Strategies for the Assessment of Matrix Effect in Quantitative Bioanalytical Methods Based on HPLC−MS/MS,

Anal. Chem. 75 (2003) 3019–3030.
[393] A. Bouabidi, E. Rozet, M. Fillet, E. Ziemons, E. Chapuzet, B. Mertens, et al., Critical analysis of several analytical method validation strategies in the framework of the fit for purpose concept, J. Chromatogr. A. 1217 (2010) 3180–3192.
[394] B. Boulanger, E. Rozet, F. Moonen, S. Rudaz, P. Hubert, A risk-based analysis of the AAPS conference report on quantitative bioanalytical methods validation and implementation, J. Chromatogr. B. 877 (2009) 2235–2243.
[395] E. Rozet, R.D. Marini, E. Ziemons, B. Boulanger, P. Hubert, Advances in validation, risk and uncertainty assessment of bioanalytical methods, J. Pharm. Biomed. Anal. 55 (2011) 848–858.
[396] Norme Française NF V 03-110, mai 2010, Association Française de Normalisation (AFNOR), Analyse des produits agricoles et alimentaires_Protocole de caractérisation en vue de la validation d'une méthode d'analyse quantitative par construction du profil d'exactitude, Saint-Denis, France., n.d.
[397] L.A. Pacheco-palencia, P. Hawken, S.T. Talcott, Juice matrix composition and ascorbic acid fortification effects on the phytochemical, antioxidant and pigment stability of açai (Euterpe oleracea Mart.), Food Chem. 105 (2007) 28–35.
[398] S. Hogan, H. Chung, L. Zhang, J. Li, Y. Lee, Y. Dai, et al., Antiproliferative and antioxidant properties of anthocyanin-rich extract from açai, Food Chem. 118 (2010) 208–214.
[399] L. Nováková, Z. Spáčil, M. Seifrtová, L. Opletal, P. Solich, Rapid qualitative and quantitative ultra high performance liquid chromatography method for simultaneous analysis of twenty nine common phenolic compounds of various structures, Talanta. 80 (2010) 1970–1979.
[400] X. Wu, R.L. Prior, Systematic Identification and Characterization of Anthocyanins by HPLC-ESI-MS/MS in Common Foods in the United States: Fruits and Berries, J. Agric. Food Chem. 53 (2005) 2589–2599.
[401] F.O. Bobbio, J.I. Druzian, P.A. AbrãO, P.A. Bobbio, S. Fadelli, Identificação e quantificação das antocianinas do fruto do açaizeiro (Euterpe oleracea) Mart, Ciênc. E Tecnol. Aliment. 20 (2000) 388–390.
[402] E. Lautié, E. Rozet, P. Hubert, J. Quetin Leclercq, Quantification of rotenone in seeds of different species of yam bean (Pachyrhizus sp.) by a SPE HPLC–UV method, Food Chem. 131 (2012) 1531–1538.
[403] M.H. Rafamantanana, E. Rozet, G.E. Raoelison, K. Cheuk, S.U. Ratsimamanga, P. Hubert, et al., An improved HPLC-UV method for the simultaneous quantification of triterpenic glycosides and aglycones in leaves of Centella asiatica (L.) Urb (APIACEAE), J. Chromatogr. B. 877 (2009) 2396–2402.
[404] J. Kang, C. Xie, Z. Li, S. Nagarajan, A.G. Schauss, T. Wu, et al., Flavonoids from acai (*Euterpe oleracea* Mart.) pulp and their antioxidant and anti-inflammatory activities, Food Chem. 128 (2011) 152–157.
[405] C. Xie, J. Kang, Z. Li, A.G. Schauss, T.M. Badger, S. Nagarajan, et al., The açaí flavonoid velutin is a potent anti-inflammatory agent: blockade of LPS-mediated TNF-α and IL-6 production through inhibiting NF-κB activation and MAPK pathway, J. Nutr. Biochem. 23 (2012) 1184–1191.
[406] A.G.V. Costa, D.F. Garcia-Diaz, P. Jimenez, P.I. Silva, Bioactive compounds and health benefits of exotic tropical red–black berries, J. Funct. Foods. 5 (2013) 539–549.
[407] J.C. Ribeiro, L.M.G. Antunes, A.F. Aissa, J.D.C. Darin, V.V. De Rosso, A.Z. Mercadante, et al., Evaluation of the genotoxic and antigenotoxic effects after acute and subacute treatments with açai pulp (*Euterpe oleracea* Mart.) on mice using the erythrocytes micronucleus test and the comet assay, Mutat. Res. Toxicol. Environ. Mutagen. 695 (2010)

22–28.
[408] I. Ojanperä, M. Kolmonen, A. Pelander, Current use of high-resolution mass spectrometry in drug screening relevant to clinical and forensic toxicology and doping control, Anal. Bioanal. Chem. 403 (2012) 1203–1220.
[409] H. Trufelli, P. Palma, G. Famiglini, A. Cappiello, An overview of matrix effects in liquid chromatography-mass spectrometry, Mass Spectrom. Rev. 30 (2011) 491–509.
[410] H. Rogez, S.N.L.T. Akwie, F.G. Moura, Y. Larondelle, Kinetic Modeling of Anthocyanin Degradation and Microorganism Growth during Postharvest Storage of Açai Fruits (*Euterpe oleracea*), J. Food Sci. 77 (2012) C1300–C1306.
[411] P. Hubert, J.-J. Nguyen-Huu, B. Boulanger, E. Chapuzet, P. Chiap, N. Cohen, et al., Harmonization of strategies for the validation of quantitative analytical procedures: a SFSTP proposal—part I, J. Pharm. Biomed. Anal. 36 (2004) 579–586.
[412] A. Bouabidi, E. Rozet, M. Fillet, E. Ziemons, E. Chapuzet, B. Mertens, et al., Critical analysis of several analytical method validation strategies in the framework of the fit for purpose concept, J. Chromatogr. A. 1217 (2010) 3180–3192.
[413] B. Boulanger, E. Rozet, F. Moonen, S. Rudaz, P. Hubert, A risk-based analysis of the AAPS conference report on quantitative bioanalytical methods validation and implementation, J. Chromatogr. B. 877 (2009) 2235–2243.
[414] E. Rozet, R.D. Marini, E. Ziemons, B. Boulanger, P. Hubert, Advances in validation, risk and uncertainty assessment of bioanalytical methods, J. Pharm. Biomed. Anal. 55 (2011) 848–858.
[415] L. Nováková, A. Vildová, J.P. Mateus, T. Gonçalves, P. Solich, Development and application of UHPLC–MS/MS method for the determination of phenolic compounds in Chamomile flowers and Chamomile tea extracts, Talanta. 82 (2010) 1271–1280.
[416] J.-B. Peng, H.-M. Jia, Y.-T. Liu, H.-W. Zhang, S. Dong, Z.-M. Zou, Qualitative and quantitative characterization of chemical constituents in Xin-Ke-Shu preparations by liquid chromatography coupled with a LTQ Orbitrap mass spectrometer, J. Pharm. Biomed. Anal. 55 (2011) 984–995.
[417] E. de Rijke, P. Out, W.M.A. Niessen, F. Ariese, C. Gooijer, U.A.T. Brinkman, Analytical separation and detection methods for flavonoids, J. Chromatogr. A. 1112 (2006) 31–63.
[418] Y.-W. Chin, H.-B. Chai, W.J. Keller, A.D. Kinghorn, Lignans and Other Constituents of the Fruits of *Euterpe oleracea* (Açai) with Antioxidant and Cytoprotective Activities, J. Agric. Food Chem. 56 (2008) 7759–7764.
[419] N. Fabre, I. Rustan, E. Hoffmann, J. Quetin-Leclercq, Determination of flavone, flavonol, and flavanone aglycones by negative ion liquid chromatography electrospray ion trap mass spectrometry, J. Am. Soc. Mass Spectrom. 12 (2001) 707–715.
[420] L.A. Pacheco-Palencia, S.T. Talcott, Chemical stability of açai fruit (*Euterpe oleracea* Mart.) anthocyanins as influenced by naturally occurring and externally added polyphenolic cofactors in model systems, Food Chem. 118 (2010) 17–25.
[421] F. Ferreres, A. Gil-Izquierdo, P.B. Andrade, P. Valentão, F.A. Tomás-Barberán, Characterization of C-glycosyl flavones O-glycosylated by liquid chromatography–tandem mass spectrometry, J. Chromatogr. A. 1161 (2007) 214–223.
[422] F. Ferreres, B.M. Silva, P.B. Andrade, R.M. Seabra, M.A. Ferreira, Approach to the study of C-glycosyl flavones by ion trap HPLC-PAD-ESI/MS/MS: application to seeds of quince (*Cydonia oblonga*), Phytochem. Anal. 14 (2003) 352–359.
[423] F. Ferreres, R.F. Gonçalves, A. Gil-Izquierdo, P. Valentão, A.M.S. Silva, J.B. Silva, et al., Further Knowledge on the Phenolic Profile of *Colocasia esculenta* (L.) Shott, J. Agric. Food Chem. 60 (2012) 7005–7015.
[424] N. Ansermot, M. Brawand-Amey, C.B. Eap, Simultaneous quantification of selective

serotonin reuptake inhibitors and metabolites in human plasma by liquid chromatography–electrospray mass spectrometry for therapeutic drug monitoring, J. Chromatogr. B. 885–886 (2012) 117–130.
[425] M.A. Bimazubute, E. Rozet, I. Dizier, P. Gustin, P. Hubert, J. Crommen, et al., Liquid chromatographic determination of enrofloxacin in nasal secretions and plasma of healthy pigs using restricted access material for on-line sample clean-up, J. Chromatogr. A. 1189 (2008) 456–466.
[426] J. Kang, L.A. Hick, W.E. Price, Using calibration approaches to compensate for remaining matrix effects in quantitative liquid chromatography/electrospray ionization multistage mass spectrometric analysis of phytoestrogens in aqueous environmental samples, Rapid Commun. Mass Spectrom. 21 (2007) 4065–4072.
[427] E. Rozet, A. Ceccato, C. Hubert, E. Ziemons, R. Oprean, S. Rudaz, et al., Analysis of recent pharmaceutical regulatory documents on analytical method validation, J. Chromatogr. A. 1158 (2007) 111–125.
[428] E. Lautié, E. Rozet, P. Hubert, J. Quetin-Leclercq, Quantification of rotenone in seeds of different species of yam bean (*Pachyrhizus* sp.) by a SPE HPLC–UV method, Food Chem. 131 (2012) 1531–1538.
[429] M.H. Rafamantanana, E. Rozet, G.E. Raoelison, K. Cheuk, S.U. Ratsimamanga, P. Hubert, et al., An improved HPLC-UV method for the simultaneous quantification of triterpenic glycosides and aglycones in leaves of *Centella asiatica* (L.) Urb (APIACEAE), J. Chromatogr. B. 877 (2009) 2396–2402.
[430] R. Chirinos, D. Campos, N. Costa, C. Arbizu, R. Pedreschi, Y. Larondelle, Phenolic profiles of andean mashua (Tropaeolum tuberosum Ruíz & Pavón) tubers: Identification by HPLC-DAD and evaluation of their antioxidant activity, Food Chem. 106 (2008) 1285–1298.
[431] A. Castañeda-Ovando, M. de L. Pacheco-Hernández, M.E. Páez-Hernández, J.A. Rodríguez, C.A. Galán-Vidal, Chemical studies of anthocyanins: A review, Food Chem. 113 (2009) 859–871.
[432] V. Mulabagal, W.J. Keller, A.I. Calderón, Quantitative analysis of anthocyanins in Euterpe oleracea (açaí) dietary supplement raw materials and capsules by Q-TOF liquid chromatography/mass spectrometry, Pharm. Biol. 50 (2012) 1289–1296.
[433] E. Loeser, P. Drumm, Using strong injection solvents with 100% aqueous mobile phase in RP-LC, J. Sep. Sci. 29 (2006) 2847–2852.
[434] S. Keunchkarian, M. Reta, L. Romero, C. Castells, Effect of sample solvent on the chromatographic peak shape of analytes eluted under reversed-phase liquid chromatogaphic conditions, J. Chromatogr. A. 1119 (2006) 20–28.
[435] J. Sun, L. Lin, P. Chen, Study of the mass spectrometric behaviors of anthocyanins in negative ionization mode and its applications for characterization of anthocyanins and non-anthocyanin polyphenols: Mass spectrometric study of anthocyanins in negative ion mode, Rapid Commun. Mass Spectrom. 26 (2012) 1123–1133.
[436] N. Ortega, M.-P. Romero, A. Macià, J. Reguant, N. Anglès, J.-R. Morelló, et al., Comparative study of UPLC–MS/MS and HPLC–MS/MS to determine procyanidins and alkaloids in cocoa samples, J. Food Compos. Anal. 23 (2010) 298–305.
[437] C. Cavaliere, P. Foglia, R. Gubbiotti, P. Sacchetti, R. Samperi, A. Laganà, Rapid-resolution liquid chromatography/mass spectrometry for determination and quantitation of polyphenols in grape berries, Rapid Commun. Mass Spectrom. 22 (2008) 3089–3099.
[438] D. Del Pozo-Insfran, C.H. Brenes, S.T. Talcott, Phytochemical composition and pigment stability of Açai (Euterpe oleracea Mart.), J. Agric. Food Chem. 52 (2004) 1539–1545.
[439] G. Cao, H.U. Muccitelli, C. Sánchez-Moreno, R.L. Prior, Anthocyanins are absorbed

in glycated forms in elderly women: a pharmacokinetic study, Am. J. Clin. Nutr. 73 (2001) 920–926.
[440] S.H. Nile, S.W. Park, Edible berries: Bioactive components and their effect on human health, Nutrition. 30 (2014) 134–144.
[441] T. Tsuda, M. Watanabe, K. Ohshima, S. Norinobu, S.-W. Choi, S. Kawakishi, et al., Antioxidative Activity of the Anthocyanin Pigments Cyanidin 3-O-.beta.-D-Glucoside and Cyanidin, J. Agric. Food Chem. 42 (1994) 2407–2410.
[442] T. Tsuda, F. Horio, J. Kitoh, T. Osawa, Protective effects of dietary cyanidin 3-O-beta-D-glucoside on liver ischemia-reperfusion injury in rats, Arch. Biochem. Biophys. 368 (1999) 361–366.
[443] R. Feng, H.-M. Ni, S.Y. Wang, I.L. Tourkova, M.R. Shurin, H. Harada, et al., Cyanidin-3-rutinoside, a natural polyphenol antioxidant, selectively kills leukemic cells by induction of oxidative stress, J. Biol. Chem. 282 (2007) 13468–13476.
[444] A.-M. Aura, P. Martin-Lopez, K.A. O'Leary, G. Williamson, K.-M. Oksman-Caldentey, K. Poutanen, et al., In vitro metabolism of anthocyanins by human gut microflora, Eur. J. Nutr. 44 (2005) 133–142.
[445] E.C.H. Yip, A.S.L. Chan, H. Pang, Y.K. Tam, Y.H. Wong, Protocatechuic acid induces cell death in HepG2 hepatocellular carcinoma cells through a c-Jun N-terminal kinase-dependent mechanism, Cell Biol. Toxicol. 22 (2006) 293–302.
[446] A. Patras, N.P. Brunton, C. O'Donnell, B.K. Tiwari, Effect of thermal processing on anthocyanin stability in foods; mechanisms and kinetics of degradation, Trends Food Sci. Technol. 21 (2010) 3–11.
[447] M. Dueñas, S. González-Manzano, A. González-Paramás, C. Santos-Buelga, Antioxidant evaluation of O-methylated metabolites of catechin, epicatechin and quercetin, J. Pharm. Biomed. Anal. 51 (2010) 443–449.
[448] D. Barreca, E. Bellocco, U. Leuzzi, G. Gattuso, First evidence of C- and O-glycosyl flavone in blood orange (Citrus sinensis (L.) Osbeck) juice and their influence on antioxidant properties, Food Chem. 149 (2014) 244–252.
[449] G. Odontuya, J.R.S. Hoult, P.J. Houghton, Structure-activity relationship for antiinflammatory effect of luteolin and its derived glycosides, Phytother. Res. 19 (2005) 782–786.
[450] T. Breiter, C. Laue, G. Kressel, S. Gröll, U.H. Engelhardt, A. Hahn, Bioavailability and antioxidant potential of rooibos flavonoids in humans following the consumption of different rooibos formulations, Food Chem. 128 (2011) 338–347.
[451] P. Bremner, M. Heinrich, Natural products as targeted modulators of the nuclear factor-KB pathway, J. Pharm. Pharmacol. 54 (2002) 453–472.
[452] H.L. Pahl, Activators and target genes of Rel/NF-kappaB transcription factors, Oncogene. 18 (1999) 6853–6866.
[453] M.P. Nair, S. Mahajan, J.L. Reynolds, R. Aalinkeel, H. Nair, S.A. Schwartz, et al., The Flavonoid Quercetin Inhibits Proinflammatory Cytokine (Tumor Necrosis Factor Alpha) Gene Expression in Normal Peripheral Blood Mononuclear Cells via Modulation of the NF-System, Clin. Vaccine Immunol. 13 (2006) 319–328.
[454] H.J. You, H.J. Ahn, G.E. Ji, Transformation of Rutin to Antiproliferative Quercetin-3-glucoside by Aspergillus niger, J. Agric. Food Chem. 58 (2010) 10886–10892.
[455] T. Makino, R. Shimizu, M. Kanemaru, Y. Suzuki, M. Moriwaki, H. Mizukami, Enzymatically modified isoquercitrin, alpha-oligoglucosyl quercetin 3-O-glucoside, is absorbed more easily than other quercetin glycosides or aglycone after oral administration in rats, Biol. Pharm. Bull. 32 (2009) 2034–2040.
[456] I. Erlund, T. Kosonen, G. Alfthan, J. Mäenpää, K. Perttunen, J. Kenraali, et al., Pharmacokinetics of quercetin from quercetin aglycone and rutin in healthy volunteers, Eur. J.

Clin. Pharmacol. 56 (2000) 545–553.
[457] L. Yuan, J. Wang, H. Xiao, W. Wu, Y. Wang, X. Liu, MAPK signaling pathways regulate mitochondrial-mediated apoptosis induced by isoorientin in human hepatoblastoma cancer cells, Food Chem. Toxicol. 53 (2013) 62–68.
[458] F. Pu, K. Mishima, K. Irie, K. Motohashi, Y. Tanaka, K. Orito, et al., Neuroprotective effects of quercetin and rutin on spatial memory impairment in an 8-arm radial maze task and neuronal death induced by repeated cerebral ischemia in rats, J. Pharmacol. Sci. 104 (2007) 329–334.
[459] M.E. Sakalem, G. Negri, R. Tabach, Chemical composition of hydroethanolic extracts from five species of the Passiflora genus, Rev. Bras. Farmacogn. 22 (2012) 1219–1232.
[460] I. Parejo, O. J�uregui, F. Viladomat, J. Bastida, C. Codina, Characterization of acylated flavonoid-O-glycosides and methoxylated flavonoids fromTagetes maxima by liquid chromatography coupled to electrospray ionization tandem mass spectrometry, Rapid Commun. Mass Spectrom. 18 (2004) 2801–2810.
[461] U. Justesen, Collision-induced fragmentation of deprotonated methoxylated flavonoids, obtained by electrospray ionization mass spectrometry, J. Mass Spectrom. 36 (2001) 169–178.
[462] J.-Y. Zhang, Q. Zhang, H.-X. Zhang, Q. Ma, J.-Q. Lu, Y.-J. Qiao, Characterization of Polymethoxylated Flavonoids (PMFs) in the Peels of “Shatangju” Mandarin (Citrus reticulata Blanco) by Online High-Performance Liquid Chromatography Coupled to Photodiode Array Detection and Electrospray Tandem Mass Spectrometry, J. Agric. Food Chem. 60 (2012) 9023–9034.
[463] E. Lautié, E. Rozet, P. Hubert, N. Vandelaer, F. Billard, T. Zum Felde, et al., Fast method for the simultaneous quantification of toxic polyphenols applied to the selection of genotypes of yam bean (Pachyrhizus sp.) seeds, Talanta. 117 (2013) 94–101.
[464] X. Shao, X. Bian, J. Liu, M. Zhang, W. Cai, Multivariate calibration methods in near infrared spectroscopic analysis, Anal. Methods. 2 (2010) 1662–1666.
[465] A. Karlsen, L. Retterstøl, P. Laake, I. Paur, S.K. Bøhn, L. Sandvik, et al., Anthocyanins inhibit nuclear factor-kappaB activation in monocytes and reduce plasma concentrations of pro-inflammatory mediators in healthy adults, J. Nutr. 137 (2007) 1951–1954.
[466] F. Aguiar, V. Menezes, H. Rogez, Spontaneous postharvest fermentation of açai (Euterpe oleracea) fruit, Postharvest Biol. Technol. 86 (2013) 294–299.